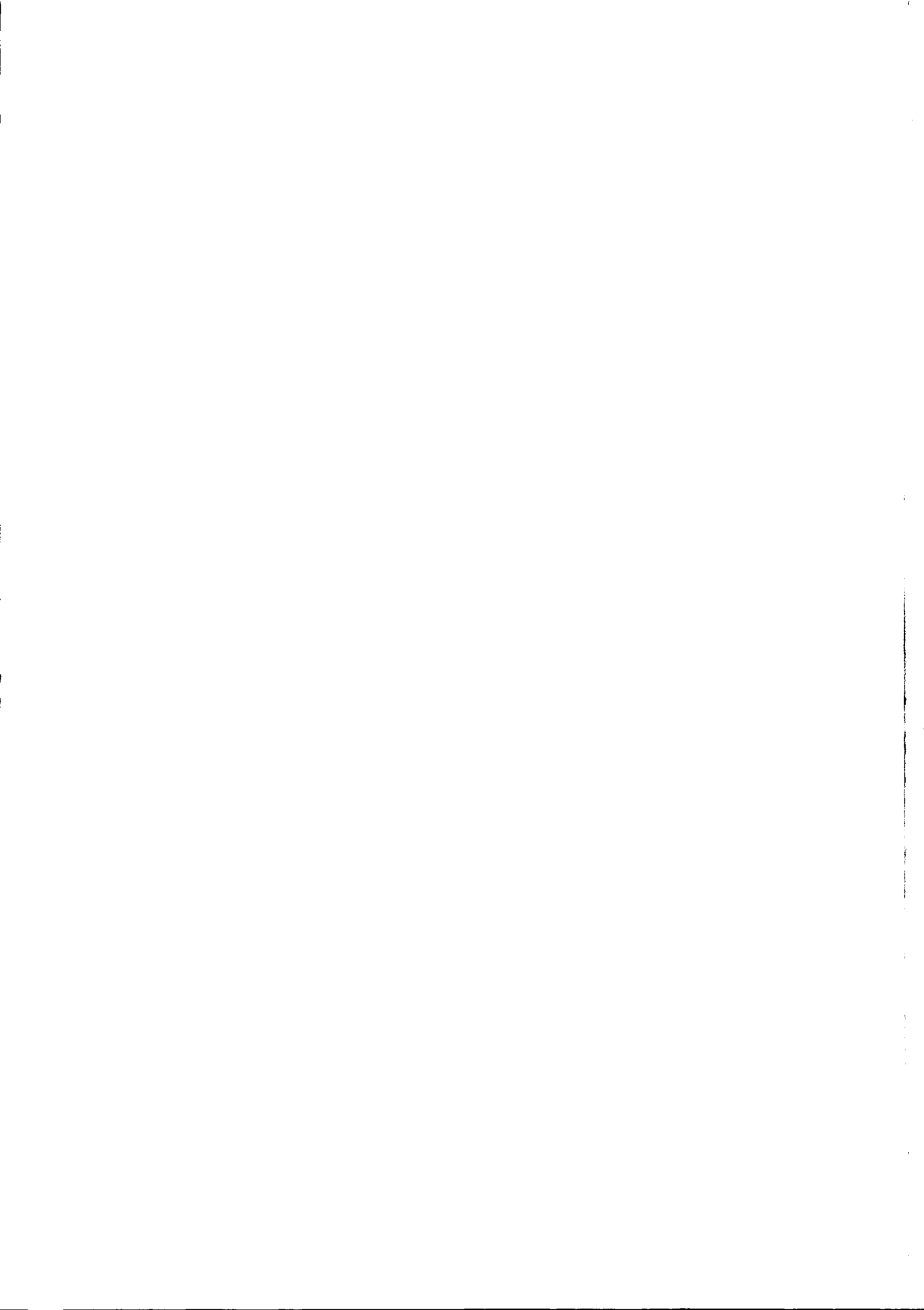


# Computational chemistry of PQQ and QH-ADH

Aldo Jongejan



Stellingen behorend bij het proefschrift "Computational chemistry of PQQ and QH-ADH door Aldo Jongejan:

- 1 In het licht van 25 jaar onderzoek van quinoproteïnen is het voorkomen van een covalent gebonden PQQ molecuul in het formaldehyde dehydrogenase uit *Methylococcus capsulatus*, zoals gesuggereerd door Zahn *et al.*, hoogst onwaarschijnlijk.  
(Zahn, J. A.; Bergmann, D. J.; Boyd, J. M.; Kunz, R. C. and DiSpirito, A. A.; *J. Bacteriol.*, **183** (2001), 6832-6840)
- 2 Het feit dat voor de twee enantiomeren van het substraat verschillende energiewaarden berekend, maakt de verklaring van Shin *et al.* voor de toename in enantioselectiviteit van lipases in organische oplosmiddelen in aanwezigheid van chirale zouten, aanvechtbaar.  
(Shin, J. -S.; Luque, S. and Klibanov, A. M.; *Biotechnol. Bioeng.*, **69** (2000), 577-583)
- 3 Het concept van "Near-Attack-Conformations" zoals gepropageerd door Bruice *et al.* voegt weinig toe aan het begrip van katalytische mechanismen in enzymatische reacties.  
(Hur, S. and Bruice, T. C.; *Proc. Natl. Acad. Sci. USA*, **99** (2002), 1176-1181; Hur, S. and Bruice, T. C.; *J. Am. Chem. Soc.*, **125** (2003), 1472-1473)
- 4 De in de literatuur beschreven nauwkeurigheid van *in silico* simulaties van biologische systemen geeft een vertekend beeld van het huidige voorspellend vermogen van deze methode van onderzoek.  
(dit proefschrift)
- 5 Glycerol, hoewel niet chiraal, wordt asymmetrisch gemetaboliseerd. Dat hier, zoals geclaimd door Chelli *et al.*, een verschil in conformatie-energie aan ten grondslag ligt is onwaarschijnlijk.  
(Chelli, R.; Gervasio, F. L.; Gellini, G. Procacci, P.; Cardini, G. and Schettino, V.; *J. Phys. Chem. A*, **104** (2000), 5351-5357)
- 6 Bij de weergave van de structuur van penicilline in biochemische leerboeken wordt aan een belangrijk drie-dimensionaal aspect voorbijgegaan.  
(Abrahamson, S.; Hodgkin, D.C. and Maslen, E.N.; *Biochem. J.*, **86** (1963) 514-535)
- 7 Eiwitvouwing *in silico* is een directe confrontatie met de Tweede Hoofdwet van de thermodynamica.
- 8 In de strijd tegen vetzucht is jarenlang de verkeerde vijand vervolgd.
- 9 Het idee dat kledingvoorschriften in het vrouwenvolleybal leiden tot verhoging van het kijkgenot is gewaagd.
- 10 In de evolutie van de computer blijkt de mens de zwakste schakel.

Deze stellingen worden verdedigbaar geacht en zijn als zodanig goedgekeurd door de promotor prof. dr. W. R. Hagen.

Propositions with the thesis "Computational chemistry of PQQ and QH-ADH" by Aldo Jongejan:

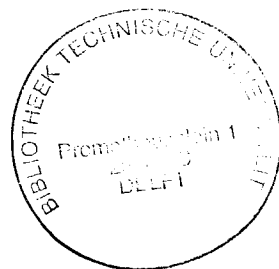
- 1 In view of 25 years of research on quinoproteins the occurrence of a covalently bound PQQ molecule in the formaldehyde dehydrogenase of *Methylococcus capsulatus* as suggested by Zahn *et al.* is unlikely.  
(Zahn, J. A.; Bergmann, D. J.; Boyd, J. M.; Kunz, R. C. and DiSpirito, A. A.; *J. Bacteriol.*, **183** (2001), 6832-6840)
- 2 Considering the fact that different values of the energy are calculated for the two enantiomers of the substrate, the explanation offered by Shin *et al.* for the increase of the enantioselectivity of lipases in organic solvents in the presence of chiral salts is disputable.  
(Shin, J. -S.; Luque, S. and Klibanov, A. M.; *Biotechnol. Bioeng.*, **69** (2000), 577-583)
- 3 The concept of "Near-Attack-Conformations" as promoted by Bruice *et al.* contributes little to our understanding of catalytic mechanisms in enzymatic reactions.  
(Hur, S. and Bruice, T. C.; *Proc. Natl. Acad. Sci. USA*, **99** (2002), 1176-1181; Hur, S. and Bruice, T. C.; *J. Am. Chem. Soc.*, **125** (2003), 1472-1473)
- 4 The accuracy of *in silico* simulations of biological systems published in literature gives a distorted picture of the current predictive capability of this technique.  
(this thesis)
- 5 Glycerol, although achiral, is metabolized asymmetrically. This property is, however, unlikely to be connected with a difference in conformational energy as claimed by Chelli *et al.*  
(Chelli, R.; Gervasio, F. L.; Gellini, G. Procacci, P.; Cardini, G. and Schettino, V.; *J. Phys. Chem. A*, **104** (2000), 5351-5357)
- 6 In biochemical textbooks an important three-dimensional feature has been omitted in the structural representation of penicillin.  
(Abrahamson, S.; Hodgkin, D.C. and Maslen, E.N.; *Biochem. J.*, **86** (1963) 514-535)
- 7 Protein folding *in silico* is a direct confrontation with the Second Law of Thermodynamics.
- 8 In the "War on Obesity" the wrong enemy has been perused for many years.
- 9 The idea that the introduction of a dress code in women's volleyball makes watching it more attractive is questionable.
- 10 In the evolution of computers man is the weakest link.

These propositions are considered defensible and as such have been approved by the supervisor prof. dr. W. R. Hagen.

2003-09-11  
2011926  
TR 4115

# Computational chemistry of PQQ and QH-ADH

proefschrift



ter verkrijging van de graad van doctor  
aan de Technische Universiteit Delft,  
op gezag van de Rector Magnificus prof. dr. ir. J. T. Fokkema,  
voorzitter van het College voor Promoties,  
in het openbaar te verdedigen op dinsdag 14 oktober 2003 om 13.00 uur

door Aldo JONGEJAN

doctorandus in de scheikunde

geboren te Delft.

Dit proefschrift is goedgekeurd door de promotor:

Prof. dr. W. R. Hagen

Samenstelling promotiecommissie:

Rector Magnificus, voorzitter

Prof. dr. W. R. Hagen, Technische Universiteit Delft, promotor

Prof. dr. C. Anthony, University of Southampton, England

Prof. dr. R. Leurs, Vrije Universiteit Amsterdam

Prof. dr. S. W. de Leeuw, Technische Universiteit Delft

Prof. dr. J. Reedijk, Rijksuniversiteit Leiden

Dr. ir. J. A. Jongejan, Technische Universiteit Delft

Dr. H. van Koningsveld, Technische Universiteit Delft

Dit onderzoek is gefinancierd door SON/NWO

*This research has been financed by the Netherlands Organization for Advancement of Pure Research (NWO).*

ISBN 90-9017352-8

Printing: Print Partners Ipskamp, Enschede, The Netherlands

*Almost in the beginning was curiosity.*

Sir Isaac Asimov

*Det er vanskeligt at spaa – især om fremtiden*

*Prediction is extremely difficult.*

*Especially about the future*

Robert Storm Petersen





# Computational chemistry of PQQ and QH-ADH

Aldo Jongejan



# CONTENTS

|   |     |
|---|-----|
| <b>CHAPTER 1</b>  | 1   |
| Computational Enzymology: in Vivo, in Vitro ...in Silico?   |     |
| <b>CHAPTER 2</b>  | 43  |
| The Enantioselectivity of Quinohemoprotein Alcohol Dehydrogenases: Mechanistic and Structural Aspects   |     |
| <b>CHAPTER 3</b>  | 107 |
| Homology Model of the Quinohemoprotein Alcohol Dehydrogenase from <i>Comamonas testosteroni</i>   |     |
| <b>CHAPTER 4</b>  | 141 |
| Direct Hydride Transfer in the Reaction Mechanism of Quinoprotein Alcohol Dehydrogenases: A Quantum Mechanical Investigation                    |     |
| <b>CHAPTER 5</b>  | 171 |
| Deuterium Isotope Effect on Enantioselectivity in the <i>Comamonas testosteroni</i> QH-ADH-catalyzed Kinetic Resolution of <i>rac</i> -Solketal |     |
| Summary   | 183 |
| Samenvatting  | 187 |
| List of publications  | 191 |
| Curriculum Vitae  | 192 |
| Dankwoord   | 193 |



# Computational Enzymology:

## *in vivo, in vitro, ...in silico ?*

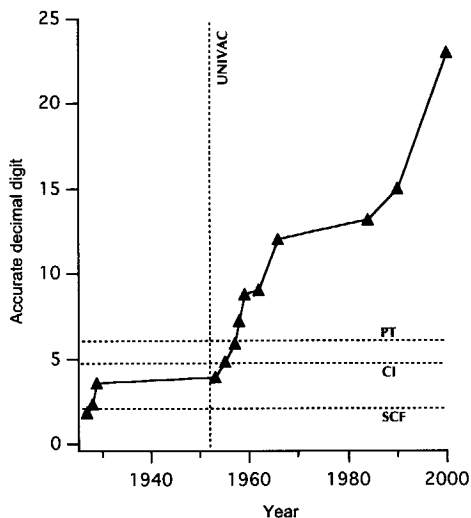
---

Science uses theories and models to uncover the physical rules that govern natural phenomena. Two strategies are commonly employed. First, the *in vivo* complexity is reduced to its *in vitro* parts. Next, hypotheses that project novel ideas into unknown territory, are judged against Occam's razor [1], providing the 'cutting edge' to separate basics from redundancies. Clearly, the first approach is bounded by the limits of reductionism. The second tool is blunted by practical limitations: the more basic a hypothesis is, the more distant to (experimental) reality it will be. This certainly holds for 'quantum theory'. In essence, the Schrödinger equation claims to hold the solution to all that can (ever) be known from black holes to black coffee. However, as Dirac expressed his concerns a long time ago "[It] leads to equations much too complicated to be soluble" [Dirac, 1929]

Since then, the quantum mechanical exploration of physico-chemical space has certainly come of age. Whereas back in the 1970's "...we were lucky if we could predict energies to within  $\pm 80$  kcal per mole" [2], calculations on (very) small systems, i.e. the helium atom, have pushed the accuracy of quantum mechanical calculations many digits beyond what can be verified experimentally [3] (Figure 1). While accurate first-principle, *ab initio*, solutions are not yet feasible for large systems, the use of powerful computers has greatly expanded the range of theories and models that can be evaluated

**Figure 1.** Accuracy of computed values for the helium ground state energy since the advent of quantum mechanics. "Accurate decimal digits" is defined as  $d = -\log_{10}|E - E_{\text{ref}}|$  in order to define a continuous scale such that the error will be less than one unit in the  $k^{\text{th}}$  place to the right of the decimal point if  $d > k$ . Points correspond to refs 6 - 17 (in order) and  $E_{\text{ref}}$  taken from ref 18 of [3]. Dashed lines show accuracies achieved by standard methods (self-consistent field (SCF), configuration interaction (CI), and perturbation theory (PT)). The first commercial computer was introduced in 1951 (UNIVAC).

Figure reproduced from [3] with permission.



in an approximate, experimental manner. In this sense, computers provide today's virtual laboratories: *in silico*.

### 1.1 Computational enzymology

Enzymes constitute a special class of polypeptides, proteins, with remarkable catalytic properties. They provide the living cell with the necessary equipment for rate enhancement, selectivity, and regulation. Understanding the basis of their proficiency is one of the major challenges of biochemistry [4-6]. Insights have been gained using traditional experimental and theoretical methods. However, certain key aspects of enzymatic catalysis appear to be elusive. This is where (quantum) mechanical simulations can complement and fill the gaps. Whether this will be successful depends critically on the interlacing of the two fields. Since the dynamical events of interest occur in the micro- to millisecond range, direct simulation of their occurrence is hampered by the femtosecond time steps needed for reliable integration of the equations of motion for molecular systems. In an alternative strategy, energy values are used to set up an interface between *wet* chemistry and *in silico* results. In Section 2, a brief outline is given of the types of energy-related experimental data obtained by traditional enzyme catalysis research. Benchmarking values for the accuracy that is required to match *wet* chemistry results are presented in Section 3.

Section 4 contains examples with increasing degree of complexity. Application to the quinohemoprotein alcohol dehydrogenase, QH-ADH, that forms the topic of this thesis, is summarized in the final Section.

## 2 Enzyme catalysis

### 2.1 Kinetic and mechanistic characterization

The formalism initiated by Michaelis and Menten still provides a strong basis for enzyme kinetic modeling. In the minimal model, Eq. 1, free enzyme,  $E$ , binds a single substrate,  $S$ , to form the Michaelis complex,  $ES$ , which subsequently transforms into the product,  $P$ , with concomitant release of the free enzyme.



$$r_{i=0} = \frac{V_{\max} \cdot [S]}{K_M + [S]} \quad (2)$$

Applying pseudo-steady state approximations, a two-parameter relation is obtained for the initial rate, Eq. 2.  $V_{\max}$  ( $= k_{\text{cat}} * [E_{\text{total}}]$ ) corresponds to the maximal rate.  $K_M$  is a measure of the affinity of free enzyme and substrate. For more complex situations appropriate lumping of the microscopic rate constants produces additional parameters [7-9]. These parameters can, in general, be retrieved from (pre/pseudo) steady-state rate measurements by regression analysis.

The kinetic framework of an enzyme-catalyzed reaction sets the boundaries for mechanistic interpretations. From the literature, it is evident that this leaves a large playground. General ideas based on the comparison of the enzymatic reaction with the corresponding uncatalyzed reaction in solution include: solvent reorganisation effects [6]; proximity and orientation effects [10-14]; hydrogen bond energetics [15,16]; tunneling phenomena [17-21]; influence of metal cofactors [22]. Recently, the role of low-barrier hydrogen bonds (LBHB) in the stabilization of the Michealis complex has been subject to much debate [15,16,23-29]. At least, the importance of the bulk protein in providing a preorganized and electrostatically favorable reaction environment is widely accepted.

The abundance of mechanistic interpretations relates in part to the success of the formalism developed in the field of (organic) chemistry. Armed with empirical relationships (Hammett, Brønstedt), quantum theoretical shortcuts (resonance, inductive and mesomeric effects), and a number of experience-based intuitions (Hammond postulate), chemists succeeded to find their way in the complexity of reacting systems. However, since (computer) calculations require numbers and not notions, there is a continuing need for adequate numerical descriptions.

## 2.2 From rates to energies

In the present setting, Eyring Transition State Theory (TST) [30] serves to outline the argument. Granting explicit assumptions, as summarized in comprehensive reviews [31,32], the (microscopic) kinetic constant,  $k$ , of an elementary reaction is expressed as in Eq. 3 (thermodynamic format, all physical constants with their usual meaning,  $\kappa$  being the transmission coefficient).

$$k = \kappa \frac{k_B T}{h} e^{-\Delta G^\ddagger / RT} \quad (3)$$

The appealing feature of this equation is that it provides a one-to-one relation between the rate (constant) and a thermodynamic state function, the Gibbs free energy difference,  $\Delta G^\ddagger$ , between the transition state, TS, and the ground state system. Although, this relation conveniently maps rate data onto the energy domain, the resulting 'energies' should be treated with caution. Of fundamental importance is the realization that the wealth of data on activation energies that can be found in the literature merely represents this change of format. Such energies should be better addressed as 'Eyring energies', to emphasize this fact. Also, whereas the numerical properties of the exponential function narrow the confidence intervals (in an absolute sense), in a reversal of fortune 'accurate' energies ( $\pm 0.5 \text{ kcal.mol}^{-1}$ ) produce large errors (200 %) for the reaction rates [31]. Despite the fact that the Eyring energies provide no new information, they are of value to reduce the complexity of kinetic equations. An example is given in Chapter 5, where the change of format serves to identify factors that are crucial for the enantioselectivity of QH-ADH.

## 2.3 Enthalpy and entropy

When additional information is collected, i.e. the temperature dependence of the reaction rate, it is possible to add extra meaning to the activation Gibbs free energy



equivalent addressed above as the Eyring energy. In principle, enthalpic and entropic contributions can be distinguished according to Eq. 4.

$$\Delta G^\# = \Delta H^\# - T\Delta S^\# \quad (4)$$

As the ratio of the rate constants for the forward and backward reaction is bounded by the value of the equilibrium constant, the enthalpy of activation difference obtained in this way is much less affected by the assumptions underlying reaction rate theory. Of course, calculation of the absolute reaction rate requires the entropic contribution to be included. When relative rates are considered, however, as is the case for enzyme enantioselectivity, cancellation of factors may again be hoped for. Extracting enthalpic and entropic differences for diastereomeric transition states from the temperature dependence of the enantiomeric ratio has been described by us [33] and others [34,35].

### 3 Computational methods

#### 3.1 Approximations

Full understanding of enzyme catalysis requires detailed knowledge of the events occurring at the atomic and electronic level. As mentioned above, solving the Schrödinger equation, Eq. 5, could provide the answers.

$$\hat{H}\Psi(r,t) = i\hbar \frac{\partial \Psi(r,t)}{\partial t} \quad (5)$$

Given the wavefunction  $\Psi(r,t)$ , the expectation value,  $\langle A \rangle$ , of the property of interest can be calculated as in Eq. 6 by introducing the appropriate operator.

$$\langle A \rangle = \int \bar{\Psi}(r,t) \hat{A} \Psi(r,t) dr \quad (6)$$

Restricting ourselves to systems for which the Hamiltonian operator,  $\hat{H}$ , is not explicitly dependent on time (i.e. no magnetic forces), the time-dependency of the wavefunction can be separated:

$$\hat{H}(r)\phi(r) = E\phi(r), \text{ and } \Psi(r,t) = \phi(r)e^{-iEt/\hbar} \quad (7)$$

leaving the *time-independent* Schrödinger equation as an eigenvalue problem. Introduction of the Born-Oppenheimer approximation allows the nuclear positions to be

treated as parameters, in which case Eq. 7 affords the electronic energy of the system at fixed internuclear positions.

Although, a classical mechanics treatment is inadequate to describe the electron configuration, the atoms themselves may well be described using Newton's equations of motion. This leads to three approaches that are commonly used to simulate molecular systems: *i. ab initio* calculations based on the Schrödinger equation, the values of fundamental constants and atomic numbers, *ii. semi-empirical* techniques using (empirical) parametrization of core electron configurations together with approximate Hamiltonians for the outer electrons, and *iii. molecular mechanics*, or *force field methods*, applying purely classical physics. An overview is provided in Table I.

**Table I.** Advantages and disadvantages of computational techniques

|                            | <b>Method</b>   | <b>Advantages</b>  | <b>Disadvantages</b>  | <b>Applicable to</b>   |
|----------------------------|---|--|---|--|
| <b>Ab initio</b>           | <ul style="list-style-type: none"> <li>⇒ uses Schrödinger Eq.</li> <li>⇒ no empirical parameters</li> <li>⇒ uses approximations</li> <li>⇒ mathematically rigorous</li> </ul> | <ul style="list-style-type: none"> <li>⇒ useful for 'new' chemistry</li> <li>⇒ no experimental data required</li> <li>⇒ electronic transitions and excited states can be calculated</li> </ul> | <ul style="list-style-type: none"> <li>⇒ computationally expensive</li> </ul>   | <ul style="list-style-type: none"> <li>⇒ small systems</li> <li>⇒ systems involving electronic transitions</li> <li>⇒ 'new' chemistry (i.e. no experimental data available)</li> </ul> |
| <b>Semi-empirical</b>      | <ul style="list-style-type: none"> <li>⇒ uses Schrödinger Eq.</li> <li>⇒ uses exp. derived empirical parameters</li> <li>⇒ uses extensive approximation</li> </ul>            | <ul style="list-style-type: none"> <li>⇒ electronic transitions and excited states can be calculated</li> <li>⇒ computationally cheaper than <i>ab initio</i> methods</li> </ul>               | <ul style="list-style-type: none"> <li>⇒ experimental data for parametrization</li> <li>⇒ less accuracy and theoretical rigor compared to <i>ab initio</i> methods</li> </ul>                       | <ul style="list-style-type: none"> <li>⇒ medium to large systems</li> <li>⇒ systems with bond breaking or formation processes</li> </ul>   |
| <b>Molecular mechanics</b> | <ul style="list-style-type: none"> <li>⇒ uses classical physics</li> <li>⇒ uses force field with empirical parameters</li> </ul>  | <ul style="list-style-type: none"> <li>⇒ fast, computationally cheap</li> <li>⇒ applicable to (very) large systems (enzymes)</li> </ul>  | <ul style="list-style-type: none"> <li>⇒ lim. applicability of force field outside test set</li> <li>⇒ no calculation of electronic properties</li> <li>⇒ expl. data for parametrization</li> </ul> | <ul style="list-style-type: none"> <li>⇒ large molecular systems (&gt;1000 atoms)</li> <li>⇒ systems without bond breaking and formation</li> </ul>                                    |

### 3.2 Chemical accuracy

Except for those cases where exact solutions to the Schrödinger equation are available, the accuracy of the computed values has to be judged from the comparison with experimental data. As Pople stated in his Nobel Prize Lecture: "Chemical accuracy is reached as chemical properties are quantitatively predicted within the standard deviation offered by the best experimental methods" [36]. Benchmarking values have been proposed in the literature for various properties of molecular systems. Spectroscopic accuracy (arbitrarily put at  $\pm 1 \text{ cm}^{-1}$ ) seems presently unattainable even for small systems due to the errors implicitly introduced by the Born-Oppenheimer approximation and the use of a non-relativistic Hamiltonian to describe molecular systems [37]. At the other end of the scale, structural and geometrical properties appear to be well within the reach of computational methods. Errors in bond lengths and bond angles of 0.01-0.02 Å and  $1^\circ - 2^\circ$ , respectively, are considered acceptable for small molecules [38,39]. Energy-related properties take up an intermediate position. Chemical accuracies that are quoted in the literature range from  $\pm 0.2$  to  $\pm 2.5 \text{ kcal.mol}^{-1}$  [38,40-43]. Extreme values ( $\pm 0.01 \text{ kcal.mol}^{-1}$  [44],  $\pm 5 \text{ kcal.mol}^{-1}$  [45]) have also been suggested. A value of  $\pm 1 \text{ kcal.mol}^{-1}$  appears to be generally accepted. This number has been related to the strength of the weakest, chemically interesting interaction, the van der Waals interaction [46].

An important aspect of *in silico* strategies is the focus on a single item of the system of interest. Macroscopic properties (equation of state, structural order parameters, free energy) are then extrapolated from the microscopic details using theoretical models. Alternatively, thermodynamical properties are obtained directly from simulations of the appropriate ensemble in the time domain. Both approaches can give rise to the introduction of additional errors.

## 4 Accuracy of computational methods

### 4.1 Quantum mechanical calculations of small molecule properties

#### 4.1.1 *Ab initio* calculations

Hartree-Fock self-consistent field methods, still the most widely applied *ab initio* computational methods, rely on the accurate description of spin orbitals by means of a comprehensive basis set. Application of a complete (i.e. infinite) basis set is computationally not feasible and hence a limit is put on the accuracy obtainable by HF-methods. Effects of applying different basis sets and their truncation errors

have been noted in the calculation of molecular geometries as well as energies. As an example, different basis sets were shown to produce opposing results for the biologically important interaction between dioxygen species and heme moieties [47].

The effects of electron correlation, although amounting to only a few % of the total energy [48], need to be included into *ab initio* calculations to arrive at reasonable estimates for absolute values of the bond dissociation energies. The neglect of electron correlation in the calculation of transition states, where the correlation energy is generally larger, leads to numbers that are too high compared to the experimental values [49]. Commonly applied coupled-cluster and perturbative methods show better accuracy, but are generally not size-consistent and very time-consuming due to slow convergence. Alternative procedures include *i*) incorporation of the interelectronic distance into the correlated wavefunction [50,51], *ii*) density functional theory (DFT) [52-54] and *iii*) combinations of additivity approximations, extrapolation and empirical correction schemes (e.g., Gaussian-2 (G2) [55] and Gaussian-3 (G3) [56]). The first method has been applied to first-row atoms only, due to rapid explosion of the number of 3- and 4-electron integrals that would have to be calculated. Nevertheless, promising results have been obtained in terms of accuracy (dissociation energy ( $\pm 0.2$  kcal.mol<sup>-1</sup>), equilibrium distance ( $\pm 1 \cdot 10^{-4}$  Å) and wavelength ( $\pm 2$  cm<sup>-1</sup>)) and speed [57].

DFT methods use an energy functional of the electron density and the nuclear positions to describe the total energy of an atomic system. The initial failure of the Local Density Approximation (LDA), used for the calculation of the exchange and correlation energy, has been overcome in the past 15 years. The exchange and correlation functionals have dramatically improved and DFT methods are now superior to Hartree-Fock methods and comparable to more elaborate post-Hartree-Fock methods. It has been argued that the commonly applied B3LYP hybrid functionals mimic pair and three-electron correlation effects, which in wave function methods can only be covered by computationally expensive coupled cluster methods [58]. However, failures of DFT methods to reproduce experimentally observed values have also been reported [59,60]. Accurate representation of hydrogen-bonded systems and aqueous solvation energetics by DFT methods is still a subject of many investigations [61-64]. A systematic overestimation of bond energies has been noted for systems with unpaired electrons, leading to large errors (max. error 31 kcal.mol<sup>-1</sup> with the popular three-parameter hybrid functional B3LYP) [59]. Artfactual effects on enzyme-induced polarization of large

anionic substrates of dihydrofolate reductase, in comparison to HF and MP2 methods have also been reported [65].

The G2 and G3 empirical schemes [55,56] consist of multiple single-point energy calculations at increasing levels of complexity based on the optimized geometry at second order Møller-Plesset (MP2) levels of theory using the 6-31G(d) basis set with all electrons included (MP2(full)/6-31G(d)) [66]. For the set of 125 molecular systems used to validate the G2 method, the average absolute deviation from experiment for the calculated enthalpies of formation is 1.21 kcal.mol<sup>-1</sup>, with deviations as large as 8.2 kcal.mol<sup>-1</sup> for individual compounds. The average for the G3 model is 1.08 kcal.mol<sup>-1</sup>. For comparison, results for the DFT method B3LYP were worse, at 2.46 kcal.mol<sup>-1</sup> and 20.25 kcal.mol<sup>-1</sup> for the outliers, respectively. Semi-empirical methods (AM1) perform even worse [67]. The accuracy decreases when computationally less-expensive variants of the initial geometry optimization method are applied (1.59 kcal.mol<sup>-1</sup>; (MP2) and 1.64 kcal.mol<sup>-1</sup> (MP2/SVP) for the G2 method and 1.30 kcal.mol<sup>-1</sup> (MP2) for the G3 method). G2 and G3 predictions for heats of formation and ionization potential values are usually within  $\pm 0.1$  eV (or  $\sim 2$  kcal.mol<sup>-1</sup>) of the experimental data. Whereas G2 results have been used to question experimental data [68], failures of the G2 method have also been reported [69].

Although assigned a higher predictive capacity than semi-empirical methods, results obtained using *ab initio* calculations should be subject to scrutiny. The computational chemist has to be aware of many possible sources of errors, e.g. the characteristics of the employed basis set, neglect of electron correlation, and relativistic effects. The effect of numerical errors in the applied algorithms [44,48] will not be discussed here.

The importance of relativistic effects has been reviewed [70]. Detailed studies have appeared for hydrogen halides [71,72]. It has been argued that agreement (if any) with experiment is fortuitous. Electron correlation and (in)complete basis sets were considered to be primary causes for concern [72].

#### 4.1.2 Semi-empirical techniques

The average accuracy of some commonly applied methods for the calculation of geometric and energetic properties of selected small molecules is summarized in Table II. It appears that geometric features are calculated with reasonable accuracy. Energy

values, on the other hand, cover a much wider range. The performance of semi-empirical methods rivals and even exceeds that of higher-level *ab initio* methods in the calculation of specific properties. However, while techniques depending on parameterization are good for interpolation, extrapolating well and consistently remains a problem. This limits the predictive power of semi-empirical methods and forms the main reason why *ab initio* calculations are the methods of choice for understanding 'new' chemistry. To extend the scope of semi-empirical methods compounds not present in the calibration set must be included followed by reparameterization. These techniques can then be applied to problems requiring both speed and accuracy. The potential of semi-empirical MO theory in applications to problems in computational chemistry has been reviewed [73].

## 4.2 Calculation of non-bonded interactions

Nonbonded interactions play an essential role in (macro)molecular folding, recognition, binding, solvation, energy transfer and chemical reactions. Their calculation presents a

**Table II.** Accuracy of computational techniques relative to experimental results

|   | computational method |                    |                    |                    |                    |                         |                             |
|---|----------------------|--------------------|--------------------|--------------------|--------------------|-------------------------|-----------------------------|
|   | MM2                  | AM1                | HF/<br>STO-<br>3G  | HF/<br>6-31G(d)    | B3LYP/<br>6-31G(d) | MP2/<br>aug-cc-<br>pVTZ | CCSD(T)<br>/aug-cc-<br>pVQZ |
| bond length (Å)                           | 0.01 <sup>a</sup>    | 0.048 <sup>a</sup> | 0.055 <sup>b</sup> | 0.032 <sup>b</sup> | 0.020 <sup>b</sup> | 0.012 <sup>b</sup>      | 0.008 <sup>b</sup>          |
| bond angle                                | 1.0 <sup>c</sup>     | 3.3 <sup>c</sup>   | 1.7 <sup>d</sup>   | 1.4 <sup>d</sup>   | 1.4 <sup>d</sup>   | 0.3 <sup>d</sup>        | 0.2 <sup>d</sup>            |
| $\angle \text{H}_i^{\text{O}}^{\text{e}}$ | 0.5                  | 8                  |                    | 4                  |                    |                         |                             |
| Total energy <sup>f</sup>                 |                      | 18.8               | 93.3               | 51.0               | 7.9                |                         |                             |
| Dipole <sup>g</sup>                       | 0.1                  | 0.5                | 0.5                | 0.2                |                    |                         |                             |
| Ionization<br>potential                   |                      | 0.6 <sup>h</sup>   |                    |                    |                    | 4.0 <sup>i</sup>        | 1.0 <sup>i</sup>            |
| Atomization<br>energy <sup>i</sup>        |                      |                    |                    |                    |                    | 5.0                     | 2.0                         |
| Frequencies <sup>j</sup>                  |                      |                    |                    |                    |                    | 60,30,120               | 25,40                       |
| Electron affinity <sup>i</sup>            |                      |                    |                    |                    |                    | 3.0                     | 1.0                         |

For comparison, the maximum error remaining in the best diffraction experiment can amount to 0.006 Å in bond lengths for small molecules [74]. Data are extracted from Young [46] and <http://www.chamotlabs.com/Freebies/Table/Methods.html>. a) Å std. dev., b) Å RMS error, c) degrees std. dev., d) degrees RMS error, e) kcal/mol std. dev., f) kcal/mol mean abs. dev., g) Debye std. dev., h) eV std. dev., i) kcal/mol mean abs. dev. j)  $\text{cm}^{-1}$  mean abs. dev.

great challenge. The current status of *ab initio* calculations of nonbonded interactions has been reviewed [64]. Small-sized dimeric systems representative for dispersion and hydrogen-bonding interactions reminiscent of low-barrier hydrogen bonding (LBHB) systems [27] have been studied. Binding energies range from 0.5 to 50 kcal.mol<sup>-1</sup>, while the *basis set superposition error* (BSSE) ranges from 0.1 to 15 kcal.mol<sup>-1</sup>. Taking the interaction energy as the difference in energy between the dimer and the separated monomeric species, BSSEs lead to an overestimate because of a nonphysical lowering of the energy of the associated dimer relative to the separated monomers. Correction is possible via the *counterpoise* method, using the same basis set for the description of both the monomeric and the dimeric species. The BSSE varies substantially depending on the size of the basis set, and can still amount to a considerable fraction of the projected 1 kcal.mol<sup>-1</sup> accuracy even when large basis sets are used [64,71].

### 4.3 PES, the potential energy surface

Dynamical aspects of molecular systems, i.e. conformational changes and redistribution of energy over various degrees of freedom, are important for the prediction of thermodynamic and spectroscopic properties [75,76]. By plotting the potential energy as a function of the molecular conformation an energy 'landscape' can be constructed. From this *potential energy surface*, PES, information regarding the structural and (thermo)dynamical properties of a molecular system can be extracted. Detailed knowledge of the PES is important for several fields of research, including reaction kinetics, protein dynamics and folding.

Stationary points on the PES include 'local' and 'global' minima, representing stable, low-energy structures. Normal-mode analysis of these structures allows for a comparison with spectroscopic data (IR and Raman) and the calculation of thermodynamic properties, i.e. free energy and heat capacity. Saddle points, in particular stationary points with exactly one imaginary normal mode frequency, represent 'transition states'. Detailed information on the atomic and electronic configuration of transition states is difficult to access experimentally because of the inherently short lifetimes [77]. Although, novel techniques are emerging, i.e. direct observation of fast, light-induced chemical reactions [78], and X-ray diffraction techniques probing the subpicosecond domain [78,79], indirect information has still to be collected from the evaluation of activation energies, entropies, kinetic isotope effects, or solvent and substituent effects on rates.

Classical TST (Section 2.2, Eq. 3) requires information of the ground state and TS energy only. More advanced theories require knowledge of the energy profile along the reaction coordinate as well [49]. Variational TST [32] stays within the classical boundaries, tunneling theories, on the other hand, require a quantum mechanical description [80]. Quantum tunneling has become an important issue in electron transfer theories. From the pioneering work of Klinman and coworkers it is now clear that quantum tunneling of hydrogen atoms must also be taken into account when studying enzyme catalysis [17-20,81]. While waiting for a comprehensive theoretical framework, quantum mechanical effects are commonly incorporated into classical TST using appropriate correction factors.

#### **4.4 Simulation of proteins and enzymes**

##### **4.4.1 Molecular mechanics and dynamics**

Proteins and enzymes are large, complex molecules showing different behaviour as compared to small molecules or relatively homogeneous systems [82]. Although, quantum mechanical calculations (*ab initio*, semi-empirical) are currently applied to small proteins [83] and selected parts of larger systems (QM/MM, see below), the size of most systems of interest precludes the direct incorporation of electrons into the simulations. Molecular mechanics simulations use a force field to describe the interactions between classical particles and apply Newton's equations of motion to study the evolution of the system in space and time. Force fields are parameterized on a test set of molecules. Force fields specifically designed for the simulation of saccharides [84], proteins [85-91], organic molecules [92-99], and transition metals [100] have been reported. Enzyme cofactors, coenzymes, and ligands or substrates often require additional parameterization specific for the applied force field [101-104]. Although, in principle, the construction of a universal force field [105] should be feasible, researchers have a tendency to fine-tune existing force fields for their specific needs. In this respect, the construction of a force field specific for transition states is worth mentioning [106,107]. Benchmarking studies on the performance of force fields with respect to the reproduction of geometrical and spectroscopic data have appeared [108]. A comparison of force fields is given in [109,110] and 'Reviews in Computational Chemistry' [111]. Requirements for proper use and validation of force fields in molecular dynamics simulations have been summarized by Lipkowitz [112] and van Gunsteren & Mark [113].



#### 4.4.2 Timescales

Due to the numerical instability of the dynamics algorithms the integration time step is limited to the femtosecond timescale. Thus, depending on system size and computational resources, simulations on the nanosecond timescale are commonly considered. Simulations extending into the millisecond timescale have, however, been reported [114,115]. Enlarging the time step leads to loss of information of the fastest motions within a protein, i.e. the vibrations of the hydrogen atom. In the study of domain movements, this loss can be overcome by focusing on the 'essential dynamics' of the system [116]. Attempts to increase the time step have been reported [117], but are not yet implemented in molecular modeling programs. Reducing the system size using united-atom representations is an option incorporated in some force fields.

#### 4.4.3 Solvation and electrostatic effects

Considering that most experimental data on proteins and enzymes relate to aqueous conditions, with defined values of pH and ionic strength, it is important to mimic these conditions *in silico*. Simulations in aqueous environments require an accurate description of the solvent, including non-bonded interactions. As discussed in Section 4.2, calculation of non-bonded interactions presents a great challenge for high-level *ab initio* quantum chemical calculations. In the case of proteins and enzymes the number of non-bonded interactions is large. Also, truncation of non-bonded, electrostatic, interactions has been shown to introduce substantial errors in protein simulations in polar solvents [118,119]. Methods representing the solvent as a continuum with a preset dielectric constant have been proposed (for reviews see [120-122]). By omitting the calculation of all solvent-solvent interactions, computation time can be reduced substantially. However, solvent molecules close to the solute and in the bulk phase display different behaviour. Explicit incorporation of water molecules allows the study of the structural and energetic role played by single molecules in ligand binding, protein conformational changes, flexibility, and enzyme catalysis [123-125]. Recent developments in both software and hardware have made computations with explicit incorporation of solvent molecules affordable.

In order to simulate solvent electrostatic screening effects a distance-dependent dielectric constant can be applied as a first approximation. A disadvantage of this strategy is the tendency of oppositely charged groups to move together, leading to the artifactual

formation of salt-bridges. A more physically rigorous approach uses the continuum electrostatic model obtained by solving the Poisson-Boltzmann equation [121]. Within this model the ionic strength and the dielectric constant of the solvent are fully determined by the experimental conditions. Other aspects are less clear, including the atomic charges and radii, the conformational fluctuations of the amino acid side chains, and the intrinsic dielectric constant of the protein. The problematic status of the latter quantity can be appreciated from studies by Antosiewicz and coworkers [126]. They observed that a value of 20 for the relative dielectric constant of the protein substantially reduced the errors in calculated  $pK_a$ -values, as opposed to the values of 2-4 that are commonly used. In line with this observation, simulations of four proteins under different conditions showed best results when the dielectric constant was taken to vary between 15 and 40 with a considerably lower value for the protein interior (2-4) [127]. Similar results have been reported earlier [128,129].

The calculation of ionization constants ( $pK_a$ s) of titratable groups within proteins constitutes an important test case for the accuracy of the applied solvation models in the description of the microscopic electrostatic details. Reactions and conformational changes often display a specific pH dependency. The individual  $pK_a$ s of ionizable amino acids can differ dramatically from those measured for the isolated residues in solution. These shifts have been attributed to the local environment of the side chains, i.e. their interactions with neighbouring groups, hydrogen bonding to nonionizable residues, and the degree of solvent exposure. Calculations suggest that electrostatic and solvation models are capable of capturing these shifts in  $pK_a$ s and can identify the amino acid residues responsible for the experimentally measured values [130-135]

Additional complications arise when enzymes are simulated in (mixtures of) non-aqueous solvents as is common practice in the study of membrane proteins and industrially interesting biocatalytic processes. Alkane/aqueous two-phase systems have been studied extensively both experimentally and theoretically. The calculated solvation free energies can be decomposed in their respective enthalpic and entropic contributions and compared with the experimentally determined quantities. This constitutes a compelling test for hydrophobic solvation models. Gallichio and coworkers studied small systems [136]. They observed partial cancellation of errors in both entropic and enthalpic contributions resulting in a relatively small error in the hydration free energy of methane

(2.0 kcal.mol<sup>-1</sup>). In general, hydration free energies calculated for the *n*-alkanes (C<sub>1</sub> – C<sub>6</sub>) were found too large by 0.5–1.0 kcal.mol<sup>-1</sup>. Examples of simulations of proteins in non-aqueous solvents are the study of the structure and dynamics of subtilisin in CCl<sub>4</sub> [137], in DMF and DMF/water mixtures [138] and chymotrypsin in hexane [139].

## 4.5 Validation and accuracy of simulations

### 4.5.1 Free energy of binding

An important criterium to validate the accuracy of molecular dynamics simulations is the calculation of the free energy of a system. Although, calculation of the *absolute* free energy is only feasible for the smallest of systems, free energy differences can be readily obtained. Various methods have been applied, ranging from theory-based free energy perturbation (FEP) methods [140] (slow) via linear interaction energy (LIE) methods [141] (faster) to fast, but theoretically less well-embedded empirical scoring schemes [142]. In any case, results of these methods should be considered with caution as even for the more rigorously defined FEP methods significant and fundamental errors have been reported. Simulation conditions have been known to play an important role [143,144]. Recently, newly developed methods, using MD in combination with solvation models, have been reported to give promising results [145-147].

An important aspect of enzyme catalysis is the formation of the Michaelis complex. Although, theoretical and practical aspects have been thoroughly studied, considerable controversy still exists regarding the basic issues [148,149]. A point of discussion is the magnitude of the loss of translational and rotational entropy upon association. Table III provides a compilation of experimental and computed data of binding affinities.

While calculated binding free energy values have been found to be in good agreement with experimental values ( $\Delta E_{\text{exp-calc}} \sim 1\text{-}2$  kcal.mol<sup>-1</sup>), this is not true for all entries. Even within series of similar ligands discrepancies are found. Obviously, these calculations are sensitive to a number of parameters. Electrostatic effects introduced by changes in the salt concentration have been observed in the binding of anthracycline antibiotics to DNA [156]. Exceptionally accurate binding energies have been calculated by Noskov and coworkers for two complexes of which high-resolution X-ray structures of both the ligand-free and ligand-bound proteins were available [151]. Using an intricate thermodynamic cycle gas-phase protein-protein interactions were separated from

**Table III.** Calculated binding free energies vs. experimental values.

| <b>System</b>   | <b>calc.</b>                                     | <b>exptl.</b> | <b>ref.</b>        |
|---|--|---------------|--------------------|
| <b><i>trypsin</i></b>                                     | binding free energy                              |               |                    |
| BPTI  | -15.7  | -18.1         | [150] <sup>a</sup> |
| BPTI  | -18.6  |               | [151]              |
| CMTI-1  | -21.8  | -14.4         | [150] <sup>a</sup> |
| Dmc-azaOrn-ONp  | -5.5   | -2.3          | [150] <sup>a</sup> |
| Dmc-azaLys-ONp  | -6.0   | -5.2          | [150] <sup>a</sup> |
| <b><i>hen egg-white lysozyme</i></b>                      |  |               |                    |
| Fv region of mouse<br>monoclonal antibody D1.3            | -9   | -11.4         | [152]              |
|   | -11.4  |               | [151]              |
| <b><i>BIV mutant Tat peptides-TAR<br/>RNA complex</i></b> | rel. free energies of binding                    |               | [153]              |
| Ile-79Ala/Val/Tyr   | 2.1/4.9/4.8                                      | 1.5/0.9/0.6   |                    |
| <b><i>MHC class I protein-peptide<br/>complexes</i></b>   | binding free energy.<br>(rel. FE in parentheses) |               | [154]              |
| H-2K/SEV-9  | -11.7  | -22.0         |                    |
| H-2K/VSV-8  | -11.5 (0.2)                                      | -26.4 (-4.4)  |                    |
| H-2K/OVA-8  | -11.4 (0.3)                                      | -26.1 (-4.1)  |                    |
| HLA-A2/HBV-10   | -11.6  | -40.6         |                    |
| HLA-A2/FLU-9  | -11.2 (0.4)                                      | -39.3 (1.3)   |                    |
| HLA-A2/TAX-9  | -10.9 (0.7)                                      | -41.3 (-0.7)  |                    |
| HLA-A2/RT-9   | -9.0 (2.6)                                       | -44.5 (-3.9)  |                    |
| HLA-A2/GP-9   | -8.9 (2.7)                                       | -40.0 (0.6)   |                    |
| <b><i>biotin</i></b>                                      |  |               | [155]              |
| streptavidin  | -16.6  | -18.3         |                    |
| <b><i>DNA</i></b>   |  |               | [156]              |
| daunomycin  | -9.4   | -11.5         |                    |
| adriamycin  | -9.9 (-0.5)                                      | -11.9 (-0.4)  |                    |
| hydroxyrubicin I  | -7.4 (2.0)                                       | -3.6 (7.9)    |                    |
| hydroxyrubicin II   | -7.4 (2.0)                                       | -9.7 (1.8)    |                    |
| 9-deoxyadriamycin   | -8.8 (0.6)                                       | -11.0 (0.5)   |                    |
| adriamycinone   | -6.3 (3.1)                                       | 2.7 (13.2)    |                    |

Table III. (continued)

|                       |       |       |       |
|-----------------------|-------|-------|-------|
| <b>Cathepsin D</b>    |       |       | [157] |
| EHMA                  | -11.5 | -11.7 |       |
| FHSA                  | -12.9 | -11.4 |       |
| (S)-EHD               | -9.8  | -9.8  |       |
| (R)-EHD               | -5.7  | >-7.3 |       |
| FHA                   | -8.7  | -9.1  |       |
| <b>HIV proteinase</b> |       |       | [158] |
| acetylpepstatin       | -8.0  | -10.2 |       |
| pepstatin             | -7.3  | -8.7  |       |
| DMP 323               | -10.4 | -13.1 |       |

a) Model C in [150]

protein-solvent and solvent-solvent interactions. This allowed calculation of the gas-phase entropy, a contribution that is not easily accessible in the solvent phase. Decomposition of the free energy of protein-protein interactions into its components showed the importance of the translational, rotational and vibrational entropy terms.  $T\Delta S^{(trans+rot)}$ -values were found to be of similar magnitude as electrostatic ( $\Delta G^{elec}$ ) and van der Waals ( $\Delta E^{vdW}$ ) contributions. The change in vibrational entropy ( $T\Delta S^{vib}$ ) can either favor or oppose binding as has been noted for the complexation of D1.3-HEL and trypsin-BPTI and is sensitive to the 3D-structure of the protein. Noteworthy, the use of decomposition schemes to assign the calculated free energy changes to particular atoms, residues or even energetic terms has been critically addressed by the group of van Gunsteren [159,160]. Although this criticism may be formally correct, decomposition schemes are helpful to identify important interactions and serve as a guide in further studies.

#### 4.5.2 Catalytic reaction

Enzymes do not just bind molecules, they also convert them into chemically different entities. Inclusion of (part of) the protein environment is an absolute requirement for a proper description of enzyme catalysis. In computational work on the characterization of hydride transfer in dihydrofolate reductase it was observed that force constants became smaller when moving from simple organic models *in vacuo* to models including the

protein environment and the solvent [161]. The protein appears to dampen the unproductive vibrations while enhancing the vibrations leading to the formation of the TS. Whereas the main source of enzyme proficiency appears to reside in the ability to lower the enthalpy of activation, entropic contributions are important as well. Although, they are difficult to calculate [162], they should not be neglected. Examples have been described for the deamination of 5,6-dihydrocytidine by cytidine deaminase [163] and hydride transfer in lactate dehydrogenase [164].

Force field methods are not well suited to simulate bond breaking and bond formation processes involved in enzyme catalysis. Quantum molecular dynamics methods, on the other hand, are not suited for long-time simulations. Empirical Valence Bond (EVB) theory [165], MD with quantum transitions (MDQT) [166,167], and IMOMM [168] are methods that have been designed to cope with this problem.

A conceptually simple approach is the use of a combined quantum mechanical and molecular mechanical procedure [169-171]. While simulating part of the enzyme, i.e. the more interesting active site region, by a quantum mechanical (QM) method, a molecular mechanics (MM) description is used to calculate the remaining interactions. A complication in these hybrid QM/MM methods is the treatment of the frontier orbitals interfacing the two parts of the system. Karplus and coworkers [172] compared two approaches addressing this problem, the "link atom" method and the "local self-consistent field" formalism. For the systems tested, tripeptides and small organic molecules, both approaches were found to be of similar accuracy provided that care was taken in the choice of the surface dividing the QM and MM region. Long-range electrostatic interactions, extending over the two parts, remain a source of error. Still, good results have been obtained using QM/MM methods, providing a better understanding of the atomic and electronic interactions responsible for enzyme catalysis [173-175]. A comparison of experimental and calculated activation barriers is presented in Table IV.

**Table IV.** Calculated activation free energies vs. experimental values. (T=300 K)

| <b>System</b>  | <b>calc.</b> | <b>exptl.</b> | <b>ref.</b> |
|--|--------------|---------------|-------------|
| <i>electrocyclic ring opening of cyclobutene</i>                         | 37.6         | 32.9          | [49]        |
| <i>phenyl ester cleavage</i>   | 18.7         | 18.6          | [176]       |
| <i>CH<sub>4</sub>+OH</i>   | 3.4/3.8      | 3.9           | [177]       |
| <i>DHFR<sup>a</sup> hydride transfer</i>                                 | 25.69/23.41  |               | [161]       |
| <i>2-phospho-D-glycerate --&gt; phosphoenolpyruvate by yeast enolase</i> | 14.4-16.8    | 15.0          | [178]       |
| <i>methyl transfer by catechol O-methyltransferase</i>                   | 24.5         | 18.0          | [179]       |
| <i>Chorismate mutase</i>   | 20.6         | 15.4          | [180]       |
| <i>proton transfer in TIM<sup>b</sup></i>                                | 21.9         | 14.0          | [181]       |
| <i>aliphatic hydrogen abstraction by citrate synthase</i>                | 15.4         | 14.6-14.8     | [182]       |

a) dihydrofolate reductase; b) triose phosphate isomerase

#### 4.5.3 Enantioselectivity

The ability to discriminate between the enantiomers of a chiral substrate is a feature of enzymes that is of both fundamental and practical interest. In particular, many industrial applications of enzymes in biocatalytic processes rely on this property for the synthesis of enantiomerically pure fine chemicals [183,184]. The intrinsic enantioselectivity of an enzyme is defined as the ratio of the specificity constants for the *R*- over the *S*-enantiomer, the enantiomeric ratio, *E*-value:

$$E = (k_{cat} / K_M)^R / (k_{cat} / K_M)^S \quad (8)$$

As discussed more fully in the following chapters, introduction of the Eyring TST expression, Eq. 3, allows the *E*-value to be expressed as the Gibbs free energy difference between the diastereomeric transition states for the reaction of the *R*- and *S*-enantiomer, Eq. 9 [185-187].

$$E = -RT \ln \Delta_{R-S} \Delta G^\ddagger \quad (9)$$

Although, the contribution of entropic differences,  $\Delta G^\ddagger = \Delta H^\ddagger - T\Delta S^\ddagger$ , is in general not negligible [188], *E*-values have been estimated using molecular modeling techniques by comparing the force field energies of the respective transition states [189-193]. The force field energy,  $\Delta V_{pot}$  appears to afford a reasonable estimate of  $\Delta H^\ddagger$ , mainly because of

cancellation of errors. Accordingly, observed accuracies in the calculated  $E$ -values must be considered fortuitous [189].

#### 4.5.4 Kinetic isotope effects

An important tool in the elucidation of enzyme reaction mechanisms is the substitution of atoms of the reacting system by their isotopes. Changes in the reaction rates originating from these substitutions are described as kinetic isotope effects (KIEs). KIEs provide information on changes in the vibrational frequencies during the proposed reaction mechanism and hence the potential energy surface of the ground- and transition states. Calculation of the (harmonic) force constants of these vibrations allows computation of theoretical KIEs applying the Bigeleisen equations [194]. However, due to the anharmonicity of the energy surface, calculated frequencies are generally 10% too high [49]. It is common practice to scale the frequencies calculated by *ab initio* methods by an empirical factor depending on the applied method [46]. Tunneling effects may also have to be included. Still: *“Comparison of calculated KIEs with experimental values provide a very stern test, and their use provides a very strong anchor to prevent theoretical modelling from drifting into unreality”* [195]. Calculated and experimental kinetic isotope effects for a selected set of examples are collected in Table V. An interesting combination of kinetic isotope effects and enantioselectivity is presented in Chapter 5

#### 4.5.5 Electron transfer in enzymes

Redox reactions play an important role in biology. The conversion of solar radiation into chemical energy by the photosynthetic systems and the redox reactions of the respiratory pathways constitute prime examples. Despite the proteins over-all insulating character, electron transfer, ET, is a common process in redox enzymes. The influence of the protein environment on ET has been studied using site-directed mutagenesis. ET kinetics is generally described in the context of Marcus theory [201-203]. For turnover rates of redox enzymes of  $10^2 - 10^3 \text{ s}^{-1}$ , transfer of electrons in proteins is still feasible over distances of 10 to 20 Å [204].

The role of the protein environment in the coupling between the two electronic states has been subject to debate [205-208]. Whereas several researchers [209-213] proposed the existence of ‘electron transfer pathways’ within the protein (‘through-bond’ model),



**Table V.** Calculated KIEs for selected systems vs. experimental values.

| <b>System</b>  | <b>calc.</b>   | <b>exptl.</b>  | <b>ref.</b> |
|--|--|--|-------------|
| hydride transfer in glutathione reductase  | 4.14/4.15<br>7.21/7.31   | 3.99±0.13<br>7.26±0.34   | [196]       |
| hydrolysis of <i>p</i> -nitrophenyl-N-acetylneuraminide;<br>Influenza B and <i>S. typhimurium</i> (in<br>parentheses) sialidases.<br><i>pro-R</i> <sup>2</sup> H, <i>pro-S</i> <sup>2</sup> H, β- <sup>2</sup> H <sub>2</sub> , lg <sup>18</sup> O,<br>respectively. | 1.024 (1.037)<br>1.142 (1.083)<br>1.177 (1.128)<br>1.047 (1.041) | 1.035 ±0.010<br>(1.051 ±0.011)<br>1.058 ±0.006<br>(1.050 ±0.014)<br>1.087 ±0.015<br>(1.097 ±0.017)<br>1.045 ±0.021<br>(1.050 ±0.010) | [195]       |
| <sup>15</sup> N KIE on hydride transfer formate to NAD <sup>+</sup>  | 1.0042   | 1.004 ±0.001   | [197]       |
| Aldol-Tischenko reaction   | 3.22/3.33  | 2.9  | [198]       |
| CH <sub>4</sub> + OH (293 K);<br><sup>12</sup> C/ <sup>13</sup> C,<br>CH <sub>4</sub> /CD <sub>4</sub> ,<br>OH/OD  | 1.033<br>4.15<br>0.83  | 1.005<br>6.75,7.49<br>0.93   | [177]       |
| benzyl alcohol → NADH  | 1.037  | 1.069  | [81]        |
| 2-phospho-D-glycerate → phosphoenolpyruvate<br>classical: TST/CVT,<br>semiclassical: TST/CVT/CVT/SCT   | 1.4/1.3<br>4.7/3.7/3.5   | 3.3  | [178]       |
| proton abstraction in glyoxalase I   | 5.0 ±1.3   | 3  | [199]       |
| mechanism of luciferase bioluminescence<br>DIE <sup>a</sup> <i>n</i> -decanal with FMNH <sub>2</sub><br>secondary KIE on electron transfer   | 1.9<br>1.88  | 1.5<br>1.9   | [200]       |

## a) deuterium isotope effect

Dutton and coworkers considered the protein to behave as an organic glass without directionality ('through-space' model) [214-216]. Observations supporting either point of view have been described [207,208,217-219]. Biological electron transfer reactions are generally considered to be non-adiabatic with weak coupling between donor and acceptor states. The rate of electron transfer,  $k_{ET}$ , is then given by Fermi's Golden Rule:

$$k_{ET} = (2\pi / \hbar) |T_{DA}|^2 (FC) \quad (10)$$

with  $T_{DA}$  the electronic tunneling matrix element between donor and acceptor and  $FC$  the

**Table VI.** Calculated midpoint potentials vs. experimental values

| <b>System</b>   | <b>calc. (mV)</b>       | <b>exptl.</b>           | <b>ref.</b> |
|---|-------------------------|-------------------------|-------------|
| <i>p</i> -benzoquinone  | 447                     | 438                     | [221]       |
| Bacteriochlorophyl ( <i>special pair</i> )  | 258                     |                         |             |
| Bacteriochlorophyl ( <i>intermediate</i> )  | 250                     | 366                     | [222]       |
| Bacteriopheophytin  | 256                     | 385                     |             |
| (I) ferredoxin ( <i>Anabaena</i> 7120)  | -1007                   | -440                    |             |
| (II) phthalate dioxygenase reductase ( <i>Ps. cepacia</i> )                                     | -812                    | -174                    | [220]       |
| $\Delta(I-II)$  | 195                     | 266                     |             |
| cytochrome $c_3$ (DvHc3; Heme I, II, III, IV)   | -272/-290/<br>-302/-242 | -274/-285/<br>-295/-248 | [223]       |
| reaction center of <i>Rh. sphaeroides</i> for different conformations of FH(M197) mutant using: |                         |                         |             |
| 1) <i>Delphi</i>  | -18 / 130 / 522 / 181   | 125 $\pm$ 10            | [224]       |
| 2) <i>Free energy perturbations</i>   | 132 / 94 / -53 / 43     |                         | [225]       |

nuclear Franck-Condon factor representing the nuclear motion associated with ET containing the standard free energy and the reorganization energy including protein and vibrational contributions. The accuracy of quantum chemical calculations of midpoint potentials is problematic. The actual configuration of the nearby amino acids has been found to play a key role in differentiating the redox potentials [220]. Some results are collected in Table VI. Application of the through-space model leads to significant discrepancies between the calculated and experimental rates (10-100 fold) [214]. The Pathways model (and its successors, [226]) of Beratan and coworkers depends on the accurate representation of the coupling matrix elements,  $T_{DA}$ .  $T_{DA}$  is taken as the product of covalent, hydrogen and through-space interactions, each with their own coupling efficiency. To convert the electronic coupling to actual ET rates usually a prefactor of  $10^{-13} \text{ sec}^{-1}$  is applied. In general, calculated ET rates still leave room for further improvement. The use of a Pathways program to obtain an educated guess for the distance and positioning of the heme and PQQ redox centers in QH-ADH homology modeling is described in Chapter 3. A comparison of calculated and experimental values for electron transfer in proteins is given in Table VII.

Molecular dynamics simulations can be of help in the description of the events occurring during electron transfer, including rearrangement of charge distributions, solvation processes and electrostatic interactions. Analysis of the interprotein ET

**Table VII.** Calculated vs. experimental electron transfer rates for selected systems.

| <b>System</b>   | <b>calc. (s<sup>-1</sup>)</b> | <b>exptl. (s<sup>-1</sup>)</b>       | <b>ref.</b> |
|---|-------------------------------|--------------------------------------|-------------|
| cyt. c <sub>2</sub> /photosynthetic reaction center   | 10 <sup>-1</sup>              | 10 <sup>7</sup>                      | [227]       |
| plastocyanin / cyt. f   | 10 <sup>1</sup>               | 3*10 <sup>3</sup> -6*10 <sup>4</sup> | [228,229]   |
| modified DNA species:   |                               |                                      |             |
| 1) [Ru(NH <sub>3</sub> ) <sub>4</sub> (py)] <sup>2+</sup> / [Ru(bpy) <sub>2</sub> (im)] <sup>3+</sup> | 1.6*10 <sup>6</sup>           | 7.1*10 <sup>6</sup>                  | [230]       |
| 2) EB <sup>+</sup> / DAP <sup>2+</sup>  | 2.5*10 <sup>6</sup>           | 2.4*10 <sup>7</sup>                  |             |
| 3) Ru(phen) <sub>2</sub> dppz <sup>2+</sup> / Rh(phi) <sub>2</sub> -phen <sup>3+</sup>                | 3.0*10 <sup>9</sup>           | 2.6*10 <sup>2</sup>                  |             |
| Ru-modified cyt. c  |                               |                                      |             |
| 1) H66  | 2.5*10 <sup>5</sup>           | 3.2*10 <sup>6</sup>                  | [231]       |
| 2) H66/F67  | 1.7*10 <sup>5</sup>           | 1.3*10 <sup>6</sup>                  |             |
| 3) H58  | 4.5*10 <sup>4</sup>           | 6.0*10 <sup>4</sup>                  |             |

reactions as a function of temperature can be helpful to unravel the kinetic complexity with regard to events coupled with ET reactions, i.e. 'gating events', changes in the nature of the rate-limiting step [232,233].

#### 4.5.6 Protein folding and homology modeling

For small molecular systems high-level computational methods can generate structures with sufficient accuracy to explain and predict properties. A state-of-the-art example is the calculation of the crystal structures of flexible hydrogen-bonded molecules [234].

For the structure of proteins and enzymes, however, one has to rely primarily on the results of X-ray crystallography, NMR spectroscopy or neutron diffraction techniques. Although, many structures have been elucidated (see current number of entries in the Protein Data Base), and additional structures become available at a high rate, there is still a need for computational efforts in this field. Whether data from X-ray crystallography faithfully represent the structure(s) of a protein in solution remains an issue [235]. Also, X-ray structures may contain spurious [236,237] as well as systematic errors, i.e. refinement procedures that bias the distribution of  $\omega$ -angles of the peptide bond to artificially narrow values [238].

As a result of ongoing sequencing projects and technical advances, protein sequences are elucidated at a pace greatly exceeding that of 3D structure elucidation. In the sequence, basically all structural and functional information for the protein is embedded. To convert sequence information into a 3D model of the protein two approaches are

commonly applied, *ab initio* and *knowledge-based* techniques. At present, accurate prediction of protein structures using first-principle approaches seems feasible only for small proteins, e.g. crambin [83]. However, the latest evaluation of the biannual Critical Assessment of Structure Prediction (CASP) meetings [<http://predictioncenter.llnl.gov>] showed an increased performance of the *ab initio* folding methods [239].

As Levinthal pointed out in his 'paradox', it would be impossible for a protein to find its way to the biologically active state via a random walk through conformation space in the allotted time [240,241]. The astronomical number of possible conformations would simply prevent it from reaching its native state in only (milli)seconds as is observed in biological systems [242]. This implies the existence of certain folding rules. Until now, however, the rules embedded in the energy landscapes of proteins [243,244] have not been disclosed, leaving us the "protein folding problem" as one of the scientific (and commercial) challenges for the next decade [245]. However, if we grant nature a certain degree of consistency, it can be assumed that a successful design is more or less retained once it has evolved. This notion is fundamental to the art of homology modeling. By identifying conserved sequence motifs proteins can be classified and compared to homologous proteins for which the structure is known, providing a lead to the structure and function of the unknown protein. Homology, however, is by no means guaranteed: "*i.* conserved amino acids are important; *ii.* very conserved amino acids are very important; *iii.* non-conserved amino acids may still be important" (G. Vriend, personal communication).

Successful attempts to construct a model of a target protein by homology modeling using the X-ray structure of a related protein as a scaffold have been reported [246-249]. Secondary structure predictions for extended sequences have appeared [250,251] while tertiary structure prediction methods reach accuracies up to 70 % [252,253]. The quality of the alignment of the sequence to the target structure is the main bottleneck to improve the quality of the models [239]. In successive CASP rounds the quality of the alignments is seen to improve in going from CASP1 (1994) to CASP2 (1996). However, from CASP3 (1998) to CASP4 (2000) only minor improvements have been reported [239,254]. Also, comparative modeling methods are not capable of predicting new folds as they rely on the sequence identity with known folds. With respect to the homology modeling efforts discussed in Chapter 2, it must be emphasized that extensive  $\beta$  structure, as in QH-ADH,

is still very difficult to predict correctly from sequence data only [239].

In an interesting study, Feig and Brooks [255] have evaluated the CASP4 predictions using energy functions. Structures similar to the native fold can be reliably distinguished from misfolded or nonfolded protein conformations using energy scoring functions in combination with implicit solvation models. The incorporation of intramolecular bonded and non-bonded energy terms as well as the free energy of solvation seems to be crucial to identify the correct conformation in the ensemble. Although protein structure predictions with a RMSD of 3-6 Å from the native topology may already provide significant detail on the function of a protein [256], better resolution is generally needed to elucidate detailed functionality, i.e. reaction mechanisms.

## 5 Molecular modeling of QH-ADH catalysis

### 5.1 Summary of topics

Alcohol dehydrogenases containing pyrroloquinoline quinone (2,7,9-tricarboxy-1*H*-pyrrolo[2,3-*f*]quinoline-4,5-dione, PQQ, Figure 2) as an organic cofactor are of fundamental and practical interest. Since their detection, a large amount of biochemical and enzymological information has been collected. The quinoprotein methanol dehydrogenases, MDHs, from methylotrophic organisms have been particularly well studied. At the start of the research described here, however, much less was known of the quino*hem*oprotein alcohol dehydrogenases (containing PQQ, Ca<sup>2+</sup> and heme *c*), of which the QH-ADH from *Comamonas testosteroni* is an example. The fundamentally interesting arrangement of redox cofactors and the potential for applications in biocatalytic kinetic resolution processes provided a strong incentive to investigate the structural and mechanistic features involved. To complement experimental data obtained earlier by wet chemistry, a computational approach was adopted. Although, this choice of strategy turned out to be demanding, it has provided exciting new insight for this class of enzymes. An overview covering (bio)chemical, enzymological, physiological, and practical aspects is given in Chapter 2.

In Chapter 3, the use of MDH as a lead structure for the PQQ-containing QH-ADHs is discussed. Based on a distinct sequence homology with the MDHs from *Methylophilus methylotrophus* W3A1 and *Methylobacterium extorquens* a 3D working model has been constructed for the QH-ADH from *C. testosteroni*. The model has been validated using biophysical and biochemical information.

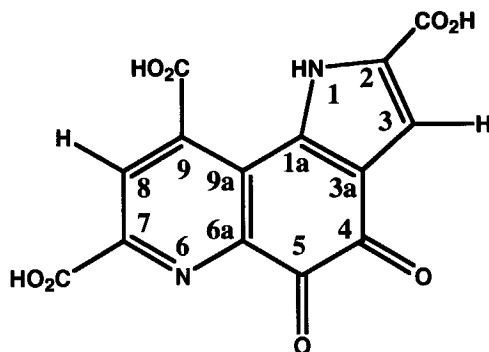


**Figure 2.** Schematic drawing of pyrroloquinoline quinone, 2,7,9-tricarboxy-1*H*-pyrrolo[2,3-*f*]quinoline-4,5-dione, PQQ

Several reaction schemes proposed for the catalytic mechanism of QH-ADHs are reviewed in relation to the constraints set by the observed enantioselectivities and reaction rates. Experimental observations are discussed in the light of the structures of MDH and homology models constructed for QH-ADHs from *C. testosteroni* and *Acetobacter pasteurianus*.

Ideas on the actual catalytic mechanism of QH-ADH from *C. testosteroni* have been pursued in Chapter 4. High-level *ab initio* calculations of probable intermediates involved in the oxidation of methanol by PQQ are described. To test the models, kinetic isotope effects have been measured for the reactions of ethanol and solketal. Enantiomerically enriched solketal and deuterium-substituted solketal mixtures were used to investigate the enantioselectivity-determining step in the catalytic reaction mechanism of QH-ADH from *C. testosteroni*. The first report of a kinetic isotope effect on enzyme enantioselectivity is included as Chapter 5.

## 5.2 Homology modeling of QHADH from *C. testosteroni*

It should be emphasized that the research reported here has been carried out while the X-ray structure determination of QH-ADH seemed at a standstill. Although efforts to crystallize and elucidate the structure started back in the 90-s [257], prohibitive problems were encountered, that have only recently been solved [258]. More or less at the same time, a second structure, QH-ADH from *Pseudomonas* HK5, has been reported [259]. Since these structures provide the opportunity for an unbiased validation of the results of

the homology modeling project, a preliminary comparison of the modeled and experimentally determined structure seems appropriate.

### **PQQ-domain**

The homology model for the PQQ-domain of QH-ADH from *C. testosteroni* has been constructed using the X-ray structures of *Methylophilus methylotrophus* W3A1 (pdb code 3AAH) [260-262] and *Methylobacterium extorquens* [263]. Approx. 34% sequence identity was found for QH-ADH and the  $\alpha$ -subunit of the MDH's. The structures are displayed in Figure 3. The RMSD values between the different structures for the  $C_{\alpha}$  atoms are shown in Table VIII. The procedure used for the construction of the 3D-working model is described in more detail in Chapter 3.

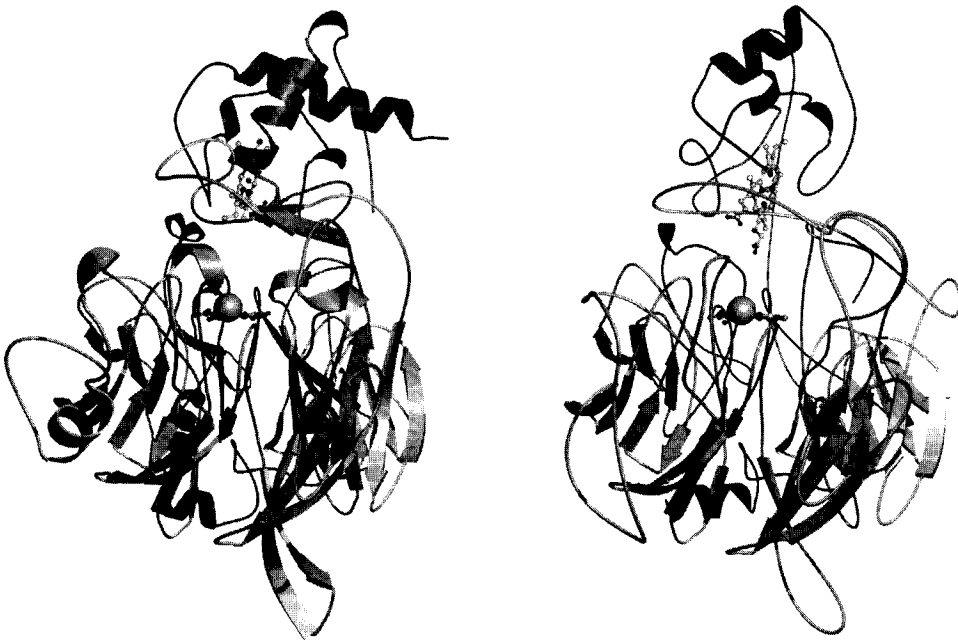


**Figure 3.** Schematic drawings of the X-ray structure (left, PDB entry 1KB0) and the model (right) of QHADH from *C. testosteroni*. Secondary structure elements were detected using an automated procedure (MolAuto [264]). Heme (top of picture), calcium ion and PQQ (behind  $Ca^{2+}$  ion) are shown in ball-and-stick representation, using the van der Waals radius for the calcium ion. The picture was generated using MolScript [264] and PovRay ([www.povray.org](http://www.povray.org)).

**Table VIII.** RMSD values calculated for the C<sub>α</sub>-atoms (in Å)

|      | 4AAH | model |
|------|------|-------|
| 1KB0 | 1.5  | 1.4   |

As the MDH structure served as the template, similar RMSD values for MDH and the model were anticipated, i.e. WYPIIWYGO ('what you put in is what you get out'). The size of the RMSD values is similar to the values obtained for X-ray structures after molecular dynamics simulations [159]. However, the smaller RMSD value obtained for the model shows that during unrestrained minimization and dynamics simulations the molecule adopts a structure more resembling the PQQ domain of the *real* QHADH than that of the template structure.

This certainly has to be considered to be fortuitous. The overall identity of the *C. testosteroni* and the *M. W3A1* sequence is relatively low and upon closer inspection many residue side chains in the model show an incorrect orientation.

The presence of a hydroxy-tryptophan has, of course, been completely missed in the model building procedure. It came as a surprise for the crystallographers as well [258]. Still, the relatively moderate numbers for the RMSD values show that the model behaved nicely during the optimization routines used to generate the overall folding.

More interesting is the comparison of the active site configurations. As can be inferred from Figure 4, the resemblance is rather good. In Table IX distances between PQQ, Ca<sup>2+</sup> and selected active site residues are compared for the X-ray structure and the model. The coordination of the Ca<sup>2+</sup> ion to the PQQ has been captured by the model quite well. Only minor deviations between the distances in the X-ray structure and the model are found (maximum deviation 0.16 Å).

Inspection of the distances of the ligands in the Ca<sup>2+</sup> coordination sphere shows the overall active site of the model to be somewhat larger. In the model Trp267 has wedged itself between Glu185 and Asn263 resulting in a widening of the active site close to the Ca<sup>2+</sup> ion. In the X-ray structure Lys335 is even better positioned for a projected role in the reaction mechanism. Due to an error in the alignment Trp479 has been positioned wrongly in the model. Alignment of two adjacent glycines was given precedence over proper alignment of a single tryptophan residue. The improper positioning of this residue



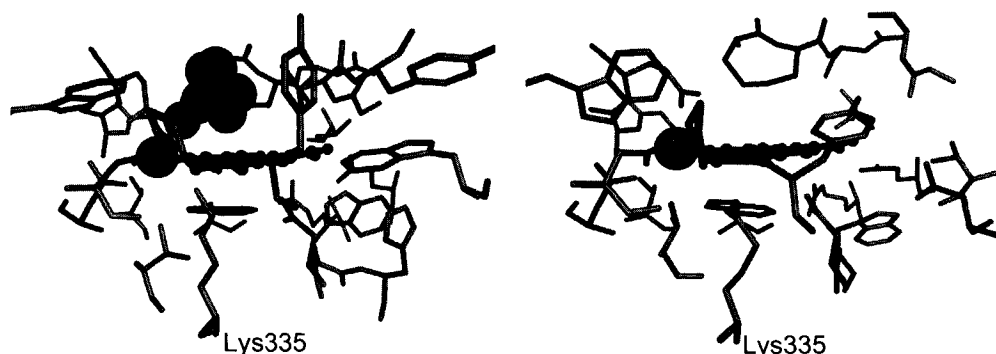


**Figure 4.** Schematic drawing of the active sites of the X-ray structure (left, PDB entry 1KB0) and the homology model (right) of the QHADH from *C. testosteroni*. PQQ is shown in a ball-and-stick representation, calcium as a ball at 0.5 times its van der Waals radius. Trp439 (below the plane of PQQ) and the disulfide ring (Cys103-Cys104, above the PQQ) are colored black. The tetrahydrofuran moiety found in the X-ray structure is shown in CPK representation. The picture was generated using [264] and PovRay ([www.povray.org](http://www.povray.org)).

**Table VII.** Distances between PQQ, Calcium and selected residues in QHADH structures.

| Atom 1    | Atom 2           | distance (Å) |       | Atom 1    | Atom 2           | distance (Å) |       |
|-----------|------------------|--------------|-------|-----------|------------------|--------------|-------|
|           |                  | 1KB0         | Model |           |                  | 1KB0         | Model |
| PQQ(O7A)  | Ca <sup>2+</sup> | 2.42         | 2.38  | D308(OD2) | Ca <sup>2+</sup> | 3.89         | 4.58  |
| PQQ(N6)   | Ca <sup>2+</sup> | 2.5          | 2.34  | K335(NZ)  | PQQ(O4)          | 2.88         | 3.22  |
| PQQ(O5)   | Ca <sup>2+</sup> | 2.53         | 2.51  | K335(NZ)  | PQQ(O5)          | 2.72         | 3.13  |
| PQQ(C5)   | Ca <sup>2+</sup> | 3.39         | 3.24  |           |                  |              |       |
| N263(OD1) | Ca <sup>2+</sup> | 2.38         | 3.76  | T310(OG1) | Ca <sup>2+</sup> | 6            | 3.42  |
| E185(OE1) | Ca <sup>2+</sup> | 2.44         | 3.14  | T310(OG1) | PQQ(O5)          | 4.86         | 3.31  |
| E185(OE2) | Ca <sup>2+</sup> | 2.55         | 3.3   | T310(OG1) | N263(OD1)        | 5.56         | 2.72  |
| D308(OD1) | Ca <sup>2+</sup> | 2.66         | 3.42  | T310(OG1) | D308(OD1)        | 5.87         | 2.71  |

could have consequences for the selectivity observed for QH-ADH. Yet, the conclusions drawn on the basis of the homology model concerning the probable reaction mechanism of QHADHs retain their validity. The role of Lys335 needs to be explored, as the presence of this residue in QHADHs and the absolute requirement of ammonia in the reaction catalyzed by related MDHs that lack a basic residue at the corresponding position, implies a functional role in the reaction mechanism of QHADH.

**Heme-domain**

At a first glance the cytochrome *c* domain of the model structure seems completely wrong (Figure 5A-C). This is not surprising considering the problems encountered during construction of this domain. No X-ray structure was available that could serve as a reliable template. Low sequence identity (approx. 20%) was found for a published sequence sharing minor resemblance to an X-ray structure that was already deemed suspicious at the time (and had been retracted from public databases).

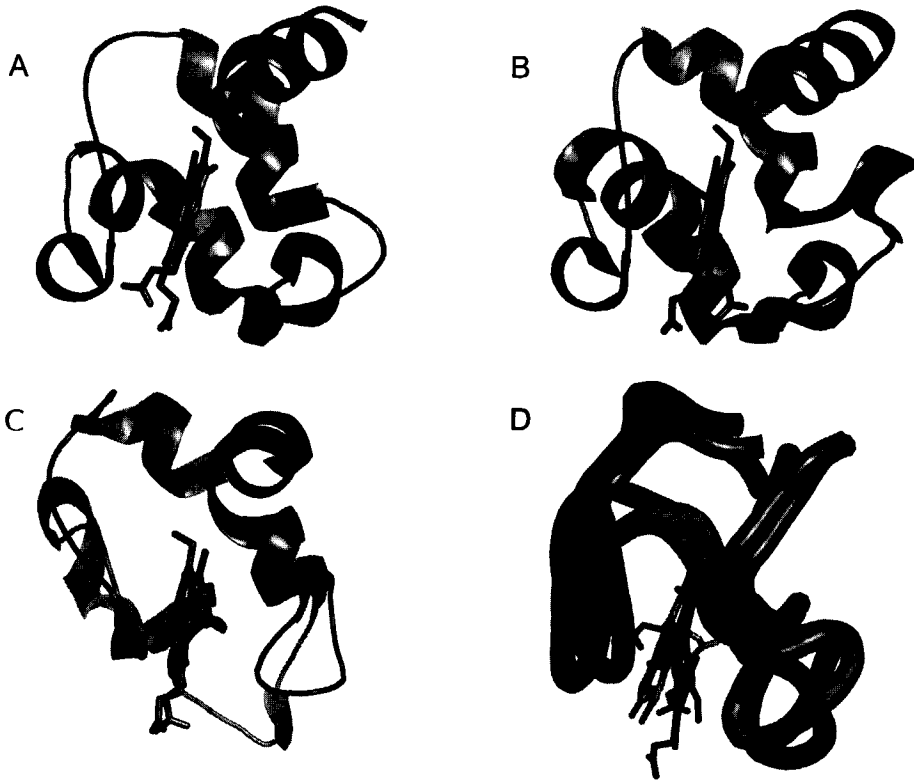


**Figure 5.** Drawing of the cytochrome *c* domains of the X-ray structures from (A) *Comamonas testosteroni* (PDB entry 1KB0), (B) *Pseudomonas putida* (PDB entry 1KV9) and (C) the homology model. (D) shows an overlay of the cytochrome *c* domains after extensive smoothing of the C $_{\alpha}$ -trace. Homology model shown in darker shadings. Haem shown in stick representation. Picture generated using Swiss-PdbViewer [265] ([www.expasy.org/spdbv](http://www.expasy.org/spdbv)) and Pymol ([pymol.sourceforge.net](http://pymol.sourceforge.net)).

Interestingly, after smoothing of the  $C_{\alpha}$ -trace, the cytochrome *c* domains show remarkable structural similarity (Figure 5D). The heme moiety shows a 90 degrees rotation compared to the X-ray structure. During the modeling procedure it was assumed that the propionate groups of the heme would point in the direction of the PQQ-domain. The X-ray structure shows this not to be the case and one might speculate about the role of the propionate groups as possible sites of interaction for electron transferring proteins (or artificial electron acceptors, i.e. ferricyanide) within the respiratory chain.

Our main interest at the time, concerning the cytochrome *c* domain, was its position relative to the PQQ-domain and the consequences for the intramolecular electron transfer reaction. From Figure 6 and Table X it is clear that we were successful in this respect. The tilting angle ( $\pm 70$  degrees), as inferred from the optical experiments by Huizinga et al, is closely matched as are the main heme-PQQ distances.

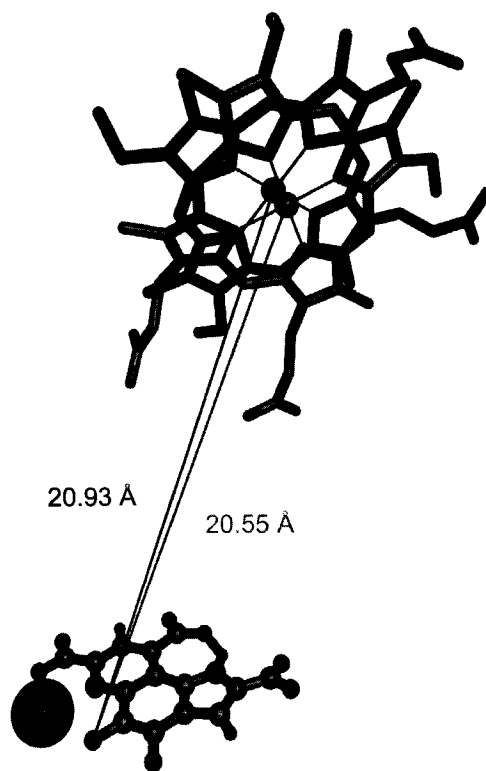


**Figure 6.**

Distance between haem and PQQ-O(5) as found in the X-ray structure (dark gray, PDB entry 1KB0) and the homology model (in light gray) of QHADH from *C. testosteroni*. Heme shown in stick representation, PQQ as ball and sticks,  $Ca^{2+}$  ion as ball using 0.5 times its van der Waals radius. Picture was generated using MolScript [264] and PovRay ([www.povray.org](http://www.povray.org)).

**Table X.** Distances between PQQ and heme moieties for QHADH

|                              | <i>X-ray</i> |          | <i>Model</i> |             |
|------------------------------|--------------|----------|--------------|-------------|
|                              | Heme-PQQ     | dist (Å) | Heme-PQQ     | dist (Å)    |
| shortest                     | HBC2-O9B     | 12.05    | O1D3-O2A     | 9.73        |
| shortest between heavy atoms | CBC-O9B      | 13.11    | <i>idem</i>  | <i>idem</i> |
| shortest between rings       | C3C-N1       | 15.12    | C3D-C2       | 14.82       |
| HEM(Fe) - PQQ(O5)            |              | 20.93    |              | 20.55       |

It can be concluded that the construction of the homology model has paid off. Although superseded by the X-ray structure, the model has played a major role in our understanding of the mechanistic aspects of the enantioselective oxidation of chiral alcohols by this interesting enzyme. It is highly rewarding to see that the model did not deviate too much with respect to the essential features of the enzyme, i.e. the active site structure and the relative positioning of the heme moiety. It indicates that computational chemistry protocols are indeed capable of providing reasonably accurate and instructive structural models at relatively short timescales.

## 6 Conclusions and prospects

Many examples documenting both successes and failures of computational methods have been reported. In general, *ab initio* methods are not yet capable of reaching the desired accuracy to predict absolute reaction rates and binding energies. Geometrical features are, however, quite accurately reproduced and predicted in most cases. Molecular systems involving weak interactions, i.e. hydrogen-bonding and metal-ligation, are described with varying success and often require additional calibration. Energy-related properties are calculated with considerably less accuracy, unless extensive parameterization is applied using available experimental data. However, extrapolation using these empirical methods is not guaranteed to be successful and experimental verification and validation remains a necessity.

The heterogeneity of the bulk protein presents a challenge for the accurate calculation of many biochemically interesting features. Using approximation methods, experimental values can be more or less accurately reproduced. Solvent effects are acknowledged as an important aspect in molecular modeling. The extra degrees of freedom are dealt with using explicit or implicit incorporation of these effects. The recent increase in

computational hard- and software further stimulates the use of computational methods.

This introduction has focused on the accurate prediction of properties of individual molecules and the interaction with their substrates. However, in the cell intricate arrays of proteins and other biomolecules interact and determine the events. The concentration and location of proteins at certain points in time appear to be at least as important as their individual characteristics. To obtain a comprehensive picture of such a complex system, the traditional view of proteins may have to be set aside. No longer can proteins be regarded as isolated and independent entities. Their role in large protein networks has to be analysed. The study of these intertwined protein networks will become a hot topic in the near future. Analytical tools have become available recently [266]. The study of protein networks is largely depending on bioinformatics, i.e. the analysis of sequence and genomic information available within the various databases. With the completion of the various genome-sequencing projects, a large amount of data has become available. The observation that various species have a similar number of genes and a similarity in the sequences of these genes, suggests an important role for the study of protein interactions rather than the properties of the individual proteins to explain the observed species differences. Computational techniques already play an important role in the analysis of these data. Mathematical models can be designed to model important interactions of the individual proteins or protein modules as 'black boxes'. However, only when we understand and can predict the intricate interactions between proteins and their substrates and ligands, can we model and predict phenomena as complex and important as the human heart in full atomic detail [267]. The predictive power of computational techniques has not yet been fully exploited. There is little doubt that *ab initio* calculations on protein structures and enzyme catalysis will become feasible in the near future. However, the accuracy of the computational methods on an absolute scale has to improve considerably in order to calculate the small, but important energetic differences that determine the properties of enzymes and proteins. Nevertheless, computational chemistry has already proven to be a unique tool to complement traditional experimental techniques with respect to understanding, explaining and prediction of biochemical phenomena.

## References

- (1) Hoffmann, R.; Minkin, V. I. and Carpenter, B. K.; *HYLE-Int. J. Philosophy of Chem.*, **3** (1997), 3-28.
- (2) Wilson, E. K.; *CENEAR*, **78** (2000), 39-45.
- (3) Summerfield, J. H.; Beltrame, G. S. and Loeser, J. G.; *J. Chem. Ed.*, **76** (1999), 1430-1438.
- (4) Jencks, W. P.; *Catalysis in chemistry and enzymology*; Dover Publications, Inc.: New York, 1987.
- (5) Radzicka, A. and Wolfenden, R.; *Science*, **267** (1995), 90-93.
- (6) Cannon, W. R. and Benkovic, S. J.; *J. Biol. Chem.*, **273** (1998), 26257-26260.
- (7) Cleland, W. W.; *Biochim. Biophys. Acta*, **67** (1963), 173-187.
- (8) Cleland, W. W.; *Biochim. Biophys. Acta*, **67** (1963), 188-196.
- (9) Cleland, W. W.; *Biochim. Biophys. Acta*, **67** (1963), 104-137.
- (10) Lightstone, F. C.; Zheng, Y.-J. and Bruice, T. C.; *J. Am. Chem. Soc.*, **120** (1998), 5611-5621.
- (11) Menger, F. M.; *Acc. Chem. Res.*, **18** (1985), 128-134.
- (12) Menger, F. M.; *Acc. Chem. Res.*, **26** (1993), 206-212.
- (13) Mesecar, A. D.; Stoddard, B. L. and Koshland, D. E.; *Science*, **277** (1997), 202-206.
- (14) Houk, K. N.; Tucker, J. A. and Doigo, A. E.; *Acc. Chem. Res.*, **23** (1990), 107-113.
- (15) Cleland, W. W.; Frey, P. A. and Gerlt, J. A.; *J. Biol. Chem.*, **273** (1998), 25529-25532.
- (16) Chen, J.; McAllister, M. A.; Lee, J. K. and Houk, K. N.; *J. Org. Chem.*, **63** (1998), 4611-4619.
- (17) Klinman, J. P.; *TIBS*, **14** (1989), 368-373.
- (18) Bahnson, B. J.; Park, D. H.; Kim, K.; Plapp, B. V. and Klinman, J. P.; *Biochemistry*, **32** (1993), 5503-5507.
- (19) Jonsson, T.; Edmondson, D. E. and Klinman, J. P.; *Biochemistry*, **33** (1994), 14871-14878.
- (20) Kohen, A.; Cannio, R.; Bartolucci, S. and Klinman, J. P.; *Nature*, **399** (1999), 497-4499.
- (21) Sutcliffe, M. J. and Scrutton, N. S.; *TIBS*, (2000), 405-408.
- (22) Zheng, Y. J. and Bruice, T. C.; *J. Am. Chem. Soc.*, **119** (1997), 8137-8145.
- (23) Ash, E. L.; Sudmeier, J. L.; De Fabo, E. C. and Bachovchin, W. W.; *Science*, **278** (1997), 1128-1132.
- (24) Garcia-Viloca, M.; Gelabert, R.; González-Lafont, A.; Moreno, M. and Lluch, J. M.; *J. Am. Chem. Soc.*, **120** (1998), 10203-10209.
- (25) Schiøtt, B.; Iversen, B. B.; Madsen, G. K. H. and Bruice, T. C.; *J. Am. Chem. Soc.*, **120** (1998), 12117-12124.
- (26) Tuckerman, M. E.; Marx, D.; Klein, M. L. and Parrinello, M.; *Science*, **275** (1997), 817-820.
- (27) Warshel, A.; Papazyan, A. and Kollman, P. A.; *Science*, **269** (1995), 102-106.
- (28) Warshel, A. and Papazyan, A.; *Proc. Natl. Acad. Sci. USA*, **93** (1996), 13665-13670.
- (29) Mulholland, A. J.; Lyne, P. D. and Karplus, M.; *J. Am. Chem. Soc.*, **122** (2000), 534-535.
- (30) Eyring, H.; *J. Chem. Phys.*, **3** (1935), 107-115.
- (31) Truhlar, D. G.; Hase, W. L. and Hynes, J. T.; *J. Phys. Chem.*, **87** (1983), 2664-2682.
- (32) Truhlar, D. G.; Garrett, B. C. and Klippenstein, S. J.; *J. Phys. Chem.*, **100** (1996), 12771-12800.
- (33) Machado, S. S.; Jongejan, A.; Geerlof, A.; Jongejan, J. A. and Duine, J. A.; *Biocat. Biotrans.*, **17** (1999), 179-207.
- (34) Overbeeke, P. L. A.; Jongejan, J. A. and Heijnen, J. J.; *Biotech. Bioeng.*, **70** (2000), 278-290.
- (35) Pham, V. T.; Phillips, R. S. and Ljungdahl, L. G.; *J. Am. Chem. Soc.*, **111** (1989), 1935-1936.

- (36) Pople, J. A.; *Angew. Chem. Int. Ed.*, **38** (1999), 1894-1902.
- (37) Handy, N. C. and Lee, A. M.; *Chem. Phys. Lett.*, **252** (1996), 425-430.
- (38) Atkins, P. W. and Friedmann, R. S.; *Molecular Quantum Mechanics*; 3rd ed.; Oxford: New York, 1997.
- (39) Foresman, J. B. and Frisch, A.; *Exploring Quantum Chemistry with Electronic Structure Methods*; Gaussian Inc.: Pittsburgh, 1995-1996.
- (40) Chipot, C.; Millot, C.; Maigret, B. and Kollman, P. A.; *J. Phys. Chem.*, **98** (1994), 11362-11372.
- (41) Flad, H.-J. and Dolg, M.; *J. Phys. Chem.*, **107** (1997), 7951-7959.
- (42) Montgomery, J. A.; Frisch, M. J.; Ochterski, J. W. and Petersson, G. A.; *J. Chem. Phys.*, **110** (1999), 2822-2827.
- (43) Smith, D. M.; Nicolaidis, A.; Golding, B. T. and Radom, L.; *J. Am. Chem. Soc.*, **120** (1998), 10223-10233.
- (44) Takashima, H.; Kitamura, K.; Tanabe, K. and Nagashima, U.; *J. Comput. Chem.*, **20** (1999), 443-454.
- (45) Tschinke, V. and Ziegler, T.; *Density Matrices and Density Functionals*; Reidel: Dordrecht, 1987.
- (46) Young, D.; *Computational Chemistry: A Practical Guide for Applying Techniques to Real World Problems*; John Wiley & Sons: 2001.
- (47) Barea, G.; Maseras, F. and Lledós, A.; *Int. J. Quantum Chem.*, **85** (2001), 100-108.
- (48) Jensen, F.; *J. Phys. Chem.*, **1110** (1999), 6601-6605.
- (49) Wiest, O.; Montiel, D. C. and Houk, K. N.; *J. Phys. Chem. A*, **101** (1997), 8378-8388.
- (50) Kutzelnigg, W.; *Theor. Chim. Acta*, **68** (1985), 445-469.
- (51) Kutzelnigg, W. and Klopper, W.; *J. Chem. Phys.*, **94** (1991), 1985-2001.
- (52) Yang, W. and Parr, R. G.; *Density-functional theory of atoms and molecules*; Oxford Science Publ.: Oxford, 1989.
- (53) Kohn, W.; Becke, A. D. and Parr, R. G.; *J. Phys. Chem.*, **100** (1996), 12974-12980.
- (54) Baerends, E. J. and Grietsenko, O. V.; *J. Phys. Chem. A*, **101** (1997), 5383-5403.
- (55) Curtiss, L. A.; Raghavachari, K.; Trucks, G. W. and Pople, J. A.; *J. Chem. Phys.*, **94** (1991), 7221-7230.
- (56) Curtiss, L. A.; Raghavachari, K.; Redfern, P. C.; Rassolov, V. and Pople, J. A.; *J. Phys. Chem.*, **109** (1998), 7764-7776.
- (57) Gdanzig, R. J.; *Chem. Phys. Lett.*, **283** (1998), 253-261.
- (58) He, Y.; Gräfenstein, J.; Kraka, E. and Cremer, D.; *Mol. Phys.*, **98** (2000), 1639-1658.
- (59) Braïda, B.; Hiberty, P. C. and Savin, A.; *J. Phys. Chem. A*, **102** (1998), 7872-7877.
- (60) King, R. A.; Crawford, T. D.; Stanton, J. F. and Schaefer, H. F. I.; *J. Am. Chem. Soc.*, **121** (1999), 10788-10793.
- (61) Hall, R. J.; Hillier, I. H. and Vincent, M. A.; *Chem. Phys. Rev.*, **320** (2000), 139-143.
- (62) Tsuzuki, S. and Lüthi, H. P.; *J. Chem. Phys.*, **114** (2001), 3949-3957.
- (63) Fonseca-Guerra, C.; Bickelhaupt, F. M.; Snijders, J. G. and Baerends, E. J.; *J. Am. Chem. Soc.*, **122** (2000), 4117-4128.
- (64) Rappé, A. K. and Bernstein, E. R.; *J. Phys. Chem. A*, **104** (2000), 6117-6128.
- (65) Greatbanks, S. P.; Gready, J. E.; Limaye, A. C. and Rendell, A. P.; *J. Comput. Chem.*, **21** (2000), 788-811.
- (66) Rodgers, J. M.; Fast, P. L. and Truhlar, D. G.; *J. Chem. Phys.*, **112** (2000), 3141-3147.

- (67) Cunningham, M. A.; Ho, L. L.; Nguyen, D. T.; Gillilan, R. E. and Bash, P. A.; *Biochemistry*, **36** (1997), 4800-4816.
- (68) Feller, D.; Dupuis, M. and Garrett, B. C.; *J. Chem. Phys.*, **113** (2000), 218-226.
- (69) Luna, A.; Alcami, M.; M6, O. and Y6fiez, M.; *Chem. Phys. Lett.*, **320** (2000), 129-138.
- (70) Pyykk6, P.; *Chem. Rev.*, **88** (1988), 563-594.
- (71) Visscher, L.; Styzyfiski, J. and Nieuwpoort, W. C.; *J. Chem. Phys.*, **105** (1996), 1987-1994.
- (72) Hennum, A. C.; Halkier, A. and Klopper, W.; *J. Mol. Struct.*, **599** (2001), 153-162.
- (73) Clark, T.; *J. Mol. Struct.*, **530** (2000), 1-10.
- (74) Jentzen, W.; Song, X. Z. and Shelnutt, J. A.; *J. Phys. Chem. B*, **101** (1997), 1684-1699.
- (75) Berens, P. H. and Wilson, K. R.; *J. Chem. Phys.*, **74** (1981), 4872-4882.
- (76) Ruud, K.; Åstrand, P.-O. and Taylor, P. R.; *J. Chem. Phys.*, **112** (2000), 2668-2683.
- (77) Zewail, A. H.; *J. Phys. Chem. A*, **104** (2000), 5660-5694.
- (78) Lobastov, V. A.; Srinivasan, R.; Goodson, B. M.; Ruan, C.-Y.; Feenstra, J. S. and Zewail, A. H.; *J. Phys. Chem. A*, **105** (2002), 11159-11164.
- (79) Rousse, A.; Rischel, C.; Fourmaux, S.; Uschmann, I.; Förster, E.; Gauthier, J.-C. and Hulin, D.; *RIKEN Rev.*, **33** (2001), 14-17.
- (80) Heller, E. J.; *J. Phys. Chem. A*, **103** (1999), 10433-10444.
- (81) Rucker, J. and Klinman, J. P.; *J. Am. Chem. Soc.*, **121** (1999), 1997-2006.
- (82) Karplus, M.; *J. Phys. Chem. B*, **104** (2000), 11-27.
- (83) Schäfer, L. and Cao, M.; *J. Mol. Struct.*, **333** (1995), 201-208.
- (84) Damm, W.; Frontera, A.; Tirado-Rives, J. and Jorgensen, W. L.; *J. Comp. Chem.*, **18** (1997), 1955-1970.
- (85) Weiner, P. K. and Kollman, P. A.; *J. Comp. Chem.*, **2** (1981), 287-302.
- (86) Weiner, S. J.; Kollmann, P. A.; Case, D. A.; Singh, U. C.; Ghio, C.; Alagona, G.; Profeta, S. and Weiner, P.; *J. Am. Chem. Soc.*, **106** (1984), 765-784.
- (87) Weiner, S. J.; Kollmann, P. A.; Nguyen, D. T. and Case, D. A.; *J. Comp. Chem.*, **7** (1986), 230-252.
- (88) Brooks, B. R.; Brucclori, R. E.; Olafson, B. D.; States, D. J.; Swaminathan, S. and Karplus, M.; *J. Comp. Chem.*, **4** (1983), 187-217.
- (89) MacKerrell, A. D.; Bashford, D.; Bellott, M.; Dunbrack, R. L.; Evanseck, J. D.; Field, M. J.; Fischer, S.; Gao, J.; Guo, H.; Ha, S.; Joseph-MacCarthy, D.; Kuchnir, L.; Kuczera, K.; Lau, F. T. K.; Mattos, C.; Michnick, S.; Ngo, T.; Nguyen, D. T.; Prodhom, B.; Reiher, W. E.; Roux, B.; Schlenkrich, M.; Smith, J. C.; Stote, R.; Straub, J.; Watanabe, M.; Wi6rkiewicz-Kuczera, J.; Yin, D. and Karplus, M.; *J. Phys. Chem. B*, **102** (1998), 3586-3616.
- (90) Dauber-Osguthorpe, P.; Roberts, V. A.; Osguthorpe, D. J.; Wolff, J.; Genest, M. and Hagler, A. T.; *Proteins: Struct., Funct. and Genetics*, **4** (1988), 31-47.
- (91) Hermans, J.; Berendsen, H. J. C.; van Gunsteren, W. F. and Postma, J. P. M.; *Biopolymers*, **23** (1984), 1513-1518.
- (92) Allinger, N. L.; *J. Am. Chem. Soc.*, **99** (1977), 8127-8134.
- (93) Allinger, N. L.; Yuh, Y. H. and Li6, J.-H.; *J. Am. Chem. Soc.*, **111** (1989), 8551-8565.
- (94) Allinger, N. L. and Fan, Y.; *J. Comp. Chem.*, **18** (1997), 1827-1847.
- (95) Halgren, T. A.; *J. Comp. Chem.*, **17** (1996), 490-519.
- (96) Halgren, T. A.; *J. Comp. Chem.*, **17** (1996), 520-552.



- (97) Halgren, T. A.; *J. Comp. Chem.*, **17** (1996), 553-586.
- (98) Halgren, T. A. and Nachbar, R. B.; *J. Comp. Chem.*, **17** (1996), 587-615.
- (99) Halgren, T. A.; *J. Comp. Chem.*, **17** (1996), 616-646.
- (100) Rappé, A. K.; Colwell, K. S. and Casewit, C. J.; *Inorg. Chem.*, **32** (1993), 3438-3450.
- (101) Foloppe, N.; Ferrand, M.; Breton, J. and Smith, J. C.; *Proteins: Structure, Fuction, and Genetics*, **22** (1995), 226-244.
- (102) Pavelites, J. J.; Gao, J.; Bash, P. A. and MacKerell Jr., A. D.; *J. Comput. Chem.*, **18** (1997), 221-239.
- (103) Laberge, M.; Vanderkooi, J. M. and Sharp, K. A.; *J. Phys. Chem.*, **100** (1996), 10793-10801.
- (104) Jongejan, A.; Jongejan, J. A. and Duine, J. A.; *Protein Engineering*, **11** (1998), 185-198.
- (105) Rappé, A. K.; Casewit, C. J.; Colwell, K. S.; Goddard Iii, W. A. and Skiff, W. M.; *J. Am. Chem. Soc.*, **114** (1992), 10024-10035.
- (106) Sherrod, M. J. and Menger, F. M.; *J. Am. Chem. Soc.*, **111** (1989), 2611-2613.
- (107) Sherrod, M. J.; *Tet. Lett.*, **31** (1990), 5085-5088.
- (108) Halgren, T. A.; *J. Comp. Chem.*, **20** (1999), 730-748.
- (109) Gundertofte, K. T.; Liljefors, T.; Norrby, P.-O. and Patteson, I.; *J. Comp. Chem.*, **17** (1996), 429-449.
- (110) Hobza, P.; Kabelac, M.; Sponer, J.; Mejzlik, P. and Vondrasek, J.; *J. Comp. Chem.*, **18** (1997), 1136-1150.
- (111) Lipkowitz, K. B. and Boyd, D. B., Ed.; *Reviews in Computational Chemistry*; Wiley-VCH: New York.
- (112) Lipkowitz, K. B.; *J. Chem. Ed.*, **72** (1995), 1070-1075.
- (113) van Gunsteren, W. F. and Mark, A. E.; *J. Chem. Phys.*, **108** (1998), 6109-6116.
- (114) Duan, Y.; Wang, L. and Kollman, P. A.; *Proc. Natl. Acad. Sci. USA*, **95** (1998), 9897-9902.
- (115) Duan, Y. and Kollman, P. A.; *Science*, **282** (1998), 740-744.
- (116) Amadei, A.; Linssen, A. B. M. and Berendsen, H. J. C.; *Proteins: Struct. Funct. Gen.*, **17** (1993), 412-425.
- (117) Elber, R.; Ghosh, A. and Cárdenas, A.; *Acc. Chem. Res.*, **35** (2002), 396-403
- (118) Åqvist, J. and Hansson, T.; *J. Phys. Chem. B.*, **102** (1998), 3837-3840.
- (119) Guenot, J. and Kollman, P. A.; *J. Comp. Chem*, **14** (1993), 295-311.
- (120) Tomasi, J. and Persico, M.; *Chem. Rev.*, **94** (1994), 2027-2094.
- (121) Honig, B. and Nicholls, A.; *Science*, **268** (1995), 1144-1149.
- (122) Cramer, C. J. and Truhlar, D. G.; *Chem. Rev.*, **99** (1999), 2161-2200.
- (123) Fischer, S. and Verma, C. S.; *Proc. Natl. Acad. Sci. USA*, **96** (1999), 9613-9615.
- (124) Mao, Y.; Ratner, M. A. and Jarrold, M. F.; *J. Am. Chem. Soc.*, **122** (2000), 2950-2951.
- (125) Denisov, V. P.; Venu, K.; Peters, J.; Hörlein, H. D. and Halle, B.; *J. Phys. Chem. B*, **101** (1997), 9380-9389
- (126) Antosiewicz, J. and McCammon, J. A.; *Biochemistry*, **35** (1996), 7819-7833.
- (127) Pitera, J. W.; Falta, M. and van Gunsteren, W. F.; *Biophys. J.*, **80** (2001), 2548-2555.
- (128) Nakamura, H.; Sakamoto, T. and Wada, A.; *Prot. Eng.*, **2** (1988), 177-183.
- (129) Simonson, T. and Brooks III, C. L.; *J. Am. Chem. Soc.*, **118** (1996), 8452-8458.
- (130) Dillet, V.; Dyson, H. J. and Bashford, D.; *Biochemistry*, **37** (1998), 10298-10306.
- (131) Warwicker, J.; *Prot. Engin.*, **10** (1997), 809-814.

- (132) Shan, S.; Loh, S. and Herschlag, D.; *Science*, **272** (1996), 97-101.
- (133) Tishmack, P. A.; Bashford, D.; Harms, E. and van Etten, R. L.; *Biochemistry*, **36** (1997), 11984-11994.
- (134) Nielsen, J. E.; Andersen, K. V.; Honig, B.; Hooft, R. W. W.; Klebe, G.; Vriend, G. and Wade, R. C.; *Prot. Engin.*, **12** (1999), 657-662.
- (135) Luo, R.; Head, M. S.; Moulton, J. and Gilson, M. K.; *J. Am. Chem. Soc.*, **120** (1998), 6138-6146.
- (136) Gallicchio, E.; Kubo, M. M. and Levy, R. M.; *J. Phys. Chem. B*, **104** (2000), 6271-6285.
- (137) Zheng, Y. J. and Ornstein, R. L.; *Protein engineering*, **9** (1996), 485-492.
- (138) Toba, S. and Merz, K. M.; *J. Am. Chem. Soc.*, **119** (1997), 9939-9948.
- (139) Toba, S.; Hartsough, D. S. and Merz, K. M. J.; *J. Am. Chem. Soc.*, **118** (1996), 6490-6498.
- (140) Jorgensen, W. L.; *Acc. Chem. Res.*, **22** (1989), 184-189.
- (141) Åqvist, J.; Medina, C. and Samuelsson, J.-E.; *Prot. Engin.*, **7** (1994), 385-391.
- (142) Bohm, H. J.; *J. Comput. Aided Mol. Des.*, **8** (1994), 243-256.
- (143) Di Nola, A. and Brünger, A. T.; *J. Comp. Chem.*, **19** (1998), 1229-1240.
- (144) Sen, S. and Nilsson, L.; *J. Comp. Chem.*, **20** (1999), 877-885.
- (145) Wang, J.; Morin, P.; Wang, W. and Kollman, P. a.; *J. Am. Chem. Soc.*, **123** (2001), 5221-5230.
- (146) Zhang, L. Y.; Gallicchio, E.; Friesner, R. A. and Levy, R. M.; *J. Comp. Chem.*, **22** (2001), 591-607.
- (147) Wang, T. and Wade, R. C.; *Proteins: Struct. Funct. Gen.*, **50** (2003), 158-169.
- (148) Gilson, M. K.; Given, J. A.; Bush, B. L. and McCammon, J. A.; *Biophys. J.*, **72** (1997), 1047-1069.
- (149) Luo, H. and Sharp, K.; *Proc. Natl. Acad. Sci.*, **99** (2002), 10399-10404.
- (150) Politicelli, F.; Ascenzi, P.; Bolognesi, M. and Honig, B.; *Protein Science*, **8** (1999), 2621-2629.
- (151) Noskov, S. Y. and Lim, C.; *Biophys. J.*, **81** (2001), 737-750.
- (152) Novotny, J.; Bruccolori, R. and Saul, F. A.; *Biochemistry*, **28** (1989), 4735-4746.
- (153) Reyes, C. M.; Nifosi, R.; Frankel, A. D. and Kollman, P. A.; *Biophys. J.*, **80** (2001), 2833-2842.
- (154) Froloff, N.; Windemuth, A. and Honig, B.; *Protein Science*, **6** (1997), 1293-1301.
- (155) Dixit, S. B. and Chipot, C.; *J. Phys. Chem. A*, **105** (2001), 9795-9799.
- (156) Baginski, M.; Fogolari, F. and Briggs, J. M.; *J. Mol. Biol.*, **274** (1997), 253-267.
- (157) Huo, S.; Wang, J.; Cieplak, P.; Kollman, P. A. and Kuntz, I. D.; *J. Med. Chem.*, **45** (2001), 1412-1419.
- (158) Hansson, T. and qvist, J.; *Prot. Engin.*, **8** (1995), 1137-1144.
- (159) Mark, A. E. and van Gunsteren, W. F.; *J. Mol. Biol.*, **240** (1994), 167-176.
- (160) Smith, P. E. and van Gunsteren, W. F.; *J. Phys. Chem.*, **98** (1994), 13735-13740.
- (161) Castillo, R.; Andrés, J. and Moliner, V.; *J. Am. Chem. Soc.*, **121** (1999), 12140-12147.
- (162) Strajbl, M.; Sham, Y. Y.; Villa, J.; Chu, Z.-T. and Warshel, A.; *J. Phys. Chem. B*, **104** (2000), 4578-4584.
- (163) Snider, M. J.; Lazarevic, D. and Wolfenden, R.; *Biochemistry*, **41** (2002), 3925-3930.
- (164) Young, L. and Post, C. B.; *Biochemistry*, **35** (1996), 15129-15133.
- (165) Åqvist, J. and Warshel, A.; *Chem. Rev.*, **93** (1993), 2523-2544.
- (166) Hammes-Schiffer, S.; *J. Phys. Chem. A*, **102** (1998), 10443-10454.
- (167) Billeter, S. R.; Webb, S. P.; Iordanov, T.; Agarwal, P. K. and Hammes-Schiffer, S.; *J. Chem. Phys.*, **114** (2001), 6925-6936.
- (168) Woo, T. K.; Cavallo, L. and Ziegler, T.; *Theor. Chem. Acc.*, **100** (1998), 307-313.
- (169) Field, M. J.; Bash, P. A. and Karplus, M.; *J. Comp. Chem.*, **11** (1990), 700-733.

- (170) Bentzen, J.; Muller, R. P.; Florián, J. and Warshel, A.; *J. Phys. Chem. B*, **102** (1998), 2293-2301.
- (171) Lyne, P. D.; Hodoscek, M. and Karplus, M.; *J. Phys. Chem. A*, **103** (1999), 3462-3471.
- (172) Reuter, N.; Dejaegere, A.; Maigret, B. and Karplus, M.; *J. Phys. Chem. A*, **104** (2000), 1720-1735.
- (173) Bruice, T. C. and Kahn, K.; *Curr. Op. Chem. Biol.*, **4** (2000), 540-544.
- (174) Field, M. J.; *J. Comput. Chem.*, **23** (2002), 48-58.
- (175) Monard, G. and Merz, K. M. J.; *Acc. Chem. Res.*, **32** (1999), 904-911.
- (176) Luzkov, V. and Åqvist, J.; *J. Am. Chem. Soc.*, **120** (1998), 6131-6137.
- (177) Espinosa-García, J. and Corchado, J. C.; *J. Chem. Phys.*, **112** (2000), 5731-5739.
- (178) Alhambra, C.; Gao, J.; Corchado, J. C.; Villá, J. and Thruhlar, D. G.; *J. Am. Chem. Soc.*, **121** (1999), 2253-2258.
- (179) Kuhn, B. and Kollman, P. A.; *J. Am. Chem. Soc.*, **122** (2000), 2586-2596.
- (180) Martí, S.; Andrés, J.; Moliner, V.; Silla, E.; Tuñón, I.; Bertrán, J. and Field, M. J.; *J. Am. Chem. Soc.*, **123** (2001), 1709-1712.
- (181) Zhang, Y.; Liu, H. and Yang, W.; *J. Chem. Phys.*, **112** (2000), 3483-3492.
- (182) Donini, O.; Darden, T. and Kollman, P. A.; *J. Am. Chem. Soc.*, **122** (2000), 12270-12280.
- (183) Sheldon, R. A.; *J. Chem. Tech. Biotechnol.*, **67** (1996), 1-14.
- (184) Faber, K.; *Biotransformations in organic chemistry: a textbook*; 3rd ed.; Springer-Verlag: Berlin, 1997.
- (185) Philips, R. S.; *Tibtech*, **14** (1996), 13-16.
- (186) Anthonsen, T. and Jongejan, J. A.; *Methods Enzymol.*, **286** (1997), 473-495.
- (187) Jongejan, A.; Machado, S. S. and Jongejan, J. A.; *J. Mol. Catalysis B*, **8** (2000), 121-163.
- (188) Overbeeke, P. L. A.; PhD Thesis, Delft University of Technology, The Netherlands, 1999.
- (189) Norin, M.; Hult, K.; Mattson, A. and Norin, T.; *Biocatalysis*, **7** (1993), 131-147.
- (190) Orrenius, C.; van Heusden, C.; van Ruiten, J.; Overbeeke, P. L. A.; Kierkels, H.; Duine, J. A. and Jongejan, J. A.; *Prot. Engin.*, **11** (1998), 1147-1153.
- (191) Ke, T.; Tidor, B. and Klibanov, A. M.; *Biotechnol. Bioengin.*, **57** (1998), 741-745.
- (192) Colombo, G.; Toba, S. and Merz Jr., K. M.; *J. Am. Chem. Soc.*, **121** (1999), 3486-3493.
- (193) Luque, S.; Ke, T. and Klibanov, A. M.; *Biocat. Biotrans.*, **16** (1998), 233-248.
- (194) Bigeleisen, J. and Wolfsberg, M.; *Adv. Chem. Phys.*, **1** (1958), 15-76.
- (195) Barnes, J. A. and Williams, I. H.; *Biochem. Soc. Trans.*, **24** (1996), 263-268.
- (196) Andrés, J.; Moliner, V.; Safoni, V. S.; Domingo, L. R. and Picher, M. T.; *J. Org. Chem.*, **61** (1996), 7777-7783.
- (197) Schiøtt, B.; Zheng, Y.-J. and C., B. T.; *J. Am. Chem. Soc.*, **120** (1998), 7192-7200.
- (198) Abu-Hasanayn, F. and Streitwieser, A.; *J. Org. Chem.*, **63** (1998), 2954-2960.
- (199) Feierberg, I.; Luzhkov, V. and Åqvist, J.; *J. Biol. Chem.*, **275** (2000), 22657-22662.
- (200) Francisco, W. A.; Abu-Soud, H. M.; DelMonte, A. J.; Singleton, D. A.; Baldwin, T. O. and Raushel, F. M.; *Biochemistry*, **377** (1998), 2596-2606.
- (201) Marcus, R. A.; *J. Chem. Phys.*, **24** (1956), 966-978.
- (202) Marcus, R. A. and Sutin, N.; *Biochim. Biophys. Acta*, **811** (1985), 265-322.
- (203) Marcus, R. A.; *Angew. Chem. Int. Ed. Engl.*, **32** (1993), 1111-1121.
- (204) Canters, G. W. and Kamp, M. v. d.; *Curr. Op. in Struct. Biol.*, **2** (1992), 859-869.
- (205) Baum, R. M.; *C&EN*, feb., **22** (1993), 20-23.
- (206) Friesner, R. A.; *Structure*, **2** (1994), 339-343.

- (207) Farver, O. and Pecht, I.; *J. Biol. Inorg. Chem.*, **2** (1997), 387-392.
- (208) Williams, R. J. P.; *J. Biol. Inorg. Chem.*, **2** (1997), 373-377.
- (209) Kuki, A. and Wolynes, P. G.; *Science*, **236** (1987), 1647-1652.
- (210) Kuki, A.; *Structure and Bonding*, **75** (1991), 49-83.
- (211) Beratan, D. N.; Nelson Onuchic, J.; Winkler, J. R. and Gray, H. B.; *Science*, **258** (1992), 1740-1741.
- (212) Regan, J. J.; Risser, S. M.; Beratan, D. N. and Onuchic, J. N.; *J. Phys. Chem.*, **97** (1993), 13083-13088.
- (213) Skourtis, S. S. and Beratan, D. N.; *J. Biol. Inorg. Chem.*, **2** (1997), 378-386.
- (214) Moser, C. C.; Keske, J. M.; Warncke, K.; Farid, R. S. and Dutton, P. L.; *Nature*, **355** (1992), 796-802.
- (215) Dutton, P. L. and Mosser, C. C.; *Proc. Natl. Acad. Sci. USA*, **91** (1994), 10247-10250.
- (216) Moser, C. C.; Page, C. C.; Chen, X. and Dutton, P. L.; *J. Biol. Inorg. Chem.*, **2** (1997), 393-398.
- (217) Bicout, D. J. and Field, M. J.; *J. Phys. Chem.*, **99** (1995), 12661-12669.
- (218) Lopez-Castillo, J. M.; Filali-Mouhim, A.; Van Binh-Otten, E. N. and Jay-Gerin, J. P.; *J. Am. Chem. Soc.*, **119** (1997), 1978-1980.
- (219) Gunner, M. R.; Nicholls, A. and Honig, B.; *J. Phys. Chem.*, **100** (1996), 4277-4291.
- (220) Li, J.; Nelson, M. R.; Peng, C. Y.; Bashford, D. and Noodleman, L.; *J. Phys. Chem. B*, **102** (1998), 6311-6324.
- (221) Wheeler, R. A.; *J. Am. Chem. Soc.*, **116** (1994), 11048-11051.
- (222) Zhang, L. Y. and Friesner, R. A.; *J. Phys. Chem.*, **99** (1995), 16479-16482.
- (223) Teixeira, V. H.; Soares, C. M. and Baptista, A. M.; *J. Biol. Inorg. Chem.*, **7** (2002), 200-216.
- (224) Muegge, I.; Apostolakis, J.; Ermler, U.; Fritzsche, G.; Lubitz, W. and Knapp, E. W.; *Biochemistry*, **35** (1996), 8359-8370.
- (225) Apostolakis, J.; Muegge, I.; Ermler, U.; Fritzsche, G. and Knapp, E. W.; *J. Am. Chem. Soc.*, **118** (1996), 3743-3752.
- (226) Balabin, I. A. and Onuchic, J. N.; *J. Phys. Chem. B*, **102** (1998), 7497-7505.
- (227) Aquino, A. J. A.; Beroza, P.; Beratan, D. N. and Onuchic, J. N.; *Chem. Phys.*, **197** (1995), 277-288.
- (228) Ullmann, G. M.; Knapp, E. W. and Kostic, N. M.; *J. Am. Chem. Soc.*, **119** (1997), 42-52.
- (229) Soriano, G. M.; Ponamarev, M. V.; Tae, G. S. and Cramer, W. A.; *Biochemistry*, **35** (1996), 14590-14598.
- (230) Priyadarshy, S.; Risser, S. M. and Beratan, D. N.; *J. Phys. Chem.*, **100** (1996), 17678-17862.
- (231) Siddarth, P. and Marcus, R. A.; *J. Phys. Chem.*, **97** (1993), 13078-13082.
- (232) Davidson, V. L.; *Biochemistry*, **35** (1996), 14035-14039.
- (233) Ivkovic-Jensen, M. M.; Ullmann, G. M.; Young, S.; Hansson, Ö.; Crnogorac, M. M.; Ejdebäck, M. and Kostic, N. M.; *Biochemistry*, **37** (1998), 9557-9569.
- (234) Mooij, W. T. M.; van Eijck, B. P. and Kroon, J.; *J. Am. Chem. Soc.*, **122** (2000), 3500-3505.
- (235) Tame, J. R. H.; *TIBS*, (1999), 372-377.
- (236) Kleywegt, G. J. and Jones, T. A.; *Structure*, **4** (1996), 1395-1400.
- (237) Hooft, R. W. W.; Vriend, G.; Sander, G. and Abola, E. E.; *Nature*, **381** (1996), 272.
- (238) Rick, S. W. and Cachau, R. E.; *J. Chem. Phys.*, **112** (2000), 5230-5241.
- (239) Venclovas, C.; Zemla, A.; Fidelis, K. and Moulton, J.; *Proteins: Struct., Funct., Gen., Suppl.*, **5**

- (2001), 163-170.
- (240) Levinthal, C.; *J. Chim. Phys.*, **65** (1968), 44-45.
- (241) Levinthal, C.; In: "Mössbauer Spectroscopy in Biological Systems"; DeBrunner, P.; Tsibris, J. C. M.; Munck, E. (eds.); Urbana: University of Illinois Press (1969); pp 22-24.
- (242) Baldwin, R. L.; *Proc. Natl. Acad. Sci. USA*, **93** (1996), 2627-2628.
- (243) Dobson, C. M.; Sali, A. and Karplus, M.; *Angew. Chem. Int. Ed.*, **37** (1998), 868-893.
- (244) Goldbeck, R. A.; Thomas, Y. G.; Chen, E.; Esquerra, R. M. and Kliger, D. S.; *Proc. Natl. Acad. Sci. USA*, **96** (1999), 2782-2787.
- (245) Allen, F.; Almasi, G.; Andreoni, W.; Beece, D.; Berne, B. J.; Bright, A.; Brunheroto, J.; C., C.; Castanos, J.; Coteus, P.; Crumley, P.; Curioni, A.; Denneau, M.; Donath, W.; Eleftheriou, M.; Fitch, B.; Fleischer, B.; Georgiou, C. J.; Germain, R.; Giampapa, M.; Gresh, D.; Gupta, M.; Haring, R.; Ho, H.; Hochschild, P.; Hummel, S.; Jonas, T.; Lieber, D.; Martyna, G.; Maturu, K.; Moreira, J.; News, D.; Newton, M.; Philhower, R.; Picunko, T.; Pitera, J.; Pitman, M.; Rand, R.; Royyutu, A.; Salapura, V.; Sanomiya, A.; Shah, R.; Sham, Y.; Singh, S.; Snir, M.; Suits, F.; Swetz, R.; Swope, W. C.; Vishnumurthy, N.; Ward, T. J. C.; Warren, H. and Zhou, R.; *IBM Systems J.*, **40** (2001), 310-327.
- (246) Sutcliffe, M. J.; Haneef, I.; Carney, D. and Blundell, T. L.; *Prot. Engin.*, **1** (1987), 377-384.
- (247) Sutcliffe, M. J.; Hayes, F. R. F. and Blundell, T. L.; *Prot. Engin.*, **1** (1987), 385-392.
- (248) Blundell, T. L.; Sibanda, B. L.; Sternbeg, M. J. E. and Thorton, J. M.; *Nature*, **326** (1987), 347-352.
- (249) Blundell, T. L.; Carney, D.; Gardner, S.; Hayes, F.; Howlin, B.; Hubbard, T.; Overington, J.; Singh, D. A.; Sibanda, B. L. and Sutcliffe, M.; *Eur. J. Biochem.*, **172** (1988), 513-520.
- (250) Chou, P. Y. and Fasman, G. D.; *Adv. Enzymol.*, **47** (1978), 45-147.
- (251) Garnier, J.; Osguthorpe, D. J. and Robson, B.; *J. Mol. Biol.*, **120** (1978), 97-120.
- (252) Zhang, K. Y. and Eisenberg, D.; *Protein. Sci.*, **3** (1994), 687-695.
- (253) Srinivansan, R. and Rose, G. D.; *Protein*, **22** (1995), 81-99.
- (254) Tramontano, A.; Lepplae, B. and Morea, V.; *Proteins: Struct., Funct., Gen., Suppl.*, **5** (2001), 22-38.
- (255) Feig, M. and Brooks III, C. L.; *Proteins: Struct., Funct., Gen.*, **49** (2002), 232-245.
- (256) Bonneau, R.; Tsai, J.; Ruczinski, I. and Baker, D.; *J. Struct. Biol.*, **134** (2001), 186-190.
- (257) Huizinga, E. G. PhD Thesis, University of Groningen, The Netherlands, 1994.
- (258) Oubrie, A.; Rozenboom, H. J.; Kalk, K. H.; Huizinga, E. G. and Dijkstra, B. W.; *J. Biol. Chem.*, **277** (2002), 3727-3732.
- (259) Chen, Z.-W.; Matsushita, K.; Yamashita, T.; Fuji, T.-A.; Toyama, H.; Adachi, O.; Bellamy, H. and Mathews, F. S.; *Structure*, **10** (2002), 837-849.
- (260) Xia, Z. X.; Dai, W. W.; Xiong, J. P.; Hao, Z. P.; Davidson, V. L.; White, S. and Mathews, FS.; *J. Biol. Chem.*, **267** (1992), 222849-22297.
- (261) White, S.; Boyd, G.; Mathews, F. S.; Xia, Z. X.; Dai, W. W.; Zhang, Y. F. and Davidson, V. L.; *Biochemistry*, **32** (1993), 12955-12958.
- (262) Xia, Z. X.; Dai, W. W.; Zhang, Y. F.; White, S. A.; Boyd, G. D. and Mathews, F. S.; *J. Mol. Biol.*, **259** (1996), 480-501.
- (263) Ghosh, M.; Anthony, C.; Harlos, K.; Goodwin, M. G. and Blake, C.; *Structure*, **3** (1995), 177-187.
- (264) Kraulis, P. J.; *J. Appl. Crystallogr.*, **24** (1991), 946-950.
- (265) Guex, N. and Peitsch, M. C.; *Electrophoresis*, **18** (1997), 2714-2723
- (266) Valencia, A. and Pazos, F.; *Curr. Opinion in Struct. Biol.*, **12** (2002), 368-373.

Chapter 1

---

(267) Noble, D.; *Science*, **295** (2002), 1678-1682.

# The Enantioselectivity of Quinohemoprotein Alcohol Dehydrogenases: Mechanistic and Structural Aspects

Aldo Jongejan, Sonia S. Machado and Jaap A. Jongejan

---

## Abstract

Quinohemoprotein alcohol dehydrogenases, QH-ADHs, isolated from *Acetobacter*, *Gluconobacter* and *Comamonas* species show appreciable enantioselectivity in the oxidation of chiral primary and secondary alcohols. Current views of the structural and mechanistic factors of importance for the understanding of the enantioselective performance of these enzymes are reviewed. Structural properties of QH-ADH, Type I, from *C. testosteroni*, and QH-ADH, Type II, from *A. pasteurianus* have been deduced from homology modeling studies based on the X-ray crystallographic data available for PQQ-containing quinoprotein methanol dehydrogenases, MDHs. Mechanisms that have been proposed for quino(hemo)protein alcohol dehydrogenase-catalyzed substrate oxidation are discussed in relation to the constraints set by the observed enantioselectivity.

**Key words**

Pyrroloquinoline quinone / quinohemoprotein / alcohol dehydrogenase / enantioselective oxidation / chiral alcohols / kinetics / mechanism / structure / molecular modeling / review

*This contribution is dedicated to Professor Hans Duine on the occasion of his retirement from the Enzymology chair of the Delft University of Technology, Delft, the Netherlands*



## **Introduction**

The identification in 1979 of pyrroloquinoline quinone, PQQ, as the cofactor of certain dye-linked methanol dehydrogenases, MDHs [1,2], and glucose dehydrogenases, GDHs [3], provided a major stimulus for the search of other enzymes that might contain this cofactor. Shortly after the detection and structure elucidation of PQQ, a number of claims regarding its presence in dehydrogenases and oxidases of both bacterial and eukaryotic origin were made [4]. With the development of more accurate and reliable analytical procedures, however, it became clear that the distribution of PQQ is most probably limited to a relatively small group of bacterial dehydrogenases [5,6]. Eventually, other quinones including topa quinone, TPQ [7], its lysyl derivative, LTQ [8], and tryptophyl-tryptophan quinone, TTQ [9], could be identified as the organic cofactors of enzymes that were once suggested to contain PQQ. Today, enzymes possessing either one of the cofactors shown in Figure 1 are collectively addressed as quinoproteins. An impressive number of comprehensive accounts of the current status of quinoprotein research covering various aspects of cofactor identification, enzyme characterization, and distribution have appeared [6,10-16].

X-ray crystallographic investigations of PQQ-containing MDHs [17-20], TPQ-containing amine oxidases, AOs [21-23], and TTQ-containing methylamine dehydrogenases, MADHs [24-30], have provided insight into the structural aspects of quinoprotein enzymes. Information regarding the distribution and physiological role of quinoproteins has become available as well [15,31,32]. As a result, the novelty of quinone cofactors among the array of organic coenzymes and cofactors of which role and function in metabolism were already firmly established, is wearing off. Still, a number of important questions remain to be solved. In this respect, the catalytic mechanism of the PQQ-containing alcohol dehydrogenases is a key issue.

Despite intensive efforts by a number of groups only limited insight into the events leading to the transfer of reducing equivalents from substrate to PQQ and from reduced PQQ to the electron acceptor has been gained. This situation is particularly frustrating when considering PQQ-containing quinoxinoprotein alcohol dehydrogenases. As shown in Table I, representatives of this class display appreciable enantioselectivity in the oxidation of low-molecular chiral alcohols of which the pure enantiomers are of interest for synthetic applications. Their performance may well be compared to enantiomeric ratio values currently realized with non-biological catalysts [33-35] where

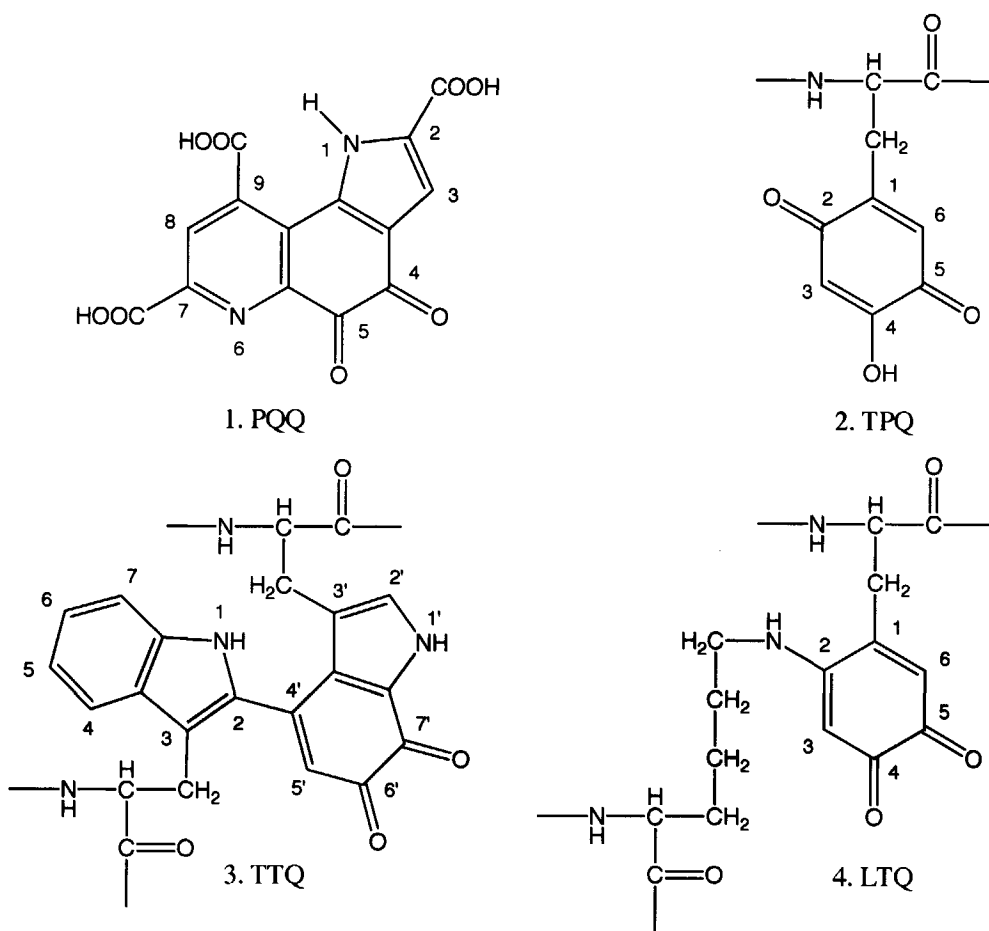


**Figure 1.** Structures of quinoprotein cofactors. 1. Pyrroloquinoline quinone, PQQ [1] [2] ; 2. Topaquinone, TPQ [7] ; 3. Tryptophyl tryptophanquinone, TTQ [9] ; 4. Lysine Tyrosylquinone, LTQ [8] . TPQ, TTQ, and LTQ are derived from the side chains of amino acids that form an integral part of the polypeptide backbone; PQQ is non-covalently bound.

$E = 40$  appears to be the rule [36], and  $E = 200$  a remarkable exception [37]. Realisation of the full potential of quinoprotein alcohol dehydrogenases in industrial processes, however, requires the enzymes not only to be enantioselective, but also to be readily available, highly active and suitably stable [38,39]. Although such properties may be eventually be attained through brute force screening, recombinant DNA techniques, or

directed evolution protocols, proper understanding of the structural and mechanistic factors involved in enantioselective catalysis will be an important tool to guide such efforts.

In addition to the prospects for applications in the fields of fine chemicals synthesis [40-42], biosensor devices [43-48] and possibly combinatorial biocatalysis, PQQ-containing quino(hemo)protein dehydrogenases represent a class of fundamentally interesting enzymes in their own right. Although the substrate specificity fingerprints show appreciable overlap with those of NAD(P)-dependent alcohol dehydrogenases, their natural electron acceptors, ubiquinone [49-52], cytochrome *c* or blue copper proteins [53,54], are found towards the oxidative end of the biological redox scale. By consequence, dehydrogenation reactions catalyzed by quinohemoproteins are strictly irreversible. Yet, the magnitude of the driving thermodynamic potential does not inspire particularly high catalytic reaction rates. Although it would appear rather naïve to expect the Gibbs free energy difference of reactants and products to be proportional to the (catalytic) reaction rate, such correlations have indeed been described for simple exothermic reactions [55,56], hypothesized for enzymatic conversions [57], and on occasion pointed to interesting phenomena obstructing the free equilibration of chemical species, i.e. the spin-restrictions governing autoxidation reactions.

**Table I.** Enantiomeric ratio of PQQ-containing quinoprotein alcohol dehydrogenases

| Enzyme              | Source                  | Substrate            | <i>E</i> -value<br>(preference) | Refs  |
|---------------------|-------------------------|----------------------|---------------------------------|-------|
| MDH                 | <i>Hyphomicrobium X</i> | solketal             | 1 (-)                           | [114] |
| QH-ADH<br>(type II) | <i>G. oxydans</i>       | glycidol             | 26 (S)                          | [115] |
|                     | .                       | solketal             | 12 (R)                          | [114] |
|                     | .                       | 1,2-cyclo-hexanediol | >50 (R)                         | [3]   |
|                     | <i>A. pasteurianus</i>  | glycidol             | 7-18 (S)                        | [200] |
|                     | .                       | 2-butanol            | 13-20 (S)                       | [200] |
| QH-ADH<br>(type I)  | <i>A. aceti</i>         | glycidol             | 17 (S)                          | [114] |
|                     | <i>C. testosteroni</i>  | solketal             | >100 (R)                        | [114] |
|                     | .                       | glycidol             | 1 (-)                           | [115] |
|                     | .                       | 2-butanol            | 14 (S)                          | [281] |
|                     | .                       | 2-hexanol            | 105 (S)                         | [281] |
|                     | .                       | 2-heptanol           | 315 (S)                         | [281] |
|                     | .                       | 2-octanol            | >800 (S)                        | [281] |

At present, comparative enzymology of quinoproteins has not provided convincing explanations for the relatively low catalytic rates of MDHs and QH-ADHs. In particular, considering the impressive turn-over numbers ( $\approx 10^5 \text{ s}^{-1}$  [58]) measured for the related PQQ-containing quinoprotein glucose dehydrogenase, GDH, it would seem that the exchange rate of reducing equivalents between substrate and cofactor in QH-ADHs ( $\approx 10^2 \text{ s}^{-1}$  [54,59]) could be further improved by several orders of magnitude. Again, knowledge of the 'enantioselectivity-controlling' step of the quinohemoprotein alcohol dehydrogenase mechanism might provide clues for the interpretation of the rate-controlling step [60] that leads to this intriguing situation.

As indicated above, the enzymology of quinoproteins has been the subject of a fair number of reviews. Comprehensive accounts of the actual chemistry occurring in the active site, on the other hand, are less numerous. In order to emphasize both the fundamental and practical aspects of this highly interesting field of research, the enantioselective properties of quinohemoproteins provide an attractive directive. In addition to its practical consequences for applications in biocatalytic kinetic resolution processes, enantioselectivity can be a valuable tool in the elucidation of kinetic mechanisms. Accordingly, this paper has been organized as follows. In Section 1 we present a brief summary of the kinetic description of enzymatic enantioselectivity in terms of the ratio of specificity constants, the enantiomeric ratio,  $E$ . The formal identification of the kinetic constants collected in  $E$ , with the Gibbs free energy barriers along the reaction coordinate is discussed in the context of Eyring Transition State Theory, TST. Implications of the location of the 'enantioselectivity-determining' reaction step(s) on the reaction coordinate are emphasized. In Section 2 an account is given of the current knowledge of structural and kinetic properties of quino(hemo)protein alcohol dehydrogenases that have a bearing on the catalytic mechanism. Subsequently, an overview of reaction mechanisms that have been proposed over the years for this class of enzymes is given in Section 3. In Section 4 we discuss the possible relevance of alternative chemical and mechanistic schemes for the catalytic and enantioselective properties of quinohemoprotein alcohol dehydrogenases. Recent results of molecular modeling experiments for representative QH-ADHs from *Acetobacter* and *Comamonas* species are proposed as a frame of reference. Perspectives for further developments in this area are addressed in Section 5.

## 1. Enantioselectivity as a mechanistic tool

Following its introduction by Sih and coworkers [61,62], the enantiomeric ratio,  $E = (k_{cat} / K_M)_R / (k_{cat} / K_M)_S$ , has gained widespread acceptance as the parameter of choice to quantify the enantioselective properties of enzymes. Comprehensive reviews on the determination and the use of  $E$ -values in the field of biotechnological applications have appeared ([63,64]). Meanwhile, it has become clear that the enantiomeric ratio can also be of fundamental importance as a valuable source of inspiration for the interpretation of kinetic properties in terms of mechanistic features. Of both practical and fundamental importance is the fact that the  $E$ -value reflects *relative* reaction rates. Since  $E$ -value determinations do not, in general, require specific knowledge of the amount of active enzyme present, experimental difficulties that are commonly encountered when measuring *absolute* reaction rates of enzyme-catalyzed reactions do not apply. Estimates of the rate-determining quality of the reaction steps involved in enantioselective catalysis under various conditions of e.g. temperature, pressure, and medium composition, can thus be readily obtained. A price has to be paid, however. Whereas measurements of absolute rates may provide data on individual reaction steps, such information is not directly available from  $E$ . A brief introduction of the theoretical background is given below. Detailed discussions have appeared elsewhere [65-67].

Eqn 1 represents the generic case of an enzyme catalyzing the conversion of mutually competitive enantiomeric substrates,  $R$ , *viz.*  $S$ , following irreversible Michaelis Menten-type kinetics:

$$\frac{r_R}{r_S} = \frac{(k_{cat}^R / K_M^R) * [E] * [R]}{(k_{cat}^S / K_M^S) * [E] * [S]} = E * \frac{[R]}{[S]} \quad (1)$$

The direct applicability of Eqn 1 for substrate and product inhibition schemes can be appreciated by noting the (redundant) presence of the concentration of free enzyme,  $[E]$ . When additional substrates and/or reversible reactions are involved, more elaborate expressions are required [68-70]. Also in these cases, the enantiomeric ratio can be formed from the kinetic parameters,  $k_{cat}$  and  $K_M$ , for the enantiomeric substrates, albeit that the number of microscopic rate constants lumped in  $E$  increases rapidly when the kinetic schemes become more realistic. This complexity tends to obscure the extent to which individual microscopic rate constants contribute to the overall enantioselective

properties. Expressing the  $E$ -value in terms of reciprocal rate constants (characteristic reaction times) is helpful. A formally equivalent and visually appealing picture is obtained when rate constants are expressed in the (thermodynamic) format of Eyring TST [71-73]:

$$k = \kappa \frac{k_B T}{h} \exp\left(-\frac{\Delta G^\ddagger}{RT}\right) \quad (2)$$

The procedure is summarized in Eqns 3, 4. Details of the derivation of Eqn 4 can be found elsewhere [66,74].

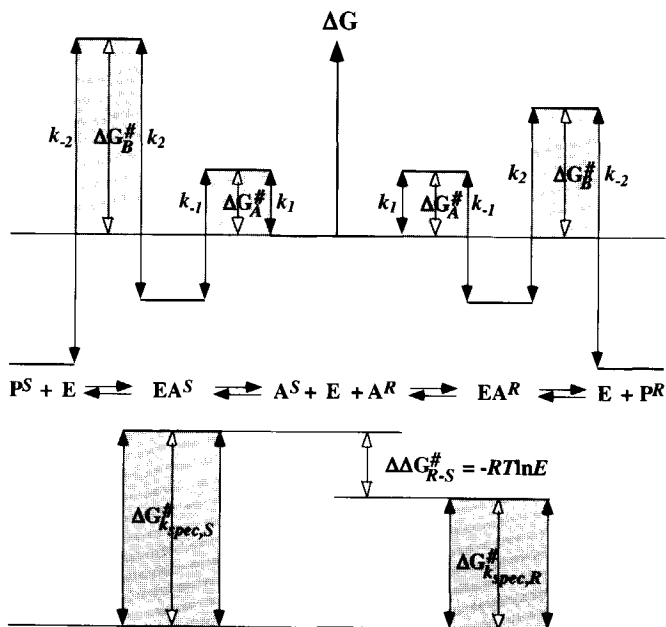
$$E = \frac{k_{spec}^R}{k_{spec}^S} = \frac{k_1^R k_2^R / (k_{-1}^R + k_2^R)}{k_1^S k_2^S / (k_{-1}^S + k_2^S)} \quad (3)$$

$$E = \frac{\exp\left(\frac{\Delta G_{spec,S}^\ddagger}{RT}\right)}{\exp\left(\frac{\Delta G_{spec,R}^\ddagger}{RT}\right)} = \frac{\exp\left(\frac{\Delta G_{A^S}^\ddagger}{RT}\right) + \exp\left(\frac{\Delta G_{B^S}^\ddagger}{RT}\right)}{\exp\left(\frac{\Delta G_{A^R}^\ddagger}{RT}\right) + \exp\left(\frac{\Delta G_{B^R}^\ddagger}{RT}\right)} \quad (4)$$

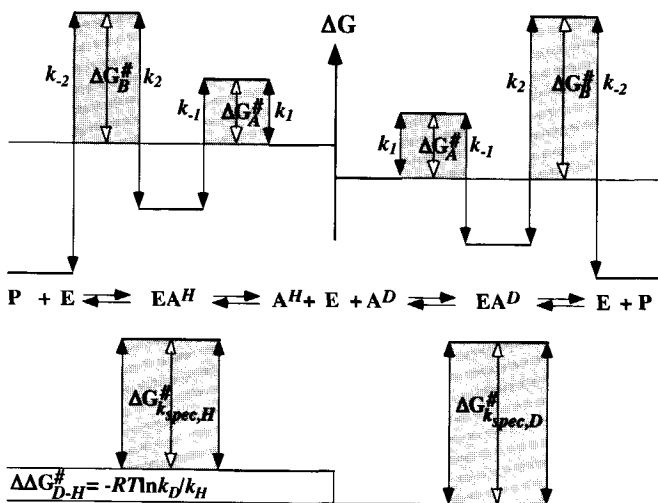
Diagrams of the full scheme, the presentation in terms of the specificity constants,  $k_{spec} = k_{cat} / K_M$  [75] (but see discussion [76-78]), and the identification of the  $E$ -value as  $RT \ln E = \Delta G_{spec,S}^\ddagger - \Delta G_{spec,R}^\ddagger = \Delta \Delta G^\ddagger$  are shown in Figure 2, Panel A, for the enantioselective branches of a ping-pong kinetic scheme. Ternary complex kinetic schemes may require slightly different representations [68]. In addition to the assumptions underlying Eyring TST [73,79-81], transmission coefficients,  $\kappa$ , for the

**Figure 2.** Panel A: Identification of microscopic rate constants contributing to the enantiomeric ratio,  $E$ , with the Gibbs free energy profile along the reaction coordinate. Transition state free energies according to the Eyring TST formalism. Pane B: Idealized presentation of Gibbs free energies to be identified with microscopic rate constants for isotopically substituted substrates. It is assumed that the potential energy surface at the TS follows the Born-Oppenheimer approximation, while the isotopic mass does not contribute to the energy of the translational mode leading from reactant to product states.

### A. Enantioselectivity



### B. Kinetic Isotope Effects



individual rate constants have been assumed identical. It must be emphasized that as a result of the numerical properties of sums of exponentials, the contribution of individual barriers to the overall enantioselectivity is governed by minor differences of the exponents ( $\Delta G^\ddagger$ -values). Since  $k_1 (= k_{on})$  is not normally rate controlling for dissolved enzymes in solution [82,83] (but see [84,85]), its contribution to the enantioselectivity will be negligible.

A great many different protocols for the representation of kinetic schemes by (free) energy profiles have been explored [86-96]. The approach taken here appears to be unique in its clear recognition of the contribution of exponentially weighted activation energies of individual barriers to the specificity constant. Extending the thermodynamic formulation of Eyring TST by including thermodynamic activities of reactants and activated complexes [97,98] has been applied to hydrolytic enzymes [70,99,100]. Preliminary results for dehydrogenases have appeared [101].

It is instructive to apply the formal approach outlined above for the case of the enzymatic discrimination of enantiomers to the effects of isotopic substitutions on enzymatic reaction rates (Figure 2, Panel B). Whereas the difference in rates observed for enantiomeric substrates has its origin in the Gibbs free energy difference of the 'enantioselectivity-determining' (diastereomeric) *transition states*, isotope effects according to the Bigeleisen-Wolfsberg formulation [102,103] reflect the perturbation of the vibrational frequencies contributing to the TS and *ground state energy* [104]. In this restricted sense, enantioselectivity can be considered to address the transition state more directly.

## 2. Characterization of quino(hemo)protein alcohol dehydrogenases

Dye-linked alcohol dehydrogenases containing pyrroloquinoline quinone (2,7,9-tricarboxy-1*H*-pyrrolo[2,3-*f*]quinoline-4,5-dione, PQQ) and  $\text{Ca}^{2+}$  as cofactors have been isolated from various Gram-negative bacteria [6,13,105]. Methanol dehydrogenases, MDHs, from methylotrophic bacteria [106-109] and ethanol dehydrogenase from *Pseudomonas* sp. [16,110] are prominent members of this class. Quinohemoprotein alcohol dehydrogenases, QH-ADHs, form a second class containing heme *c* as an additional organometallic cofactor probably involved in the electron acceptor interaction [69]. Type I QH-ADHs are monomeric proteins (70 to 80 kDa) containing one molecule



of PQQ, one  $\text{Ca}^{2+}$ , and a single c-type heme. Examples have been isolated from ethanol grown *C. testosteroni* [54,111], vanillyl alcohol grown *Rhodopseudomonas acidophila* [112,113] and *Pseudomonas putida* [114]. Type II QH-ADHs have been isolated from various acetic acid bacteria. They are membrane-associated enzymes composed of different subunits. A large subunit (72 to 80 kDa, subunit I) containing one molecule of non-covalently-bound PQQ, one  $\text{Ca}^{2+}$ , and one heme c, is thought to possess the dehydrogenase activity [32]. A medium-sized subunit (43 to 53 kDa, subunit II), most likely involved in electron transport, contains three heme c moieties and shows a high degree of similarity to the CO-binding cytochrome  $c_{553}$  [51]. A small subunit (15 to 20 kDa, subunit III) has been speculated to promote the proper association of the subunits at the membrane interface [50]. In Type II QH-ADH from *A. pasteurianus* and *A. aceti* all three subunits appear to be essential for enzymatic activity. Note that the distinction between *classes* (heme/non-heme) and *types* (subunit composition) used here differs from that used by other authors [32,115].

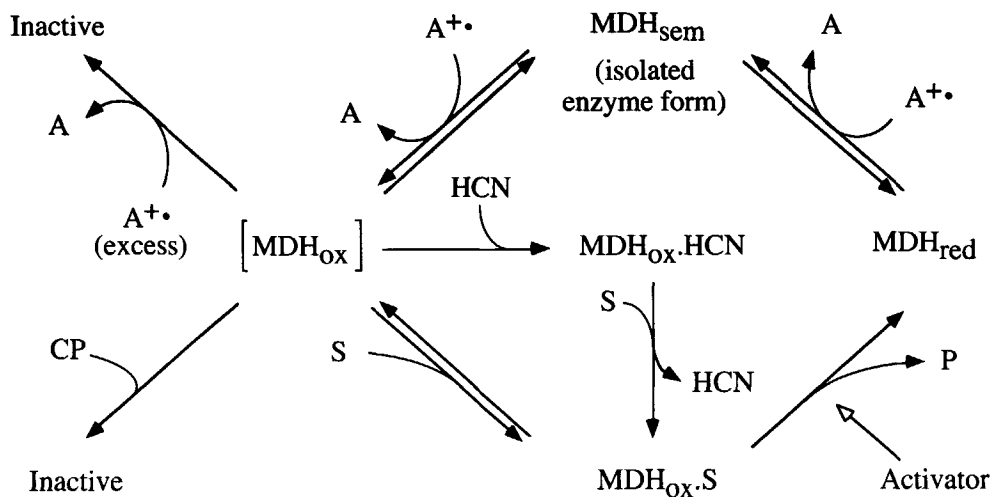
## **2.1. PQQ-containing methanol dehydrogenases, MDHs**

### **2.1.1. Kinetic properties**

Before discussing the enzymological characterization of the quino*hem*oprotein alcohol dehydrogenases a short survey of the non-heme PQQ-containing alcohol dehydrogenases will be given. Soluble methanol dehydrogenases occurring in the periplasmic space of methylotrophic bacteria have played an important role in the development of quinoprotein enzymology. Although the presence of a cofactor of unknown structure, later to be identified as PQQ, was first reported for glucose dehydrogenase in the sixties [116,117], methanol dehydrogenases from methylotrophic bacteria became the source for the actual isolation and structure elucidation of PQQ [1,2,118]. In addition, MDH (from *Methylophilus methylotrophus* and bacterium W3A1) was the first quinoprotein for which the three-dimensional structure was solved [17].

NAD(P)-independent methanol dehydrogenase activity was originally described by Anthony and Zatman [119]. A large number of MDHs (EC 1.1.99.8) with similar properties have been characterized since [120]. As isolated, MDHs are dye-linked enzymes, requiring cationic electron acceptors, the presence of ammonia (which can sometimes be substituted with higher primary amines) as an activator, and  $\text{pH} \approx 9$  for *in vitro* activity. Most MDHs are dimeric proteins containing two molecules of PQQ [121].

Despite its ready availability from various methylotrophes, with *Hyphomicrobium X* as a particularly abundant source [122], MDH turned out not to be an easy target for the study of the catalytic mechanism. Several complications exist: 1. MDHs are usually isolated with their cofactor in a semiquinone form, a redox state that is unreactive with substrate [123]; 2. oxidation with artificial electron acceptors leads to inactivation unless substrate or carbonyl group reagents are present [120,123,124]; 3. enzyme preparations appear to be inevitably contaminated with large amounts of endogenous substrate(s) of unknown origin [119,122,125,126]. By combining spectroscopic and kinetic techniques a convincing kinetic scheme could nevertheless be devised [123,127-129] (Scheme 1). Key observations comprised the radical nature of the MDH semiquinone form [130], the acid extraction of stoichiometric amounts of PQQ and PQQH<sub>2</sub> from this enzyme form [128], and the structure elucidation of the PQQ-adduct extracted from cyclopropanol-inactivated MDH [129] (Figure 3).



**Scheme 1.** MDH<sub>red</sub>, reduced MDH; MDH<sub>sem</sub>, semiquinone form of MDH (EPR active); MDH<sub>ox</sub>, fully oxidized form of MDH; MDH<sub>ox</sub>.HCN, the complex of MDH with cyanide; MDH<sub>ox</sub>.S, the complex of MDH with substrate alcohol or aldehyde; CP, cyclopropanol; activator, ammonia or low molecular primary amine; A and A<sup>+</sup>, reduced and oxidized form of the electron acceptor (Wurster's Blue)(adapted from [123])

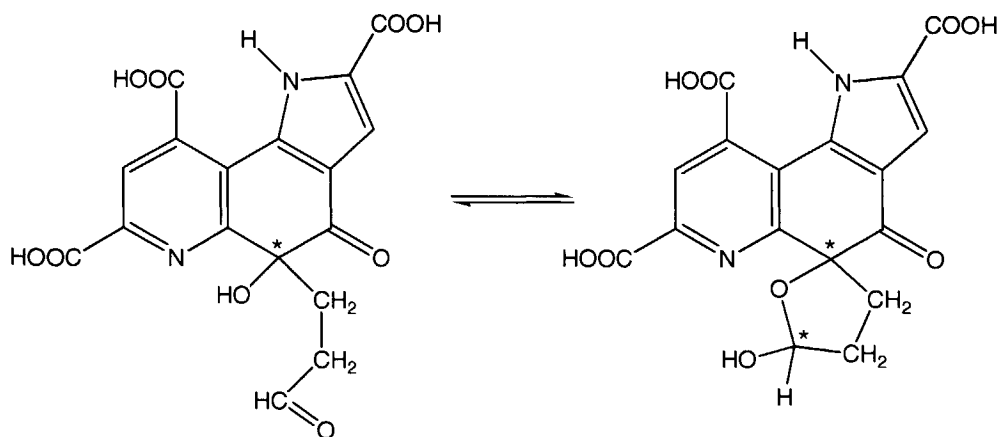


**Figure 3.** Structures of the interconverting PQQ-adducts isolated from cyclopropyl alcohol-inactivated MDH [129]. Note presence of two chiral centers giving rise to diastereomeric mixtures.

The chemical mechanism that has been proposed on the basis of these findings will be discussed in Section 3.

### 2.1.2. The structure of PQQ-containing methanol dehydrogenases

X-Ray crystallography of MDHs from *Methylophilus methylotrophus* and *Methylophilus* W3A1 [17] showed the basic structure of the PQQ-containing  $\alpha$  subunit to be a 'propeller fold' barrel consisting of eight 'blades', also called 'tryptophan motifs' (Ws) since these residues hold together small stretches of  $\beta$  sheets around the superbarrel. Similar propeller motifs have been observed in a large family of proteins [131,132]. The small  $\beta$  subunit is nested in a zipper-like fashion along one side of the  $\alpha$  subunit. The orientation originally assigned to PQQ in the active site has created confusion [133]. A detailed study of *M. W3A1* (crystal form A) at 2.4 Å resolution [19,134] as well as the determination of the structure of MDH from *Methylobacterium extorquens* AM1 at 1.94 Å resolution [18] confirmed the position and orientation of PQQ as shown in Figure 4. A detailed description of the active site of MDH from *M. W3A1* at 1.9 Å resolution revealed the presence of a substrate molecule in the vicinity of the cofactor [20].

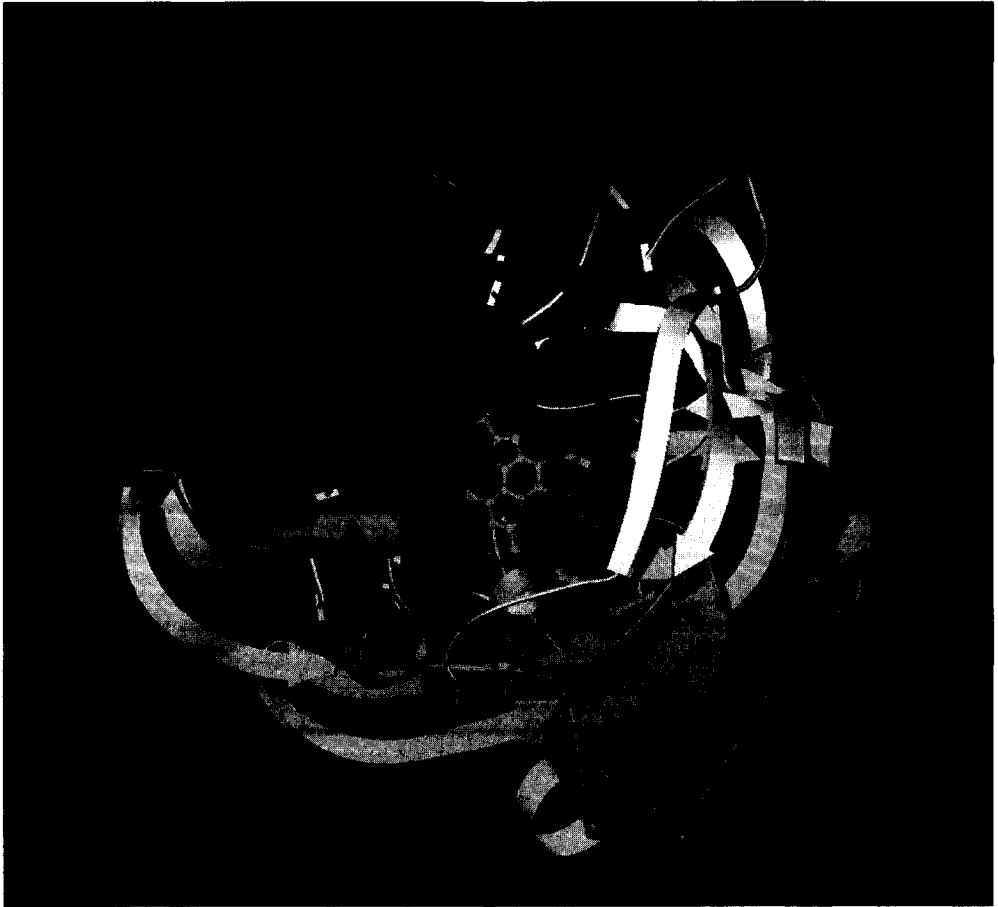


**Figure 4.** Schematic representation of MDH from *Methylophilus methylotrophus* W3A1 showing the 8 bladed  $\beta$ -propeller fold. PQQ shown in a ball and stick representation, calcium as dark grey sphere. This figure was generated using coordinates from pdb entry 1BN2 and MOLSCRIPT version 2.0.2 [326].

Crystal structures have shown the presence of a rather unique non-planar eight-membered ring formed by two vicinal cysteines (residues 103 and 104). The disulfide-bridge was originally taken to be part of a *cis*-peptide bond [17,134], refined X-ray structures, however, have shown the cysteines to be in a *trans* configuration both in the

MDH structures of *M. W3A1* [19] and *M. extorquens* [18]. The disulfide bridge is positioned on top of the cofactor with its sulfur atoms at  $\pm 3.5$  Å parallel to the plane of the PQQ molecule. The bridge is solvent accessible forming one side of the active site funnel with the opposite wall made up of various hydrophobic residues. Tryptophan 243 (*M. extorquens*) forms the bottom of the active site cavity. PQQ is positioned parallel to this residue with the phenyl moiety of the indole group in what appears to be a  $\pi$ -stacking interaction with the pyridine ring of PQQ, thus sandwiching PQQ between Trp 243 and the disulfide bridge. The calcium ion is liganded by the  $\gamma$ -carboxyl oxygens of Glu 177 (axial position), the amide oxygen of Asn 261, and the C(5)-carbonyl oxygen, the C(7)-carboxyl group and the pyridine nitrogen from PQQ occupying equatorial positions (residue numbering refers to MDH from *M. extorquens*). The remaining axial position is filled by an Ala 305. All distances of ligands to  $\text{Ca}^{2+}$  range between 2.4 – 2.8 Å. These values that are in fair agreement with data collected in the Cambridge database for i.e.  $\text{Ca}^{2+}$ -carboxylates [135]. In the high resolution structures, water molecules are seen nearby the C(7)-carboxyl group and C(5)-carbonyl oxygen of PQQ. The proposed active site base, Asp 303, is located opposite the *o*-quinone moiety of PQQ. As a result of its limited dimensions, the funnel-shaped active site cavity places severe restrictions on the size of possible substrates. In accordance with experimental findings, it appears that only primary alcohols may enter the active site (Figure 5).

The hydrophobic residues in the active-site funnel might play an important role in the docking of the natural electron acceptor of MDH, cytochrome  $c_L$ . Originally, it was thought that the small  $\beta$ -subunit was responsible for the interaction with this cytochrome due to the excess of lysines present (15 out of 74 residues) [124,136]. However, those lysines are not conserved in all MDHs. Further chemical studies suggested interaction of lysines at the surface of the  $\alpha$ -subunit with carboxylates on the cytochrome. The importance of these ionic interactions was confirmed by the influence of the ionic strength on the rate of electron transfer [137,138]. For effective electron transfer, PQQ and the heme of cytochrome  $c_L$  need to be in close contact. The shortest possible pathway would be via the hydrophobic funnel. No lysines are present in the vicinity of the funnel entrance. Current ideas involve alignment and initial docking of the two proteins by electrostatic interactions via lysines at the surface of the  $\alpha$ -subunit and carboxylates on the cytochrome followed by a change in docking position due to hydrophobic interactions between the active site funnel and the natural electron acceptor [139].

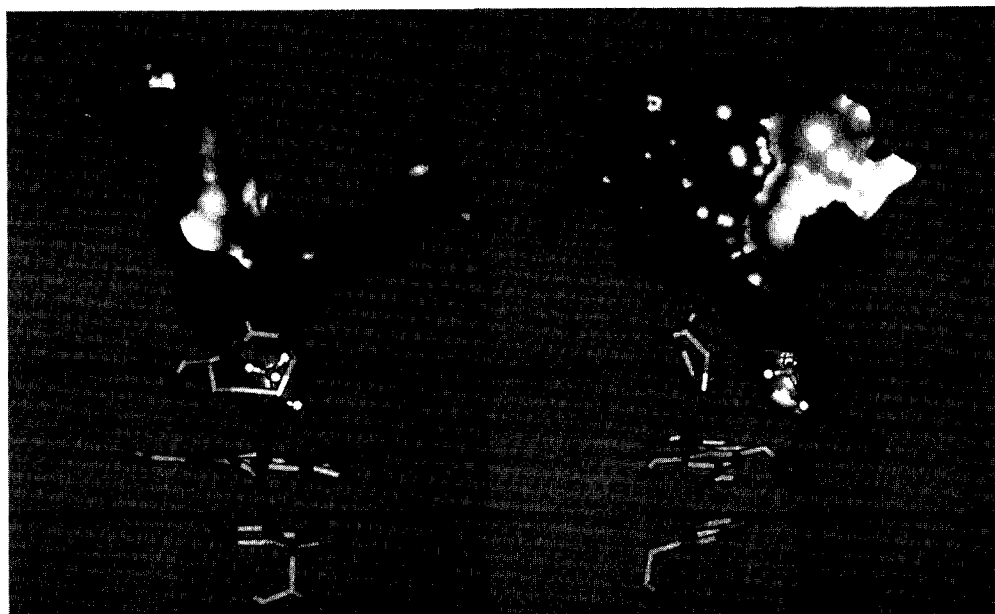


**Figure 5.** View on the active site of MDH from *Methylophilus methylotrophus* W3A1 showing the 8-membered disulfide bridge in stacking interaction with PQQ and underlying tryptophan residue (Trp 237). The molecule of methanol (or formaldehyde) present in the crystal structure is represented as a ball and stick model. The solvent accessible surfaces were generated while omitting the substrate molecule. Residues and PQQ shown as stick models, calcium as CPK model (radius divided by two). Figures generated using INSIGHT (Biosym, Inc.).

Determination of the three-dimensional structure of a macromolecule by X-ray crystallography is commonly regarded as the cornerstone of the structural characterization. While protein crystallographers feel confident that uncertainties in the structure are properly acknowledged by specifying the resolution and by giving reference to the protocols used, researchers that are less familiar with this discipline, on the other hand, tend to overlook the assumptions underlying the fitting and regression analyses and express too much faith in the description of the structure that is provided. On occasion, this widely held belief has been challenged (see [140,141] and comments [142]). In this respect, the erroneous orientation of PQQ in the structure originally proposed for MDHs of *M. methylotrophus* and *M. W3A1* [17] may serve as an example of the fact that the information implied in X-ray structures may be biased by the underlying assumptions. Of course, this bias will be less severe when better resolutions are obtained. In the context

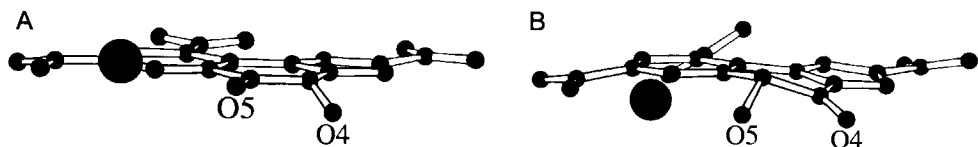


**Figure 6.** Structures of PQQ in the active site of MDH. Panel A, detailed view of the active site of MDH from *M. extorquens* (1.94 Å resolution, coordinates were kindly provided by the authors) [18]. Panel B, corresponding view of MDH from *M. W3A1* (1.9 Å resolution, pdb entry 1B2N) [20]. Figures were generated using MOLSCRIPT version 2.0.2 [326].

of the present survey, two details stand out from the high-resolution structure reported for MDH from *M. W3A1* [20]. Of these, the interpretation of the elongated electron density in the active site cavity in terms of the presence of a molecule of methanol is well supported by earlier findings of a single tightly-bound methanol (or formaldehyde?) to MDH [126]. The out-of-plane position of the oxygen atom in the PQQ-C(5)-carbonyl group is more surprising, however, especially since a similar observation has been reported for the atom attached to the PQQ-C(4) position in the MDH from *Methylobacterium extorquens* [18]. Both structures are shown in Figure 6. Discussion of the possible relevance of these observations will be deferred until Section 4.

In addition to the remarks made above, the question may be raised whether the determination of good-quality structures has provided insight into the complications that have hampered kinetic investigations of MDHs (see 2.1.1). Clearly, the peculiar geometry of the PQQ-C(4) oxygen in MDH from *M. extorquens* and the PQQ-C(5) oxygen in MDH from *M. W3A1* may pertain to the impaired interaction with substrate. There appears to be little reason, however, why fully oxidized PQQ would be unstable in the environment of the active site. The large amount of endogenous substrate equivalents (up to 90! [126]) likewise remains a mystery.

## 2.2. QH-ADHs from *Acetobacter* and *Gluconobacter*

### 2.2.1. Kinetic description

Type II QH-ADHs have been isolated from various acetic acid bacteria. They are membrane-associated enzymes composed of different subunits [32,50-52,59,143]. The QH-ADHs isolated from *A. aceti*, *A. pasteurianus*, and *G. oxydans* appear to follow regular ping-pong kinetics for a variety of substrates. Both natural (ubiquinone) and

artificial (ferricyanide, Wurster's Blue) electron acceptors have been used. Ammonia or amines are not required for activity. pH optima are generally around pH 6. Substantial data sets have been reported for the conversion of non-chiral substrates, detailed analyses of the kinetic schemes in terms of Michaelis and inhibition constants, however, are not yet available [51,143,144]. The kinetic features of the conversion of chiral glycidol using whole cells and isolated QH-ADH from *A. pasteurianus* have been described [59]. The conspicuous presence of (chiral) glycidaldehyde as an intermediate in the reaction has been noted. While whole cells catalyze the conversion of glycidol to glycidic acid with concomitant release of only minute amounts of intermediate glycidaldehyde into the medium, conversions with isolated QH-ADH give rise to substantial accumulation of glycidaldehyde, eventually bringing the reaction to a complete halt. In analogy with the kinetic bi-bi ping-pong scheme including uncompetitive substrate inhibition reported for the mechanistically similar reaction catalyzed by the QH-ADH Type I of *Comamonas testosteroni* [69] (see below), the oxidation rate of a single enantiomer of the alcohol in the presence of aldehyde by the Type II enzyme has been expressed as:

$$r_{alc} = \frac{\left(k_{cat(alc)} / K_{M(alc)}\right) [alc][E]}{D_{Fe,alc,ald}}$$

$$D_{Fe,alc,ald} = 1 +$$

$$+ \frac{[alc]}{K_{M(alc)}} + \frac{[alc] / K_{M(alc)}}{[Fe] / K_{M(Fe,alc)}} + \frac{[alc]^2}{K_{M(alc)} K_{i(alc)}}$$

$$+ \frac{[ald]}{K_{M(ald)}} + \frac{[ald] / K_{M(ald)}}{[Fe] / K_{M(Fe,ald)}} + \frac{[ald]^2}{K_{M(ald)} K_{i(ald)}}$$

With  $[alc]$ ,  $[ald]$ ,  $[E]$ , and  $[Fe]$ , the concentration of the alcohol, aldehyde, active enzyme, and ferricyanide, respectively. Experimental support for the consistency of this kinetic equation has been derived from the determination of the time course of the reaction of racemic glycidol catalyzed by purified QH-ADH [59]. Curiously, dimerization of the intermediate aldehyde had to be included in the overall model as a reversible reaction. Inactivation of the enzyme by the aldehyde and inhibition by the dimer accounted for the abortion of the catalytic reaction that is observed to take place



before glycidol is fully converted.

### **2.2.2. Structural characterization**

All three subunits of Type II QH-ADH from *A. pasteurianus* and *A. aceti* appear to be essential for enzymatic activity. The indispensibility of the small subunit (15-20 kDa, subunit III) in the QH-ADH from *C. suboxydans* has, however, recently been questioned [51,52]. The large subunit (72 to 80 kDa, subunit I) of Type II QH-ADHs, which possesses the dehydrogenase activity, contains one molecule of non-covalently-bound PQQ and one heme *c* [32,143,145]. The genes of QH-ADH from *A. aceti* [146-148], *A. polyoxygenus* [149] *A. pasteurianus* [50,150] and *C. suboxydans* [52] have been cloned and sequenced. X-ray structures of Type II QH-ADHs are still lacking. A working model has been obtained by molecular modeling. Cozier and coworkers [49] constructed a homology model of the QH-ADH from *A. aceti* based the 31% sequence identity and 66% sequence similarity of the residues 1-590 of the QH-ADH of *A. aceti* [106,146,147] and residues 1-595 of MDH from *M. extorquens* [136]. Alignment was determined using a Needleman-Wunsch algorithm and a protein-sequence score matrix, followed by refinement by inspection and modification. Quanta/CHARMm was used to generate and relax side chain positions. Clashes were removed by hand and a force field-derived energy minimization was carried out with partial constraints on the backbone atom positions in order to preserve the basic structure as found in MDH. Thus, the resulting model of the N-terminal domain of *A. aceti* (QH-)ADH retains the characteristics of the MDH structure [49]. No attempts were made to model or position the C-terminal heme-containing domain.

Recently, we succeeded to construct a model of the PQQ-containing domain of the large subunit of the Type II QH-ADH from *A. pasteurianus* [67] using the same approach as adopted to obtain a structural model for the QH-ADH from *C. testosteroni*. The amino acid sequence of QH-ADH from *A. pasteurianus* as reported by Takemura and coworkers [150] (accession number D13893) was used. Considering the extent of sequence identity (> 90%) between QH-ADH from *A. aceti* and QH-ADH from *A. pasteurianus* the alignment [151] of the former sequence with that of MDH from *M. extorquens* was used for the initial comparison. Alignments performed using ClustalW 1.6 [152] did not differ significantly. Coordinates were assigned going from the core to the surface residues of the protein. Configurations of loops were suggested by database searches and assigned.

The unique cysteine-bridge was formed prior to refinement. PQQ and calcium were placed according to optimal superpositioning of the crude model and the MDH structure. Molecular dynamics, using CVFF, was used to remove sidechain clashes. Structures were checked using PROCHECK [153] and ProStat and although some deviation from normally observed values was found, the results were satisfactory. As a control the X-ray structure of MDH was run against ProStat which gave some unsatisfactory amino acid conformations as well. Because the model is build on the MDH structure it is obvious that it will inherit the errors present. Since no obvious errors were observed for the active site residues, further refinement was not considered. No attempts were made to model the heme domain.

### 2.3. QH-ADH from *Comamonas testosteroni*

Quinohemoprotein alcohol dehydrogenase Type I was isolated from *C. testosteroni* (at that time known as *Pseudomonas testosteroni*) as the apoenzyme [111,154]. Only two other representatives of this single subunit type have been reported since: a PQQ-containing holoenzyme from *Pseudomonas putida* [155], and a holoenzyme from *Rhodopseudomonas acidophila* [112]. Like the Type II enzymes, QH-ADH from *C. testosteroni* does not require ammonia or amines for activity. Its pH optimum is around 7.5. PQQ-free QH-ADH apoenzyme is isolated from ethanol-grown *C. testosteroni* in the absence of extraneous PQQ. Purified apoenzyme, showing a single band on native gel electrophoresis (71 kDa) can be converted into active holoenzyme by addition of PQQ in the presence of calcium ions [54]. Incomplete reconstitution has been ascribed to the presence of 'nicked' apoprotein showing up as two band of 51 and 25 kDa, respectively, on SDS/PAGE. Analysis of the N-terminal sequences of the fragments and comparison with the DNA sequence of the gene [156] suggests (proteolytic) scission to occur between two phenylalanine residues (450-451). Following reconstitution with PQQ, active holoenzyme and nicked, inactive, enzyme can be separated [54]. Binding of PQQ apparently leads to structural changes, as reflected by changes of spectral and chromatographic properties. Reconstitution of apoenzyme with PQQ analogues results in a decreased activity [157] and enantioselectivity [63,158] for the oxidation of chiral alcohols.

The interaction between PQQ and heme c has been characterized by the shift of the maximum absorption of the heme moiety in reduced and oxidized QH-ADH as well as by a 60 mV increase in the heme midpoint redox potential upon reconstitution of

apoenzyme with PQQ [53]. A shift of the  $^1\text{H-NMR}$  porphyrin methyl group resonances has been observed for the binding of PQQ in the oxidized form of the enzyme, while a shift of the methionine heme ligand accompanies binding in the reduced form [53]. The redox-dependent reorganization of surface residues at the heme edge of horse heart cytochrome *c* has similarly been related to the redox behaviour of the protein [159,160]. Spectroelectrochemical evidence for a conformational change triggered by heme reduction has been reported to accompany electron transfer in tetrahemic cytochromes  $c_3$  [161]. Distance constraints on the intramolecular positioning of the heme *c* and PQQ redox centers have been deduced from  $^{19}\text{F-NMR}$  relaxation studies employing fluorine-labeled phenylhydrazones of PQQ [162].

### **2.3.1. Kinetics of QH-ADH Type I from *C. testosteroni***

The kinetic mechanism of QH-ADH Type I has been described in detail for the oxidation of primary (chiral) alcohols and aldehydes using ferricyanide as an electron acceptor [69]. Initial rate data could be described by hexa uni ping pong kinetic schemes in which the alcohols are oxidized to the corresponding carboxylic acids and the intermediate aldehydes are released from the enzyme. For some substrates uncompetitive inhibition had to be invoked. In general, oxidation of aldehydes is much faster than the oxidation of the alcohols from which they are derived. Progression curve analysis suggested reversible inactivation of the enzyme to take place in proportion to the concentration of ferricyanide present at the start of the conversion. Simpler kinetic schemes are expected for the oxidation of secondary alcohols [163].

### **2.3.2. Structural model of QH-ADH Type I**

So far, X-ray crystallography of Type I QH-ADH from *C. testosteroni* has not been successful. A structural model has been constructed by homology modeling based on the sequence similarity of *N*-terminal residues 1-570 with the  $\alpha$  subunit of MDHs from *M. W3A1* and *M. extorquens*. [164]. The amino acid sequence of QH-ADH of *C. testosteroni* has been compared to other QH-ADHs and related MDHs by Stoorvogel and coworkers [156]. Only 34 % sequence identity was found with the sequences of MDHs. However, salient structural features appeared to be conserved on the primary sequence level. The repeated 'tryptophan motif' that constitutes the eight-bladed  $\beta$ -propeller fold is also present in QH-ADH. The active site residues, involved in PQQ and calcium binding, are completely conserved as well. The unique disulfide bridge and the

tryptophan responsible for the stacking of PQQ are found at the primary sequence level of the N-terminal domain of QH-ADH in the same position. The conservation of these residues strongly suggested a similar arrangement of the active site structure for QH-ADH. The presence of the tryptophan motif served as a scaffold for the building of the overall folding of the PQQ-binding domain. The C-terminal heme-binding domain, residues 571-677, absent in MDHs, has been modeled using minimal sequence similarity with cytochrome  $c_5$  from *Azotobacter vinelandii*, cytochrome  $c$  from *Plectonema boryanum*, and cytochrome  $c_{551}$  from *Ectothiorhodospira halophila* [165]. Using distant constraints inferred from  $^{19}\text{F}$ -NMR relaxation studies of trifluoromethylphenylhydrazine-derivatized PQQ bound to QH-ADH apoenzyme [162], as well as theoretical relations for optimal electron transfer [166,167], the relative positioning of the heme- and PQQ-binding domains was estimated (Figure 7).

The model successfully accounted for the site of proteolytic attack (see Section 2.2), the substrate specificity, the change of spectral properties upon reconstitution of apoenzyme with PQQ [53], and the electronic interaction between heme  $c$  and PQQ. A discussion on the implications of the model for the enantioselectivity displayed by the enzyme in the oxidation of chiral alcohols and aldehydes is presented in Section 4.

### **3. Mechanism of action of quino(hemo)proteins**

#### **3.1. Structural and chemical properties of PQQ and derivatives**

X-ray crystallography has played an important role in the detection and structure elucidation of PQQ. Kennard and coworkers reported the structure of the PQQ-acetone adduct which led to the identification of PQQ as a novel cofactor [1,118]. The structure of the dinitrophenylhydrazone of PQQ triester, an important derivative in early analytical protocols [168], was determined by van Koningsveld [169]. The structure of the pentahydrated disodium salt of PQQ has been reported by Urakami and coworkers [170], who also described quantum-mechanical calculations on the stacking ability of PQQ important for the formation of charge-transfer complexes with aromatic amino acids. Although the reaction of PQQ with tryptophan has recently been shown to lead to a different product [171], the stacking interaction clearly plays a role in the accommodation of PQQ in quinoproteins. X-ray crystallographic data for free PQQ and PQQ monopotassium salt are available as well [172]. The X-ray structure determination of C(4) and C(5) adducts of PQQ triester and methanol and their possible relevance to quinoprotein

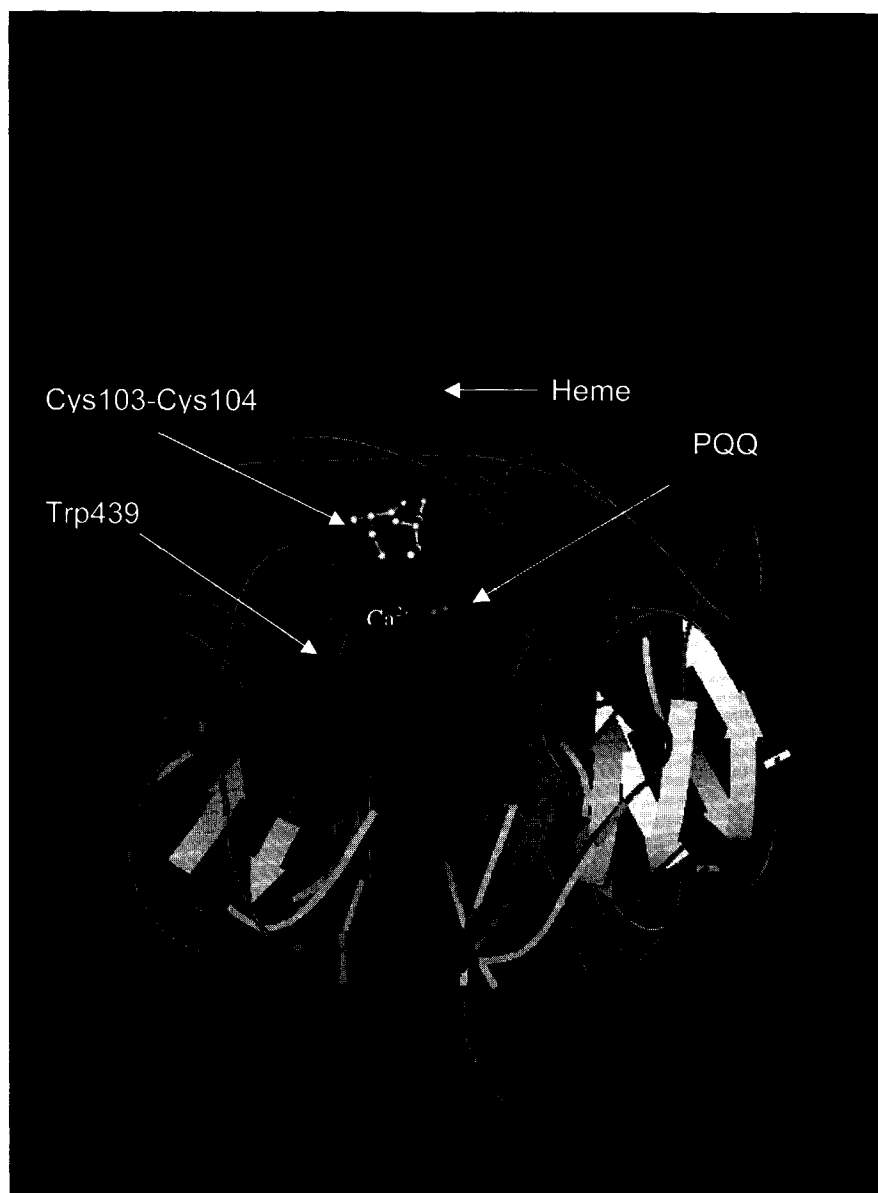


**Figure 7.** Representation of homology model for QH-ADH from *Comamonas testosteroni*. Heme, 8-membered cysteine bridge, PQQ and tryptophan shown using ball-and-stick representation, calcium using CPK representation. Picture generated with MOLSCRIPT version 2.0.2 [326].

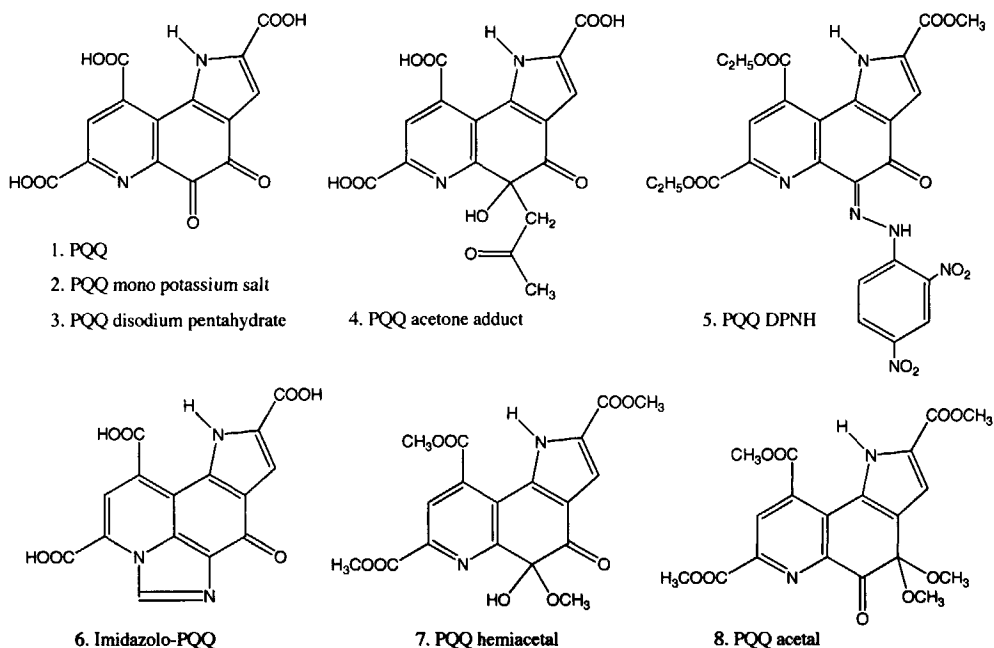


**Figure 8.** PQQ and PQQ-related compounds for which structures have been determined by X-ray crystallography. 1. PQQ [172]; 2. PQQ mono potassium salt [172]; 3. PQQ disodium pentahydrate [170]; 4. PQQ acetone adduct [1,118]; 5. PQQ dinitrophenyl hydrazone [169]; 6. Imidazolo-PQQ [171]; 7. PQQ-C(5) hemiacetal [133]; 8. PQQ-C(4) acetal [133].

catalysis have been reported [133]. An overview of X-ray structures that are currently known is given in Figure 8.

The X-ray structures show the PQQ molecule to be almost completely flat with only a slight dihedral angle between the heterocyclic rings ( $\pm 10^\circ$ ). The C(2) and C(7)-carboxylic groups are in the plane of the tricyclic ring system. The C(9)-carboxylic group is tilted by  $\pm 22^\circ$ . The non-planarity of this group has also been reproduced using high level *ab Initio* quantum chemical calculations [173-175]. Adducts of PQQ show a slight twist in the ring system most probably to accommodate the substituted  $sp^3$  carbon at the C(4) or C(5)-positions. In the mono-potassium complex [172] the  $K^+$  atom is liganded by the C(7) carboxyl group, the carbonyl O(5) and two waters in diad symmetry with another PQQ molecule. The resulting structure shows a high resemblance with the  $Ca^{2+}$ -complexes

found in the X-ray structures of the MDHs. Surprisingly, the positive charge of the potassium ion is balanced by complete ionization of the C(9) carboxyl group of the neighbouring PQQ molecule, leading to a reasonably strong hydrogen bond to the pyrrole N(1). Quantum chemical calculations show that this hydrogen bond may also be present in the non-ionized form of the C(9) carboxyl group.

Studies of the chemical reactivity of PQQ were greatly stimulated when various routes for its chemical synthesis became available [176-181]. Although the original procedures suffered from low overall yields, synthetic bottle-necks could be relieved [182-185] by appropriate adaptation of the procedure devised by Corey and Tramontano [176] or by novel strategies [186,187]. Methods for the microbiological production of PQQ have been described [188-190]. However, the commercial availability of PQQ (FLUKA, Buchs) still relies on chemical synthesis [191].

The pivotal role of the *o*-quinone moiety of PQQ in quinoprotein catalysis was recognized even before its structure was fully known [192]. The semiquinone, PQQH<sup>•</sup> (2), the quinol, PQQH<sub>2</sub> (3), and the tetrahydro derivative, PQQH<sub>4</sub> (4), can be obtained upon reduction (Figure 9). The biological relevance of compounds 1-3 has been well established [128]. A possible role for the keto alcohol derivative (5), a likely intermediate during borohydride reduction of PQQ to PQQH<sub>4</sub> under aerobic conditions [193], has been suggested (see Section 3.2). The existence of a two-electron oxidized lactone of PQQ has been claimed on the basis of mass spectroscopic data [194]. PQQ can be considered a medium-potential biological oxidant distinct from the high-potential quinones that have been applied in organic synthesis [195]. The redox chemistry of PQQ has been investigated by several groups. From potentiometric titrations of PQQH<sub>2</sub> at several pHs Duine and coworkers [196,197] determined the redox potential of the PQQ/PQQH<sub>2</sub> couple. Bergethon [198] investigated the amperometric detection of PQQ in HPLC analysis. Redox behaviour at acid pHs was determined by cyclic voltammetry [199]. McWhirter and Klapper [200] obtained a value for the redox potential of the PQQ/PQQH<sup>•</sup> couple at neutral pH from pulse radiolysis experiments. Eckert and coworkers compared redox properties of PQQ with those of related *o*-phenanthroline quinones [201,202].

The redox properties of a PQQ-ruthenium complex were determined by Schwederski

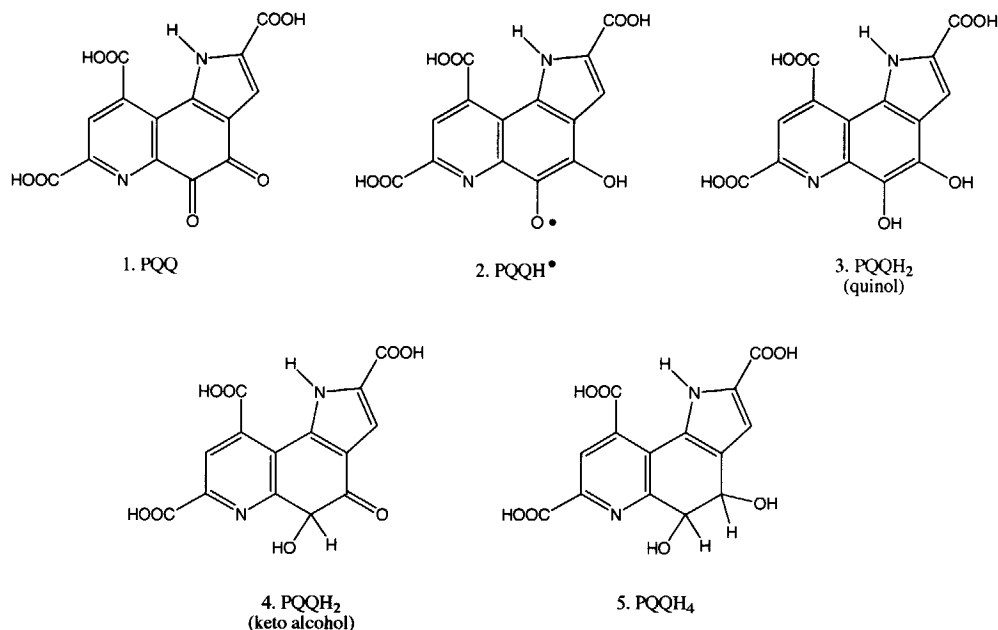


**Figure 9.** Currently known redox forms of PQQ. 1. PQQ; 2. PQQ semiquinone; 3. PQQH<sub>2</sub> (quinol form); 4. PQQH<sub>2</sub> (keto alcohol form); 5. PQQH<sub>4</sub>

and coworkers [203]. Itoh and coworkers described the electrochemical behaviour of the trimethyl esters of PQQ and its N(1)-methylated analogue in aprotic organic solvents [204]. Redox properties of PQQ are collected in Table II. These numbers may be compared to the value of +80 mV (vs NHE) of the heme *c* in *C. testosteroni* QH-ADH apoenzyme and +140 mV (NHE) in the holoenzyme [53].

The close resemblance of the structural features of PQQ and well-established chelating agents, e.g.  $\alpha$ -picolinic acid [205] and 8-hydroxyquinoline [206], has been noticed [207,208]. Equilibrium complexing of 9-decarboxyPQQ with Cd(II) at pH 4.0 (ionic strength 1.0, NaClO<sub>4</sub>) has been reported [207]. Formation of a 1:1 complex was deduced from titration plots [209]. Addition of Cu(II) apparently gave rise to 2:3 complexes. Both 1:1 and 1:2 complexes were observed in the titration of PQQ and several derivatives lacking oxygen substituents at C(4), and C(5), respectively, with Cu(II) [191].

In all cases, equilibrium constants were of order  $10^6 \text{ M}^{-1}$  [210]. Strong indications



**Table II.** Redox properties of PQQ and PQQ-Metal complexes

| Couple                     | Redox potential, V     |                   | Method                        | Refs.     |
|----------------------------|------------------------|-------------------|-------------------------------|-----------|
|                            | $E_m$ (NHE)            | $E_m$ (SCE)       |                               |           |
| PQQ/PQQH <sub>2</sub>      | 0.090 <sup>a</sup>     |                   | Potentiometric titration      | [197]     |
|                            | 0.15 <sup>b</sup>      |                   | Thin-layer cyclic voltammetry | [202]     |
| + Zn(II)                   | 0.17/0.23 <sup>b</sup> |                   | Thin-layer cyclic voltammetry | [202]     |
|                            | 0.053 <sup>c</sup>     | 1.75 <sup>d</sup> | Cyclic voltammetry            | [198,199] |
| PQQ/PQQH·                  | -0.122 <sup>e</sup>    |                   | Pulse radiolysis              | [200]     |
|                            | -0.218 <sup>f</sup>    |                   | Potentiometric titration      | [197]     |
| PQQH/PQQH <sub>2</sub>     | 0.22 <sup>e</sup>      |                   | Pulse radiolysis              | [200]     |
|                            | -0.242 <sup>f</sup>    |                   | Potentiometric titration      | [197]     |
| PQQ/PQQH-Ru                |                        | 0.82 <sup>g</sup> | Cyclic voltammetry            | [203]     |
| PQQH/PQQH <sub>2</sub> -Ru |                        | 0.26 <sup>g</sup> | Cyclic voltammetry            | [203]     |

a.  $10^{-4}$  M PQQ, 0.1 M phosphate, pH 7.0,  $5 \times 10^{-6}$  M phenazine methosulfate,  $K_3Fe(CN)_6$ ;

b. 0.5 M sodium acetate, pH 5.6;

c.  $10^{-4}$  M PQQ, 0.016 M phosphate/0.1 M NaCl, pH 7.0;

d.  $3 \times 10^{-4}$  M PQQ, 0.5 M KCl, pH 7.2;

e. Pulse radiolysis-generated  $CO_2^{\cdot-}$  in  $O_2$ -saturated 0.1 M formate, 5 mM phosphate, mmolar quantities of PQQ, pH 7.2;

f.  $10^{-4}$  M PQQ, 2 M salicylate, pH 13,  $K_3Fe(CN)_6$ , from semiquinone formation constant of 2.54;

g. Acetonitrile, 0.1 M  $(Bu_4N)PF_6$ . Adapted from [82]

were found for the involvement of the C(5)-covalent hydrate in complex formation [191]. Complexation of PQQ and PQQH<sub>2</sub> with calcium requires higher concentrations. Equilibrium complexation (50  $\mu$ M PQQ) was observed to occur at 100 mM  $Ca^{2+}$  in 20 mM MOPS/KOH, pH 7.5 suggesting an equilibrium constant of order  $10^3$   $M^{-1}$  [162]. Changes of the UV/Vis-spectrum are in accordance with the formation of a PQQ-hydrate- $Ca^{2+}$  complex. Similar changes have been observed upon addition of  $Ca^{2+}$  and  $Mg^{2+}$  to PQQ solutions [211]. Complex formation of PQQH<sub>2</sub> with calcium in the presence of dithiothreitol (1 mM) required similar concentrations of  $Ca^{2+}$  [162].

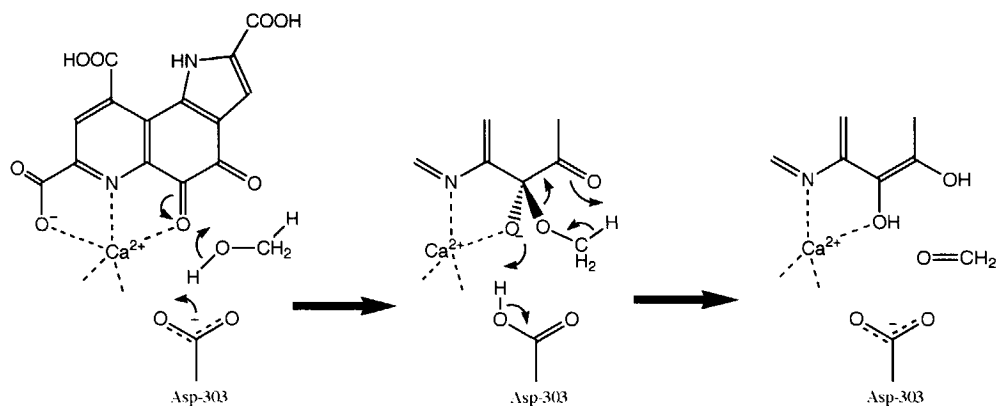
The affinity of PQQ for nucleophiles adding to the C(5) carbonyl group was discovered at an early stage [128,212-214]. Formation of C(4) adducts has been observed to occur when PQQ trimethyl ester is treated with methanol under acidic conditions [133]. Addition of amines as a first step in the oxidative deamination that was at one time believed to be a role of PQQ in quinoprotein amine oxidases and dehydrogenases that are now known to harbor different quinones, has been investigated by Itoh and

coworkers [215-218]. The relevance of these model systems for the understanding of the mode of action of TPQ [219-221] and TTQ [222,223] containing quinoproteins, as well as of the reactivity of PQQ in biological samples [224,225] has been addressed [6]. Reactions of PQQ with various carbonyl group reagents, aimed at the formation of stable derivatives for the extraction and identification of PQQ in alleged quinoproteins have obtained due attention. Competing activities of hydrazones in the reduction [226] and derivatization of PQQ [172,227] have been reported.

### 3.2. Proposed reaction mechanisms

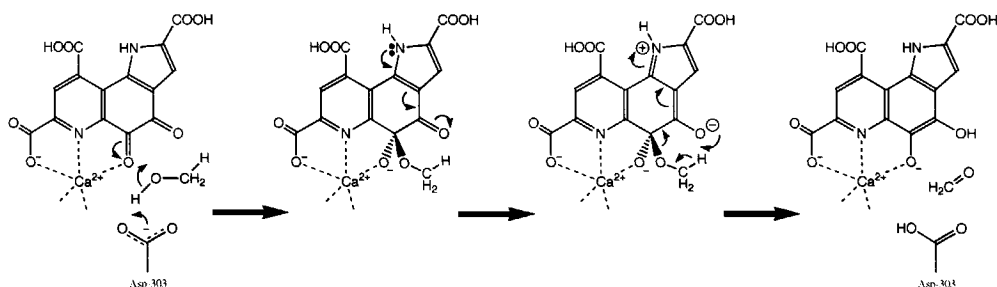
Methanol dehydrogenases have been the prime subject of investigations into the chemical mechanism of quinoprotein alcohol dehydrogenase catalysis. Early suggestions on the participation of three-electron reduced enzyme species [228] could not be substantiated [229]. A revised reaction scheme [230] was rejected in favor of the kinetic scheme presented in Section 2.2.1. (Scheme 1). Conversion of the oxidized, substrate-containing, complex into the reduced enzyme and product is generally considered to be the rate-limiting step in the reductive half reaction [123,129] (for a review see [11]). This is also the only step requiring ammonia or primary amines as activators for the enzyme as isolated. A covalent PQQ-substrate adduct appears to be a prime candidate for this role (Scheme 2). Evidence for the actual participation of such an adduct is, however, largely circumstantial. An important motivation has been provided by the well-documented reactivity of PQQ with a variety of nucleophiles [212,231], giving rise to the formation of C(5) carbonyl adducts [133]. The central position of such adducts in early mechanistic proposals is illustrated in Scheme 2.

The isolation of the corresponding PQQ-adducts (Figure 3) from cyclopropanol- (and cyclopropanal-) inhibited MDH has been considered as a major indication for the involvement of an active site base setting up the alcohol for nucleophilic addition. This assumption was further supported when the X-ray structures revealed an aspartate residue (Asp303 in *M. extorquens* MDH) situated in an appropriate position for proton abstraction. Curiously, changing this residue into a glutamate by site-directed mutagenesis resulted in a highly active enzyme with, however, a much lower substrate affinity [115]. This situation appears to be in contrast with observations on the flavoprotein-catalyzed oxidation of acyl-CoA [232] where replacement of a glutamate



**Scheme 2.** Proposed reaction mechanism of MDH involving covalent adduct formation of PQQ and methanol followed by deprotonation and rearrangement

residue with very similar function by an aspartate leads to severe reduction of the reaction rate, suggesting a crucial dependence on the correct “spacing”. Also, while hemiketal formation at C(5) would position the substrate  $\alpha$ -hydrogen in a geometrically favorable configuration for transfer to PQQ via a six-membered transient, several objections can be raised. Of trivial importance is the notion that whereas free PQQ hardly requires catalysis for adduct formation, PQQ in MDH would require explicit base catalysis. This, of course, may well be caused by the specific environment of PQQ in MDH. An issue of more importance is the proton abstraction by the remaining carbonyl at C(4), an entity that is not normally known for its high basicity. Scheme 3 addresses a possible role of the pyrrole nitrogen in the promotion of the basic strength of this carbonyl group by conjugation [233] (Scheme 3).



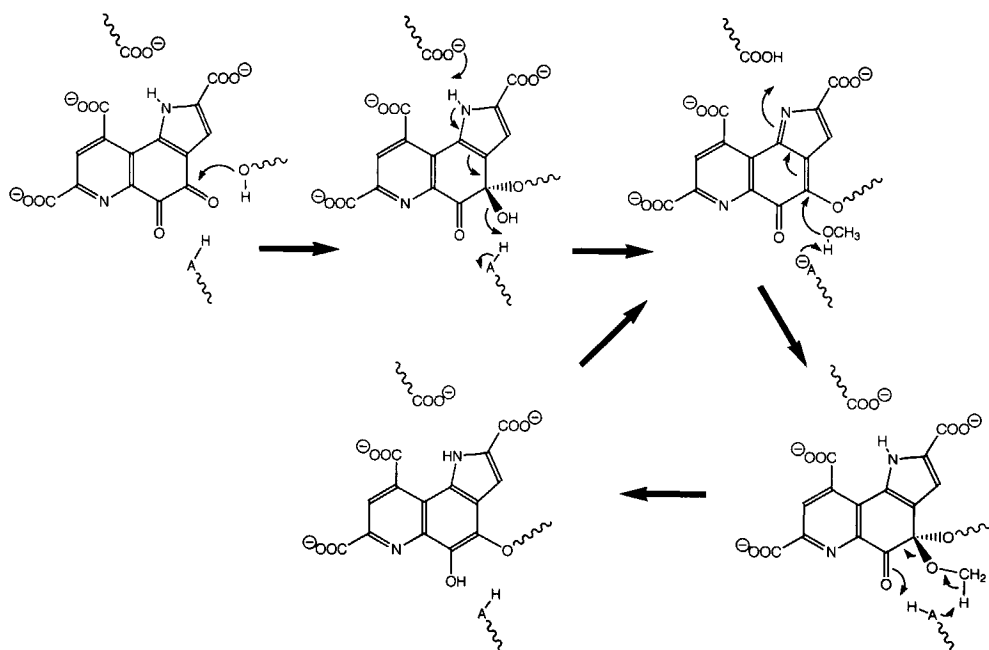
**Scheme 3.** Proton abstraction facilitated by charge separation.

It is not clear whether charge separation as shown in Scheme 3 will be an important contribution to the basic properties of the C(4)-carbonyl group. Comparison of the  $^{13}\text{C}$  NMR chemical shifts of the C(5) and C(4) carbons indeed shows the C(4) atom to be slightly more shielded (DMSO- $d_6$ , ppm, 173.3 (C-4); 179.3 (C-5); [231]). The (slight) difference of the electrophilic characteristics of the carbonyl groups that form the *o*-quinone moiety of PQQ has been investigated by Itoh and coworkers in terms of the formation and relative stability of (hemi)ketals [133]. A mechanistic proposal was designed that elaborated earlier suggestions [196,234] on the possible participation of a *p*-quinonoid tautomeric structure of PQQ (Scheme 4).

It must be emphasized that N(1)-alkylated PQQ analogs show low but definite activity in the reconstitution of Type I QH-ADH apoenzyme from *C. testosteroni* [157]. In these experiments possible contamination of the derivative with authentic PQQ could be rigorously excluded by determining the different enantioselectivity of the resulting holoenzyme [158].

Although the possibility that PQQ might behave as a *p*-quinone cannot be rejected as yet, the physiological relevance of the proposed mechanism [133] depends strongly on the alleged presence of a suitably situated serine or threonine residue in the active site (see Section 2.1.2 for discussion of the erroneous assignment of the orientation of PQQ in early crystal structure). Currently available high-resolution X-ray data, however, do not support this view.

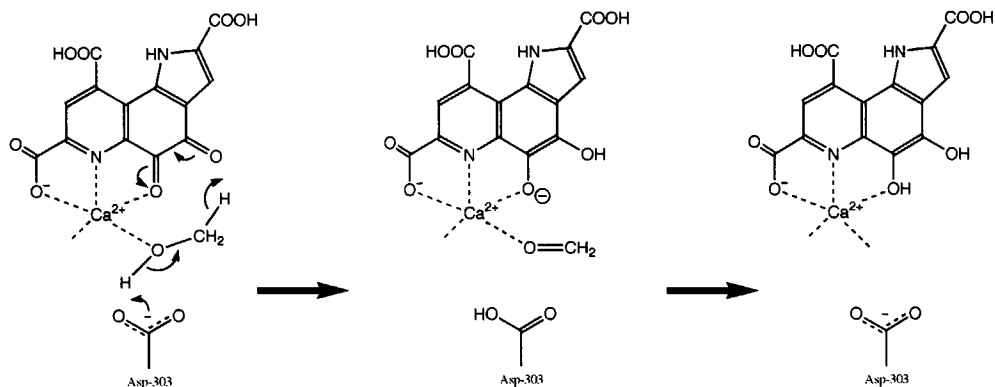
While these proposals considered covalent addition of the substrate alcohol to PQQ as a primary event, an interesting possibility was raised when the importance of  $\text{Ca}^{2+}$ , both as a structural and as a catalytic factor became evident (in the structures of MDH from *M. extorquens* and *M. W3A1*,  $\text{Ca}^{2+}$  is situated in the plane of the PQQ molecule with the C(7) carboxy group, the N(6) pyridine nitrogen and the C(5) oxygen as equatorial PQQ-derived ligands. Contributions from Asn 261, Glu 177, and a solvent water molecule complete the coordination. The role of  $\text{Ca}^{2+}$  in the catalytic mechanism is supported by a series of interesting observations, including a  $\text{Ca}^{2+}$ -lacking mutant enzyme devoid of activity [235], of which the activity could be restored (in part) by addition of  $\text{Ca}^{2+}$ ,  $\text{Ba}^{2+}$  or  $\text{Sr}^{2+}$  [108,236-238]. In the mechanisms shown in Schemes 5 and 6,  $\text{Ca}^{2+}$  is portrayed as a Lewis acid promoting the polarization of the C(5) carbonyl for the transfer of a hydride [11,107].



**Scheme 4.** Possible participation of enzyme-bound *p*-quinonoid vinyllog ester

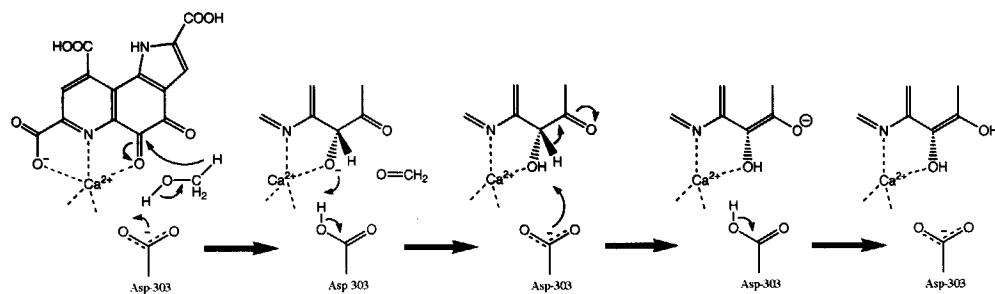
**Table III.** PQQ-containing (hemo)quinoproteins for which the presence of  $\text{Ca}^{2+}$  (and closely related metal ions) has been established

| Enzyme               | Source                      | Metal ion                       | Metal ions capable of replacing $\text{Ca}^{2+}$  | Refs.         |
|----------------------|-----------------------------|---------------------------------|---|---------------|
| MDH                  | <i>Hyphomicrobium X</i>     | $\text{Ca}^{2+}$                |   | [309]         |
|                      | <i>M. W3A1</i>              |                                 |   | [76,322]      |
|                      | <i>M. extorquens</i>        | $\text{Ca}^{2+}$                | $\text{Sr}^{2+}$ , $\text{Ba}^{2+}$   | [119,255]     |
|                      | <i>P. denitrificans</i>     | $\text{Ca}^{2+}$                | $\text{Sr}^{2+}$  | [64,128,129]  |
| QH-ADH (Type I)      | <i>C. testosteroni</i>      | $\text{Ca}^{2+}$                | $\text{Mg}^{2+}$ , $\text{Sr}^{2+}$ , $\text{Co}^{2+}$ , $\text{Cd}^{2+}$ , $\text{Ba}^{2+}$ , $\text{Ni}^{2+}$ , $\text{Fe}^{2+}$ , $\text{VO}^{2+}$ | [66,123]      |
| QH-ADH (Type II)     | <i>Acetobacter sp.</i>      | $\text{Ca}^{2+}$                | $\text{Sr}^{2+}$  | [66]          |
| EDH                  | <i>P. aeruginosa</i>        | $\text{Ca}^{2+}$                | $\text{Sr}^{2+}$  | [228]         |
| GDH (soluble)        | <i>A. calcoaceticus</i>     | $\text{Ca}^{2+}$                | $\text{Mn}^{2+}$ , $\text{Cd}^{2+}$   | [77,116]      |
| GDH (membrane bound) | <i>E. coli</i>              | $\text{Ca}^{2+}/\text{Mg}^{2+}$ | $\text{Sr}^{2+}$ , $\text{Co}^{2+}$ , $\text{Cd}^{2+}$ , $\text{Ba}^{2+}$ , $\text{Fe}^{2+}$ , $\text{Zn}^{2+}$                                       | [72,208]      |
| PVA-DH               | <i>Pseudomonas sp.VM15C</i> | $\text{Ca}^{2+}$                |   | [131,270,271] |



**Scheme 5.** Hydride transfer by Lewis acid catalysis (I)

A variation of the hydride transfer mechanism, based on high-level quantum mechanical calculations [175] is shown in Scheme 6.



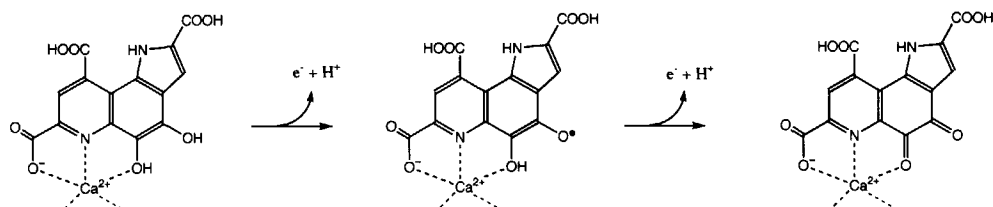
**Scheme 6.** Hydride transfer by Lewis acid catalysis (II)

Despite the great variety of mechanisms, some of the basic features of MDH catalysis are not covered by these proposals. Except, possibly, for some of the early suggestions [196,234], none of the schemes addresses the role of the activator ammonia. There may be some justification in the fact that ammonia (as the free base) is required as an activator only when the enzyme is assayed with artificial electron acceptors. With cytochrome as an electron acceptor, ammonia is not usually needed [124,128,236,239]. In this respect, both Type I and II QH-ADHs behave quite differently. No activator is required. It might

be argued that a lysine residue, conspicuously present in the active site cavity of the QH-ADH homology models, assumes this role. An alternative function for this residue in the accomodation of product aldehydes has been proposed [157]. If one accepts the possibility that the natural electron acceptor, cytochrome  $c_L$  of MDHs overcomes the need for an amine-type activator in the oxidized enzyme-substrate complex, i.e. by providing a lysine of suitable basicity under physiological conditions, it would appear that the kinetic scheme of a hexa-uni ping-pong reaction [123,124] is no longer valid and should be replaced by ternary complex kinetics involving oxidized enzyme, substrate/product, and cytochrome, most probably in a rate-controlling step. The ability of ammonia to restore enzyme activity when critical catalytic basic residues have been mutated has been described [240]. In this respect, restoration of activity by addition of ammonia for an inactive Lys258Ala mutant of *Escherichia coli* aspartate aminotransferase is of interest [241,242]. Not only was the degree of restoration found to be dependent on the type and concentration of the amine added, also a correlation between the logarithm of the efficiency and the pKa of the amine was observed. These results suggest that exogenous amines would substitute the functional role of Lys258. This approach has been applied to Lys296-substituted rhodopsin [243], Lys80-substituted leucine dehydrogenase [244], and Lys329-substituted ribulose 1,5-bisphosphate carboxylase/oxygenase [245].

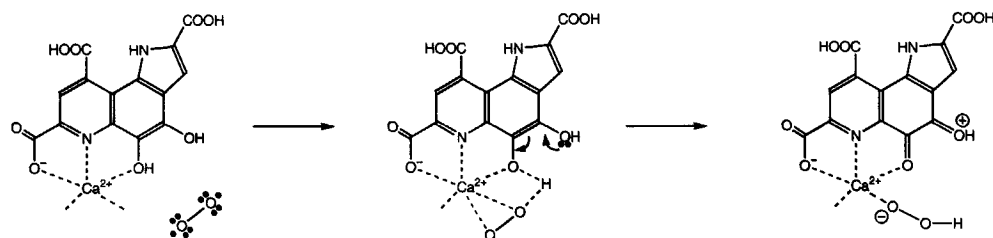
Suggestions for the oxidative half-reaction of MDHs feature the free-radical semiquinone form of PQQ with the unpaired electron localized in the *o*-quinone moiety (Scheme 7). There would appear to be little reason to speculate on the possible localization of the unpaired electron at the C(4) oxygen of MDH from *M. extorquens* [11] (or the C(5) oxygen in MDH from *M. W3A1*, for that matter [20]) in order to rationalize the out-of-plane positions of these atoms in the respective X-ray structures. Neither the extent of refinement, nor the hybridization state warrants such a proposal. Structures reported in the literature for cation-stabilized radicals derived from *o*-benzoquinones give no indication for out-of-plane positions of the oxygen atoms [246,247].

Although MDHs and QH-ADHs reported to date are dehydrogenases, with the possible exception of an extracellular quinoprotein oxidase that catalyzes conversion of enacyloxin IVa to enacyloxin IIa, for which the involvement of PQQ has not been unequivocally established [248], models for the reaction of PQQH<sub>2</sub> with dioxygen have



**Scheme 7.** Oxidative half-reaction of MDH.

been investigated. Indications for the role of  $\text{Ca}^{2+}$  in the oxidation of PQQH<sub>2</sub> trimethyl ester in acetonitrile have been found [249].  $\text{Ca}^{2+}$  was shown to have a catalytic effect on this oxidation. An electron-transfer mechanism (SET) was proposed analogous to the reaction of 1,5-dihydroflavins with  $^3\text{O}_2$ . Schürer and Clark used the results of semiempirical (PM3) MO calculations to propose that the oxidation of PQQH<sub>2</sub> with dioxygen may proceed by successive hydrogen-atom-transfer steps [250] (Scheme 8).



**Scheme 8.** Oxidation of PQQH<sub>2</sub> with dioxygen.

An electron-transfer mechanism is deemed unlikely. The authors conclude that the reaction of PQQH<sub>2</sub> trimethylester with  $^3\text{O}_2$  to give a triplet radical pair is a spin allowed reaction with  $\text{Ca}^{2+}$  acting as an electrostatic catalyst in the reoxidation of reduced PQQ. The suggestion that ‘..this might possibly be the best documented example of this type of catalysis in biological systems..’ [250], completely disregards the fact that PQQ-containing *oxidases* are not particularly abundant in nature. So far, the X-ray structures of MDHs do not provide a clear answer as to the reason for the fact that dioxygen does not function as an electron acceptor for these enzymes. It could be argued, though, that dioxygen can not, in the enzyme, compete favorably with other calcium ligands so that the situation created in the model systems simply does not arise. Similar insensitivity to



dioxygen is observed for reduced QH-ADHs. An observation that may be of interest to rationalize the presence of TPQ in oxidases and PQQ in dehydrogenases has been reported by Kalyanaraman and coworkers [251] who found that semiquinones of certain catechol(amine)s react with oxygen with rates of order  $10^5 \text{ M}^{-1} \cdot \text{s}^{-1}$  (a value corresponding to  $25 \text{ s}^{-1}$  for ambient (8-9 ppm) oxygen concentrations), while those of hydroxy-substituted catechol(amine)s react with rates two to three orders of magnitude higher.

The possible role of the disulphide bridge in the release of protons concomitant with the successive single electron oxidations of PQQH<sub>2</sub> (Scheme 7) has been investigated [252,253]. Reduction with dithiothreitol aborts the activity with cytochrome, however, oxidation with artificial electron acceptors was not impaired [252], most probably because these oxidants rapidly restore the disulphide bridge. Mechanistic involvement as proposed for the rare thiol-disulphide oxidoreductase family [254,255] is unlikely. A role in the stabilization of the semiquinone intermediate has been suggested [253].

#### 4. Alternative mechanistic possibilities

Despite the plethora of proposals discussed in Section 3, more than twenty years of intense research has provided only limited insight into the chemical mechanism of quinoprotein alcohol dehydrogenase catalysis. An important aspect of this quest has been the lack of chemically relevant model systems that might be of value to probe various effects thought to contribute to catalysis in the physiologically active enzyme. Whereas model systems for the reaction of PQQ with amines [216-218], amino acids [215,225], thiols [256], glucose [257], pyridoxamine phosphate [258], and even epoxidation reactions [259], have been explored, similar reactions of free PQQ with alcohols mimicking its function in MDHs and QH-ADHs have been hard to design. Curiously, the adduct (Figure 3) resulting from the reaction of PQQ with cyclopropanol has been found to rearrange under basic conditions (pH 11, [230]) or in the NMR tube (neutral pH, 30 °C [129]) to give PQQH<sub>2</sub> and propenal. This observation summarizes a most peculiar situation: 1. The *non-natural* reaction, i.e. redox-neutral formation of PQQ-cyclopropanol adduct, occurs "for free" in MDH, while it takes intricate chemistry in the laboratory [129], whereas: 2. The *natural* reaction, i.e. exchange of redox equivalents between PQQ and cyclopropanol in the preformed adduct occurs readily in the NMR tube and not at all in the enzyme that is supposed to be equipped with the full machinery for just this type of (redox) reaction! Clearly, this anomaly should inspire some caution as

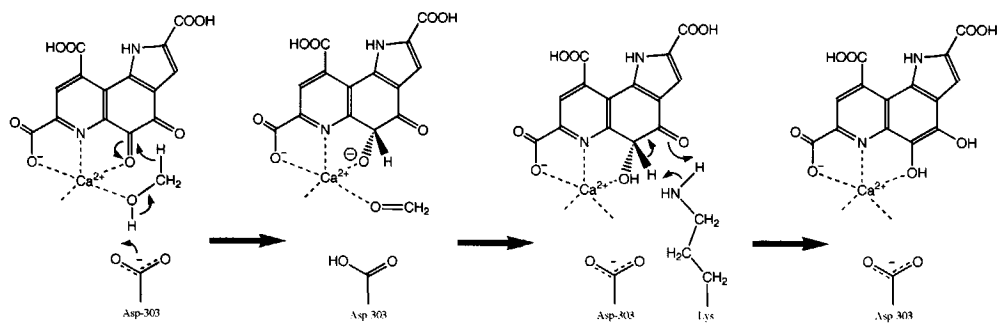
to the mechanistic relevance placed on the inhibition of MDHs with cyclopropanol. Another reason for concern is provided by the fact that the stereochemical features of the PQQ-cyclopropanol adduct extracted from cyclopropanol-inhibited MDH have not been established, leaving the possibility open that the adduct may contain both configurations at the C(5) position. In comparison: the PQQ-acetone adduct isolated upon extraction of PQQ from MDH of a methylotrophic bacterium could be identified as the racemic mixture [1,118], suggesting its formation outside the active site. This conclusion has found support in the finding that QH-ADH apoenzyme from *C. testosteroni* accepts only one enantiomer of synthetic racemic PQQ-acetone adduct mixture upon reconstitution [157]. In summary, the emphasis that has been put in the past on the exemplary role of cyclopropanol inhibition in MDH catalysis may have been misplaced. Again, this notion is supported by the fact that QH-ADHs that catalyze essentially the same reaction type using the same cofactor are not inhibited by cyclopropanol [260].

#### 4.1. Lewis acid catalysis

In this respect, the recent suggestions for a more dominant role of  $\text{Ca}^{2+}$  in catalysis (Scheme 6) deserve proper attention. Model studies by Itoh and coworkers [261] using the trimethyl ester of PQQ in organic solvent with DBU as a base, showed the oxidation of methanol to formaldehyde to be significantly enhanced by addition of calcium [233]. Some caution is due, however, since the system is very similar to the conditions described by Skibo and Lee [262] for the rather unnatural oxidation of methanol with a heterocyclic quinone in the presence of strong base (methanolate). Still, it would appear that the generation of negative charge on the alcohol oxygen does set up the system for the hydride transfer, a line of reasoning that has been investigated recently using quantum chemical calculations by Bruice and coworkers [175]. If their suggestions hold, the chemistry involved would be very similar to the well-studied Meerwein-Ponndorf-Verley, Oppenauer, and Cannizzaro reactions. In retrospect, an early report on Lewis acid chemistry using aluminum *t*-butoxide as a catalyst for the biomimetic oxidation of alcohols by PQQ trimethyl ester in organic solvent deserves to be mentioned [263].

Considering the experimental evidence for the formation of a covalent adduct during methanol dehydrogenation, some support can be obtained from the observation of a slight shift in the UV-Vis spectrum, attributed to a possible intermediate in the reaction of MDH with deuterated methanol [128,264]. However, finding similar values for the

energies of the covalent adduct and the  $\text{Ca}^{2+}$ -ligated alcoholate calculated by Zheng and Bruice [175] suggests another possibility. As these authors concluded, the covalent adduct may well be at a mechanistic side road. Partitioning into this non-committed species could then occur for the deuterated alcohol. For MDH, the conversion from the oxidized enzyme-substrate complex [ $\text{MDH}_{\text{ox}}\cdot\text{S}$ ] to reduced MDH and product has been proposed as a rate-limiting step in the catalytic cycle. To get beyond this step requires the presence of activator. Compared to unlabeled methanol, use of  $^2\text{H}_3\text{COH}$  (1 mM) leads to a sevenfold decrease in the rate bringing it to  $8.5 \times 10^{-3} \text{ s}^{-1}$ , clearly indicating that an intramolecular hydrogen transfer from substrate to PQQ is involved. In the absence of activator, this step is independent of pH, suggesting that acid- or base-catalyzed proton transfers are not rate-limiting. In the presence of saturating concentrations of the activator, the rate constant increases more than 400-fold, while the deuterium isotope effect decreases from 7 to 1.4 [128]. In a preliminary attempt to rationalize these findings on the basis of current ideas, we propose a mechanistic scheme in which the activator functions in the equilibration of a primary keto alcohol form of PQQ and the tautomeric diol,  $\text{PQQH}_2$ . The situation as it might apply to QH-ADH-catalyzed reactions is shown in Scheme 9.



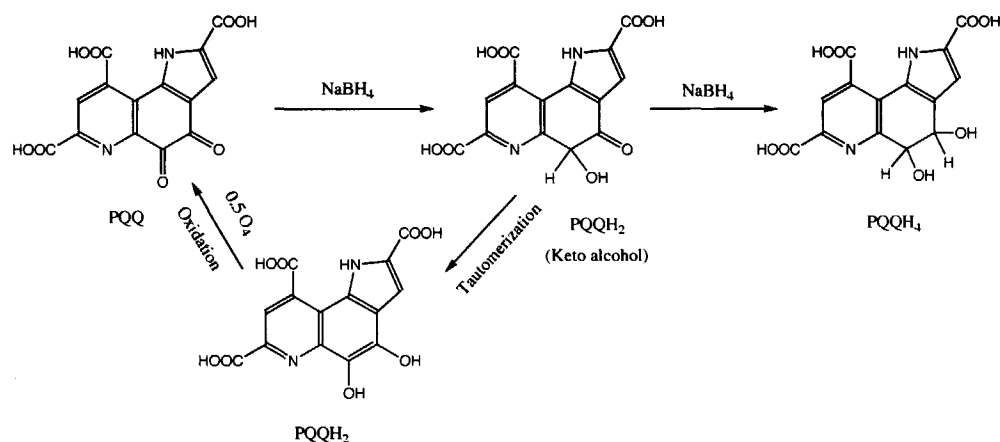
**Scheme 9.** Proposed role for lysine in QH-ADHs as a natural activator in quinoprotein alcohol dehydrogenase catalysis.

It must be emphasized that the experimentally found release of product aldehyde *after* addition of ammonia in the reaction catalyzed by MDH does not necessarily invalidate this proposal, since it may be hypothesized that a prolonged lifetime of the primary C(5)-reduced PQQ in the absence of activator could well force the substrate into a different

mode of action characterized by a substantial kinetic isotope effect, KIE. Also, the binding of aldehydes to calcium is almost as strong as that of the alcohols [265]. In view of the structural similarity of C(5) hemiketals and the  $\text{PQQH}_2$  tautomeric form, its UV-Vis and fluorescence spectroscopic properties are likely to be similar. So far, indirect, but highly compelling evidence has been obtained for the existence and chemical stability of this tautomeric form of  $\text{PQQH}_2$  [191]. As shown in Scheme 10, this species most probably occurs as an intermediate during the complete reduction of PQQ to give the non-physiological  $\text{PQQH}_4$  compound. A similar mechanism has been proposed for the reduction of 1,10-phenanthroline-5,6-dione [2] and the synthesis of (trans)-dihydroquinols [266,267].

In view of the 100-fold excess of borohydride that is required to bring the reduction to completion (in the presence of dioxygen to recycle  $\text{PQQH}_2$ ) the stability of the primary reduction product is expected to be low, however, the conversion is carried out at high pH (0.1 M NaOH) which may promote rearrangement to the more stable  $\text{PQQH}_2$  tautomer. Its lifetime under neutral conditions may well be extended.

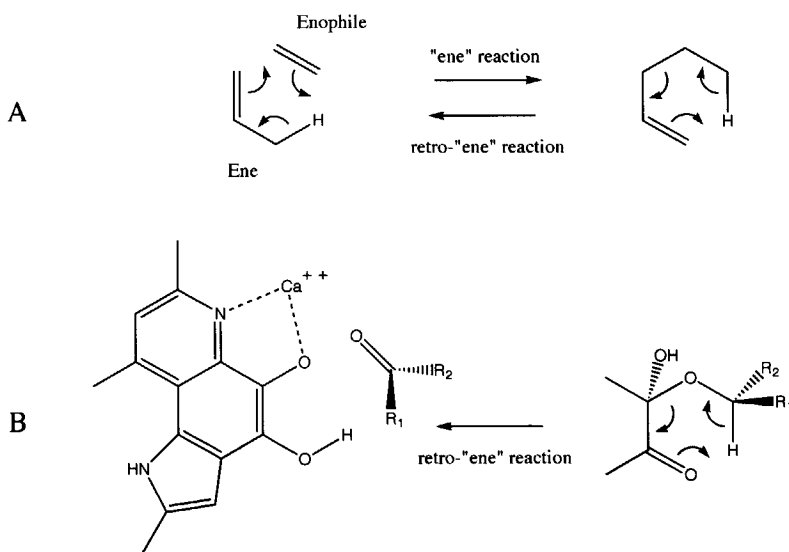
The computational studies by Zheng and Bruice [175] addressed above were initiated with the intention to explore the possible involvement of a PQQ hemiketal intermediate



**Scheme 10.** Occurrence of the intermediate keto alcohol as a tautomeric form of  $\text{PQQH}_2$  in the synthesis of  $\text{PQQH}_4$  from PQQ under aerobic conditions.

followed by a 'retro-ene' rearrangement [268] leading to oxidized substrate and reduced PQQ (Scheme 11)

From the results of high-level quantum mechanical calculations it was concluded that hydride transfer might be driven by the generation of a negative charge on the incoming alcohol. Subsequently, the possible formation of a hemiketal intermediate followed by a 'retro-ene' reaction was rejected since these reactions are known to be slow and proceed at high temperatures only [269-271]. Direct hydride transfer to the C(4) carbonyl oxygen, as implied in Scheme 11 would be possible, but not very likely. The authors conclude from their *ab Initio* calculations that formation of the hemiketal intermediate might not be on the primary reaction path. Instead, the alcoholate complexed to the calcium, has been proposed as the mechanistically relevant configuration. Facilitation of alcoholate formation by a cation that is not normally considered a typical Lewis acid appears feasible. For comparison, study of the proton transfer kinetics in carbonic anhydrase suggested that the proton from a water molecule ligated to the  $Zn^{2+}$  ion acquires  $pK_a \approx 7$  [272]. A similar effect in the case of methanol complexing with  $Ca^{2+}$  would bring its  $pK_a$  in the range for proton abstraction by the active site base (Asp303 in MDHs). On this basis, a comparison with the more general hydrogen transfer reactions mentioned above

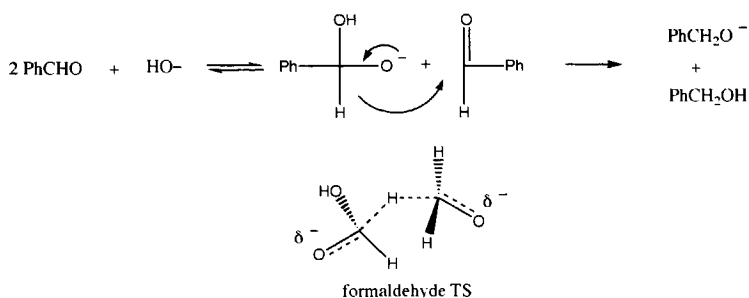


**Scheme 11.** Retro-ene reaction. A. General mechanism. B. Applied to PQQ/ $Ca^{2+}$

could be of interest.

Meerwein-Ponndorf-Verley reductions (and the complementary Oppenauer oxidations) normally require mild reaction conditions. A readily oxidizable hydrogen donor and a simple ketone are the prerequisites for this reaction to occur. The reaction is catalyzed by metal alkoxides such as  $\text{Al}(\text{O}i\text{-Pr})_3$ . The activity of these catalyst is related to their Lewis acid character in combination with ligand exchangeability. The reaction mechanism is commonly believed to involve a six-membered transition-state. The alcohol reactant is coordinated as an alkoxide to the metal centre. Activation of the carbonyl by coordination to the metal initiates the hydride transfer from alcoholate to the carbonyl function. The use of calcium as Lewis acid has not been frequently mentioned, however, interesting observations have been made using barium as a Lewis acid in the reaction with 4-hydroxycyclohexanone [273]. In a series of experiments using constant ratios of  $i\text{-PrO}^-/i\text{-PrOH}$  in the reaction medium, the rate of *intermolecular* hydride transfer was seen to increase with increasing Lewis acid character of the cation with  $\text{Al}^{3+} > \text{Li}^+ > \text{Ba}^{2+} > \text{Na}^+ > \text{K}^+$ . Under identical conditions, it was found that the *intramolecular* hydride transfer increased in a reversed order with  $\text{Ba}^{2+} > \text{K}^+ > \text{Na}^+ > \text{Li}^+ > \text{Al}^{3+}$ , in line with increasing metal-oxygen basic character. It was concluded that the reversal of the rate order must be a function of the way in which the oxygens are configured in the transition state for hydride transfer. If a cyclic transition state is possible, the reaction catalyzed by the better Lewis acid will be favored whether intra- or intermolecular. On the other hand, when a cation-linked cyclic transition state is stereochemically prohibited, hydride transfer is favored by the greater negative charge build-up on the oxygen atoms, i.e. by the poorer Lewis acid and the stronger base. This might well be the way in which  $\text{Ca}^{2+}$  functions in MDH and QH-ADH catalysis since a *planar* cyclic transition state cannot be readily adopted in the enzyme active site due to steric constraints. Interestingly, single electron transfers (SET), i.e. radical reactions, have on occasion been observed in the MPV reaction [274-278]. By analogy, an earlier suggestion for the mechanism of inactivation of MDH with cyclopropanol, involving the formation of a radical pair [279] might be reconsidered.

Current ideas with respect to the mechanism of the related Cannizzaro reaction favor a hydride transfer from  $\text{RCH}(\text{OH})\text{O}^-$  to  $\text{RCHO}$  in an inefficient stepwise mechanism [280].



**Scheme 12.** Cannizzaro reaction of benzaldehyde and proposed TS for formaldehyde reaction (according to [280]).

These views are in complete support of the mechanism as originally proposed by Swain [281,282]. *Ab Initio* calculations on the HO<sup>-</sup>/CH<sub>2</sub>O model system infer a low lying energy state for the tetrahedral species HOCH<sub>2</sub>O<sup>-</sup>. When this species approaches formaldehyde two competitive reactions can occur. The first alternative is nucleophilic attack of the alkoxide center of the energized ion at the electrophilic carbon of formaldehyde. This proceeds without barrier and via a deep channel to form HOCH<sub>2</sub>OCH<sub>2</sub>O<sup>-</sup>. The second reaction is the Cannizzaro process and is essentially irreversible. The hydride transfer is not linear, the activation barrier is low, but the reaction channel is narrow. The unfavorable orientation of the reacting species, HOCH<sub>2</sub>O<sup>-</sup> and CH<sub>2</sub>O, required to allow passage over the saddle point of the potential energy surface makes the probability of the Cannizzaro reaction low and less likely to be of relevance for the reaction mechanism of quinoprotein alcohol dehydrogenases. On the other hand, both MDHs and QH-ADHs have been found to catalyze the oxidation of aldehydes, in most cases with higher efficiency than the corresponding alcohols [69]. The measured deuterium isotope effects of Cannizzaro reactions are generally low (1.8 in the case of benzaldehyde) [283], these numbers compare favorably with the numbers found for MDH catalyzed oxidations in the presence of activator [129].

Both the MPV, and the Cannizzaro reaction involve hydride transfer to a carbon centre while the proposal by Zheng and Bruice [175] favors hydride transfer to the C(4)-oxygen. Preliminary calculations carried out by the present authors suggest that the reason for this difference could be caused by the undue relaxation of the position of the Ca<sup>2+</sup>-ion in the computational protocol of Zheng and Bruice which disregards the full

coordination shell of  $\text{Ca}^{2+}$  in MDH (and has the stereochemistry of the  $\text{Ca}^{2+}$ /PQQ complex inverted!). From the data provided [175] it appears that the metal-ion has shifted position towards the *o*-quinone moiety allowing the hydrogen that is to be transferred to come within reach of the accepting oxygen at C(4). Within the geometrical constraint set by the active sites of MDH (and QH-ADHs, see below), hydride transfer to C(5) carbon appears to be preferred. At this point, the enantioselectivity of QH-ADHs for secondary alcohols has been used to provide corroborative evidence [67,164].

#### 4.2. Molecular modeling of QH-ADH enantioselectivity

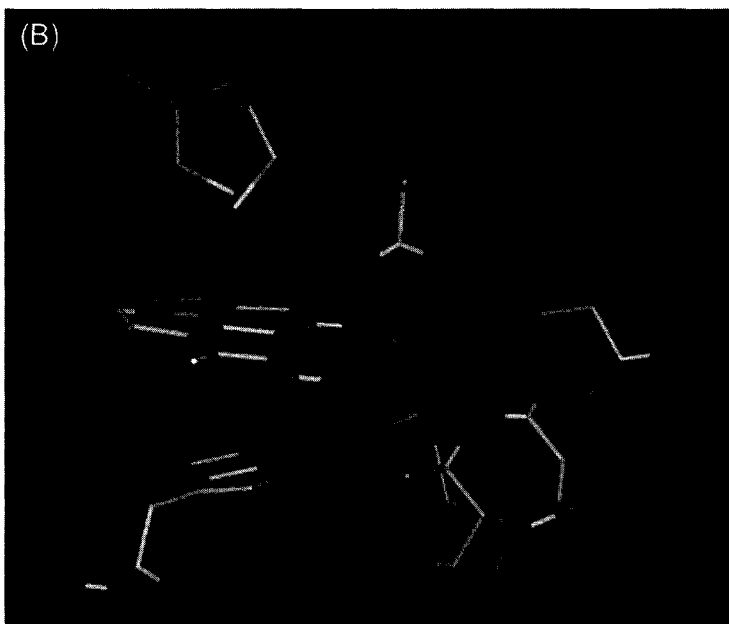
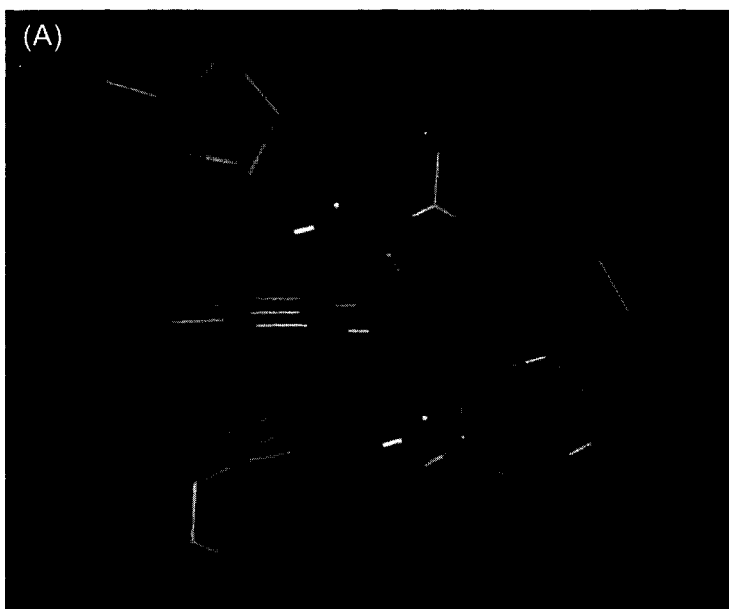
Molecular modeling of enzyme enantioselectivity has gained some popularity in the field of hydrolases, notably proteases [284-288] and lipases [289-295]. The protocols that have been developed for this purpose aim at the estimation of the Gibbs free energy difference between the two enantiomer-enzyme complexes in the enantioselectivity-determining step of the catalytic cycle. The tetrahedral intermediate formed upon nucleophilic addition of the catalytic serine to the substrate (peptide or ester) carbonyl function is accepted to be a reasonable approximation of the actual transition state [296-298]. Recalling the relation between the enantiomeric ratio,  $E$ , and the Gibbs free energy difference,  $\Delta\Delta G^\ddagger$ , of the relevant transition states, one has  $RT \ln E = \Delta G_{spec,S}^\ddagger - \Delta G_{spec,R}^\ddagger = \Delta\Delta G^\ddagger$  (Section 1). Assessing  $\Delta\Delta G^\ddagger$  directly requires extensive computational efforts. Thermodynamic integration, TI, protocols have been reported [289], as have the reasons for their failure [299]. Hybrid quantum mechanical and molecular mechanical, QM/MM, methods have been developed [300] and used [301,302] to obtain values for free energy differences. A computationally less expensive approach is to calculate forcefield potential energies and equate these to the corresponding  $\Delta\Delta G^\ddagger$ -value. Clearly, the entropic contribution, which has been shown to be of substantial magnitude [66,74], will then be neglected. This may not be warranted for QH-ADH-catalyzed enantioselective conversions. Examples of QH-ADH enantioselectivity have been reported where the entropic contribution actually exceeds the enthalpic contribution [67]. A simple and computationally inexpensive method starts by constructing the TS model structure and searches the conformation space by suitable molecular dynamics algorithms [295]. In principle, a qualitative estimate of the relative stabilities of the TSs can be obtained when certain criteria satisfied. Such criteria include the number of hydrogen bonds, absence of clashes, and most importantly limited root-mean-square, rms, deviations of the structures searched during the dynamics runs as



compared to the starting structure. For this condition to hold, the starting structure has to be of good quality. This requirement is also commonly acknowledged from a slightly different perspective [303]: "In order to understand the mechanism of action of an enzyme, it is necessary to determine, as precisely as possible, the tertiary structure of the protein ...". Clearly then, when good quality structures (MDH) do not provide the answers homology models (QH-ADH) will be even less meaningful. Still, computational efforts on QH-ADH homology models may not be completely wasted. Firstly, it is quite conceivable that the active site area of QH-ADHs will be as closely similar to that of MDHs as the models predict, while secondly, QH-ADH's active site chemistry may be more akin to the physiologically functional situation than that of the rather artefactually behaving MDHs. With respect to the active site residues, some differences occur (Figure 10).

The cysteines involved in the disulfide bridge were linked in their final *trans* -position prior to the structural refinement. The conserved position of all other active site residues is inherent to the modeling procedure. The position of the non-conserved Trp 477 in MDH from *M. extorquens* is taken up by Val 479 in the model for QH-ADH from *C. testosteroni* and by Gly 479 in the model of QH-ADH from *A. pasteurianus*. These changes lead to a significant increase in the active site dimensions of the QH-ADHs, as compared to those of MDH. This might explain the observed difference in substrate specificity i.e. the conversion of bulky alcohols (and even sterols) by QH-ADHs as opposed to the more restricted substrate specificity of MDHs. The non-conserved Arg 331 (*M. extorquens*) is replaced by Lys 335 in both QH-ADHs. It has been suggested that this arginine residue might play a role in the reaction mechanism of MDH by forming a hydrogen bond to the C(5)-carbonyl oxygen thus promoting build-up of positive charge on this atom [19]. Its replacement by an amino group might offer an explanation for the fact that QH-ADHs do not need to be activated by ammonia (Scheme 9).

As pointed out above, structural information for quinoprotein dehydrogenases has been deduced largely from homology modeling experiments. Of the currently existing models no coordinates are available for the PQQ-binding domain of QH-ADH from *A. acetii* [49]. 3D models of the Type I QH-ADH from *C. testosteroni* [164] and the PQQ-



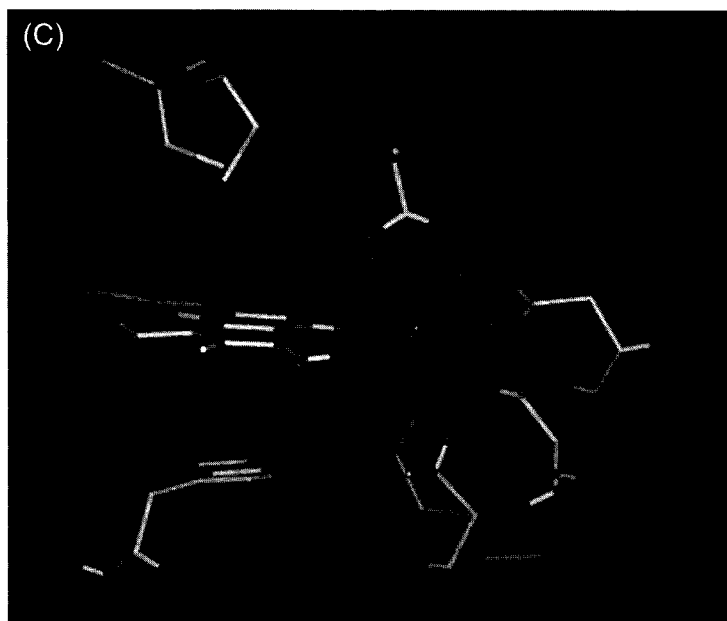


**Figure 10.** Stick representation of active site residues from A) MDH from *Methylotrophus W3A1* (crystal structure at 1.9 Å resolution; B) QH-ADH from *Acetobacter pasteurianus* (homology model), and C) QH-ADH from *Comamonas testosteroni* (homology model). The stacking of PQQ between the disulfide bridge and underlying tryptophan is a recurring theme in the pictures. A glutamate is conserved as a ligand for the calcium as is an asparagine residue. The active site base (aspartate) is present in all three structures. The apical position in the calcium ligation is taken up by an alanine in MDH(A) and a threonine in QH-ADH (B and C). The arginine that is in close contact to the O(4) position of PQQ in MDH (A) is replaced by a lysine in both QH-ADHs (B and C). Figures generated using INSIGHT (Biosym, Inc.).

containing domain of the large subunit of the Type II QH-ADH from *A. pasteurianus* [67] have been described (See Section 2 for details). In order to gain insight into the reaction mechanism and the enantioselectivity of this class of enzymes, preliminary molecular modeling experiments were performed aimed at the validation of proposed transition state structures with respect to the enantioselective features of these enzymes. Reaction intermediates leading to the respective transition states for the covalent PQQ-adduct reaction mechanism (the hemiketal intermediate, i.e. Schemes 2, 3) and the hydride transfer mechanism (i.e. Schemes 5, 6, and 9) were subjected to closer examination. To evaluate the stability of the hemiketal intermediate, PQQ-substrate adducts were build

and placed in the active site. To study the intermediates in which the alcoholate anion is complexed to the calcium ion, docking simulations were performed starting from outside the active site. Force field-derived energies for all complexes with substrates of opposite chirality were monitored and analyzed.

Conformational searching for the most stable PQQ-adduct structures was carried out by placing torsions on two dihedral angles. Rotations around the (PQQ)-C(5)-O(substrate) bond as well as the O(substrate)-C( $\alpha$ )-(substrate) bond were introduced. In case of the PQQ-(*R,S*)-2-hexanol adducts this was done for free PQQ as well as the for PQQ in the active site. The results for the (*S*)-2-hexanol PQQ-C(5)-adduct are shown in Figure 11.

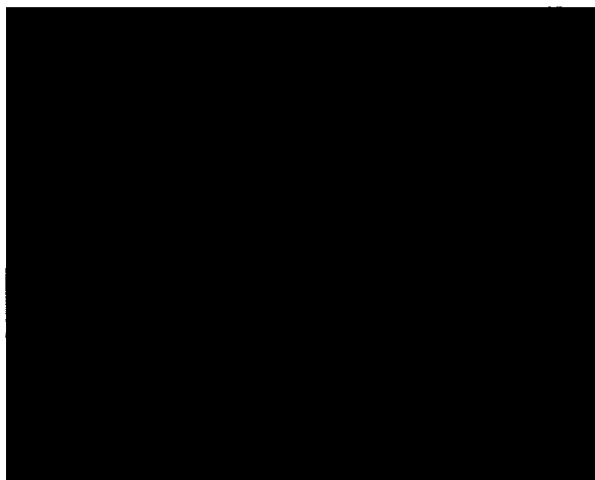


**Figure 11.** Conformational search for the hemiketal intermediate formed by addition of (*S*)-2-hexanol to PQQ-C(5). Torsion angles around PQQ-C(5)-(O)-alcohol and alcohol-(O)-chiral C were rotated using steps of 10 degrees. 400 conformations were generated using DISCOVER. Picture made using INSIGHT (Biosym, Inc.).

In order to fully search the active site, several different conformations of the PQQ-adduct were generated and placed in the active site. The dielectric constant was set to 1 in all cases. MNDO runs were performed, within the GAMESS-US program [304], on the diastereomeric PQQ-(*R,S*)-2-hexanol adducts. Energies for the final structures were compared and found to give no significant difference between (*R*)- and (*S*)-substrate-

PQQ-adduct (such differences have been reported to occur for hydrolase tetrahedral intermediate structures in which only the atoms of the active site serine were included [305]).

#### **4.3.2. Enantioselectivity of QH-ADH from *C. testosteroni***

PQQ-C(5) adducts of (*R*)- and (*S*)-pentan-2-ol, hemiketal intermediates, were placed in the active site and subjected to minimization and molecular dynamics. Water molecules were added according to their coordinates in the reference structures. Waters showing substantial overlap with the PQQ-adducts were discarded. The whole structure was solvated during the dynamic runs. Although this is a very crude approximation of an enzyme performing a reaction, the idea holds that by calculating the energies for the different (enantiomeric) reaction intermediates, insight can be gained on the overall reaction mechanism. Similar force field energies were found for both adducts. The energy differences between the favorable conformations of the adducts with opposite chirality were sufficiently small to be in line with the observed enantiomeric ratio for this substrate [164].

#### **4.3.3. Enantioselectivity of QH-ADH from *A. pasteurianus***

Both the hemiketal mechanism and the mechanism involving direct hydride transfer were tested. For studying the intermediates resulting from covalent adduct formation the same approach was used as for the QH-ADH from *C. testosteroni*. From the resulting favorable conformations and their corresponding force field energies a clear preference for the (*S*)-enantiomer could not be inferred (Figure 12, A-C). This kind of simulation depends very much on the initial placement of the cofactor-substrate adduct, as was already known from the simulation performed on QH-ADH from *C. testosteroni*. To simulate the mechanism involving direct hydride transfer, substrate molecules were pulled into the active site, by applying a force at their alcohol oxygen. In order to use the coordinating power of the calcium ion, the opposite end of the pulling vector was located at this ion. Substrate molecules were docked into the active site and analyzed for their ability to transfer a hydride when in their lowest energy conformation. The results of this combined 'energy-distance' criterium are shown in Figure 12 (D,E).

Preference for the (*S*)-enantiomer is in agreement with experimental data [59,67]. Considering the large number of assumptions made, it is hardly possible to discriminate

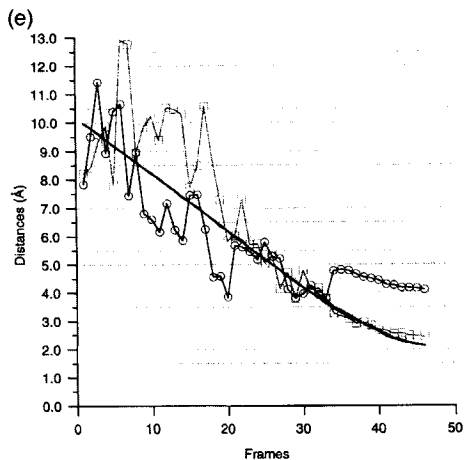
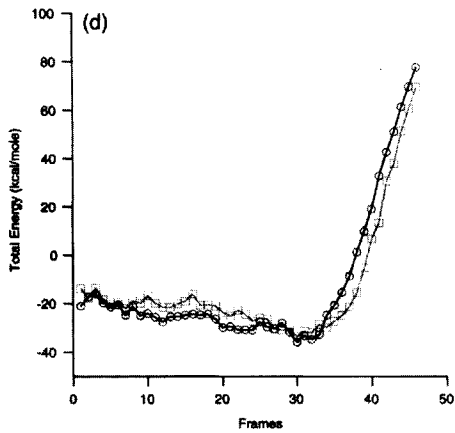
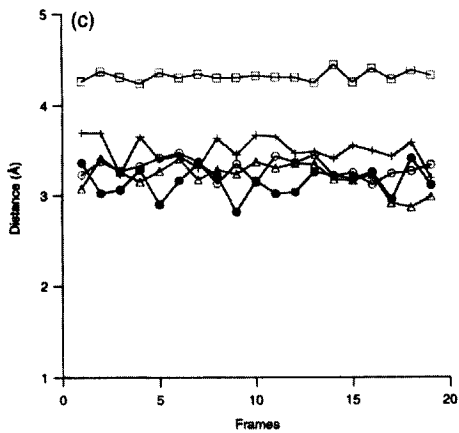
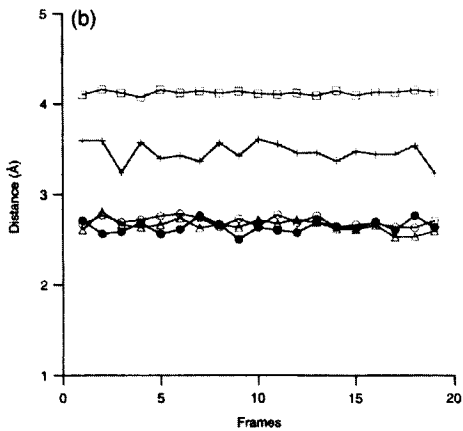
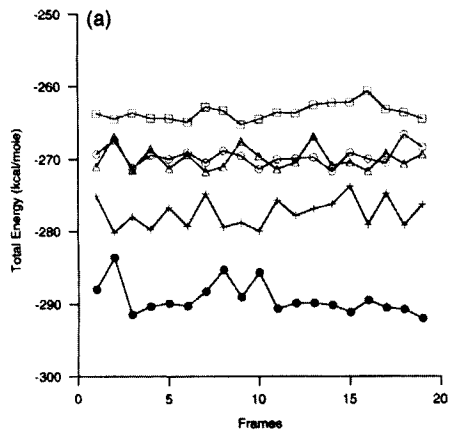


**Figure. 12.** Results of different approaches to simulate the reaction mechanism with respect to enantioselectivity determining transition states of PQQ containing quinoproteins. All calculations used the homology model of QH-ADH from *A. pasteurianus* and (*R*)- and (*S*)-2-butanol as substrate. Calculations were performed using DISCOVER. Net atomic charges for PQQ and PQQ-adducts and substrates were calculated using MOPAC. Parameters for calcium were adapted from Wavefunction Inc. Docking was performed by pulling the oxygen of the substrates towards the calcium position with a maximum force of  $100 \text{ kcal.mol}^{-1}.\text{\AA}^{-1}$ . Initially, substrates were placed well away from the protein surface ( $\pm 10 \text{ \AA}$ ). Following each pull the substrate was submitted to a short (1000 cycles) molecular dynamics run at 400 K with subsequent cooling to 50 K before energy minimization and archiving of the resulting structure. Each structure was analyzed for its force field energy components and for the distance between the hydrogen to be transferred and the C(5)-position of PQQ. Runs were also carried out allowing relaxation of residues in a  $10 \text{ \AA}$  sphere around PQQ in which case the substrates were initially placed at a distance of  $19.0 \text{ \AA}$  from PQQ. Up to  $10 \text{ \AA}$  the substrates were pulled in steps of  $1.0 \text{ \AA}$ , from  $10 - 1 \text{ \AA}$  in steps of  $0.5 - 0.2 \text{ \AA}$ . The same simulated annealing approach as described above was used. Runs were carried out for (*S*)-2-butanol and (*R*)-2-butanol. Interestingly, in these runs the disulfide bridge had to be constrained to its position. Due to non-balanced charges and van der Waals interactions, the disulfide bridge slowly swung away from its original position when no constraints were applied. Whether this points to a severe error in the model, or is a feature exhibited by the original MDH-crystal structure as well, is not clear at the moment. The importance of well balanced charge-charge interactions has been shown to be of major importance in protein simulations. Because of non-balanced charge-charge interactions or the absence of proper counter-charges (as in the case of MDH without its  $\beta$ -subunit) protein unfolding is likely to occur.

*Figure 12A-C* show the results of calculations performed assuming the covalent adduct to be the enantioselectivity determining step in the oxidation of (*R*)- and (*S*)-2-butanol. *Graph A* displays the calculated forcefield energies of a subset of residues containing the active site and the hemiketal intermediate corresponding to the (*R*)- or (*S*)-substrate PQQ-adduct. As the calculation was only performed on a subset of residues contained in a sphere with a radius of  $10 \text{ \AA}$ , no long-range electrostatic forces are incorporated. *Graphs B,C* show the distance of the hydrogen to be abstracted to the PQQ-C(4) and PQQ-O(4) position, respectively. —●— (*R*)-2-Butanol (run 1#); —†— (*R*)-2-Butanol (run 2#); — — (*S*)-2-Butanol (run 1#); —◆— (*S*)-2-Butanol (run 2#); —△— (*S*)-2-Butanol (run 3#);

*Figure 12D,E* show the results of "docking" runs, performed by pulling a molecule of substrate into the active site and onto the calcium. *Graph D* shows the energies involved. No emphasis should be given to the absolute values of the energies, as residues have been fixed to their positions and only a subset of residues has been used. — — (*S*)-2-Butanol; —○— (*R*)-2-Butanol. In *Graph E* the distance from the alcohol oxygen to the calcium and the hydrogen-to-be-transferred to the PQQ-C(5) position is displayed. Runs were performed on the alcohol, not on the alcoholate. — — (*S*)-2-Butanol; —○— (*R*)-2-Butanol; — Distance to calcium atom.

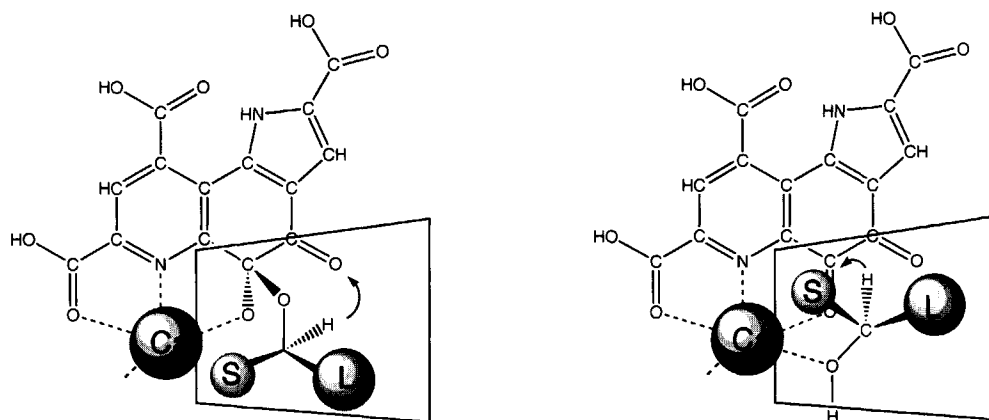


**Figure 13.** Structures of intermediates preceding the enantioselectivity determining transition state. On the left: "best fit" of secondary alcohols for the covalent adduct mechanism as proposed in Schemes 2, 3, leading to wrong prediction of QH-ADH enantioselectivity; on the right: "best fit" for Calcium-ligated secondary alcohols as proposed in Schemes 5, 6, 9, leading to correct prediction of QH-ADH enantioselectivity. S, small substituent, L, large substituent on chiral carbon. Boxes indicate active site limitations as deduced from homology models of QH-ADHs

between the mechanistic proposals. Yet, it appears that the intermediate calcium-alcohol complex that is invoked in Schemes 5, 6, and 9 as a precursor for hydride transfer, is more likely to predict the correct enantioselectivity than the PQQ-C(5) adduct presented in Schemes 2, 3. Diagrams of the preferred configurations involved in these mechanisms are given in Figure 13.

## 5. Prospects

Unlike the situation in related areas of enantioselective biocatalysis, i.e. "Kazlauskas rule" for lipases [306,307], "Prelog's rule" for yeast-mediated reductions [39,308] and, of historical interest, "Bertrand's rule" for acetic acid bacteria in the conversion of vicinal diols [310], "rules of thumb" for the prediction of the enantioselectivity have not been formulated for the enantioselectivity of quino(hemo)protein alcohol dehydrogenases. Qualitative correlations of enzyme enantioselectivity and substrate structure were originally proposed for liver alcohol dehydrogenase [311]. Similar approaches have been documented since [312-315]. An attempt to rationalize the observed enantioselectivity



for quinoproteins has been reported [67]. Figure 14 summarizes the results in a "substrate overlay" diagram.

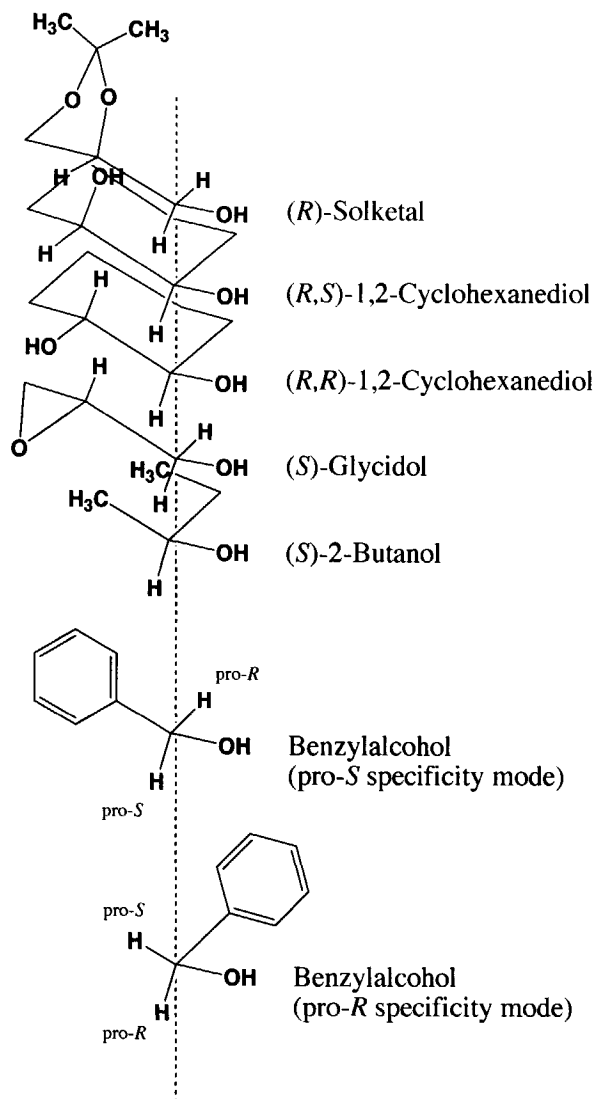


**Figure. 14.** Overlay of substrate enantiomers that are preferentially oxidized by quinohemoprotein dehydrogenases of *Acetobacter*, *Gluconobacter* and *Comamonas* sp. as compared to the pro-chiral specificity for benzylalcohol reported for MDH (adapted from [67])

Clearly, such diagrams should be treated with due care. Not only because "averaging" the preferred structures does not lend credit to the fact that some of the "preferred" enantiomers may not be "preferred" substrates, and may actually perform worse than "non-preferred" enantiomers of good substrates. Also, one would ideally like to compare transition state structures and *not* Michaelis-type complexes (see Section 1 for analysis). Thirdly, there may be appreciable ambiguity with respect to the ordering of ligands. In this respect, the possible orientation of benzylalcohol is of interest. MDH has been reported to catalyze removal of the pro-*S* hydrogen (ref. 16 in [124]). Whereas comparison with the enantioselectivity for secondary alcohols would suggest pro-*R* specificity, comparison with glycidol and solketal suggests the observed pro-*S* specificity (Figure 14). Finally then, the characteristics of the individual enzymes may defy correlations of this type.

An important aspect of quinoxinoprotein enantioselectivity is the location of the enantioselectivity determining reaction step on the reaction coordinate. Since this step may not be identical to the rate-controlling step, appropriate analysis of the mechanism is required. In this respect, the study of (deuterium) isotope effects on the reaction rate as well as on the enantioselectivity may be helpful. It must be emphasized that location of the rate controlling step following the enantioselectivity determining step has no influence on the enantiomeric ratio. This situation has been verified in the case of QH-ADH Type I from *C. testosteroni* [69], and QH-ADH Type II from *A. pasteurianus* [59] for the electron acceptors ferricyanide and decylubiquinone (U. Wandel, personal communication). Even though ferricyanide is rate controlling, no effect of ferricyanide concentrations of *E* were found. It will be interesting to investigate possible effects of intramolecular, *viz.* intermolecular electron transfer as well. Kinetic studies of quinoxinoprotein *D*-fructose dehydrogenase from *Gluconobacter industrius*, a three-subunit enzyme containing PQQ and heme *c* [316,317] showed parallel reciprocal plots in the oxidation of *D*-fructose with varying concentrations of ferricyanide indicative of ping-pong kinetics [318]. A reciprocal plot of the reduction of ferricyanide at saturating concentrations of *D*-fructose gave a break which was considered to result from the involvement of two active centers, namely PQQ and heme *c*. The electron transfer rate between PQQH<sub>2</sub> and heme *c* was calculated as  $2.2 \pm 0.4 \cdot 10^4 \text{ M}^{-1} \cdot \text{s}^{-1}$ , with  $k_{\text{cat}}$ 's of  $93 \pm 14 \text{ s}^{-1}$  and  $162 \pm 7 \text{ s}^{-1}$  for the slow (reduced heme at low ferricyanide concentrations) and fast (oxidized heme at high concentrations) branches of the pathway, respectively. Rate

limitations of this kind for QH-ADH alcohol dehydrogenases should thus be considered.

Current knowledge of the structure of PQQ-containing dehydrogenases relies heavily on the X-ray crystallographic data obtained for MDHs. The structure elucidation of glucose dehydrogenase from *Acinetobacter calcoaceticus* (soluble form, expressed in recombinant *E. coli*) has been announced (B.W. Dijkstra, personal communication) and will probably add to our understanding of the role of PQQ in quinoprotein-mediated redox reactions. Kinetic and mechanistic details of the reactions catalyzed by this enzyme have been reported [58,319,320]. Presumably even more interesting will be the eventual structure elucidation of the membrane-bound GDH from this and related organisms. This enzyme catalyzes the oxidation of *D*-glucose and other monosaccharides to the corresponding lactones. The electron acceptor is ubiquinone [321,322]. A low extent of sequence identity with MDHs has been found, based on which a model has been constructed [323]. In the model, a histidine residue is seen to replace the disulphide bridge present in MDHs, a finding consistent with earlier data on the involvement of a histidine residue in the binding of PQQ to this enzyme [324]. Recent isolation of a new quinoprotein dehydrogenase from *G. oxydans* DSM 4025 that effectively oxidizes L-sorbose as well as a broad variety of primary and secondary alcohols, aldehydes, aldoses, and ketoses, but not methanol or formaldehyde might bridge the gap between PQQ-containing glucose dehydrogenases and alcohol dehydrogenases [325]. Some of the structural constraints deduced to be of importance for the enantioselectivity of e.g. QH-ADHs may have to be reconsidered once new structures become available.

### **Acknowledgements**

We gratefully acknowledge financial support from the Organization for the Advancement of Pure Research/NWO, Foundation for Chemical Research/SON, The Netherlands (A.J.) and the Conselho Nacional de Desenvolvimento Científico e Tecnológico/CNPq, Brasil (S.S.M.).

## References

- (1) Salisbury, S. A.; Forrest, H. S.; Cruse, W. B. T. and Kennard, O.; *Nature*, **280** (1979), 843-844.
- (2) Duine, J. A.; Frank, J. J. and Verwiel, P. E. J.; *Eur. J. Biochem.*, **108** (1980), 187-192.
- (3) Duine, J. A.; Frank, J. J. and van Zeeland, J. K.; *FEBS Lett*, **108** (1979), 443-445.
- (4) Duine, J. A. and Jongejan, J. A.; *Annu. Rev. Biochem.*, **58** (1989), 403-426.
- (5) Klinman, J. P.; Dooley, D. M.; Duine, J. A.; Knowles, P. F.; Mondovi, B. and Villafranca, J. J.; *FEBS Lett*, **282** (1991), 1-4.
- (6) Duine, J. A.; *Eur. J. Biochem.*, **200** (1991), 271-284.
- (7) Janes, S. M.; Mu, D.; Wemmer, D.; Smith, A. J.; Kau, R. S.; Maltby, D.; Burlingame, A. L. and Klinman, J. P.; *Science*, **248** (1990), 981-987.
- (8) Wang, S. X.; Mure, M.; Medzihradzky, K. F.; Burlingame, A. L.; Brown, D. E.; Dooley, D. M.; Smith, A. J.; Kagan, H. M. and Klinman, J. P.; *Science*, **273** (1996), 1078-1084.
- (9) McIntire, W. S.; Wemmer, D. E.; Chistoserdov, A. and Lidstrom, M. E.; *Science*, **252** (1991), 817-824.
- (10) Davidson, V. L.; *Principles and applications of quinoproteins*; Marcel Dekker: New York, 1993, pp 1-453.
- (11) Anthony, C.; *Biochem. J.*, **320** (1996), 697-711.
- (12) Klinman, J. P.; *J. Biol. Chem.*, **271** (1996), 27189-27192.
- (13) Anthony, C. and Ghosh, M.; *Current Science*, **72** (1997), 716-726.
- (14) Anthony, C. and Ghosh, M.; *Prog. Biophys. Mol. Biol.*, **69** (1998), 1-21.
- (15) McIntire, W. S.; *Annual Review Of Nutrition*, **18** (1998), 145-77.
- (16) Goodwin, P. M. and Anthony, C.; In: "*Advances in Microbial Physiology*", R. K. Poole, Ed., Academic Press: San Diego, 1998; Vol. 40; pp 1-82.
- (17) Xia, Z.-X.; Dai, W.-W.; Xiong, J.-P.; Hao, Z.-P.; Davidson, V. L.; White, S. and Mathews, F. S.; *J. Biol. Chem.*, **267** (1992), 22289-22297.
- (18) Ghosh, M.; Anthony, C.; Harlos, K.; Goodwin, M. G. and Blake, C.; *Structure*, **3** (1995), 177-187.
- (19) Xia, Z.-X.; Dai, W.-W.; Zhang, Y.-F.; White, S. A.; Boyd, G. D. and Mathews, F. S.; *J. Mol. Biol.*, **259** (1996), 480-501.
- (20) Xia, Z.-X.; He, Y.-N.; Dai, W.-W.; White, S. A.; Boyd, G. D. and Mathews, F. S.; *Biochemistry*, **38** (1999), 1214-1220.
- (21) Kumar, V.; Dooley, D. M.; Freeman, H. C.; Guss, J. M.; Harvey, I.; McGuirl, M. A.; Wilce, M. C. J. and Zubak, V. M.; *Structure*, **4** (1996), 943-955.
- (22) Wilmot, C. M.; Murray, J. M.; Alton, G.; Parsons, M. R.; Convery, M. A.; Blakeley, V.; Corner, A. S.; Palcic, M. M.; Knowles, P. F.; McPherson, M. J. and Phillips, S. E. V.; *Biochemistry*, **36** (1997), 1608-1620.
- (23) Wilce, M. C. J.; Dooley, D. M.; Freeman, H. C.; Guss, J. M.; Matsunami, H.; McIntire, W. S.; Ruggiero, C. E.; Tanizawa, K. and Yamaguchi, H.; *Biochemistry*, **36** (1997), 16116-16133.
- (24) Vellieux, F. M. D.; Huitema, F.; Groendijk, H.; Kalk, K. H.; Frank, J. J.; Jongejan, J. A.; Duine, J. A.; Petratos, K.; Drenth, J. and Hol, W. G. J.; *EMBO Journal*, **8** (1989), 2171-2178.
- (25) Vellieux, F. M. D. K. K. H. D. J. and Hol, W. G. J.; *Acta Cryst. B46*, (1990), 806-823.
- (26) Chen, L.; Durley, R.; Poliks, B. J.; Hamada, K.; Chen, Z.; Mathews, F. S.; Davidson, V. L.; Satow, Y.; Huizinga, E.; Vellieux, F. M. D. and Hol, W. G. J.; *Biochemistry*, **31** (1992), 4959-4964.

- (27) Huizinga, E. G.; Zanten, B. A. M. v.; Duine, J. A.; Jongejan, J. A.; Huitema, F.; Wilson, K. S. and Hol, W. G. J.; *Biochemistry*, **31** (1992), 9789-9795.
- (28) Chen, L.; Mathews, F. S.; Davidson, V. L.; Huizinga, E. G.; Vellieux, F. M. D. and Hol, W. G. J.; *Proteins: Structure, Function, and Genetics*, **14** (1992), 288-299.
- (29) Chen, L.; Durley, R. C. E.; Mathews, F. S. and Davidson, V. L.; *Science*, **264** (1994), 86-89.
- (30) Chen, L.; Doi, M.; Durley, R. C. E.; Chistoserdov, A. Y.; Lidstrom, M. E.; Davidson, V. L. and Mathews, F. S.; *J. Mol. Biol.*, **276** (1998), 131-149.
- (31) Smidt, C. R.; Steinberg, F. M. and Rucker, R. B.; *Proc. Soc. Exptl. Biol. Med.*, **197** (1991), 19-26.
- (32) Matsushita, K.; Toyama, H. and Adachi, O.; *Adv. Microb. Physiol.*, **36** (1994), 247-301.
- (33) Gao, Y.; Hanson, R. M.; Klunder, J. M.; Ko, S. Y.; Masamune, H. and Sharpless, K. B.; *J. Am. Chem. Soc.*, **109** (1987), 5765-5780.
- (34) Noyori, R. and Hashiguchi, S.; *Acc. Chem. Res.*, **30** (1997), 97-102.
- (35) Tokunaga, M.; Larrow, J. F.; Kakiuchi, F. and Jacobsen, E. N.; *Science*, **277** (1997), 936-938.
- (36) Vedejs, E. and Chen, X.; *J. Am. Chem. Soc.*, **118** (1996), 1809-1810.
- (37) Corey, E. J.; Loh, T.-P.; Roper, T. D.; Azimioara, M. D. and Noe, M. C.; *J. Am. Chem. Soc.*, **114** (1992), 8290-8292.
- (38) Sheldon, R. A.; *J. Chem. Tech. Biotechnol.*, **67** (1996), 1-14.
- (39) Faber, K.; *Biotransformations in organic chemistry*; 3rd ed.; Springer-Verlag: Berlin, 1997.
- (40) Geerlof, A.; Stoorvogel, J.; Jongejan, J. A.; Leenen, E. J. T. M.; van Dooren, T. J. G. M.; van den Tweel, W. J. J. and Duine, J. A.; *Appl. Microbiol. Biotechnol.*, **42** (1994), 8-15.
- (41) Geerlof, A.; Jongejan, J. A.; van Dooren, T. J. G. M.; Raemakers-Franken, P. C.; van den Tweel, W. J. J. and Duine, J. A.; *Enzyme Microb. Technol.*, **16** (1994), 1059-1063.
- (42) Stigter, E. C. A.; Jong, G. A. H. de.; Jongejan, J. A.; Duine, J. A.; Lugt, J. P. v. d. and Somers, W. A. C.; *Enzyme Microb. Technol.*, **18** (1996), 489-494.
- (43) Karube, I.; Yokoyama, K. and Kitagawa, Y.; In; "*Principles and applications of quinoproteins*", V. L. Davidson, Ed., Marcel Dekker, Inc: New York, 1992; pp 429-446.
- (44) Khan, G. F.; Kobatake, E.; Ikariyama, Y. and Aizawa, M.; *Analytica Chimica Acta*, **281** (1993), 527-533.
- (45) Ye, L.; Haemmerle, M.; Olsthoorn, A. J. J.; Schuhmann, W.; Schmidt, H.-L.; Duine, J. A. and Heller, A.; *Anal. Chem.*, **65** (1993), 238-241.
- (46) Kuwabata, O. and Martin, C. R.; *Anal. chem.*, **66** (1994), 2757-2762.
- (47) Schmidt, H.-L. and Schuhmann, W.; *Biosensors & Bioelectronics*, **11** (1996), 127-135.
- (48) Somers, W. A. C.; van Hartingsveldt, W.; Stigter, E. C. A. and van der Lugt, J. P.; *TIBTECH*, **15** (1997), 495-500.
- (49) Cozier, G. E.; Giles, I. G. and Anthony, C.; *Biochem. J.*, **308** (1995), 375-379.
- (50) Kondo, K.; Beppu, T. and Horinouchi, S.; *J. Bacteriol.*, **177** (1995), 5048-5055.
- (51) Matsushita, K.; Yakushi, T.; Toyama, H.; Shinagawa, E. and Adachi, O.; *J. Biol. Chem.*, **271** (1996), 4850-4857.
- (52) Kondo, K. and Horinouchi, S.; *Appl. Environmental Microbiol.*, **63** (1997), 1131-1138.
- (53) de Jong, G. A. H.; Caldeira, J.; Sun, J.; Jongejan, J. A.; de Vries, S.; Loehr, T. M.; Moura, I.; Moura, J. J. G. and Duine, J. A.; *Biochemistry*, **34** (1995), 9451-9458.
- (54) de Jong, G. A. H.; Geerlof, A.; Stoorvogel, J.; Jongejan, J. A.; de Vries, S. and Duine, J. A.; *Eur. J. Biochem.*, **230** (1995), 899-905.

- (55) Semenov, N. N.; *Some problems in Chemical Kinetics and Reactivity, Chap. 1*; Pergamon: London, 1958.
- (56) Laidler, K. J.; *Chemical Kinetics*; 3rd ed.; Harper & Row: New York, 1987.
- (57) Stoner, C. D.; *Biochem. J.*, **283** (1992), 541-552.
- (58) Olsthoorn, A. J. J.; Otsuki, T. and Duine, J. A.; *Eur. J. Biochem.*, **255** (1998), 255-261.
- (59) Machado, S. S.; Wandel, U.; Jongejan, J. A.; Straathof, A. J. J. and Duine, J. A.; *Biosci. Biotechnol. Biochem.*, **63** (1998), 10-20.
- (60) Laidler, K. J.; *J. Chem. Educ.*, **65** (1988), 250-254.
- (61) Chen, C. S.; Fujimoto, Y.; Girdaukas, G. and Sih, S. J.; *J. Am. Chem. Soc.*, **104** (1982), 7294-7299.
- (62) Chen, C. S.; Wu, S. H.; Girdaukas, G. and Sih, C. J.; *J. Am. Chem. Soc.*, **109** (1987), 2812-2817.
- (63) Jongejan, J. A.; van Tol, J. B. A.; Geerlof, A. and Duine, J. A. In *5th European Congress on Biotechnology*; Munksgaard Intl. Publisher: Copenhagen, 1990; pp 268.
- (64) Straathof, A. J. J. and Jongejan, J. A.; *Enzyme Microb. Technol.*, **21** (1997), 559-571.
- (65) Anthonsen, T. and Jongejan, J. A.; *Methods Enzymol.*, **286** (1997), 473-495.
- (66) Overbeeke, P. L. A.; Ottosson, J.; Hult, K.; Jongejan, J. A. and Duine, J. A.; *Biocatalysis and Biotransformations*, **17** (1998), 61-79.
- (67) Machado, S. S.; Jongejan, A.; Geerlof, A.; Jongejan, J. A. and Duine, J. A.; *Biocatalysis and Biotransformations*, **16** (1999), 1-29.
- (68) Straathof, A. J. J.; Rakels, J. L. L. and Heijnen, J. J.; *Biocatalysis*, **7** (1992), 13-27.
- (69) Geerlof, A.; Rakels, J. J. L.; Straathof, A. J. J.; Heijnen, J. J.; Jongejan, J. A. and Duine, J. A.; *Eur. J. Biochem.*, **226** (1994), 537-546.
- (70) van Tol, J. B. A.; Jongejan, J. A. and Duine, J. A.; *Biocatalysis and Biotransformations*, **12** (1995), 99-117.
- (71) Eyring, H.; *J. Chem. Phys.*, **3** (1935), 107-115.
- (72) Truhlar, D. G.; Hase, W. L. and Hynes, J. T.; *J. Phys. Chem.*, **87** (1983), 2664-2682.
- (73) Truhlar, D. G.; Garrett, B. C. and Klippenstein, S. J.; *J. Phys. Chem.*, **100** (1996), 12771-12800.
- (74) Overbeeke, P. L. A.; Orrenius, S. C.; Jongejan, J. A. and Duine, J. A.; *Chemistry and Physics of Lipids*, **93** (1998), 81-93.
- (75) NC-IUB; *Eur. J. Biochem.*, **128** (1982), 281-291.
- (76) Crompton, I. E. and Waley, S. G.; *Biochem. J.*, **239** (1986), 221-224.
- (77) Barnsley, E. A.; *Biochem. J.*, **291** (1993), 323-328.
- (78) Engel, P. C.; *Biochem. J.*, **291** (1993), 324-325.
- (79) Demchenko, A. P.; *FEBS Lett.*, **310** (1992), 211-215.
- (80) Hill, T. L.; *Proc. natl. Acad. Sci. USA*, **77** (1980), 205-209.
- (81) Hwang, J.-K. and Warshel, A.; *J. Phys. Chem.*, **97** (1993), 10053-10058.
- (82) Benner, S. A.; *Chem. Rev.*, **89** (1989), 789-806.
- (83) McCammon, J. A.; *Proc. Natl. Acad. Sci. USA*, **93** (1996), 11426-11427.
- (84) Job, D.; Jones, P. and Dunford, H. B.; *J. Phys. Chem.*, **97** (1993), 9259-9262.
- (85) Szegletes, T.; Mallender, W. D.; Thomas, P. J. and Rosenberry, T. L.; *Biochemistry*, **38** (1999), 122-133.
- (86) Burbaum, J. J.; Raines, R. T.; Albery, W. J. and Knowles, J. R.; *Biochemistry*, **28** (1989), 9293-9305.

- (87) Yagisawa, S.; *Biochem. J.*, **263** (1989), 985-988.
- (88) Suedi, J.; *Biochem. J.*, **276** (1991), 265-268.
- (89) Menger, F. M.; *Biochemistry*, **31** (1992), 5368-5373.
- (90) Murphy, D. J.; *Biochemistry*, **34** (1995), 4507-4510.
- (91) Kodaka, M. and Hase, A.; *J. Phys. Chem.*, **99** (1995), 10686-10689.
- (92) Yagisawa, S.; *Biochem. J.*, **308** (1995), 305-311.
- (93) Fersht, A. R.; *Proc. Natl. Acad. Sci. USA*, **92** (1995), 10869-10873.
- (94) Cannon, W. R.; Singleton, S. F. and Benkovic, S. J.; *Nature structural biology*, **3** (1996), 821-833.
- (95) Dunford, H. B.; Job, D. and Jones, P.; *J. Phys. Chem. B*, **101** (1997), 4349-4350.
- (96) Kodaka, M.; *J. Phys. Chem. B*, **101** (1997), 4351.
- (97) Eyring, H.; Ma, S.-M. and Ueda, I.; *Proc. Natl. Acad. Sci. USA*, **78** (1981), 5549-5553.
- (98) Mazo, R. M. and Guslander, J.; *J. Phys. Chem.*, **96** (1992), 3958-3962.
- (99) Smith, R. R. and Canady, W. J.; *Biophysical Chemistry*, **43** (1992), 173-187.
- (100) Smith, R. R. and Canady, W. J.; *Biophysical Chemistry*, **43** (1992), 189-195.
- (101) van Tol, J. B. A. PhD Thesis, Delft University of Technology, 1994.
- (102) Bigeleisen, J. and Wolfsberg, M.; *Adv. Chem. Phys.*, **1** (1958), 15-76.
- (103) Huskey, W. P.; In: "Enzyme Mechanisms from Isotope effects", P. F. Cook, Ed., CRC Press, Inc.: Boca raton, FL, 1991.
- (104) Schramm, V. L.; Horenstein, B. A. and Kline, P. C.; *J. Biol. Chem.*, **269** (1994), 18259-18262.
- (105) McIntire, W. S.; *FASEB Journal*, **8** (1994), 513-521.
- (106) Anthony, C.; *Int. J. Biochem.*, **24** (1992), 29-39.
- (107) Anthony, C.; Ghosh, M. and Blake, C. C. F.; *Biochem. J.*, **304** (1994), 665-674.
- (108) Goodwin, M. G. and Anthony, C.; *Biochem. J.*, **318** (1996), 673-679.
- (109) Matsushita, K.; Takahashi, K. and Adachi, O.; *Biochemistry*, **32** (1993), 5576-5582.
- (110) Schrover, J. M. J.; Frank, J.; van Wielink, J. E. and Duine, J. A.; *Biochem. J.*, **290** (1993), 123-127.
- (111) Groen, B. W.; Frank, J. J. and Duine, J. A.; *Biochem. J.*, **223** (1986), 921-924.
- (112) Yamanaka, K. and Tsuyuki; *Agric. Biol. Chem.*, **47** (1983), 2173-2183.
- (113) Yasuda, M.; Cherepanov, A. and Duine, J. A.; *FEMS Microbiol. Lett.*, **138** (1996), 23-28.
- (114) Toyama, H.; Fujii, A.; Matsushita, K.; Shinagawa, E.; Ameyama, M. and Adachi, O.; *J. Bacteriol.*, **177** (1995), 2442-2450.
- (115) Anthony, C.; *Biochem. Soc. Trans.*, **26** (1998), 413-417.
- (116) Hauge, J. G.; *Biochim. Biophys. Acta*, **45** (1960), 263-269.
- (117) Hauge, J. G.; *J. Biol. Chem.*, **239** (1964), 3630-3639.
- (118) Cruse, W. B. T.; Kennard, O. and Salisbury, S. A.; *Acta Cryst. B36*, (1980), 751-754.
- (119) Anthony, C. and Zatman, L. J.; *Biochem. J.*, **92** (1964), 614-627.
- (120) Anthony, C.; *Adv. Microbial. Physiol.*, **27** (1986), 113-210.
- (121) Dijkstra, M.; van den Tweel, W. J. J.; de Bont, J. A. M.; Frank, J. J. and Duine, J. A.; *J. Gen. Microbiol.*, **131** (1985), 3163-3169.
- (122) Duine, J. A.; Frank, J. and Westerling, J. A.; *Biochim. Biophys. Acta*, **524** (1978), 277-287.
- (123) Frank, J.; Dijkstra, M.; Balny, C.; Verwiel, P. E. J. and Duine, J. A.; In: "PQQ and Quinoproteins", J. A. Jongejan and J. A. Duine, Ed., Kluwer Academic Publishers: Dordrecht, 1989; pp 13-22.
- (124) Anthony, C.; In: "Principles and applications of quinoproteins", V. L. Davidson, Ed., Marcel

- Dekker, Inc: New York, 1993; pp 17-45.
- (125) Bamforth, C. W. and Quayle, J. R.; *Biochem. J.*, **169** (1978), 677-686.
- (126) Ghosh, R. and Quayle, J. R.; *Biochem. J.*, **199** (1981), 245-250.
- (127) Duine, J. A.; Frank, J. J.; Jongejan, J. A. and Dijkstra, M.; In; "Microbial growth on C1 compounds", R. S. H. R.L. Crawford, Ed., American Society for Microbiology: Washington, D.C., 1984; pp 91-96.
- (128) Frank, J. J.; Dijkstra, M.; Duine, J. A. and Balny, C.; *Eur. J. Biochem.*, **174** (1988), 331-338.
- (129) Frank, J. J.; van Krimpen, S. H.; Verwiël, P. E. J.; Jongejan, J. A.; Mulder, A. C. and Duine, J. A.; *Eur. J. Biochem.*, **184** (1989), 187-195.
- (130) Duine, J. A.; Frank, J. J. and de Beer, R.; *Arch. Biochem. Biophys.*, **233** (1984), 708-711.
- (131) Garcia-Higuera, I.; Fenoglio, J.; Li, Y.; Lewis, C.; Panchenko, M. P.; Reiner, O.; Smith, T. F. and Neer, E. J.; *Biochemistry*, **35** (1996), 13985-13994.
- (132) Smith, T. F.; Gaitatzes, C.; Saxena, K. and Neer, E. J.; *Trends in Biochemical Sciences* (1999), 181-185.
- (133) Itoh, S.; Ogino, M.; Fukui, Y.; Murao, H.; Komatsu, M.; Ohshiro, Y.; Inoue, T.; Kai, Y. and Kasai, N.; *J. Am. Chem. Soc.*, **115** (1993), 9960-9967.
- (134) White, S.; Boyd, G.; Mathews, F. S.; Xia, Z.-X.; Dai, W.-W.; Zhang, Y.-F. and Davidson, V. L.; *Biochemistry*, **32** (1993), 12955-12958.
- (135) Carrell, C. J.; Carrell, H. L.; Erlebacher, J. and Glusker, J. P.; *J. Am. Chem. Soc.*, **110** (1988), 8651-8656.
- (136) Nunn, D. N.; Day, D. and Anthony, C.; *Biochem. J.*, **260** (1989), 857-862.
- (137) Chan, H. T. C. and Anthony, C.; *Biochem. J.*, **280** (1991), 139-146.
- (138) Cox, J. M.; Day, D. J. and Anthony, C.; *Biochim. Biophys. Acta*, **1119** (1992), 97-106.
- (139) Dales, S. L. and Anthony, C.; *Biochem. J.*, **312** (1995), 261-265.
- (140) Hooft, R. W. W.; Vriend, G.; Sander, C. and Abola, E. E.; *Nature*, **381** (1996), 272.
- (141) Schulze, P. and Feigon, J.; *Nature*, **387** (1997), 668.
- (142) Jones, T. A.; Kleywegt, G. J. and Bruenger, A. T.; *Nature*, **383** (1996), 18-19.
- (143) Adachi, O.; Miyagawa, E.; Shinagawa, E.; Matsushita, K. and Ameyama, M.; *Agric. Biol. Chem.*, **42** (1978), 2331-2340.
- (144) Matsushita, K.; Takaki, Y.; Shinagawa, E.; Ameyama, M. and Adachi, O.; *Biosci. Biotech. Biochem.*, **56** (1992), 304-310.
- (145) Tayama, K.; Fujaya, M.; Okumura, H.; Kawamura, Y. and Beppu, T.; *Appl. Microbiol. Biotechnol.*, **32** (1989), 181-185.
- (146) Inoue, T.; Sunagawa, M.; Mori, A.; Imai, C.; Fukuda, M.; Tagaki, M. and Yano, K.; *J. Bacteriol.*, **171** (1989), 3115-3122.
- (147) Inoue, T.; Sunagawa, M.; Mori, A.; Imai, C.; Fukuda, M.; Takagi, M. and Yano, K.; *J. Ferment. Bioeng.*, **70** (1990), 58-60.
- (148) Inoue, T.; Sunagawa, M.; Mori, A.; Imai, C.; Fukuda, M.; Tagaki, M. and Yano, K.; *J. Ferment. Bioeng.*, **73** (1992), 419-424.
- (149) Tamaki, T.; Fukaya, M.; Takemura, H.; Tayama, K.; Okamura, H.; Kawamura, Y.; Nishiyama, M.; Horinouchi, S. and Beppu, T.; *Biochim. Biophys. Acta*, **1088** (1991), 292-300.
- (150) Takemura, H.; Kondo, K.; Horinouchi, S. and Beppu, T.; *J. Bacteriol.*, **175** (1993), 6857-6866.
- (151) Anthony, C.; *Biochem. J.*, **308** (1995), 375-379.



- (152) Thompson, J. D.; Higgins, D. G. and Gibson, T. J.; *Nucleic Acids Research*, **22** (1994), 4673-4680.
- (153) Laskowski, R. A.; MacArthur, M. W.; Moss, D. S. and Thornton, J. M.; *J. Appl. Cryst.*, **26** (1993), 283-291.
- (154) Groen, B. W. and Duine, J. A.; *Meth. Enzymol.*, **188** (1990), 33-39.
- (155) Matsushita, K. and Adachi, O.; In: "*Principles and Applications of Quinoproteins*", V. L. Davidson, Ed., Marcel Dekker Inc.: New York, 1993; pp 47-63.
- (156) Stoorvogel, J.; Kraayveld, D. E.; van Sluis, C. A.; Jongejan, J. A.; de Vries, S. and Duine, J. A.; *Eur. J. Biochem.*, **235** (1996), 690-698.
- (157) Jongejan, J. A.; Groen, B. W. and Duine, J. A.; In: "*PQQ and Quinoproteins*", J. A. Jongejan and J. A. Duine, Ed., Kluwer Academic Publishers: Dordrecht, 1989; pp 205-216.
- (158) Duine, J. A.; *TibTech*, **9** (1991), 343-346.
- (159) Qi, P. X.; Di Stefano, D. L. and Wand, A. J.; *Biochemistry*, **33** (1994), 6408-6417.
- (160) Qi, P. X.; Beckman, R. A. and Wand, A. J.; *Biochemistry*, **35** (1996), 12275-12286.
- (161) Kazanskaya, I.; Lexa, D.; Bruschi, M. and Chottard, G.; *Biochemistry*, **35** (1996), 13411-13418.
- (162) de Jong, P. A. H. PhD Thesis, Delft University of technology, 1995.
- (163) Stigter, E. C. A.; Lugt, J. P. v. d. and Somers, W. A. C.; *J. Mol. Catal. B: Enzymatic*, **2** (1997), 291-297.
- (164) Jongejan, A.; Jongejan, J. A. and Duine, J. A.; *Protein Engineering*, **11** (1998), 185-198.
- (165) Bersch, B.; Brutscher, B.; Meyer, T. E. and Marion, D.; *Eur. J. Biochem.*, **227** (1995), 249-260.
- (166) Beratan, D. N.; Betts, J. N. and Onuchic, J. N.; *Science*, **252** (1991), 1285-1288.
- (167) Canters, G. W. and van de Kamp, M.; *Curr. Opin. Struct. Biol.*, **2** (1992), 859-869.
- (168) van der Meer, R. A.; Jongejan, J. A. and Duine, J. A.; *FEBS Lett*, **221** (1987), 299-304.
- (169) van Koningsveld, H.; Jansen, J. C.; Jongejan, J. A.; Frank, J. J. and Duine, J. A.; *Acta Cryst. C41*, (1985), 89-92.
- (170) Ishida, T.; Doi, M.; Tomita, K.; Hayashi, H.; Inoue, M. and Urakami, T.; *J. Am. Chem. Soc.*, **111** (1989), 6822-6828.
- (171) Ishida, T.; Kawamoto, E.; In, Y.; Amano, T.; Kanayama, J. and Doi, M.; *J. Am. Chem. Soc.*, **117** (1995), 3278-3279.
- (172) van Koningsveld, H.; Jongejan, J. A. and Duine, J. A.; In: "*PQQ and Quinoproteins*", J. A. Jongejan and J. A. Duine, Ed., Kluwer Academic Publishers: Dordrecht, 1989; pp 243-251.
- (173) Andres, J.; Moliner, V. and Krechl, J.; *Bioorganic Chemistry*, **22** (1994), 58-71.
- (174) Andres, J.; Moliner, V.; Domingo, L. R.; Picher, M. T. and Krechl, J.; *J. Am. Chem. Soc.*, **117** (1995), 8807-8815.
- (175) Zheng, Y.-J. and Bruice, T. C.; *Proc. Natl. Acad. Sci. USA*, **94** (1997), 11881-11886.
- (176) Corey, E. J. and Tramontano, A.; *J. Am. Chem. Soc.*, **103** (1981), 5599-5600.
- (177) Gainor, J. A. and Weinreb, S. M.; *J. Org. Chem.*, **46** (1981), 4317-4319.
- (178) Gainor, J. A. and Weinreb, S. M.; *J. Org. Chem.*, **47** (1982), 2833-2837.
- (179) Hendrickson, J. B. and de Vries, J. G.; *J. Org. Chem.*, **47** (1982), 1148-1150.
- (180) Hendrickson, J. B. and de Vries, J. G.; *J. Org. Chem.*, **50** (1985), 1688-1695.
- (181) Buechi, G. B. J. H. L. G. C. M. and Yakushijin, K.; *J. Am. Chem. Soc.*, **107** (1985), 5555-5556.
- (182) Jongejan, J. A. B. R. P. and Duine, J. A.; *Tetrahedron Lett*, **29** (1988), 3709-3712.
- (183) van der Meer, R. A.; Groen, B. W.; van Kleef, M. A. G.; Frank, J.; Jongejan, J. A. and Duine, J. A.;

- Meth. Enzymol.*, **188** (1990), 260-283.
- (184) Martin, P.; *Helv. Chim. Acta*, **76** (1993), 988-992.
- (185) Martin, P.; *Helv. Chim. Acta*, **76** (1993), 1667-1673.
- (186) MacKenzie, A. R.; Moody, C. J. and Rees, C. W.; *J. Chem. Soc., Chem. Commun.*, (1983), 1372-1373.
- (187) MacKenzie, A. R.; Moody, C. J. and Rees, C. W.; *Tetrahedron*, **42** (1986), 3259-3268.
- (188) Ameyama, M.; Hayashi, M.; Matsushita, K.; Shinagawa, E. and Adachi, O.; *Agric. Biol. Chem.*, **48** (1984), 561-565.
- (189) Iwayama, A. and Ohita, S.; *Jp.*, **63** (1988), 1-9.
- (190) Urakami, T.; Yashima, K.; Kobayashi, H.; Yoshida, A. and Ito-Yoshida, C.; *Appl. Environ. Microbiol.*, **58** (1992), 3970-3976.
- (191) Jongejan, J. A. PhD Thesis, Delft University of Technology, 1989.
- (192) Westerling, J.; Frank, J. J. and Duine, J. A.; *Biochem. Biophys. Res. Commun.*, **87** (1979), 719-724.
- (193) Duine, J. A.; Frank, J. J. and Jongejan, J. A.; *Anal. Biochem.*, **133** (1983), 239-243.
- (194) Gallop, P. M.; Henson, E.; Paz, M. A.; Greenspan, S. L. and Flückiger, R.; *Biochem. Biophys. Res. Commun.*, **163** (1989), 755-763.
- (195) Corey, E. J. and Achiwa, K.; *J. Am. Chem. Soc.*, **91** (1969), 1429-.
- (196) Duine, J. A.; Frank, J. J. and Jongejan, J. A.; *Adv. Enzymol.*, **59** (1987), 169-212.
- (197) Duine, J. A.; Frank, J. J. and Verwiël, P. E. J.; *Eur. J. Biochem.*, **118** (1981), 395-399.
- (198) Bergethon, P. R.; *Anal. Biochem.*, **186** (1990), 324-327.
- (199) Kano, K.; Mori, K.; Uno, B.; Kubota, T.; Ikeda, T. and Senda, M.; *Bioelectrochemistry and Bioenergetics*, **24** (1990), 193-201.
- (200) McWhirter, R. B. and Klapper, M. H.; *Biochemistry*, **29** (1990), 6919-6926.
- (201) Eckert, T. S.; Bruice, T. C.; Gainor, J. A. and Weinreb, S. M.; *Proc. Natl. Acad. Sci. USA*, **79** (1982), 2533-2536.
- (202) Eckert, T. S. and Bruice, T. C.; *J. Am. Chem. Soc.*, **105** (1983), 4431-4441.
- (203) Schwederski, B.; Kasack, V.; Kaim, W.; Roth, E. and Jordanov, J.; *Angew. Chem.*, **102** (1990), 74-76.
- (204) Itoh, S.; Kawakami, H. and Fukuzumi, S.; *J. Am. Chem. Soc.*, **120** (1998), 7271-7277.
- (205) Suzuki, K.; Yasuda, M. and Yamasaki, K.; *J. Phys. Chem.*, **61** (1957), 229.
- (206) Dwyer, F. P. and Mellor, D. P.; *Chelating agents and metal chelates*; Academic Press: New York, 1964.
- (207) Noar, J. B.; Rodriguez, E. J. and Bruice, T. C.; *J. Am. Chem. Soc.*, **107** (1985), 7198-7199.
- (208) Jongejan, J. A.; van der Meer, R. A.; Zuylen, G. A. v. and Duine, J. A.; *Recl. Trav. Chim. Pays-Bas*, **106** (1987), 365.
- (209) Walker, F. A.; Lo, M. W. and Ree, M. T.; *J. Am. Chem. Soc.*, **98** (1976), 5552-5560.
- (210) Duine, J. A. and Jongejan, J. A.; In: "*Bioinorganic Catalysis*", J. Reedijk, Ed., Marcel Dekker, Inc.: New York, 1993; pp 447-468.
- (211) Geiger, O. and Görisch, H.; *Biochem. J.*, **261** (1989), 415-421.
- (212) Dekker, R. H.; Duine, J. A.; Frank, J. J.; Verwiël, J. P. E. and Westerling, J.; *Eur. J. Chem.*, **125** (1982), 69-73.
- (213) Sleath, P. R.; Noar, J. B.; Eberlein, G. A. and Bruice, T. C.; *J. Am. Chem. Soc.*, **107** (1985), 3328-

3338.

- (214) Rodriguez, E. J. and Bruce, T. C.; *J. Am. Chem. Soc.*, **111** (1989), 7947-7956.
- (215) Itoh, S.; Kato, N.; Ohshiro, Y. and Agawa, T.; *Tetrahedron Lett.*, **25** (1984), 4753-4756.
- (216) Itoh, S.; Kitamura, Y.; Ohshiro, Y. and Agawa, T.; *Bull. Chem. Soc. Jpn.*, **59** (1986), 1907-1910.
- (217) Itoh, S.; Mure, M.; Ogino, M. and Ohshiro, Y.; *J. Org. Chem.*, **56** (1991), 6857-6865.
- (218) Itoh, S.; Mure, M.; Suzuki, A.; Murao, H. and Ohshiro, Y.; *J. Chem. Soc. Perkin Trans. 2*, (1992), 1245-1251.
- (219) Mure, M. and Klinman, J. P.; *J. Am. Chem. Soc.*, **117** (1995), 8698-8706.
- (220) Mure, M. and Klinman, J. P.; *J. Am. Chem. Soc.*, **117** (1995), 8707-8718.
- (221) Wang, F.; Bae, J.-Y.; Jacobson, A. R.; Lee, Y. and Sayre, L. M.; *J. Org. Chem.*, **59** (1994), 2409-2417.
- (222) Itoh, S. and Ohshiro, Y.; *Methods Enzymol.*, **258** (1995), 164-176.
- (223) Itoh, S.; Takada, N.; Haranou, S.; Ando, T.; Komatsu, M.; Ohshiro, Y. and Fukuzumi, S.; *J. Org. Chem.*, **61** (1996), 8967-8974.
- (224) van Kleef, M. A. G.; Jongejan, J. A. and Duine, J. A.; In: "PQQ and Quinoproteins", J. A. Jongejan and J. A. Duine, Ed., Kluwer Academic Publishers: Dordrecht, 1989; pp 217-226.
- (225) van Kleef, M. A. G.; Jongejan, J. A. and Duine, J. A.; *Eur. J. Biochem.*, **183** (1989), 41-47.
- (226) Mure, M.; Nii, K.; Inoue, T.; Itoh, S. and Ohshiro, Y.; *J. Chem. Soc. Perkin trans*, **2** (1990), 315-320.
- (227) Mure, M.; Nii, K.; Itoh, S. and Ohshiro, Y.; *Bull. Chem. Soc. Jpn.*, **63** (1990), 417-420.
- (228) Mincey, T. C.; Bell, J. A.; Mildvan, A. S. and Abeles, R. H.; *Biochemistry*, **20** (1981), 7502-7509.
- (229) de Beer, R.; Duine, J. A.; Frank, J. J. and Westerling, J.; *Eur. J. Biochem.*, **130** (1983), 105-109.
- (230) Parkes, C. and Abeles, R. H.; *Biochemistry*, **23** (1984), 6355-6363.
- (231) Ohshiro, Y. and Itoh, S.; In: "Principles and applications of quinoproteins", V. L. Davidson, Ed., Marcel Dekker, Inc: New York, 1993; pp 309-329.
- (232) Peterson, K. L.; Galitz, D. S. and Srivastava, D. K.; *Biochemistry*, **37** (1998), 1697-1705.
- (233) Itoh, S.; Kawakami, H. and Fukuzumi, S.; *Biochemistry*, **37** (1998), 6562-6571.
- (234) Forrest, H. S.; Salisbury, S. A. and Kilty, C. G.; *Biochem. Biophys. Res. Commun.*, **97** (1980), 248-251.
- (235) Richardson, I. W. and Anthony, C.; *Biochemical Journal*, **287 ( Pt 3)** (1992), 709-15.
- (236) Harris, T. K. and Davidson, V. L.; *Biochemistry*, **32** (1993), 4362-4368.
- (237) Harris, T. K. and Davidson, V. L.; *Biochem. J.*, **300** (1994), 175-182.
- (238) Goodwin, M. G.; Avezoux, A.; Dales, S. L. and Anthony, C.; *Biochem. J.*, **319** (1996), 839-842.
- (239) Dijkstra, M.; Frank, J. J. and Duine, J. A.; *FEBS Lett*, **227** (1988), 198-202.
- (240) Inoue, J.; Tomioka, N.; Itai, A. and Harayama, S.; *Biochemistry*, **37** (1998), 3305-3311.
- (241) Toney, A. and Kirsch, B.; *Science*, **243** (1989), 1485-1488.
- (242) Toney, A. and Kirsch, B.; *Protein Sci.*, **1** (1992), 107-119.
- (243) Zhukovski, A.; *Science*, **251** (1991), 558-560.
- (244) Sekimoto, A.; *J. Biol. Chem.*, **268** (1993), 27039-27045.
- (245) Harpel, A. and Hartman, B.; *Biochemistry*, **33** (1994), 5553-5561.
- (246) Kalyanaraman, B.; Premovic, P. I. and Sealy, R. C.; *J. Biol. Chem.*, **262** (1987), 11080-87.
- (247) Rodriguez, J. H.; Wheeler, D. E. and McCusker, J. K.; *J. Am. Chem. Soc.*, **120** (1998), 12051-12068.

- (248) Oyama, R.; Watanabe, T.; Hanzawa, H.; Sano, T.; Sugiyama, T. and Izaki, K.; *Biosci. Biotech. Biochem.*, **58** (1994), 1914-1917.
- (249) Itoh, S.; Kawakami, H. and Fukuzumi, S.; *J. Chem. Soc., Chem. Commun.*, (1997), 29-30.
- (250) Schürer, G. and Clark, T.; *J. Chem. Soc., Chem. Commun.*, (1998), 257-258.
- (251) Kalyanaraman, B.; Korytowski, W.; Pilas, B.; Sarna, T.; Land, E. J. and Truscott, T. G.; *Arch. Biochem. Biophys.*, **266** (1988), 277-284.
- (252) Blake, C. C. F.; Ghosh, M.; Harlos, K.; Avezoux, A. and Anthony, C.; *Structural Biology*, **1** (1994), 102-105.
- (253) Avezoux, A.; Goodwin, M. G. and Anthony, C.; *Biochem. J.*, **307** (1995), 735-741.
- (254) Williams, C. H. J.; In; "Chemistry and Biochemistry of Flavoenzymes", F. Müller, Ed., CRC Press, Inc.: Boca Raton, 1992; Vol. 3; pp 121-211.
- (255) Dhaiman, A. S. and Rabbani, N.; *Biochem. Biophys. Res. Commun.*, **221** (1996), 229-233.
- (256) Itoh, S.; Kato, N.; Ohshiro, Y. and Agawa, T.; *Chemistry Letters*, (1985), 135-136.
- (257) Itoh, S.; Mure, M. and Ohshiro, Y.; *J. Chem. Soc. Chem. Commun.*, (1987), 1580-1581.
- (258) Churchich, J. E.; *Biofactors*, **2** (1989), 113-6.
- (259) Hirao, T.; Ohno, M. and Ohshiro, Y.; *Tetrahedron Lett.*, **31** (1990), 6039-6042.
- (260) Groeneveld, A.; Dijkstra, M. and Duine, J. A.; *FEMS Microbiol. Lett.*, **25** (1984), 311-314.
- (261) Itoh, S.; Kawakami, H. and Fukuzumi, S.; *J. Am. Chem. Soc.*, **119** (1997), 439-440.
- (262) Skibo, E. B. and Lee, C. H.; *J. Am. Chem. Soc.*, **107** (1985), 4591-4593.
- (263) Itoh, S.; Mure, M.; Ohshiro, Y. and Agawa, T.; *Tetrahedron Lett.*, **26** (1985), 4225-4228.
- (264) Dijkstra, M.; Frank, J. J. and Duine, J. A.; *Biochem. J.*, **257** (1989), 87-94.
- (265) Remko, M.; Liedl, K. R. and Rode, B. M.; *J. Phys. Chem. A*, **102** (1998), 771-777.
- (266) Platt, K. L. and Oesch, F.; *Synthesis*, (1982), 459-461.
- (267) Platt, K. L. and Oesch, F.; *J. Org. Chem.*, **48** (1983), 265-268.
- (268) Snider, B. B.; *Acc. Chem. Res.*, **13** (1980), 426-432.
- (269) Evans, D. A. and Golob, A. M.; *J. Am. Chem. Soc.*, **97** (1975), 4765-4766.
- (270) Loncharich, R. J. and Houk, K. N.; *J. Am. Chem. Soc.*, **109** (1987), 6947-6952.
- (271) Bunnage, M. E. and Nicolaou, K. C.; *Chem. Eur. J.*, **3** (1997), 187-192.
- (272) Lu, D. and Voth, G. A.; *J. Am. Chem. Soc.*, **120** (1998), 4006-4014.
- (273) Warnhoff, E. W.; Reynolds-Warnhoff, P. and Wong, M. Y. H.; *J. Am. Chem. Soc.*, **102** (1980), 5956-5957.
- (274) Ashby, E. C.; Goel, A. B. and Argyropoulos, J. N.; *Tetrahedron Lett.*, **23** (1982), 2273-2276.
- (275) Ashby, E. C. and Argyropoulos, J. N.; *Tetrahedron Lett.*, **27** (1986), 465-468.
- (276) Ashby, E. C. and Argyropoulos, J. N.; *J. Org. Chem.*, **51** (1986), 3593-3597.
- (277) Nasipuri, D.; Gupta, M. D. and Banerjee, S.; *tetrahedron Lett.*, **25** (1984), 5551-5554.
- (278) Lewis, E. S.; *J. Am. Chem. Soc.*, **111** (1989), 7576-7578.
- (279) Dijkstra, M.; Frank, J. J.; Jongejan, J. A. and Duine, J. A.; *Eur. J. Biochem.*, **140** (1984), 369-373.
- (280) Sheldon, J. C.; Bowie, J. H.; Dua, S.; Smith, J. D. and O'Hair, R. A. J.; *J. Org. Chem.*, **62** (1997), 3931-3937.
- (281) Swain, C. G.; Powell, A. L.; Lynch, T. J.; Alpha, S. R. and Dunlap, R. P.; *J. Am. Chem. Soc.*, **101** (1979), 3584-3587.
- (282) Swain, C. G.; Powell, A. L.; Sheppard, W. A. and Morgan, C. R.; *J. Am. Chem. Soc.*, **101** (1979), 3576-3583.

- (283) Wiberg, K. B.; *J. Am. Chem. Soc.*, **76** (1954), 5371-5375.
- (284) DeTar, D. F.; *Biochemistry*, **20** (1981), 1730-1743.
- (285) Wipff, G.; Dearing, A.; Weiner, P. K.; Blaney, J. M. and Kollman, P. A.; *J. Am. Chem. Soc.*, **105** (1983), 997.
- (286) Bemis, G. W.; Carlson-Golab, G. and Katzenellenbogen, J. A.; *J. Am. Chem. Soc.*, **114** (1992), 570-578.
- (287) Norin, M.; Hult, K.; Mattson, A. and Norin, T.; *Biocatalysis*, **7** (1993), 131-147.
- (288) Ke, T.; Tidor, B. and Klibanov, A. M.; *Biotechnol. Bioeng.*, **57** (1998), 741-745.
- (289) Norin, M.; Haeffner, F.; Achour, A.; Norin, T. and Hult, K.; *Protein Science*, **3** (1994), 1493-1503.
- (290) Aerts, J.; *J. Comput. Chem.*, **16** (1995), 914-922.
- (291) Bencsura, A.; Enyedy, I. Y. and Kovach, I. M.; *J. Am. Chem. Soc.*, **118** (1996), 8531-8541.
- (292) Benedetti, F.; Berti, F.; Linda, P.; Miertus, S. and Sabot, A.; *Bioorganic & Medicinal Chemistry Letters*, **6** (1996), 839-844.
- (293) Botta, M.; Cernia, E.; Corelli, F.; Manetti, F. and Soro, S.; *Biochim. Biophys. Acta*, **1337** (1997), 302-310.
- (294) Haeffner, F.; Norin, T. and Hult, K.; *Biophys. J.*, **74** (1998), 1251-1262.
- (295) Orrenius, C.; van Heusden, C.; van Ruiten, J.; Overbeeke, P. L. A.; Kierkels, H.; Duine, J. A. and Jongejans, J. A.; *Protein Engineering*, **11** (1998), 1147-1153.
- (296) Warshel, A.; Åqvist, J. and Creighton, S.; *Proc. Natl. Acad. Sci. USA*, **86** (1989), 5820-5824.
- (297) Warshel, A.; *Modelling enzyme reactions*; Wiley Interscience: 1997.
- (298) Hu, C.-H.; Brinck, T. and Hult, K.; *Int. J. Quant. Chem.*, **69** (1998), 89-103.
- (299) Edholm, O. and Ghosh, I.; *Mol. Simul.*, **10** (1993), 241-253.
- (300) Warshel, A. and Levitt, A.; *Biochemistry*, **28** (1976), 3629-3637.
- (301) Harrison, M. J.; Burton, N. A. and Hillier, I. H.; *J. Am. Chem. Soc.*, **119** (1997), 12285-12291.
- (302) Colombo, G.; Toba, S. and Merz, K. M. J.; *J. Am. Chem. Soc.*, **121** (1999), 3486-3493.
- (303) Cid, H. and Bunster, M.; *Biol. Res.*, **29** (1996), 77-100.
- (304) Schmidt, M. W.; Baldrige, K. K.; Boatz, J. A.; Elbert, S. T.; Gordon, M. S.; Jensen, J. H.; Koseki, S.; Matsunaga, N.; Nguyen, K. A.; Su, S. J.; Windus, T. L.; Dupuis, M. and Montgomery Jr., J. A.; *J. Comput. Chem.*, **14** (1993), 1347-1363.
- (305) O'Hagan, D. and Rzepa, H. S.; *J. Chem. Soc., Perkin Trans II*, **2** (1994), 3-4.
- (306) Kazlauskas, R. J.; Weissfloch, A. N. E.; Rappaport, A. T. and Cuccia, L. A.; *J. Org. Chem.*, **56** (1991), 2656-65.
- (307) Janes, L. E. and Kazlauskas, R. J.; *Tetrahedron: Asymmetry*, **8** (1997), 3719-3733.
- (308) Prelog, V.; *Pure & Appl. Chem.*, **9** (1964), 119-130.
- (309) Adachi, O.; Matsushita, K.; Shinagawa, E.; Ameyama, M.; *Agric. Biol. Chem.*, **54** (1990), 2123-2129.
- (310) Bertrand, G.; *Ann. Chim. Phys.*, **3** (1904), 181-288.
- (311) Jones, J. B. and Jakovac, I. J.; *Can. J. Chem.*, **60** (1982), 19-28.
- (312) Toone, E. J.; Werth, M. J. and Jones, J. B.; *J. Am. Chem. Soc.*, **112** (1990), 4946-4952.
- (313) Naemura, K.; Fukuda, R.; Konishi, M.; Hirose, K. and Tobé, *Chem. Soc., Perkin Trans. I*, **1** (1994), 1253-1256.
- (314) Ottolina, G.; Carrea, G.; Colonna, S. and Rueckemann, A.; *Tetrahedron: Asymmetry*, **7** (1996), 1123-1136.

- (315) Ljubovic, E. and Sunjic, V.; *Tetrahedron: Asymmetry*, **8** (1997), 1-4.
- (316) Yamada, Y. K.; Aida, K. and Uemura, T.; *J. Biochem.*, **61** (1967), 636-646.
- (317) Ameyama, M.; Shinegawa, E.; Matsushita, K. and Adachi, O.; *J. Bacteriol.*, **145** (1981), 814-823.
- (318) Marcinkeviciene, J. and Johansson, G.; *FEBS Lett.*, **318** (1993), 23-26.
- (319) Olsthoorn, A. J.; Otsuki, T. and Duine, J. A.; *European Journal Of Biochemistry*, **247** (1997), 659-65.
- (320) Olsthoorn, A. J. J. and Duine, J. A.; *Biochemistry*, **37** (1998), 13854-13861.
- (321) Matsushita, K.; Shinagawa, E.; Inoue, T.; Adachi, O. and Ameyama, M.; *FEMS Microbiol. Lett.*, **37** (1986), 141-144.
- (322) Matsushita, K.; Shinagawa, E.; Adachi, O. and Ameyama, M.; *J. Biochem.*, **105** (1989), 633-637.
- (323) Cozier, G. E. and Anthony, C.; *Biochem. J.*, **312** (1995), 679-685.
- (324) Imanaga, Y.; In; "PQQ and Quinoproteins", J. A. Jongejan and J. A. Duine, Ed., Kluwer Academic Publishers: Dordrecht, 1989; pp 87-95.
- (325) Asakura, A. and Hoshino, T.; *Biosci. Biotechnol. Biochem.*, **63** (1999), 46-53.
- (326) Kraulis, P. J.; *J. Appl. Cryst.*, **24** (1991), 946-950.

# Homology Model of the Quinohemoprotein Alcohol Dehydrogenase from *Comamonas testosteroni*

Aldo Jongejan, Jaap A. Jongejan and Johannes A. Duine

---

## Abstract

A molecular model of QH-ADH, the quinohemoprotein alcohol dehydrogenase from *Comamonas testosteroni*, has been built by homology modeling. Sequence similarity of N-terminal residues 1-570 with the  $\alpha$ -subunit of quinoprotein methanol dehydrogenases, MDHs, from *Methylophilus W3A1* and *Methylobacterium extorquens* provided a basis for the design of the PQQ-binding domain of QH-ADH. Minimal sequence similarity with cytochrome  $c_{551}$  from *Ectothiorhodospira halophila* and cytochrome  $c_5$  from *Azotobacter vinelandii* has been used to model the C-terminal heme c-binding domain, residues 571-677, absent in MDHs. Distance constraints inferred from  $^{19}\text{F}$ -NMR relaxation studies of trifluoromethylphenylhydrazine-derivatized PQQ bound to QH-ADH apoenzyme as well as theoretical relations for optimal electron transfer have been employed to position the heme- and PQQ-binding domains relative to each other. The homology model obtained shows overall topological similarity with the crystal structure of  $cd_1$ -nitrite reductase from *Thiosphera pantotropha*. Experimental findings including (i) the site sensitive to *in vivo* proteolytic attack, (ii) the substrate specificity in comparison to MDHs, (iii) changes of the spectral properties of the heme c upon reconstitution of apoenzyme with PQQ, (iv) electronic interaction between heme and PQQ, and (v) enantioselectivity in the conversion of a chiral sec alcohol are adequately accounted for by the proposed model.

Published in *Protein Engineering*, **11** (1998), 185-198.

**Keywords**

Quinhemoprotein alcohol dehydrogenase / PQQ / Homology modeling /  $\beta$ -propeller fold  
/ *Comamonas testosteroni*



## Introduction

Alcohol dehydrogenases containing pyrroloquinoline quinone (2,7,9-tricarboxy-1*H*-pyrrolo[2,3-*f*]quinoline-4,5-dione, PQQ) (Figure 1), as a cofactor have been isolated from various Gram negative bacteria [1-3]. Based on the cofactor requirement two classes can be distinguished: quinoprotein alcohol dehydrogenases (containing PQQ and Ca<sup>2+</sup>) and quinohemoprotein alcohol dehydrogenases (containing PQQ, Ca<sup>2+</sup> and heme c).

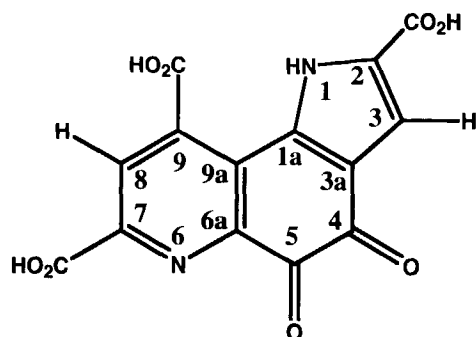


**Figure 1.** Structure of pyrroloquinoline quinone, PQQ

The first class includes methanol dehydrogenases, MDHs, from methylotrophic bacteria [4-8], and ethanol dehydrogenases, EDHs, occurring in Pseudomonads [9-12]. Both MDHs and EDHs possess an  $\alpha_2\beta_2$  configuration with subunits of 66 kDa( $\alpha$ ) and 8.5 kDa( $\beta$ ). The  $\alpha$  subunits contain one molecule each of non-covalently bound PQQ and calcium. The electrons accepted upon oxidation of the substrate are transferred to the natural electron acceptors, cytochrome  $c_1$  in the case of MDH [5,6,13], cytochrome  $c_{EDH}$  for EDH from *Pseudomonas aeruginosa* [12]. Only positively charged dyes, e.g. TMPD<sup>+</sup>, PMS, PES, appear to function as artificial electron acceptors in the *in vitro* assay. Primary amines or ammonia are required as activators. Whereas an optimum pH of 9.0-9.5 is observed in both cases, EDH has a  $K_M$  value for methanol that is 1000 times that for ethanol. High-resolution crystal structures are available for MDHs from *Methylophilus W3A1* [14-16] and *Methylobacterium extorquens* [17]. Crystals have been obtained for EDH [18].

Two types of quinohemoprotein alcohol dehydrogenases, QH-ADHs, have been described. Type II comprises membrane-bound enzymes composed of at least three different subunits. Examples have been found in *Acetobacter* and *Gluconobacter* species

[19]. The  $\alpha$ -subunit (72 kDa), thought to possess dehydrogenase activity, contains one molecule of PQQ and one heme c. The other subunits contain several heme-c-binding motifs [20-22]. The genes of QH-ADH from *A. polyoxygenus* [21], *A. acetii* [23] and *A. pasteurianus* [24,25] have been cloned and sequenced.

Type I quinohemoprotein alcohol dehydrogenases are monomeric proteins containing one molecule of PQQ and a single c-type heme. Examples have been isolated from ethanol grown *Comamonas testosteroni* [9,26-29] and *Comamonas acidovorans* (Kraayveld *et al.*, unpublished), vanillyl alcohol grown *Rhodopseudomonas acidophila* [30,31], *Pseudomonas putida* [32] and poly(vinyl alcohol) grown *Pseudomonas* sp. [33]. Whereas the latter species produce QH-ADH in the holo-form, *C. testosteroni* has so far been found unable to synthesize PQQ and produces a PQQ-free apo-enzyme when grown in the absence of PQQ. The protein is isolated as a 73 kDa soluble, inactive, heme c containing monomeric apo-enzyme [9,26,27]. Upon reconstitution with PQQ in the presence of calcium, active holoenzyme is formed both *in vitro* as well as *in vivo*. Part of the apo-enzyme appears to be nicked at a specific site during growth of the organism in the absence of PQQ, resulting in strongly associated fragments of 51 kDa and 25 kDa unable to bind PQQ upon reconstitution [27]. Once formed, holo-enzyme is less sensitive to proteolytic attack. Upon substrate oxidation two electrons are transferred to PQQ. Reoxidation of PQQH<sub>2</sub> has been proposed to occur by subsequent intramolecular electron transfer to the heme c moiety [34]. Compared to MDH and EDH a broader range of artificial electron acceptors including negatively charged ferricyanide is accepted, suggesting the heme cofactor to be involved in the electron acceptor interaction. The physiological redox partner is not known (preliminary results suggest a role for an azurin-type blue-copper protein under certain growth conditions (Kraayveld *et al.*, 1996, unpublished). The two types of quinohemoprotein alcohol dehydrogenase differ in substrate specificity and enantioselectivity for chiral C3-alcohols [34]. Whereas Type II QH-ADHs specifically oxidize primary and secondary alcohols ranging from ethanol to hexanol and have low activity for formaldehyde and acetaldehyde, Type I QH-ADH from *C. testosteroni* also converts sterols, polyethylene glycols [27,30] and secondary alcohols [35] as well as various aldehydes implying a more accessible active site. The pH optima for the two types differ by 2-3 units (7.7 for Type I and 4-6 for Type II). No activator is required for catalysis. Recently, the gene for QH-ADH from *C. testosteroni* has been cloned and sequenced [36]. X-ray crystallography has been attempted [37]. No crystal structures are available for QH-ADHs.

For a better understanding of the observed differences in catalytic behaviour and the intramolecular electron transfer processes, knowledge of the three-dimensional structure of QH-ADHs is required. A molecular model for the Type II enzyme from *Acetobacter acetii* lacking the essential heme-domain has been presented [38]. In view of the large body of experimental observations, the fundamentally interesting cofactor arrangement and the potentials for application of Type I QH-ADH [39-42], further investigations would benefit greatly from the availability of an appropriate structural model. We investigated the potential of homology modeling protocols for the construction of a 3D-model of *C. testosteroni* QH-ADH, comprising both PQQ-binding and heme c-containing domains.

### Homology modeling

In the absence of comprehensive *a priori* folding rules accurate protein structure elucidations based solely on the amino acid sequence are not feasible. Secondary structures have, however, been assigned for extended sequences [43,44] while methods for the prediction of tertiary structures have appeared [45,46]. Since the three-dimensional structures of related proteins tend to be conserved X-ray structures of related proteins have been used as a scaffold to construct a model of the target protein by homology modeling. The merits of this approach for the understanding and organization of experimental observations have been documented. Examples include: lignin peroxidase [47], D-glyceraldehyde-3-phosphate dehydrogenase [48], glutathione S-transferases [49], a monocyte chemo-attractant [50], leader peptidase NisP [51], interleukin-13 [52], interleukin-4, serine & cysteine proteases [53,54], hypothetical model flavodoxin-tetraheme cytochrome  $c_3$  [55], D-lactate dehydrogenase [56], phenylalanine dehydrogenase [57] and rap-1A protein [58].

Structures proposed using homology modeling that have been subsequently confirmed by X-ray crystallography include immunoglobulin D1.3 [59] and angiogenin ([60] and references therein). The extent of amino acid sequence identity appears to be the most critical parameter for the accuracy of the model building [61].

### Reference structures for modeling of Type I QH-ADH

Amino acids sequences have been compared for Type I QH-ADH and related quinoproteins [36]. Up to 43 % amino acid identity is observed for the sequences of QH-ADH from *Comamonas testosteroni* and the QH-ADHs of *Acetobacter* species. However,



a reliable starting point for homology modeling based on a single reference structure [61]. Lower sequence identity scores may, however, be acceptable when a number of related structures is available [54,56,62-65]. In the present case, salient features of the MDH structures appear to be highly conserved on the primary sequence level in the N-terminal domain of QH-ADH. The 'tryptophan-motif' [7,14-17] that constitutes the eight-bladed  $\beta$ -propeller fold found in MDHs is distinctly present on the primary sequence level in QH-ADH as well (Figure 3A).

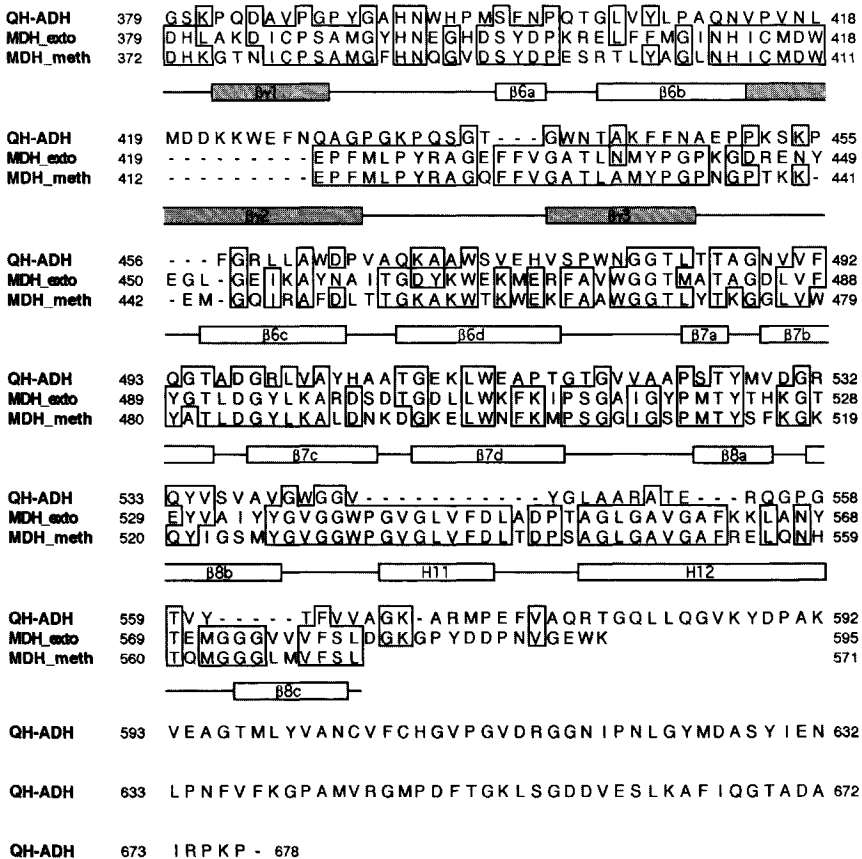


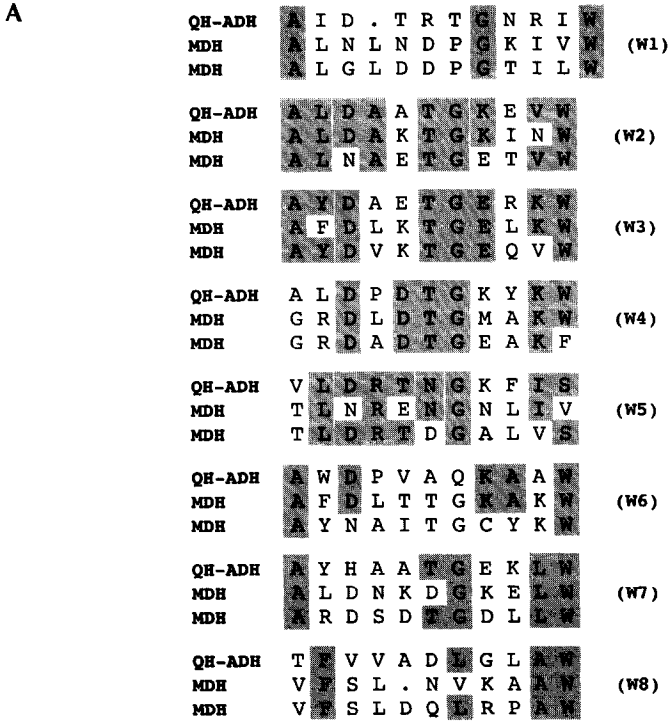
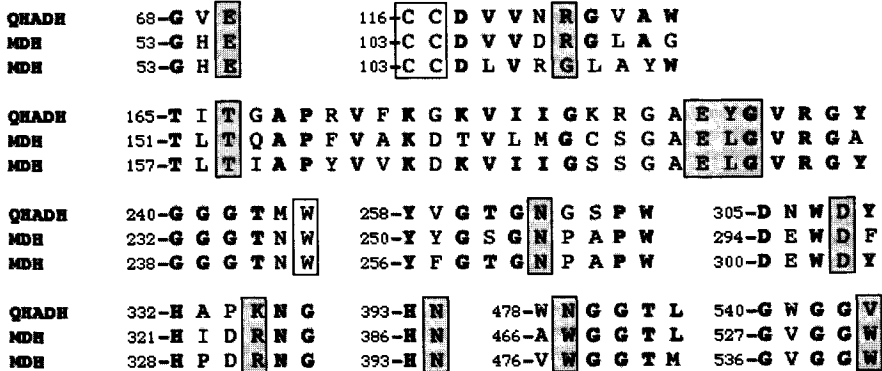
**Figure 2.** Sequence alignment of the primary sequence of QH-ADH from *C. testosteroni* and MDHs from *M. extorquens* and *M. methylophilus*, respectively. Structural motives as found in MDH from *M. methylophilus* are depicted beneath its sequence (H designates an helix,  $\beta$  a beta-sheet).

The amino acids involved in PQQ and  $\text{Ca}^{2+}$  binding in MDH appear to be completely conserved in QH-ADH (Figure 3B). In particular, the conservation of the vicinal cysteines 103 and 104 and tryptophan 243 lining the characteristic PQQ sandwich in the active site of both MDHs (numbers refer to *M. extorquens*) strongly suggests a similar arrangement in the active site of QH-ADH. Since the residues conserved between the MDHs and QH-ADH are evenly distributed in space structure predictions based on their positions might well be more accurate than could be expected on the basis of the 34% overall sequence identity.

UV/Vis, EPR and NMR spectroscopy have shown QH-ADH to contain a low-spin, six-coordinated heme, most probably liganded by methionine and histidine residues [28]. The methionyl-histidinyl-Fe-coordination is also implied by the presence of a heme c-binding motif in the C-terminal domain of QH-ADH. For QH-ADH no sequence similarity in this region was found with the natural electron acceptors of MDH and EDH, cytochrome  $c_L$  and cytochrome  $c_{\text{EDH}}$ , respectively. Low similarity is observed for the heme-domain of QH-ADH of *C. testosteroni* and the C-terminal part of the 44 kDa cytochrome  $c$  subunit of QH-ADH from *A. polyoxygenus* (20 % identity, accepting gaps in the alignment) and that of cytochromes  $c_{553}$  of cyanobacteria and algae (23 % identity with cytochrome  $c_{553}$  from *Plectonema boryanum* [36]. X-ray structures are not available for these cytochromes. The primary sequence and NMR structure determination of cytochrome  $c_{551}$  from the purple phototrophic bacterium *Ectothiorhodospira halophila* is available [66]. For this cytochrome low sequence identity (23 % identity) with the heme-domain of QH-ADH is also observed (Figure 4). Since, based on the NMR assignment, this cytochrome is proposed to be structurally homologous to cytochrome  $c_5$  from *Azotobacter vinelandii* for which an X-ray structure is available [67] the structure of the latter cytochrome provided a starting point for the construction of a model for the heme-domain of QH-ADH.

### **The relative positions of heme- and PQQ-domains**

In order to construct the full model appropriate spatial positioning of the heme- and PQQ domains is required. An estimate of the separation of the heme-Fe and PQQ cofactors has been obtained from  $^{19}\text{F}$  NMR-relaxation measurements of QH-ADH containing fluorine-labeled PQQ-derivatives [29]. A distance of ca. 20 Å between PQQ-C5 and the heme Fe has been deduced. Kinetic measurements [34] have indicated the heme to be involved in intramolecular electron transfer processes between the electron-acceptor

**B**

**Figure 3. (A)** Tryptophan motif conserved for QH-ADH from *C. testosteroni* and MDH from *M. methylophilus* and *M. extorquens*, respectively. **(B)** Sequence alignment for active site residues in QH-ADH from *C. testosteroni* and MDH from *M. methylophilus* and *M. extorquens*, respectively. PQQ-ligands in shaded boxes, cysteine-bridge and tryptophan boxed, conserved residues in bold typeface.

and the primary PQQ redox-site. Distinct changes of the heme Soret band upon reconstitution of QH-ADH apoprotein with PQQ do not contradict the presence of an electronic link between the heme and PQQ cofactors (although other possibilities have been pointed out, see below). Analysis of the probable electron transfer pathways [68] leading from PQQ to the surface of the N-terminal domain in the proposed model might thus provide an estimate of the relative location of the heme-containing domain.

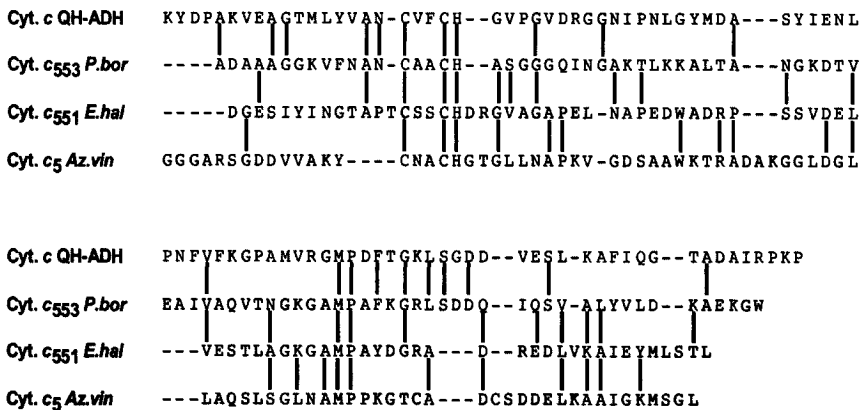


**Figure 4.** Sequence alignment of the C-terminal cytochrome part of QH-ADH of *C. testosteroni* with the sequence of cytochrome *c*<sub>553</sub> (*P. boryanum*), cytochrome *c*<sub>551</sub> (*E. halophila*) and cytochrome *c*<sub>5</sub> (*A. vinelandii*). For cytochrome *c*<sub>551</sub> and cytochrome *c*<sub>553</sub> identical residues are shown relative to cytochrome *c* from QH-ADH, and for cytochrome *c*<sub>551</sub> [66]

## Materials and methods

Modeling experiments were performed on a Silicon Graphics Indigo XZ4000 using InsightII/Discover/Homology (BIOSYM Technology, San Diego). GREENPATH v0.97 was kindly provided by J. J. Regan, MolScript v1.4 by P. Kraulis [69], Raster3D [70,71] was obtained by anonymous ftp from ftp.bmsc.washington.edu.

Protein volumes were calculated using InsightII.

## Force field parameters, minimizations and dynamics

Energy minimizations have been carried out using the Consistent Valence Force Field (CVFF, Biosym Inc.) disregarding cross terms and Morse bond stretching potentials. A double cut-off was applied at 14.0 Å and 20.0 Å, with a switching distance of 1.5 Å. A dielectric constant of 1 was used in all minimizations. Structures were minimized using



steepest descent (maximum derivative  $< 5.0 \text{ kcal } \text{\AA}^{-1} \text{ mol}^{-1}$ ) and conjugate gradient (maximum derivative  $< 0.1 \text{ kcal } \text{\AA}^{-1} \text{ mol}^{-1}$ ) algorithms followed by molecular dynamics protocols. In consecutive MD rounds the temperature was varied between 50 and 300 K.  $C_{\alpha}$  atoms were restrained to their initial position by applying a force of  $2 \text{ kcal}/\text{\AA}$  and allowing a maximum force of  $10 \text{ kcal}/\text{\AA}$  while the PQQ molecule and calcium-ion were kept at their initial coordinates. After a 1-5 ps equilibration period dynamics was performed for 10 ps before cooling down to 50 K (2-5 ps). The constraints on the  $C_{\alpha}$  atoms prevented unfolding at temperatures up to 250 K. At higher temperatures further optimization was not successful, probably due to the overriding importance of correct charge assignments to maintain the structural integrity. The final model was obtained after several rounds of minimization and molecular dynamics to monitor its stability. The MDH structure of *M. extorquens* was subjected to similar protocols for comparison.

**Note:** Molecular dynamics performed on MDH structures (previously 'relaxed' using standard procedures) at 300 K without its  $\beta$ -subunit showed the structure to be highly unstable, while including the  $\beta$ -subunit and using the same protocol left the structure intact. The relative abundance of charged residues in this small subunit, illustrates the importance of the correct and well-balanced positioning of charges for successful performance of energy minimizations of protein structures. Apparently, the  $\beta$ -subunit functions as a zipper to stabilize the structure of the  $\alpha$ -subunit of MDH. Assessing a similar role for the heme-domain is outside the scope of this project.

The literature was searched for force field parameters for the heme moiety [72-77]. Parameters of the CHARMM force field as described by Brooks and coworkers [78] were used and transferred to the CVFF force field. New potential types were introduced for iron, nitrogen and carbon atoms in the porphyrin ring as described by Lopez & Kollman [72] (Figure 5). However, most force field parameters describe heme molecules that have CO, O<sub>2</sub> or H<sub>2</sub>O as a sixth ligand. Bond and angle parameters for the methionine sulphur as the sixth ligand were taken from the crystal structure of cytochrome *c*<sub>5</sub> from *Az. vinelandii*. Partial charges were adapted from Lopez & Kollman and from calculations using MOPAC (implemented in INSIGHT). The structure of the macrocycle and its two axial ligands of cytochrome *c*<sub>5</sub> from *Az. vinelandii* served as a template for optimization of the parameters. The structure was further minimized and compared with the original after 100 steps of steepest descent followed by dynamics runs of 10 ps (300

K) and 2 ps (50 K). Force constants were adapted to meet geometric constraints. The parameter set leading to a final RMS deviation for the nitrogen, carbon and iron atoms of 0.71 Å and for all atoms of 1.02 Å was used in further minimization and dynamics runs. Final values of the parameters have been collected in Table I. Similar values have been presented while this work was in progress [79].

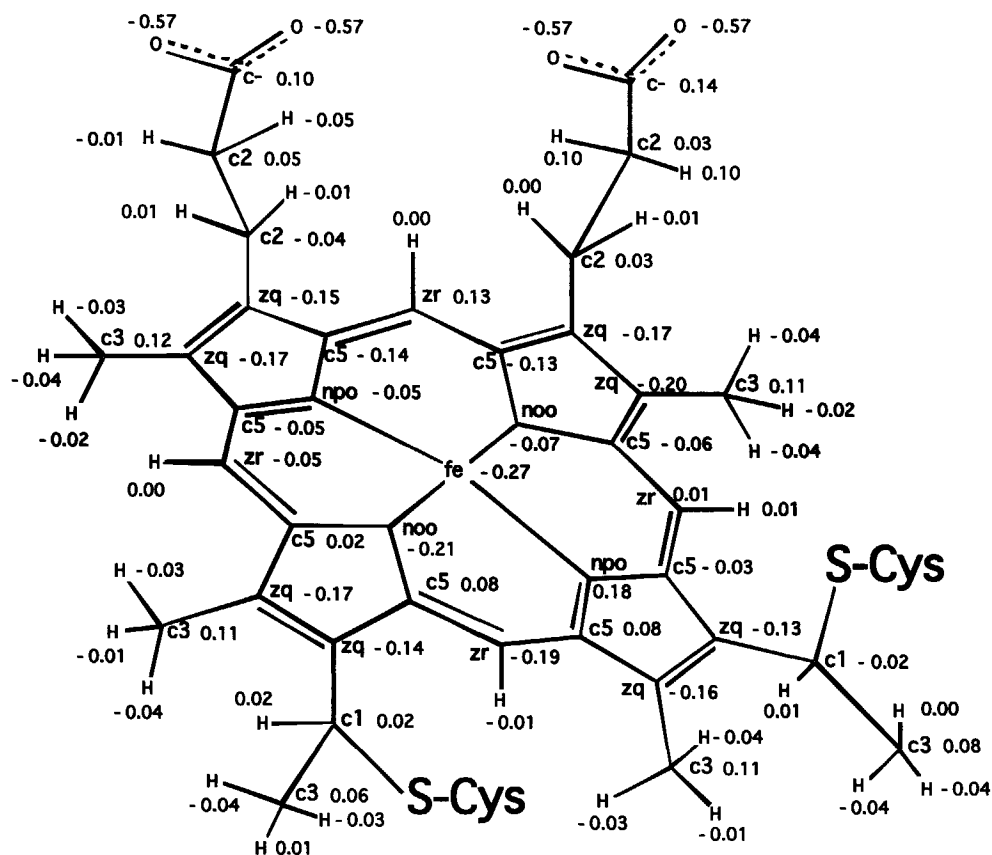


**Figure 5.** Potential types (according to [72]) and charges for the porphyrin ring as used in the mechanics and dynamics calculations.

**Table I.** Parameters used for description of a low-spin heme in the CVFF force field.**Quadratic bond stretching potential:  $E = K_2 (R - R_0)^2$** 

| Bond          | $R_0$ (Å) | $K_2$ (kcal mol <sup>-1</sup> Å <sup>-2</sup> ) |
|---------------|-----------|---|
| fe - npo/noo  | 1.98      | 275.00  |
| fe - s (Met)  | 2.36      | 100.00  |
| fe - np (His) | 2.08      | 100.00  |

**Quadratic angle bending potential:  $E = K_2 (\theta - \theta_0)^2$** 

| Angle                    | $\theta_0$ (deg) | $K_2$ (kcal mol <sup>-1</sup> rad <sup>-2</sup> ) <sup>a</sup> |
|--------------------------|------------------|--|
| npo/noo - c5 - zq        | 109.00           | 70.00  |
| npo - fe - npo           | 179.90           | 50.00  |
| np (His) - fe - noo/npo  | 90.00            | 50.00  |
| npo - fe - noo           | 90.00            | 50.00  |
| zr - c5 - c5             | 125.00           | 70.00  |
| c5 - zr - c5             | 125.00           | 70.00  |
| npo/noo - fe - s (Met)   | 90.00            | 50.00  |
| np (His) - fe - s (Met)  | 179.90           | 50.00  |
| c (Met) - s (Met) - fe   | 120.00           | 50.00  |
| fe - npo/noo - c5        | 125.00           | 70.00  |
| fe - np (His) - c5 (His) | 130.00           | 20.00  |
| zr - c5 - npo/noo        | 125.00           | 70.00  |
| c5 - npo/noo - c5        | 108.80           | 70.00  |
| zq - c5 - npo/noo        | 125.00           | 70.00  |

**Dihedral angle potential:  $E = K_\phi [1 + \cos(n\phi - \phi_0)]$** 

| Angle                | $K_\phi$ (deg) | n | $\phi_0$ (deg) |
|----------------------|----------------|---|----------------|
| X - npo/noo - c5 - X | 11.40          | 2 | 180.00         |
| X - fe - X - X       | 0.00           | 2 | 180.00         |
| fe - X - X - X       | 0.00           | 2 | 180.00         |

<sup>a</sup>Discover converts angles to radians

### Model building

**PQQ-domain.** Crystal structures of quinoprotein methanol dehydrogenase from *Methylophilus methylotrophus* W3A1 (pdb entry 3aah) and *Methylobacterium extorquens* were kindly provided by the authors (F.S. Mathews and M. Ghosh, respectively). Four blocks of structurally conserved regions, SCRs, were identified by pairwise sequence and structure alignment of the MDH sequences (Block 1 from Thr10/Ser10 to Ala115/Pro115, block 2 from Gly116/Ala122 to Val311/Asp317, block 3 from Ala313/Gly320 to Asn436/Lys443 and block 4 from Gly444/Gly453 to Leu571/Leu580. Residue numbers of MDH are given as *M. methylotrophus* W3A1 / *M. extorquens*). Partial sequences of MDHs and QH-ADH were aligned according to Stoorvogel *et al.* (Figure 2). Two procedures were tested to model the structure of the PQQ-domain of QH-ADH.

*Procedure A.* The center of MDH was located by visual inspection at Trp 345. Non-conserved residues within a radius of 10 Å were mutated in the MDH structure. The orientations of the side chains were retained as much as possible. After each round of 'accelerated evolution', energy minimization was applied to the residues within this sphere, keeping the surrounding residues fixed at their initial positions. This procedure was repeated after increasing the radius another 10 Å until all non-conserved residues were mutated. Loops were generated using an energy-based procedure. Candidate loops were picked by visual inspection of the resulting structure ignoring RMS deviations if needed. High priority was given to the topological similarity with the overall MDH structure. An extra round of energy minimization was performed in order to relax the residues in the loops using the surrounding residues as constraints.

*Procedure B.* Structures of both MDH's were superimposed guided by the SCRs. Coordinates for all residues were transferred and loops were constructed in a single round. Several rounds of energy minimization were performed. Areas with close contacts were allowed to move freely while their surroundings were kept fixed serving as constraints for the minimizations. Residues showing bad contacts were replaced with their rotamers as well as manually adapted. Molecular dynamics simulations were performed starting at low temperature (50 K). C $\alpha$ -atoms were restrained to their initial position with a force of 2 kcal/Å and a maximum force of 10 kcal/Å. In consecutive rounds the temperature was raised to 250 K.

In both procedures the disulfide bridge between the vicinal cysteines was constructed after completion of the initial minimizations. The PQQ cofactor and the calcium ion

were introduced in this stage of the modeling by superposition of the active site residues from QH-ADH on these of the MDH structures. Charges for PQQ were calculated using MOPAC.

**Heme-domain.** The coordinates of cytochrome  $c_5$  from *Az. vinelandii* were obtained from the crystal structure (pdb entry 1cc5, [67]). Residues 587-677 of QH-ADH were first aligned to the sequence of cytochrome  $c_{551}$  from *E. halophila* using the Biosym Homology module (gap penalty = 6, gap length penalty = 1.65). The resulting sequence was then aligned to the sequence of cytochrome  $c_5$  from *Az. vinelandii* [66]. Results are collected in Figure 4. Secondary structure elements were determined using the methods of Garnier-Osguthorpe-Robson [44] and Chou-Fasman [43]. All coordinates were transferred and loops constructed using an energy-based procedure. The domain was extended with residues 571-586 using the BIOSYM Biopolymer-module. One round of minimization (300 steps of steepest descent and 500 steps of conjugate gradient) was performed while keeping the conserved residues restrained to their initial positions in order to relax the loops. Initially, the heme macrocycle together with its axial ligands was kept fixed using a restraint-file. Deviations from starting values were allowed as follows: 0.5 degrees for dihedral angles, 0.05 Å for distances within the macrocycle and 0.1 Å for distances between the macrocycle and its closest neighbouring residues. In subsequent runs the heme was minimized using parameters described by the home-made force field. Minimization of the full model was performed similarly.

### Positioning of the PQQ and heme domains

**Electronic coupling to surface residues.** Surface residues of the PQQ-domain were identified by rolling a probe with a radius of 3.0 Å over the surface [68]. Electronic coupling with the PQQ cofactor was calculated for these residues using GREENPATH [80-82]. The C(5) carbonyl bond of PQQ was taken as the donor state while the respective surface residues were taken as acceptor states. The highest coupling value calculated for a specific bond in the residue was taken as the coupling value for that particular residue. Surface residues colored according to their relative coupling intensity with PQQ are shown in Figure 6.

As the heme edge is exposed to the solvent no calculation of the electronic coupling to the surface residues was performed for this domain.

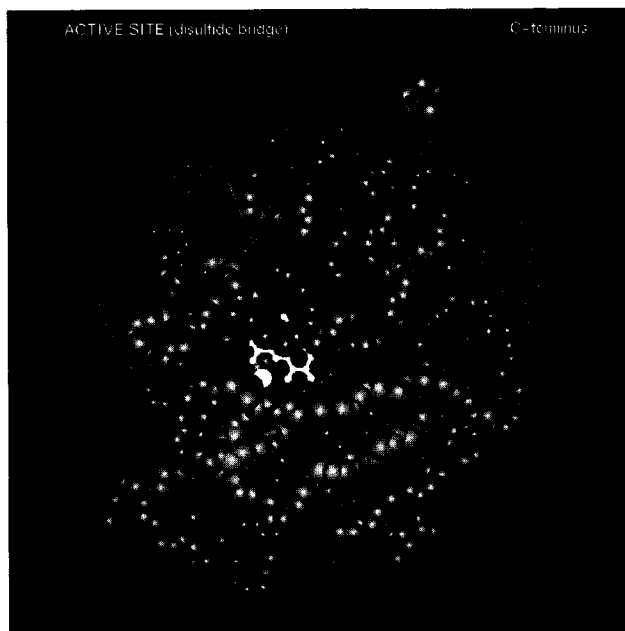


**Figure 6.** Electronic coupling from PQQ (in white) to surface residues as calculated with GREENPATH [80-82]. Colouring is according to the value of coupling (increasing from dark grey to white). Only backbone atoms of the amino acids are displayed. The highest value found within an amino acid has been as the value for that particular residue.

**Docking.** The heme-domain was placed manually at  $\sim 30.0$  Å along the pseudo C2-axis from the PQQ with the heme edge pointing towards the active site cavity. A force of  $100 \text{ kcal } \text{Å}^{-1}$  was assigned to pull the heme-iron towards PQQ. A step size of  $1$  Å was applied initially. On closer approach the step size was decreased to  $0.1$  Å. Each pull was followed by a round of minimization (300 steps of conjugate gradient). Initially, the PQQ-domain was kept fixed while the complete heme-domain was allowed to move freely. In subsequent runs residues constituting the alleged docking site were allowed to move freely, while the surrounding residues were kept fixed. The energy of the complete protein was monitored during the process in order to determine optimal docking under the conditions applied.

### Enantioselectivity

C(5)-(R)- and (S)-pentan-2-ol adducts of PQQ were built on the basis of the PQQ X-ray

structure available to us [83]. After replacement of the C(5)-carbonyl group with the appropriate hemiketal moiety charges were set using MOPAC. Subsequent minimizations were performed using CVFF parameters. The adducts were introduced into the active site cavity using maximum overlap of the atoms belonging to PQQ. The conformation of the alkyl side chains was allowed to relax during dynamics runs with and without Coulombic interactions (1000 iterations at 300 K). Except for the calcium ion, the hemiketal alkoxy and the hemiketal hydroxy group, all atoms were kept fixed to their model coordinates. In subsequent runs water molecules were included from the pdb-file of MDH from *M. extorquens*. Those waters showing a large interaction with the hemiketal groups ( $> 10$  kcal/mol) were deleted. The residual waters were allowed to move during the dynamic runs but confined to the active site by waters placed in a solvent box around the protein.

## Results

**PQQ-domain.** The distinct sequence similarity between QH-ADH and the related quinoproteins, methanol dehydrogenases from *M. extorquens* and *M. methylophilus* W3A1, allowed stepwise construction (Procedure A) of a model for the PQQ-domain of quinohemoprotein alcohol dehydrogenase. Application of a single round of mutagenesis (Procedure B) was not successful: excessive sidechain clashes occurred. Procedure A allowed relaxation of the side chains in between the different rounds of 'mutation'. The initial alignment of both MDHs provided four blocks of structurally conserved regions comprising 91 % of all residues in 588 pairs. RMS deviation of 0.64 Å was found for the C $\alpha$  atoms upon alignment of the structures. Two major variational regions were observed (residues 114-116 vs 114-122 and 435-443 vs 442-451 in *M. methylophilus* W3A1 and *M. extorquens*, respectively). Both loops are exposed on the outside of the proteins. Only minor loops had to be included in the PQQ domain of QH-ADH. Results of the minimizations and molecular dynamics runs (solvent molecules not included) are depicted. (Figure 7)

**Heme-domain.** The results of the model building protocol using the coordinates of *Az. vinelandii* cytochrome  $c_3$  as a template are shown in Figure 8.

**Full model.** Application of GREENPATH for the analysis of the electronic coupling between PQQ and the surface residues of the N-terminal domain identified a favorable

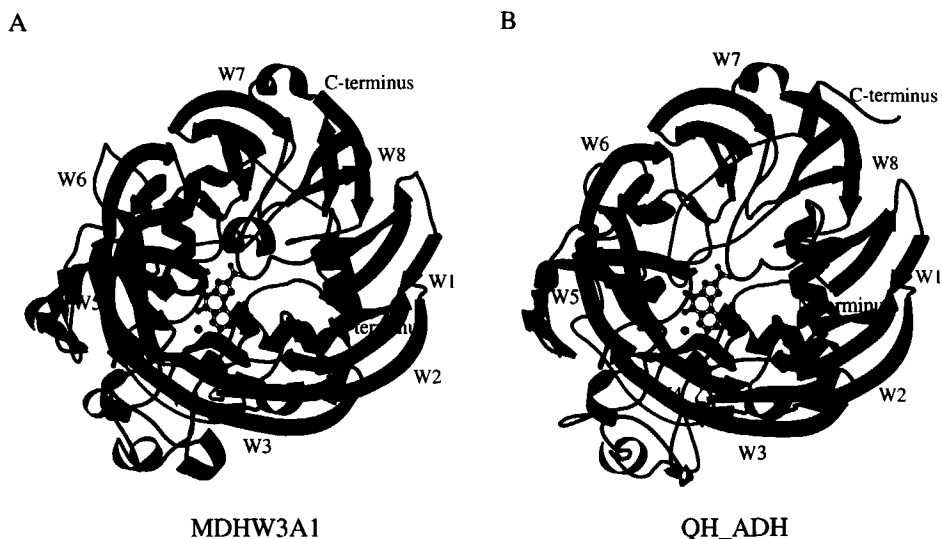


**Figure 7.** (A) Secondary structure of the  $\alpha$ -subunit of MDH from *M. methylotrophus* W3A1. PQQ is shown as ball and stick structure,  $\text{Ca}^{2+}$  as a small sphere. (B) Secondary structure of the model QH-ADH structure (N-terminal part). PQQ is shown as a ball and stick structure,  $\text{Ca}^{2+}$  as a small sphere. Figures are generated with MolScript [69].

region directly over the active site entrance. The docking position located directly over the active site cleft allowed the heme to approach the PQQ C(5)-bond to within 20 Å. The full model obtained by joining the PQQ-domain with the heme-domain via the long loop of sufficient length (~ 25 residues) to span the distance is shown (Figure 10). In view of the many degrees of freedom involved no further attempts were made to refine the position of this loop relative to the PQQ-domain.

#### Validation of the model structure

Several procedures for the evaluation of structural models have been described [84-87]. Analysis of the QH-ADH model structure using PROCHECK [88], WHAT\_CHECK [89] and the protein check software as implemented in the BIOSYM Homology module identified residues in 'unlikely' sections of the plots during initial stages of the minimizations and dynamics runs. After further minimizations and relaxations while constraining the surrounding residues improved scores where obtained. In the final





**Figure 8.** Constructed heme-domain of QH-ADH from *C. testosteroni*. Heme, methionine and histidine shown in dark grey (histidine above heme, methionine below), cysteines in light grey and heme iron depicted as a small sphere. Helices are represented as solid ribbons.

model low scores of residues in positions outside the region of our prime interest, the PQQ-binding and active site pocket, were disregarded. During initial rounds of energy minimizations several amino acids were forced into D-configurations. These were replaced by their L-counterparts. After several rounds of minimization and replacement inversions at  $C_{\alpha}$  were no longer observed. The total protein volume was measured to be  $63138 \text{ \AA}^3$ . This value compares favorably to the value of  $55732 \text{ \AA}^3$  obtained for MDH.

## Discussion

As a consequence of the assumptions and constraints embedded in the modeling strategy the final model incorporates the features present in the MDH structures. Thus, the 8-bladed  $\beta$ -propeller fold is clearly retained. The amino acids involved in this structure motif appear to be either conserved or replaced by similar residues in QH-ADH. No major disturbance of the overall folding pattern revealed itself during the modeling procedure (Figure 7). A similar observation has been reported for the homology modeling of the Type II QH-ADH from *A. acetii* [7].

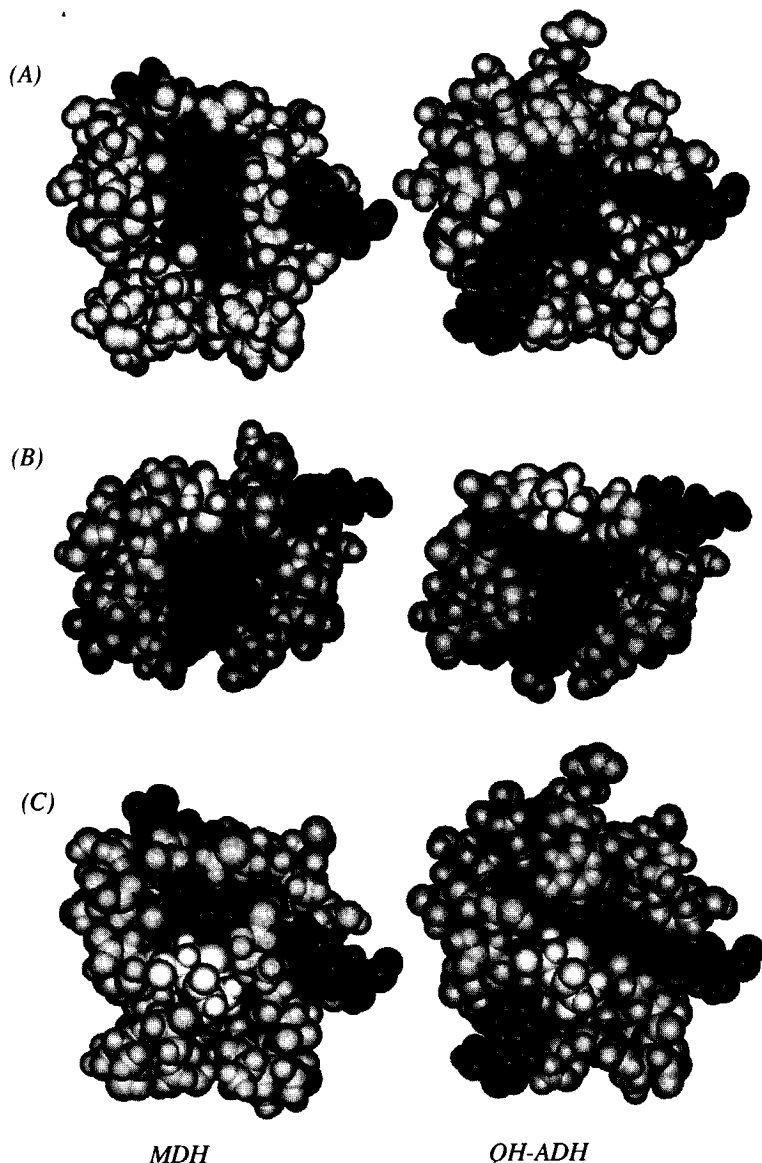


**Figure 9.** Views of the active site of MDH from *M. extorquens* and QHADH of *C. testosteroni*. All residues within 6 Å are included. PQQ is shown in grey, cysteine bridge in light grey, calcium in grey and tryptophan in dark grey. (A) Top view on the active site entrance of MDH and QH-ADH. The disulfide bridges have been removed for clarity. (B) Side view of the active

The vicinal disulfide bridge (Cys103-Cys104 in the primary sequence of *M. extorquens*) that is conspicuously present in the MDH structures is conserved on the primary level in the QH-ADH sequence (Cys116-Cys117). The cysteines form a unique non-planar eight-membered ring. At one time, the disulfide-bridge was proposed to be linked by a *cis*-peptide bond [90], as predicted [87,91] and observed for disulfide containing peptides [92,93]. High resolution crystal structures, however, have subsequently shown the cysteines to be in a *trans* configuration [16,17]. In the model structure the ring is accommodated in *trans* configuration on top of the cofactor with its sulfur atoms at  $\sim 3.5$  Å parallel to the plane of the PQQ molecule. Tryptophan 245 (Trp243 in *M. extorquens*) is positioned at the bottom of the active site cavity, its phenyl ring in a  $\pi$ -stacking interaction with the pyridine ring of PQQ. In MDH from *M. extorquens* the calcium ion is liganded by the  $\gamma$ -carboxyl oxygens of Glu 177, the amide oxygen of Asn 261, the C5-carbonyl oxygen, one oxygen of the C7-carboxyl group and the pyridine nitrogen of PQQ. In QH-ADH the coordination sphere of the calcium is provided similarly by the Glu 185  $\gamma$ -carboxyl oxygens, the amide oxygen of Asn 263 and the PQQ atoms mentioned above. Despite the fact that the calcium ligands were not restricted to their positions during the energy minimizations only a slight increase (2.4 - 3.1 Å in QH-ADH vs. 2.4 - 2.8 Å in MDH) in the distances between the calcium ion and its ligands is observed.

The overall appearance of the active sites of the model QH-ADH and MDHs is strikingly similar. However, the position of the non-conserved tryptophan (Trp 477 in *M. extorquens*, Trp 467 in *M. methylophilus* W3A1) is taken up by Val 479 in the present model, the loop to which this tryptophan belongs being absent in QH-ADH. As a consequence the active site entrance is widened into a cleft-like structure, whereas in MDH it is funnel-shaped [13]. This provides a suitable explanation for the observed difference in substrate specificity e.g. the conversion of bulky alcohols and even sterols by QH-ADH as opposed to the more restricted substrate specificity of MDHs.

Comparative cross-sections are depicted in Figure 9. As a possible consequence of the increased size of the cavity, PQQ was observed to occupy slightly tilted positions with

---

site of MDH and QHADH. All residues in the plane in front of the PQQ were subsequently removed to get a better view of the active site. **(C)** Top view of the active site of MDH and QH-ADH. The disulfide bridges have been included to show the clear difference in the active site dimensions between MDH and QH-ADH.

respect to the underlying tryptophan and the disulfide bridge in initial energy minimizations. Parallel sandwiching was restored, however, by transferring structurally defined waters from the active site of MDH (*M. extorquens*) to their analogous positions in the QH-ADH structure and minimization of the complete active site cavity following suitable relaxation of the water molecules.

Accommodation of bulky substrates by QH-ADH may well follow a similar pattern. While displacing water molecules the PQQ cofactor could easily tilt to facilitate the formation of a PQQ-substrate adduct at the C(5) position. Restricted entrance by the blocking tryptophan residue and the smaller size of the active site most probably prevent MDHs from oxidizing alcohols other than methanol to the corresponding acids (Figure 9B).

Compared to MDHs the active site of QH-ADH also shows a slight increase in size around the alleged positions of the N1- and C3- atoms of PQQ (Figure 9A & B). Thus, the model rationalizes the observation that PQQ derivatives carrying (small) alkyl groups in these positions [94] fit into the active site most probably replacing water molecules. Meanwhile, it has become clear that reconstitution of apoQH-ADH with PQQ derivatives carrying bulky alkyl groups in these positions is not successful. Reconstitution experiments with PQQ attached to pyrrole by way of a C6-alkyl spacer arm were equally unsuccessful (to be published elsewhere).

Construction of a model for the heme domain was considerably less straightforward due to the low degree of sequence similarity on the primary sequence level with cytochromes *c* for which crystal structures are currently available. Although the sequences may not show major similarities a common folding pattern is observed for many cytochromes *c*, called the 'cytochrome *c* fold'. The residues thought to be involved appear to be conserved to a certain extent in the cytochrome domain of QH-ADH (Figure 4). We therefore assumed the heme-domain of QH-ADH to possess the overall topology present in the small cytochromes *c*. Sequence similarity with cytochromes of phototrophic bacteria was found. The low degree of sequence similarity with cytochrome *c*<sub>551</sub> from *E. thiorhodospira* [66] and the observed degree of similarity of this cytochrome with cytochrome *c*<sub>5</sub> from *Az. vinelandii* (X-ray structure available) prompted us to accept the latter as a reference structure. The alignment used by Bersch *et al.* has been based on

the crystal structures of cytochrome  $c_{555}$  from *Chlorobium limicola* [95] and cytochrome  $c_5$  from *Az. vinelandii* [67]. As mentioned by Bersch *et al.*, these structures have to be treated with caution. The low-resolution structure of the cytochrome  $c_{555}$  has never been refined and is no longer available from the Brookhaven Protein Data Bank. The cytochrome  $c_5$  structure has been the subject of a critical discussion as to whether or not the crystal structures correspond to the biochemically relevant form [96]. Despite these limitations we accepted this structure as the basis for a crude model of the cytochrome  $c$  domain of QH-ADH. In this cytochrome the heme-iron is also liganded to a histidine and a methionine, and contains a low-spin heme as is observed for QH-ADH (Figure 8).

The final model results from the docking procedure in which the heme-domain has been placed manually in the vicinity of the two favorable electron transfer pathway patches identified by the GREENPATH program, one directly over the active site area and one at the opposite side of the pseudo C2-axis, running through the PQQ-domain. As the docking position and orientation is unknown we used experimental data to support allocation of the heme-domain. The value of 20 Å between the PQQ-C5 and the heme iron obtained from NMR-relaxation experiments with  $^{19}\text{F}$ -labeled PQQ-derivatives [29] is acceptable for electron-transfer to occur at rates faster than the observed enzyme turnover rate (approx.  $35\text{ s}^{-1}$ ) [97,98]. Based on energetic demands we decided in favor of the docking position located directly over the active site cleft since this position appeared to be most favorable allowing the heme to approach the PQQ C(5)-bond to less than 20 Å (Figure 10). The alternate position away from the active site appeared to be less likely since approach of the heme-iron and PQQ-C5 to within 24 Å required unrealistically high energies. In both cases the residues in the contact-regions were allowed to move during the minimizations in a naive attempt to mimic the dynamic properties of the encounter. Flexibility in the loops located further away on the protein surface might actually allow an even closer approach.

In the final model, 6 well-defined hydrogen bonds are formed at the perimeter of the contact area (diameter of ca. 20 Å). One of the hydrogen bonds formed is between the backbone hydrogen of Val 119, a residue in the PQQ-domain, and one of the propionic acid side chains of the heme moiety. The central part of the contact area consists of residues that are mainly hydrophobic in nature. Two of these residues, Tyr 545 and Phe 113, protrude from the PQQ-domain into the heme-domain and appear to play an

anchoring role.

The loop connecting the PQQ-domain with the heme-domain clearly belongs to the class of long-open loops as defined recently [99]. The distribution of residues in the loop does not deviate significantly from that found for other members of this class. In particular, no accumulation of (positively) charged residues was found in this loop. Although this seems to exclude a role for the loop as proposed for the small  $\beta$ -domain of MDH [14,17] a restraining interaction with the PQQ-domain can not be excluded.

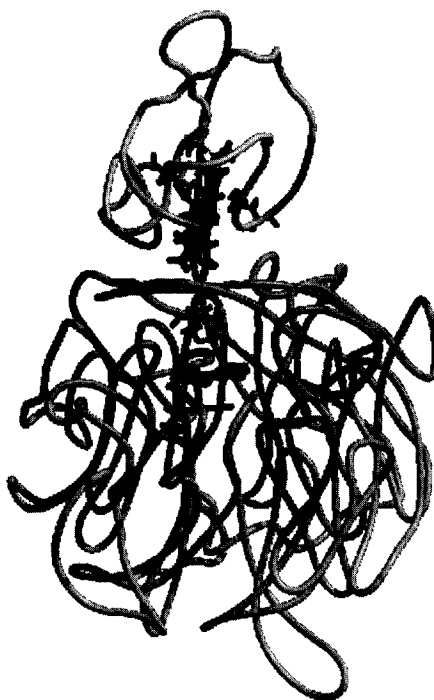


**Figure 10.** Total view of QH-ADH from *C. testosteroni* and positioning of the cofactors and important residues (shown in ball and stick representation). Going from top to bottom: heme *c* with His608 to the left, Met647 (right) and Cys604 and Cys607 and PQQ sandwiched between the disulfide bridge (Cys116 and 117, above PQQ) and Trp245. Calcium shown as grey sphere with its van der Waals radius. Backbone shown in grey. Figure generated with MolScript [69].

A feature in support of the current model that can be readily visualized concerns the site of the proteolytic attack that is observed to take place to a certain extent during cultivation of *Comamonas testosteroni* in the absence of PQQ. As is to be expected, the two phenylalanines (450 and 451) between which breakage of the bond occurs are located at the surface, however, they are not part of the long loop connecting the PQQ- and heme-domain. Although the close association of the fragments formed after the proteolytic nick well may be supported by the hydrophobic interactions between the separate heme- and PQQ-domains a curious topological feature is revealed in the model: the N-terminal extension of the loop connecting the heme- and the PQQ-domain is partially tucked underneath the  $\beta$ 8d-sheet. In order to fully separate both fragments the severed sequence would have to move through a small opening, thus obstructing the physical separation of the fragments. In addition, the extra degrees of freedom acquired after proteolysis might give rise to the formation of an association complex in which the heme-domain is more firmly anchored onto the active-site region. This could well explain the observed resistance of the nicked protein to reconstitution with PQQ resulting in an inactive complex, still showing almost the same chromatographic properties as the fully intact (apo-)enzyme [27,28].

A comparison of the spectroscopic properties of the heme in oxidized apo- and holoenzyme reveals a shift of the absorption maximum of the  $\gamma$  band from 410 nm (apo) to 412 nm (holo). Concomitantly, the midpoint potential of the heme changes from +80 mV (apo) to +140 mV (holo) when PQQ is bound [27-29]. Significant changes are also observed in the  $^1\text{H-NMR}$  spectra of the apo- and holoenzyme. The most downfield signal of the heme methyl groups (37.0 ppm in apoQH-ADH) changes upon binding of PQQ (43.7 ppm in reconstituted QH-ADH). No such shift is observed for the signals of the other methyl groups. This might be taken as an indication that the electron density on the pyrrole ring carrying that methyl group decreases.

Resonance Raman spectroscopic investigations of the different enzyme forms, on the other hand, have not shown any significant changes in the porphyrin and  $\text{C}\alpha\text{-S}$  (cysteines 604 and 607, methionine 647) bonds to occur. These observations have been explained by implying a rotation of the methionine liganding the heme-iron. The current model fully supports the possibility of a conformational change involving the heme-domain, incorporation of PQQ by the apo-enzyme triggering the proposed rotation [28].

It must be emphasized that the deductions stated above provide additional support for the particular choice of the spatial location of the heme-domain on the basis of the electron pathway analysis and distance minimization protocols. On positioning the heme-domain at alternative locations effects of PQQ-reconstitution on the spectroscopic properties of the heme would hardly be expected. Also, reconstitution of nicked apoenzyme might still be considered feasible since no blocking of the active site cleft would occur.

The overall topology of the model is strikingly similar to that described for the *cd*<sub>1</sub>-nitrite reductase from *Thiosphera pantotropha* [100]. This enzyme, responsible for the one-electron reduction of nitrite to nitric oxide, and the four-electron reduction of oxygen to water, is isolated as a soluble dimer of 62 kDa subunits. The cytochrome *d*<sub>1</sub> containing domain (C-terminal residues 135-567) forms a rigid eight-bladed  $\beta$ -propeller fold. However, the overall primary sequence identity with QH-ADH is low (21 %). Profile searches using the Profiler-3D programs developed by Eisenberg and coworkers [101,102] did not show significant similarity between the profiles calculated for QH-ADH and *cd*<sub>1</sub>-nitrite reductase. None of the tryptophan-motifs could be found either. The characteristic vicinal cysteines are absent as are the residues involved in PQQ and calcium binding in MDHs. Another difference revealed upon inspection of both sequences concerns the location of the cytochrome *c* binding motif. Whereas it is located near the C-terminus in QH-ADH, the N-terminal residues 1-134 make up the  $\alpha$ -helical cytochrome *c* domain in the *cd*<sub>1</sub>-nitrite reductase. Quite similarly, however, the cytochrome *c* containing domain is connected via a long loop to the 8-bladed propeller-fold domain. A detailed comparison of the two structures has to await deposition of the coordinates.

### **Mechanistic implications**

Several mechanisms have been proposed for the role of PQQ (Figure 1) in the oxidation of alcohols by quinoprotein alcohol dehydrogenases [1,103-107]. Limited evidence for the involvement of various functionalities present in PQQ has been obtained from the reconstitution of apo-quinoproteins with PQQ analogues and derivatives [94,108,109] as well as from inhibitor studies [107,110]. In a few cases, reconstitution experiments have been designed to discriminate between effects on binding and activity. Thus, the importance of the PQQ *o*-quinone moiety could be established from reconstitution experiments involving QH-ADH apo-enzyme and pyrroloquinoline derivatives in which



this functionality was abolished. The effect of the carboxylic acid moiety at C(9) may, however, well be related to the affinity for the apo-enzyme [108]. Nucleophilic addition of the substrate alcohol at the C(5) carbonyl group of PQQ has been suggested as a primary step in substrate oxidation, leading to the formation of PQQ-5-hemiketal. Alternative formation of PQQ-4-adducts has been suggested as well [2,111]. In both cases an active site base is supposed to be responsible for proton abstraction from the incoming alcohol enhancing its nucleophilic properties. Initial formation of an alcoholate anion has gained support from inhibitor studies employing cyclopropanol [107]. In the active site cavity of MDHs Asp303 (Asp 308 in QH-ADH) would be located appropriately to fulfill this role [17,103]. Whether or not the subsequent reorganization leading to PQQH<sub>2</sub> and aldehyde involves a concerted or a step-wise hydride transfer has not been unequivocally established. It has been argued that the C4-carbonyl oxygen might not be a likely candidate for either hydride or proton abstraction in a concerted mechanism involving a 6-ring transition state. Concerted general acid-base catalysis involving proton abstraction by an active site base followed by electron rearrangement has also been proposed [104]. A role for an active site lysine residue in transient binding and release of the aldehyde formed upon substrate oxidation has been suggested [94]. In view of the uncertainties outlined above, evaluation of the model in terms of its implications for *absolute* reaction rates is not feasible. With respect to *relative* reaction rates, however, a different situation applies. As shown by Geerlof *et al.* [34], QH-ADH catalyzes the oxidation of chiral primary alcohols with good enantioselectivity. Appreciable enantioselectivity has also been reported by Somers *et al.* [35], for the oxidation of certain secondary alcohols. The enantioselective properties of enzymes are conveniently expressed as the enantiomeric ratio, *E*, the ratio of specificity constants for the two enantiomers of a chiral substrate, [112-114]

$$E = (k_{cat} / K_M)^R / (k_{cat} / K_M)^S$$

The enantiomeric ratio for the enantioselective oxidation of chiral alcohols can be determined using the steady-state kinetic relation for the ratio of rates for the conversion of (R)- and (S)-enantiomeric alcohols [34]. The relation between the *E*-value and the Gibbs free energy profile of the reaction is obtained from Eyring transition state theory, TST. Application of the TST expression for the microscopic rate constant:

$$k = \kappa \frac{k_b T}{h} e^{-\beta \Delta G^\ddagger}$$

to the ratio of specificity constants gives:

$$(k_{cat} / K_M)^R / (k_{cat} / K_M)^S = k_{sp}^R / k_{sp}^S = e^{-\beta(\Delta G_R^\ddagger - \Delta G_S^\ddagger)} = e^{-\beta \Delta \Delta G_{RS}^\ddagger} = E$$

(all symbols with their regular meaning,  $\Delta G^\ddagger$  the difference in Gibbs free energy between the ground state and activated state for (R)- and (S)-enantiomer conversion, respectively). The physical meaning of  $\Delta \Delta G_{RS}^\ddagger$  is questionable in the sense that both TST itself, the identity of the transmission coefficients, and the lumped character of the specificity constants, imply certain assumptions. However, as has been pointed out [115,116], the relation  $\Delta \Delta G_{RS}^\ddagger = -RT \ln E$  appears to be of general applicability, provided that the Gibbs free energy difference is understood to represent the 'selectivity determining' energy barriers. Using the relation for the prediction of *E*-values of enzymes, stimulating results have been obtained by calculating the difference of force field energies of the tetrahedral intermediates on the reaction coordinate of serine-type hydrolases [117]. Guided by the kinetic analogy between bi-bi ping-pong mechanistic schemes for serine-type hydrolases and the kinetic pattern of QH-ADH catalysis [34], we identified the PQQ-5-hemiketal adducts of the alcohol enantiomers as likely candidates for this analysis. PQQ-5-hemiketals of (R)- and (S)-pentan-2-ol were build and subjected to energy minimization using MOPAC. The compounds were docked into the position determined for PQQ in the model structure. Extensive minimization and dynamics runs were performed to determine energy minima for the total structure. A set of closely similar conformations of virtually equal force field energy (within 2 kcal/mol) were obtained for each adduct. Favorable conformations of both adducts are shown and compared (Figure 11). It appears that the difference in force field energy calculated for the favorable conformations of the adducts of opposite chirality are sufficiently small (differences are of order 10 kcal/mol) to be in agreement with the observed enantiomeric ratio ( $E \cong 70$ , [35] requires  $\Delta \Delta G^\ddagger = 2.5$  kcal/mol at room temperature) for this substrate. Further refinement has to await elucidation of the three-dimensional structure, kinetic evaluation of the importance of the hemiketals for enantioselectivity, and the possible importance of entropic contributions to  $\Delta \Delta G^\ddagger = \Delta \Delta H^\ddagger - T \Delta \Delta S^\ddagger$ . Regarding the latter contribution, preliminary results of the temperature (in)dependence of the enantiomeric ratio for the kinetic resolution of (R)- and (S)-solketal (A. Geerlof, personal communication), suggest that for this case, the enantioselectivity results almost exclusively from entropic effects. The temperature dependence of the *E*-value for 2-butanol has not been determined.

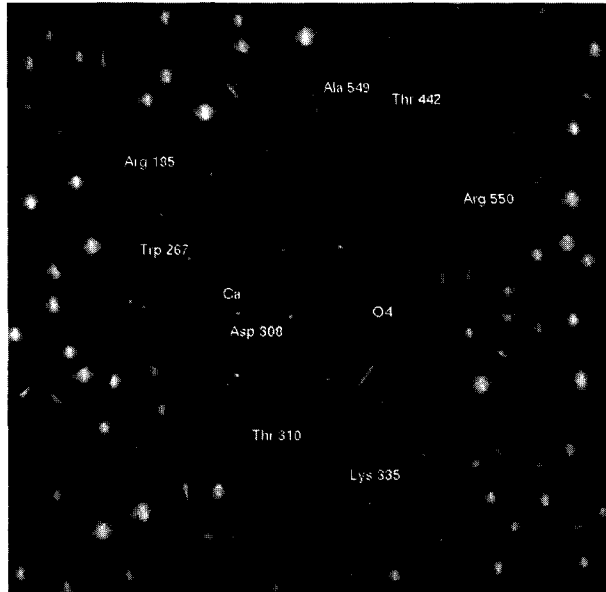


**Figure 11.** View of the active site of QH-ADH from *C. testosteroni*. Residues blocking the view are removed. Important residues are shown in different shades of grey. Hydrogen at the chiral carbon is shown in white, PQQ-O4 in dark grey, S-2-pentanol in dark grey, R-2-pentanol and PQQ in light grey and calcium in black. The distance between hydrogen (R-enantiomer) and Asp308 is 3.67 Å, hydrogen (S-enantiomer) and Asp308 3.17 Å and between PQQ-O4 carbonyl and Lys335 2.74 Å.

The conspicuous presence of Lys335 (absent in MDHs) as well as the (conserved) Asp308 in the vicinity of the substrate  $\alpha$ -hydrogen to be abstracted during the oxidation by QH-ADH is noted. These residues can be considered prime candidates for mutagenesis studies aimed at the unraveling of the catalytic mechanism.

## Conclusions

It must be emphasized that the accuracy of the model proposed here for the structure of the quinohemoprotein alcohol dehydrogenase from *Comamonas testosteroni* rests completely on the validity of the underlying assumptions. Considering the large number of additional simplifications that have been introduced, the presentation is highly questionable on the level of the conformation of individual amino acids and secondary structure elements. On the level of the overall topology of the model, however, a more

realistic picture may have been obtained. In particular, the model summarizes currently available experimental observations in a concise and organized fashion. Since determination of the structure of QH-ADH by X-ray crystallography is not anticipated in the immediate future, the present model serves as a guide for the allocation of amino acid residues of importance for further investigations. Engineering of the enantioselectivity by mutational protocols, mechanistic studies of the crucial aspects of hydride and/or electron transfer, and structural investigations on the importance of cofactor interactions are currently explored.

### **Acknowledgements**

This research has been financed by the Netherlands Organization for the Advancement of Pure Research (NWO) and the Netherlands Foundation for Chemical Research (SON).

## References

- (1) Duine, J. A.; Frank, J. and Jongejan, J. A.; *In: Adv. in Enzymol. and Rel. Areas. of Mol. Biol.*, **198** (1987), 169-212.
- (2) Duine, J. A. and Jongejan, J. A.; *Annu. Rev. Biochem.*, **58** (1989), 403-426.
- (3) McIntire, W. S.; *FASEB Journal*, **8** (1994), 513-521.
- (4) Westerling, J. F. J. J. and Duine, J. A.; *Biochem. Biophys. Res. Commun.*, **87** (1979), 719-724.
- (5) Anthony, C.; *Int. J. Biochem.*, **24** (1992), 29-39.
- (6) Anthony, C.; *Biochim. Biophys. Acta*, **1099** (1992), 1-15.
- (7) Anthony, C.; Ghosh, M. and Blake, C. C. F.; *Biochem. J.*, **304** (1994), 665-674.
- (8) Goodwin, P. M. and Anthony, C.; *Microbiology*, **141** (1995), 1051-1064.
- (9) Groen, B. W. and Duine, J. A.; *Methods in Enzymology*, **188** (1990), 33-39.
- (10) Rupp, M. and Görisch, H.; *Biol. Chem. Hoppe Seyler*, **369** (1988), 431-439.
- (11) Görisch, H. and Rupp, M.; *Antonie Van Leeuwenhoek*, **56** (1989), 35-45.
- (12) Schrover, J. M. J.; Frank, J.; Wielink, J. E. v. and Duine, J. A.; *Biochem. J.*, **290** (1993), 123-127.
- (13) Dales, S. L. and Anthony, C.; *Biochem. J.*, **312** (1995), 261-265.
- (14) Xia, Z. X.; Dai, W. W.; Xiong, J. P.; Hao, Z. P.; Davidson, V. L.; White, S. and Mathews, F. S.; *J. Biol. Chem.*, **267** (1992), 222849-22297.
- (15) White, S.; Boyd, G.; Mathews, F. S.; Xia, Z. x.; Dai, W. w.; Zhang, Y. f. and Davidson, V. L.; *Biochemistry*, **32** (1993), 12955-12958.
- (16) Xia, Z. x.; Dai, W. w.; Zhang, Y. f.; White, S. A.; Boyd, G. D. and Mathews, F. S.; *J. Mol. Biol.*, **259** (1996), 480-501.
- (17) Ghosh, M.; Anthony, C.; Harlos, K.; Goodwin, M. G. and Blake, C.; *Structure*, **3** (1995), 177-187.
- (18) Stezowski, J. J.; Görisch, H.; Dauter, Z.; Rupp, M.; Hoh, A.; Englmaier, R. and Wilson, K.; *Journal of Molecular Biology*, **205**, 617-8.
- (19) Ameyama, M. and Adachi, O.; *Meth. Enzymol.*, **89** (1982), 451-457.
- (20) Inoue, T.; Sunagawa, M.; Mori, A.; Imai, C.; Fukuda, M.; Tagaki, M. and Yano, K.; *J. Ferment. Bioeng.*, **73** (1992), 419-424.
- (21) Tamaki, T.; Fukaya, M.; Takemura, H.; Tayama, K.; Okamura, H.; Kawamura, Y.; Nishiyama, M.; Horinouchi, S. and Beppu, T.; *Biochim. Biophys. Acta*, **1088** (1991), 292-300.
- (22) Matsushita, K.; Yakushi, T.; Toyama, H. and Shinagawa, E.; *J. Biol. Chem.*, **271** (1996), 4850-4857.
- (23) Inoue, T.; M., S.; A., M.; C., I.; M., F.; M., T. and Yano, K.; *J. Bacteriol.*, **171** (1989), 3115-3122.
- (24) Takemura, H.; Kondo, K.; Horinouchi, S. and Beppu, T.; *J. Bacteriol.*, **175** (1993), 6857-6866.
- (25) Kondo, K.; Beppu, T. and Horinouchi, S.; *J. Bacteriol.*, **177** (1995), 5048-5055.
- (26) Groen, B. W.; van Kleef, M. A. G. and Duine, J. A.; *Biochem. J.*, **234** (1986), 611-615.
- (27) de Jong, G. A. H.; Geerlof, A.; Stoorvogel, J.; Jongejan, J. A.; de Vries, S. and Duine, J. A.; *Eur. J. Biochem.*, **230** (1995), 899-905.
- (28) de Jong, G. A. H.; Caldeira, J.; Sun, J.; Jongejan, J. A.; de Vries, S.; Loehr, T. M.; Moura, I.; Moura, J. J. G. and Duine, J. A.; *Biochemistry*, **34** (1995), 9451-9458.
- (29) de Jong, G. A. H. PhD Thesis, Delft University of technology, 1995.
- (30) Yasuda, M.; Cherepanov, A. and Duine, J. A.; *FEMS Microbiol. Lett.*, **138** (1996), 23-28.
- (31) Yamanaka, K. and Tsuyuki; *Agric. Biol. Chem.*, **47** (1983), 2173-2183.
- (32) Toyama, H.; Fujii, A.; Matsushita, K.; Shinagawa, E.; Ameyama, M. and Adachi, O.; *J. Bacteriol.*,

- 177 (1995), 2442-2450.
- (33) Shimao, M.; Tamogami, T.; Nishi, K. and Harayama, S.; *Biosci. Biotech. Biochem.*, **60** (1996), 1056-1062.
- (34) Geerlof, A.; Rakels, J. J. L.; Straathof, A. J. J.; Heijnen, J. J.; Jongejan, J. A. and Duine, J. A.; *Eur. J. Biochem.*, **226** (1994), 537-546.
- (35) Somers, W. A. C.; Stigter, E. C. A. and van der Lugt, J. P.; *J. Mol. Catal. B: Enzym.*, **2** (1997), 291-297.
- (36) Stoorvogel, J.; Kraayveld, D. E.; Sluis, C. A. v.; Jongejan, J. A.; de Vries, S. and Duine, J. A.; *Eur. J. Biochem.*, **235** (1996), 690-698.
- (37) Huizinga, E. G. PhD Thesis, University of Groningen, The Netherlands, 1994.
- (38) Cozier, G. E.; Giles, I. G. and Anthony, C.; *Biochem. J.*, **308** (1995), 375-379.
- (39) Geerlof, A.; Groen, B. W. and Duine, J. A. In *Eur. Patent Appl.* 412,585, 1991.
- (40) Geerlof, A.; Groen, B. W. and Duine, J. A. In *US Patent* 5,182,209, 1993.
- (41) Somers, W.; van den Dool, R. T. M.; de Jong, G. A. H.; Jongejan, J. A. and Duine, J. A.; *Biotechnol. Techniq.*, **8** (1994), 407-412.
- (42) Stigter, E. C. A.; de Jong, G. A. H.; Jongejan, J. A.; Duine, J. A.; van der Lugt, J. P. and Somers, W. A. C.; *J. Chem. Tech. Biotechnol.*, **68** (1997), 110-116.
- (43) Chou, P. Y. and Fasman, G. D.; *Adv. Enzymol.*, **47** (1978), 45-147.
- (44) Garnier, J.; Osguthorpe, D. J. and Robson, B.; *J. Mol. Biol.*, **120** (1978), 97-120.
- (45) Srinivansan, R. and Rose, G. D.; *Protein*, **22** (1995), 81-99.
- (46) Zhang, K. Y. and Eisenberg, D.; *Protein. Sci.*, **3** (1994), 687-695.
- (47) Du, P.; Collins, J. R. and Loew, G. H.; *Prot. Engin.*, **5** (1992), 679-691.
- (48) Szilágyi, A. and Závodszy, P.; *Prot. Engin.*, **8** (1995), 779-789.
- (49) Cachau, R. E.; Erickson, J. W. and Villar, H. O.; *Prot. Engin.*, **7** (1994), 831-839.
- (50) Gronenborn, A. M. and Clore, G. M.; *Prot. Engin.*, **4** (1991), 263-269.
- (51) Siezen, R. J.; Rollema, H. S.; Kuipers, O. P. and Vos, W. H. d.; *Prot. Engin.*, **8** (1995), 117-125.
- (52) Bamborough, P.; Duncan, D. and Richards, W. G.; *Prot. Engin.*, **7** (1994), 1077-1082.
- (53) Ring, C. S. and Cohen, F. E.; *Faseb J*, **7** (1993), 783-790.
- (54) Greer, J.; *Prot.: Struct., Funct., Gen.*, **7** (1990), 317-334.
- (55) Stewart, D. E.; LeGall, J.; Moura, I.; Moura, J. J. G.; Peck, H. D.; Xavier, A. V.; Weiner, P. K. and Wampler, J. E.; *Biochemistry*, **27** (1988), 2444-2450.
- (56) Vinals, C.; De Bolle, X.; Depiereux, E. and Feytmans, E.; *Prot.: Struct., Funct., Gen.*, **21** (1995), 307-318.
- (57) Seah, S. Y. K.; Britton, K. L.; Baker, P. J.; Rice, D. W.; Asano, Y. and Engel, P. C.; *FEBS Lett*, **370** (1995), 93-96.
- (58) Chen, J. M.; Grad, R.; Monaco, R. and Pincus, M. R.; *J. Prot. Chem.*, **15** (1996), 11-16.
- (59) Chothia, C.; Lesk, A. M.; Levitt, M.; Amit, A. G.; Mariuzza, R. A.; Phillips, S. E. V. and Poljak, R. J.; *Science*, **233** (1986), 754-758.
- (60) Allen, S. C.; Acharaya, K. R.; Palmer, K. A.; Shapiro, R.; Vallee, B. L. and Scheraga, H. A.; *J. Prot. Chem.*, **13** (1994), 649-658.
- (61) Chothia, C. and Lesk, A. M.; *EMBO J.*, **5** (1986), 823-826.
- (62) Sutcliffe, M. J.; Haneef, I.; Carney, D. and Blundell, T. L.; *Prot. Engin.*, **1** (1987), 377-384.
- (63) Blundell, T. L.; Carney, D.; Gardner, S.; Hayes, F.; Howlin, B.; Hubbard, T.; Overington, J.; Singh, D.

- A.; Sibanda, B. L. and Sutcliffe, M.; *Eur. J. Biochem.*, **172** (1988), 513-520.
- (64) Blundell, T. L.; Sibanda, B. L.; Sternberg, M. J. E. and Thornton, J. M.; *Nature*, **326** (1987), 347-352.
- (65) Bajorath, J.; Stenkamp, R. and Aruffo, A.; *Prot. Sci.*, **2** (1993), 1798-1810.
- (66) Bersch, B.; Brutscher, B.; Meyer, T. E. and Marion, D.; *Eur. J. Biochem.*, **227** (1995), 249-260.
- (67) Carter, D. C.; Meli, K. A.; O'Donnell, S. E.; Burgess, B. K.; Furey, W. F., Jr.; Wang, B.-C. and Stout, C. D.; *J. Mol. Biol.*, **184** (1985), 279-285.
- (68) Aquino, A. J. A.; Beroza, P.; Beratan, D. N. and Onuchic, J. N.; *Chem. Phys.*, **197** (1995), 277-288.
- (69) Kraulis, P. J.; *J. Appl. Crystallogr.*, **24** (1991), 946-950.
- (70) Merritt, E. A. and Murphy, M. E. P.; *Acta Crystallogr.*, **D50** (1994), 869-873.
- (71) Bacon, D. J. and Anderson, W. F.; *J. Mol. Graph.*, **6** (1988), 219-220.
- (72) Lopez, M. A. and Kollman, P. A.; *J. Am. Chem. Soc.*, **111** (1989), 6212-6222.
- (73) Kuczera, K.; Kuriyan, J. and Karplus, M.; *J. Mol. Biol.*, **213** (1990), 351-373.
- (74) Foloppe, N.; Ferrand, M.; Breton, J. and Smith, J. C.; *Proteins: Structure, Function, and Genetics*, **22** (1995), 226-244.
- (75) Munro, O. Q.; Marques, H. M.; Debrunner, P. G.; Mohanrao, K. and Scheidt, W. R.; *J. Am. Chem. Soc.*, **117** (1995), 935-954.
- (76) Munro, O. Q.; Bradley, J. C.; Hancock, R. D.; Marques, H. M.; Marsicano, F. and Wade, P. W.; *J. Am. Chem. Soc.*, **114** (1992), 7218-7230.
- (77) Svensson, B. PhD Thesis, University of Stockholm, Sweden, 1995.
- (78) Brooks, B. R.; Brucceolori, R. E.; Olafson, B. D.; States, D. J.; Swaminathan, S. and Karplus, M.; *J. Comp. Chem.*, **4** (1983), 187-217.
- (79) Laberge, M.; Vanderkooi, J. M. and Sharp, K. A.; *J. Phys. Chem.*, **100** (1996), 10793-10801.
- (80) Skourtis, S. S.; Beratan, D. N. and Onuchic, J. N.; *Chem. Phys.*, **176** (1993), 501-520.
- (81) Regan, J. J.; Risser, S. M.; Beratan, D. N. and Onuchic, J. N.; *J. Phys. Chem.*, **97** (1993), 13083-13088.
- (82) Beratan, O. N.; Betts, J. N. and Onuchic, J. N.; *Science*, **252** (1991), 1285-1288.
- (83) van Koningsveld, H.; Jongejan, J. A. and Duine, J. A.; In: "PQQ and Quinoproteins", J. A. Jongejan and J. A. Duine, Ed., Kluwer Academic Publishers: Dordrecht, 1989; pp 243-251.
- (84) Sippl, M. J.; *Prot.: Struct., Funct., Gen.*, **17** (1993), 355-362.
- (85) Colovos, C. and Yeates, T. O.; *Prot. Sci.*, **2** (1993), 1511-1519.
- (86) Novotny, J.; Bruccolieri, R. and Karplus, M.; *J. Mol. Biol.*, **177** (1984), 787-818.
- (87) Ramachandran, G. N. and Sasisekharan, V.; *Adv. Protein Chem.*, **23** (1968), 283-437.
- (88) Laskowski, R. A.; MacArthur, M. W.; Moss, D. S. and Thornton, J. M.; *J. Appl. Crystallogr.*, **26** (1993), 283-291.
- (89) Hooft, R. W. W.; Vriend, G.; Sander, G. and Abola, E. E.; *Nature*, **381** (1996), 272.
- (90) Blake, C. C. F.; Ghosh, M.; Harlos, K.; Avezoux, A. and Anthony, C.; *Struct. Biol.*, **1** (1994), 102-105.
- (91) Chandrasekharan, R. and Balasubramanian, R.; *Biochim. Biophys. Acta*, **188** (1969), 1-9.
- (92) Capasso, S.; Mattia, C. and Mazzarella, L.; *Acta Crystallogr.*, **833** (1977), 2080-2083.
- (93) Mez, H.-C.; *Cryst. Struct. Commun.*, **3** (1993), 657-660.
- (94) Jongejan, J. A.; Groen, B. W. and Duine, J. A.; In: "PQQ and Quinoproteins", J. A. Jongejan and J. A. Duine, Ed., Kluwer Academic Publishers: Dordrecht, 1989; pp 205-216.
- (95) Korszun, Z. R. and Salemme, F. R.; *Proc. Natl. Acad. Sci. USA*, **74** (1977), 5244-5247.

- (96) Moore, G. R. and Pettigrew, G. W.; *Cytochromes c - Evolutionary, Structural and Physicochemical Aspects*; Springer Verlag: Berlin, Heidelberg, 1990.
- (97) Canters, G. W. and Kamp, M. v. d.; *Curr. Op. in Struct. Biol.*, **2** (1992), 859-869.
- (98) Beratan, D. N.; Nelson Onuchic, J.; Winkler, J. R. and Gray, H. B.; *Science*, **258** (1992), 1740-1741.
- (99) Martin, A. C. R.; Toda, K.; Stirk, H. J. and Thornton, J. M.; *Prot. Engin.*, **8** (1995), 1093-1101.
- (100) Fülöp, V.; Moir, J. W. B.; Ferguson, S. J. and Hajdu, J.; *Cell*, **81** (1995), 369-377.
- (101) Bowie, J. U.; Lüthy, R. and Eisenberg, D.; *Science*, **253** (1991), 164-170.
- (102) Lüthy, R.; Bowie, J. U. and Eisenberg, D.; *Nature*, **356** (1992), 83-85.
- (103) Anthony, C.; *Biochem. J.*, **320** (1996), 697-711.
- (104) Itoh, S.; Mure, M.; Ohshiro, Y. and Agawa, T.; *Tetrahedron Lett*, **26** (1985), 4225-4228.
- (105) Sleath, P.; Noar, J.; Berlein, G. A.; Bruce, T. C.; *Am. Chem. Soc.*, **107** (1985), 3328-3338.
- (106) Frank, J. J.; M., D.; A., D. J. and Balny, C.; *Eur. J. Biochem.*, **174** (1988), 331-338.
- (107) Frank, J. J.; van Krimpen, S. H.; Verwiël, P. E. J.; Jongejan, J. A.; Mulder, A. C. and Duine, J. A.; *Eur. J. Biochem.*, **184** (1989), 187-195.
- (108) Shinagawa, E.; Matsushita, K.; Nonobe, M.; Adachi, O.; Ameyama, M.; Ohshiro, Y.; Itoh, S. and Kitamura, Y.; *Biochem. Biophys. Res. Commun.*, **139** (1986), 1279-1284.
- (109) Conlin, M. F. H. S. and Bruce, T. C.; *Biochem. Biophys. Res. Commun.*, **131** (1985), 564-566.
- (110) Dijkstra, M.; Frank, J.; Jongejan, J. A. and Duine, J. A.; *Eur. J. Biochem.*, **140** (1984), 369-373.
- (111) Itoh, S. and Oshiro, Y.; *Natural Product Reports*, (1995), 45-53.
- (112) Chen, C.-S.; Fujimoto, Y.; Girdaukas, G. and Sih, C.; *J. Am. Chem. Soc.*, **104** (1982), 7294-7299.
- (113) Chen, C.-S.; Wu, S.-H.; Girdaukas, G. and Sih, C.; *J. Am. Chem. Soc.*, **109** (1987), 2812-2817.
- (114) Straathof, A. J. J. and Jongejan, J. A.; *Enzyme Microbiol. Technol.*, **21** (1997), 559-571.
- (115) Phillips, R. S.; *Tibtech*, **14** (1996), 13-16.
- (116) Anthonson, T. and Jongejan, J. A.; *Methods Enzymol.*, **286** (1997), 473-495.
- (117) Norin, M.; Hult, K.; Mattson, A. and Norin, T.; *Biocatalysis*, **7** (1993), 131-147.



# Direct Hydride Transfer in the Reaction Mechanism of Quinoprotein Alcohol Dehydrogenases: A Quantum Mechanical Investigation

Aldo Jongejan, Jaap A. Jongejan and Wilfred. R. Hagen

---

## Abstract

Oxidation of alcohols by direct hydride transfer to the pyrroloquinoline quinone (PQQ) cofactor of quinoprotein alcohol dehydrogenases has been studied using *ab initio* quantum mechanical methods. Energies and geometries were calculated at the 6-31G(d,p) level of theory. Comparison of the results obtained for PQQ and several derivatives with available structural and spectroscopic data served to judge the feasibility of the calculations. The role of calcium in the enzymatic reaction mechanism has been investigated. Transition state searches have been conducted at the semi-empirical and STO-3G(d) level of theory. It is concluded that hydride transfer from the C $\alpha$ -position of the substrate alcohol (or aldehyde) directly to the C(5) carbon of PQQ is energetically feasible.

**Key words**

PQQ / direct hydride transfer / pyrroloquinoline quinone / quinoprotein alcohol dehydrogenase / transition state

## 1. Introduction

Alcohol dehydrogenases containing pyrroloquinoline quinone (2,7,9-tricarboxy-1*H*-pyrrolo[2,3-*f*]quinoline-4,5-dione, PQQ) (Figure 1) as a cofactor have been isolated from several sources [1-3]. Enzymes belonging to this class have been characterized as dye-linked enzymes following ping-pong kinetic schemes [4]. Quinones, cytochromes and blue copper proteins have been found to act as the natural electron acceptors [5-9]. The enzymology of PQQ-containing alcohol dehydrogenases has been extensively reviewed [1-3,10-12]. Methanol dehydrogenases (MDHs), isolated from methylotrophic bacteria, catalyze the oxidation of short-chain primary alcohols whereas ethanol dehydrogenases (Q-ADHs) oxidize a range of primary alcohols as well as secondary alcohols [13-15].

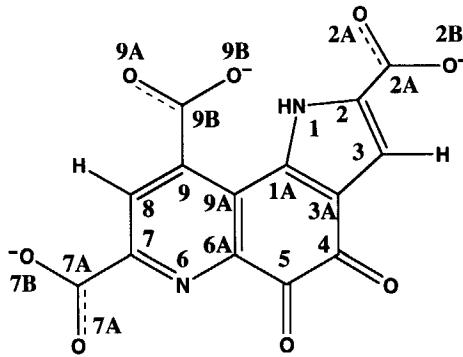
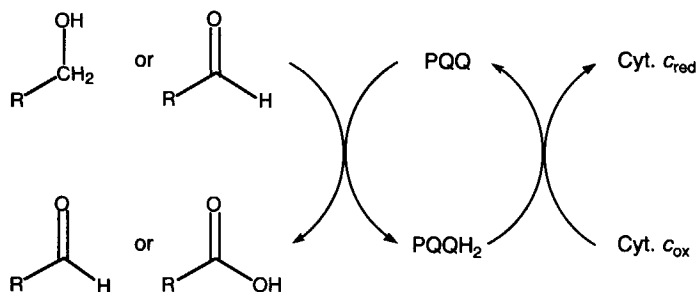


**Figure 1.** Structure of pyrroloquinoline quinone, PQQ

Quinohemoprotein alcohol dehydrogenases (QH-ADHs) contain a heme *c* as an additional redox-active cofactor. Two types of QH-ADH's can be distinguished based on differences in cofactor requirements and subunit composition (for reviews see ref. [12,16]). In the first step of the alcohol dehydrogenase-catalyzed reaction, the reducing equivalents are passed from the substrates to PQQ (Scheme 1). The involvement of an active site base has been inferred from the isolation of the corresponding PQQ-adducts from cyclopropanol- (and cyclopropanal-) inhibited MDHs [17]. Mutagenesis studies have identified an aspartic acid residue as a likely candidate [12]. An important mechanistic role has been suggested for the calcium ion complexed to PQQ [18]. Calcium is also involved in the oxidation of glucose by PQQ-containing glucose dehydrogenases [19]. In the soluble GDH isolated from *Acinetobacter calcoaceticus*, for which a high-resolution x-ray structure has recently become available [20], a histidine

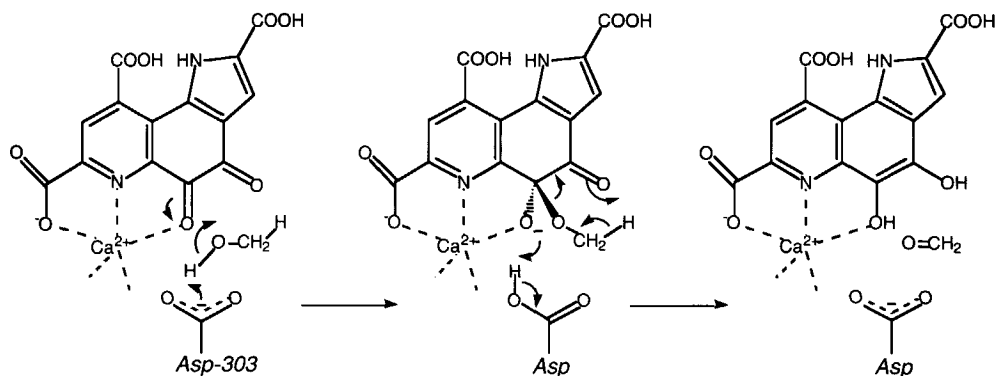


**Scheme 1.** Oxidation of alcohols and aldehydes by PQQ.

is found to act as the active-site base [21]. Reduced PQQ is subsequently oxidized by either inter- or intra-molecular electron transfer.

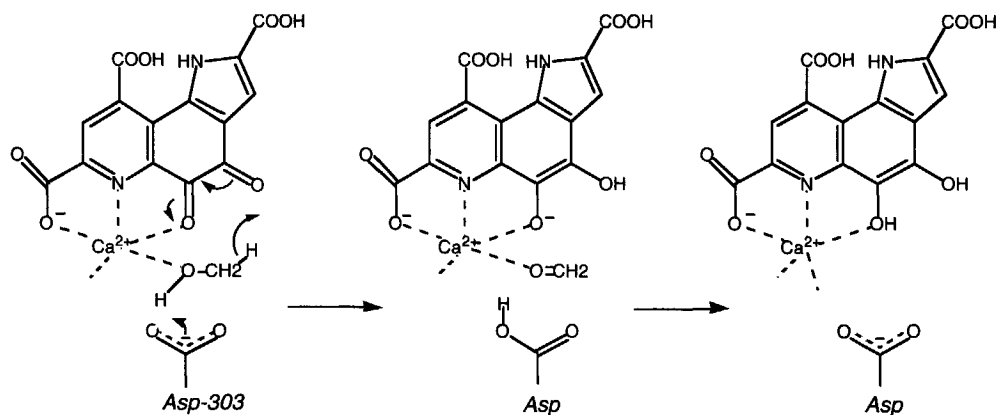
A number of mechanistic schemes for the reduction of PQQ by substrate have been proposed (for reviews see ref. [11,22]). An enzymatic mechanism featuring covalent adduct formation of PQQ and substrate as a key step has been presented in analogy to the *in vitro* reactivity of PQQ with various nucleophiles (Scheme 2) [23,24]. Valuable information has been obtained from mechanistic studies of the oxidation of methanol catalyzed by MDHs [17,25,26]. Although high-resolution crystal structures are available for MDHs from *Methylophilus methylotrophus* and *Methylobacterium extorquens*, mechanistic studies were hampered by the complexity of the assays: (1) MDH's are usually isolated with their cofactor in the semiquinone state, a redox state that is unreactive with substrate [26]; (2) oxidation with artificial electron acceptors leads to inactivation unless substrate or carbonyl group reagents are present [6,26,27]; (3) enzyme preparations are inevitably contaminated with excess endogenous substrate(s) of unknown origin [28-31]; (4) *in vitro* activity requires the use of cationic electron acceptors and activation with ammonia at high pH.

Quinohemoprotein ADHs appear to be less demanding. X-ray crystallographic data of quinohemoprotein ADHs are, however, not yet available. It is commonly accepted that the special characteristics of MDHs, notably the requirement for ammonia and high pH in the *in vitro* assays, may well be artefacts introduced during isolation. Thus, these properties have been routinely disregarded as part of the 'consensus' mechanism of quinoprotein alcohol dehydrogenases. Theoretical studies of the formation of a hemiketal intermediate have been reported by Andrés *et al.* [32,33] and Zheng and



**Scheme 2.** Proposed reaction mechanism of MDH involving covalent adduct formation of PQQ and methanol followed by deprotonation and rearrangement.

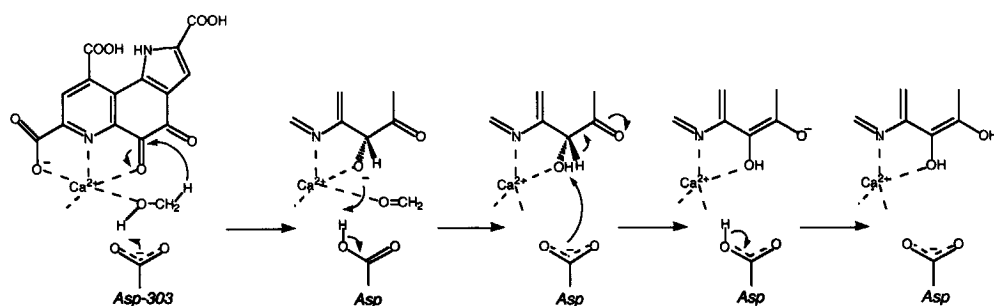
Bruice [18]. Formation of the intermediate followed by a 'retro-ene' rearrangement has been rejected [18] in favor of hydride transfer to the oxygen at the C(4) position of PQQ (Scheme 3A). A role for the active site calcium ion in the mobilisation of the substrate  $\alpha$ -hydrogen atom has been proposed [11,18,34,35].



**Scheme 3A.** Hydride transfer by Lewis acid catalysis to the C(4)-carbon of PQQ.

Since the catalytic reaction bears a formal resemblance to the well-studied Meerwein-Ponndorf-Verley reduction (Oppenauer oxidation) [36] and Canizzarro reaction [37], we investigated the feasibility of hydride transfer from the alcohol  $\alpha$ -position directly to the C(5)-carbon of PQQ (Scheme 3B). The following strategy has been adopted: 1. Ground

state energies of PQQ derivatives of known structure and physical properties were calculated at the 6-31G(d,p) level of theory and compared with available experimental results; 2. Energies and structures of probable reaction intermediates were determined with calcium included using the basis set developed by McLean and Chandler [38]. 3. Potential energy differences of ground-state and transition-state structures for the postulated hydride transfer mechanism were calculated. Results have been evaluated by comparing measured reaction rates with those predicted by Eyring's transition state theory (TST) [39-41].



**Scheme 3B.** Direct hydride transfer by Lewis acid catalysis to the C(5) carbon of PQQ followed by tautomerisation and formation of product and PQQH<sub>2</sub>.

## 2. Computational methods

*Ab initio* calculations were performed using GAMESS-US (version Dec. 1998) [42]. Geometry optimizations were carried out at different levels of theory, ranging from PM3 to 6-31G(d,p). Final calculations were performed using the unrestricted HF method. The McLean/Chandler triple split basis set (12s,9p)/[6s,5p] (MC) was employed for calcium [38].

Transition state calculations on the calcium containing model complex were performed using the MC basis set. Natural internal coordinates as described by Fogarasi et al [43,44] or delocalized coordinates as implemented in GAMESS-US were used [45]. Initial Hessian force matrices were used when available.

Calculations were performed on a single processor SGI-O2 R10K workstation or the multi-processor CRAY-T3E at the High Performance Applied Computing (HPaC) Centre of the Delft University of Technology, The Netherlands. Output was visualized using MOLDEN [46] or MacMolPlt [47].

### 3. Results and Discussion

Mechanistic details of enzyme-catalyzed reactions may be beyond the reach of currently available biophysical and biochemical experimental methods. In such cases, insight into the atomic, energetic and electronic aspects of the reaction mechanisms can be obtained by computational methods. However, proper validation of the results obtained from theoretical calculations is required. In the first section we describe the calibration of the methodology. X-ray crystallographic data and physical properties of PQQ and derivatives determined by  $^1\text{H-NMR}$ -, fluorescence- and UV-Vis spectroscopy are compared with the calculated energy differences. In the second section, energies of ground-state structures and postulated intermediates are determined. Calculations including the calcium are presented in section 3. The geometry of the transition state and the energy barriers involved in the proposed reaction are discussed in the final section.

#### 3.1 Calibration.

PQQ and PQQH<sub>2</sub> represent the cofactor ground states for the reductive half-reaction (Scheme 1). Semiempirical calculations at the AM1 or PM3 level of theory appeared to be unsuitable for proper computation of the orientation of the carboxylic acid groups of PQQ. Including the  $\pi$ -orbital interaction of the aromatic rings and the carboxylic acid moieties required the use of higher level basis sets. In addition it was found essential to include polarization functions in order to reproduce the geometry of the carboxylic acid groups as found in the high-resolution X-ray structures of the PQQ Na<sup>+</sup> [48] and K<sup>+</sup> salts [49] and of the PQQ structure present in s-GDH [20] and refined MDH [50] X-ray structures. For free PQQ in solution nucleophilic attack is known to take place at the C(5) carbon of the quinone moiety, suggesting hemiketal formation to be energetically favorable. Dekker *et al.* investigated the partial hydration of PQQ at the C(5)-position using  $^1\text{H NMR}$ - and fluorescence spectroscopy [23]. In order to compare the computed relative energies with the equilibrium free energies deduced from these observations, the ionized form of PQQ and its derivatives were considered. The pK<sub>a</sub>-values of the carboxylic acid groups of PQQ in aqueous solution [51] favor the fully deprotonated state at pH 7. At first sight, the presence of triply negatively charged PQQ in the enzyme active site would appear unlikely. The charges on the carboxylic acid groups are neutralized due to hydrogen bonding and pair-ion interactions within the protein environment (Glu55, Arg109, Thr159, Ser174, Thr241, Arg331, Asn394 and Trp476 in MDH from *M. extorquens* [52], Arg408, Lys377 and Arg406 in s-GDH from *A.*

*calcoaceticus* [20,21]), the charge on the C(7)-carboxylic acid also being neutralized by complexation of the divalent calcium cation. To mimick this situation in subsequent calculations, hydrogens were attached to the C(2)- and C(9)-carboxylic acid moieties during the final stages of the transition state searches.

Hydrated forms of three methyl-substituted PQQ derivatives, for which data of their relative degrees of hydration exist, have also been included in the calculations.

*Ground state PQQ.* The fully-converged structure of free, trianionic PQQ at the HF/6-31G(d,p) level of theory shows values for single and double bond lengths well within the range that is normally observed. The greater part of the molecule is planar, as has been found for the X-ray structures determined for PQQ and its K<sup>+</sup>-salt [49]. Coplanarity of the pyrrole and pyridine rings is slightly off (9.3 degrees for the dihedral N(1)-C(1A)-C(9A)-C(9) bond). This angle compares well with the values that have been reported for the X-ray structures of the C(4)-dimethylacetal (9.6 degrees) and C(5)-hemiacetal (9.9 degrees) forms of PQQ-triester [53]). Butterfly dihedral values close to 180 degrees are observed for the connection of the pyridine ring to the quinone ring as well as for the connection of the pyrrole to the quinone ring. Puckering is observed for the quinone ring forcing the C(4) carbon atom out of the plane of the PQQ, resulting in a value for the O(4)-C(4)-C(5)-O(5) dihedral angle of 16.5 degrees. Except for the group at C(2), the carboxylic acid groups are not in the plane of the PQQ tricyclic ring-system. The C(7)-carboxylic acid group is rotated by 22.9 degrees with the oxygen (O7B) closest to the C(8) position above the pyridine ring (see Footnote). In the case of the negatively charged C(9)-carboxylic acid group the rotation is more pronounced (41.98 degrees). Flexibility in the rotational disposition of this group has been observed in the structures of PQQ and its K<sup>+</sup>-salt [49].

All calculations confirm the presence of a hydrogen bond between the pyrrole-nitrogen and the carboxylic acid group at the C(9) position. All of the above values are in line with X-ray crystallographic data. A slight overestimation of the rotation computed for the carboxylic acid groups is noted. Most probably these highly charged anionic species require higher level basis-sets including additional diffuse functions (6-311G\*\*) to obtain

---

**Footnote:** Positions relative to the plane of the molecule are considered with respect to the face of PQQ that is turned towards the active site entrance. In MDHs and (probably also) QH-ADHs "above" indicates the 5*Si*,4*Re*-face. In sGDH this is the 5*Re*,4*Si*-face of PQQ.



proper geometries. Such calculations, however, turned out to be computationally too expensive.

For neutral PQQ the situation is similar. Bond lengths for the carboxylic acid oxygens change from partial double bond (1.23 Å) to double bond (carbonyl 1.19 Å) and single bond (hydroxyl 1.32 Å). Bond lengths between carboxylic acid carbon and connected ring atom decrease slightly (by 0.05 Å). The rotation of the C(9)-carboxylic acid group does not change, although the quinone ring adopts a more planar configuration as indicated by a decrease in the dihedral angle O(4)-C(4)-C(5)-O(5) (from 16.54 to 9.71 degrees). The largest change observed concerns the rotation of the C(7)-carboxylic acid group by 25 degrees to a position almost coplanar with the pyridine ring. The oxygen atom O(7B), above the plane of the PQQ in the trianionic form, is now slightly below the plane of the pyridine ring ( 2.54 degrees).

*Reduced PQQ (PQQH<sub>2</sub>, compound II).* PQQH<sub>2</sub> is nearly flat. The C(4)-C(5) bond length is that of an aromatic ring bond (1.38 Å) in agreement with the aromatic character of the quinone ring. The pyrrole- and pyridine rings are virtually coplanar (the dihedral angle N(1)-C(1A)-C(9A)-C(9) reduces to 3.70 degrees). The two phenolic oxygens are in the plane of the tricyclic system (the dihedral angle O(4)-C(4)-C(5)-O(5) decreases to zero).

Final structures for anionic PQQ, neutral PQQ and PQQH<sub>2</sub> are given Figure 2. Selected geometrical features and energies for the three structures are summarized in Table I.

*Hydration of PQQ (compounds III and IV).* Upon addition of water, the planarity of the tricyclic ring system is reduced compared to that of the trianionic form of PQQ. The dihedral angle for C(3A)-C(4)-C(5)-C(6A) increases from 18.2 to 36.3 degrees, while the dihedral angle for N(1)-C(1A)-C(9A)-C(9) only increases with 3 degrees (to 12.7). The configuration around the C(4)-C(5) bond becomes increasingly more skewed. However, the sign of the torsional distortion is opposite for the two hydrated forms of PQQ. In the case of the C(5)-hydrated PQQ (III), the C(5) carbon atom is raised above the plane of the PQQ, whereas in the C(4)-hydrated form (IV) it is the C(4) carbon. In the structure of PQQ-C(5)(OH)<sub>2</sub> the C(7)-carboxylic acid group is rotated out of the pyridine plane by 12.8 degrees (O(7B) above the plane). In PQQ-C(4)(OH)<sub>2</sub> the rotation amounts to 12.0 degrees (O(7B) below the plane). The rotation of the C(9)-carboxylic acid group stays roughly the same at 35 degrees for both compounds. Experimentally, the C(5)-adduct is

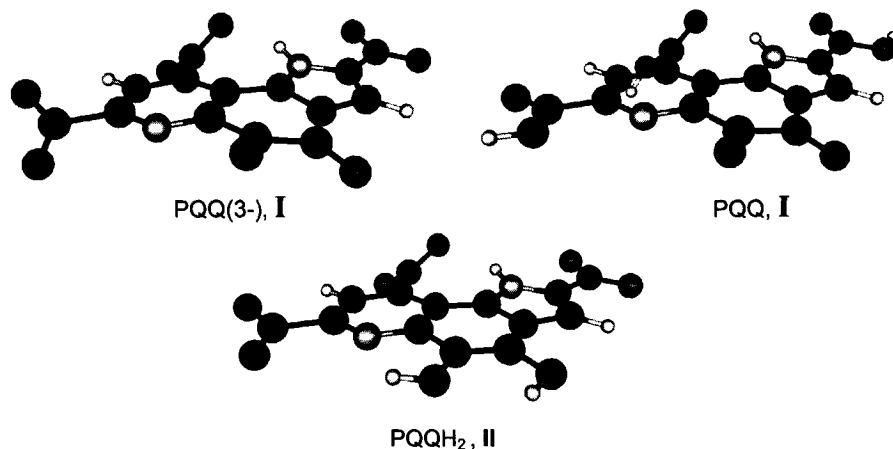


**Figure 2.** Structures of anionic PQQ, neutral PQQ and reduced PQQ (PQQH<sub>2</sub>). All compounds were optimized at the 6-31G(d,p) level of theory. Pictures were created with MacMolPlt<sup>47</sup>.

**Table I.** Energies and selected geometrical features of anionic, neutral and reduced PQQ

|                                 |     |     |     | PQQ(3-)    | PQQ        | PQQH <sub>2</sub> |
|---------------------------------|-----|-----|-----|------------|------------|-------------------|
| <b>Energy (Hartree/mole)</b>    |     |     |     | -1239.6369 | -1241.5225 | -1240.8031        |
| <b>Bond length (Å)</b>          |     |     |     |            |            |                   |
| C4                              | C5  |     |     | 1.54       | 1.54       | 1.34              |
| C4                              | O4  |     |     | 1.21       | 1.19       | 1.37              |
| C5                              | O5  |     |     | 1.19       | 1.18       | 1.37              |
| C7A                             | O7B |     |     | 1.19       | 1.24       | 1.24              |
| C7A                             | O7A |     |     | 1.31       | 1.23       | 1.23              |
| <b>Dihedral angle (degrees)</b> |     |     |     |            |            |                   |
| N1                              | C1A | C9A | C9  | 9.26       | 9.00       | 3.70              |
| C3A                             | C4  | C5  | C6A | 18.19      | 11.59      | 1.38              |
| C8                              | C7  | C7A | O7B | -22.92     | 2.54       | -7.82             |
| C9A                             | C9  | C9B | O9B | -41.99     | -44.92     | -38.73            |
| O4                              | C4  | C5  | O5  | 16.54      | 9.71       | -0.08             |

found to be more stable than the corresponding C(4)-adduct [23,53]. Also in the calculated structures it is found that the change from carbonyl  $sp^2$  to hydrate  $sp^3$ -hybridisation of the ring carbon leads to larger geometrical differences for the PQQ-C(4)-hydrate as compared to free PQQ. In order to accommodate this change in orbital

hybridization the C(7)-carboxylic acid group has to rotate. This induces a change in the relative positions of the pyridine and pyrrole ring. In water at pH 7 and 24 °C, PQQ is found to be hydrated for 39% at the C(5)-position exclusively, although exchange of oxygen is observed to occur for both the C(5) and C(4) carbonyls upon exposure to H<sub>2</sub><sup>18</sup>O [23]. From these data the free energy difference between PQQ and its C(5)-hydrate is estimated to be close to 0.25 kcal/mol at 24 °C. The enthalpic difference calculated on the basis of the temperature dependence of the hydration amounts to 3.6 kcal/mol in favor of the C(5)-hydrate. Calculated energy differences between PQQ and H<sub>2</sub>O and the C(5)-hydrate amount to 9.7 kcal/mol, again in favor of the hydrate (Table II). Clearly, the magnitude of the calculated difference is almost twice the measured value, reflecting the poor approximation of thermodynamic quantities by gas phase electronic energies. Assuming a similar entropic contribution to the hydration at C(4), the calculated equilibrium constant (24 °C) would be of the order 10<sup>-5</sup> M, in agreement with the fact that the C(4)-hydrate appears to be absent in the equilibrium mixture.

*PQQ derivatives and their corresponding C(5)-hydrated forms (XII-XIV).* Upon introduction of a methyl-group at the N(1)-position of PQQ (XII) the dihedral angle N(1)-C(1A)-C(9A)-C(9) is seen to increase from 9.3 in PQQ to 28.4 degrees. The C(9)-carboxylic acid group rotates in a clockwise fashion increasing the dihedral angle. The C(7)-carboxylic acid group rotates through the plane of the pyridine ring bringing the O(7B) oxygen below the plane. The final dihedral angle for O7B-C(7)A-C(7)-C(8) is 23.3 degrees (Table III.A).

**Table II.** Calculated energy differences between PQQ + H<sub>2</sub>O and C(4)- and C(5)-hydrated forms of PQQ. All energies have been calculated at the 6-31G(d,p) level of theory

| Compound(s)  | Hartree/mole | kcal/mole    |
|--|--------------|--------------|
| PQQ  | -1239.6369   | -777822.6956 |
| H <sub>2</sub> O   | -76.0236     | -47701.7871  |
| PQQ-C4-(OH) <sub>2</sub>   | -1315.6557   | -825521.5048 |
| PQQ-C5-(OH) <sub>2</sub>   | -1315.6760   | -825534.2176 |
| $\Delta E(\text{PQQ-C4-(OH)}_2 - \text{PQQ} + \text{H}_2\text{O})$ | 0.0047       | 2.9779       |
| $\Delta E(\text{PQQ-C5-(OH)}_2 - \text{PQQ} + \text{H}_2\text{O})$ | -0.0155      | -9.7349      |

**Table III.A.** Selected dihedral angles for anionic and N(1)-, C(3)- and C(8)-methyl-PQQ derivatives and their C(5)-hydrated forms.

| Dihedral angle<br>(degrees) |     |     |     | PQQ(3-) | PQQ-N1-<br>Me | PQQ-N1-<br>Me-<br>C5(OH) <sub>2</sub> | PQQ-C3-<br>Me | PQQ-C3-<br>Me-<br>C5(OH) <sub>2</sub> | PQQ-<br>C8-Me | PQQ-C8-<br>Me<br>C5(OH) <sub>2</sub> |
|-----------------------------|-----|-----|-----|---------|---------------|---------------------------------------|---------------|---------------------------------------|---------------|--------------------------------------|
| N1                          | C1A | C9A | C9  | 9.26    | 28.35         | 28.64                                 | 10.42         | 13.30                                 | 11.30         | 15.50                                |
| C3A                         | C4  | C5  | C6A | 18.19   | 24.88         | 41.31                                 | 22.04         | 36.95                                 | 14.32         | 35.11                                |
| C8                          | C7  | C7A | O7B | -22.92  | 23.28         | -7.22                                 | -23.08        | -11.66                                | -73.30        | -58.33                               |
| C9A                         | C9  | C9B | O9B | -41.99  | -137.03       | -130.33                               | -42.98        | -40.81                                | -64.24        | -63.47                               |

Formation of an sp<sup>3</sup>-carbon atom at C(5) following hydration (XIIa) causes the dihedral angle C(3A)-C(4)-C(5)-C(6A) to increase to 41.3 degrees. The C(7)-carboxylic acid group rotates back to a position that keeps the O(7B) 7.2 degrees above the pyridine plane. Replacement of the hydrogen at the C(8) position of PQQ by a methyl group (XIV) forces the two neighboring carboxylic acid groups out of the plane of the PQQ. The overall structure of PQQ is not altered. Rotation of the C(7)- and C(9) carboxylic acid groups increases to 60 degrees for both the free and hydrated forms (XIVa) of PQQ-C(8)-Me. In the non-hydrated form the rotational angle for the C(7) carboxylic acid group is slightly larger at 73 degrees.

The C(3)-methyl-PQQ derivative (XIII) shows the least distortions. The methyl group does not sterically interact with the C(2)-carboxylic acid group, which stays largely in the plane. No major effect is observed on the rest of the PQQ molecule. Hydration (XIIIa) only affects the dihedral involving the C(4)-C(5) bond and allows the C(7)-carboxylic acid to move into the plane of the molecule.

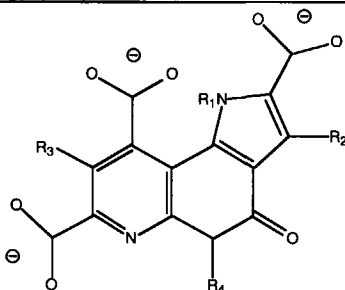
Comparing the energies computed for the N(1)-, C(3)- and C(8)-methyl substituted PQQ derivatives and their respective C(5)-hydrated forms matches the experimentally observed trend [54]. Although equi-electronic, the PQQ-C(3)-Me derivative is computed to be significantly more stable than its N(1)- and C(8)-counterparts (by 3.8 and 19.4 kcal/mol, respectively). This holds for the hydrated forms as well (6.3 and 20.1 kcal/mol, respectively). The N(1)-methylated PQQ being the least stable species is not surprising as in this case the hydrogen bond between the N(1)-proton and the C(9)-carboxylic acid group is absent. Introducing a methyl group at the C(8) position seems to have negligible influence on the formation of this hydrogen bond and by consequence it is more stable than the N(1)-methylated PQQ. In this case the methyl-group can be easily accommodated and does not disturb the original PQQ structure. However, the C(7)

carboxylic acid group is forced to rotate out of the plane of the pyridine ring making this derivative less stable than its C(3)-methylated counterpart. By and large, the computed energies (Table III.B) appear to follow the trend that is observed experimentally. From the comparison, discrepancies would be estimated to be less than 10 kcal/mol.

#### Redox reaction of PQQ/PQQH<sub>2</sub>.

The energies obtained for the molecules involved in the overall redox reaction (Scheme 1) provide an indication of the correctness of the used methods. The redox-potential of the PQQ/PQQH<sub>2</sub> couple has been measured to be +90 mV (pH 7) [55], whereas for the methanol/formaldehyde couple a redox-potential of -182 mV (pH 7) has been reported [56]. The equilibrium thus lies completely to the PQQH<sub>2</sub>/formaldehyde side. A severe shortcoming of the (gas phase) calculations becomes evident when we compare the computed energies of PQQ+methanol (reactants) and PQQH<sub>2</sub>+formaldehyde (products).

**Table III.B.** Structures and energies of several methyl-PQQ derivatives. All energies are calculated at the 6-31G(d,p) level.



| Entry | R1               | R2               | R3               | R4                      | Energy (Hartrees/mol) |
|-------|------------------|------------------|------------------|-------------------------|-----------------------|
| XII   | -CH <sub>3</sub> | -H               | -H               | $\text{C}=\text{O}$     | -1278.6436            |
| XIIa  | -CH <sub>3</sub> | -H               | -H               | $\text{C}(\text{OH})_2$ | -1354.6838            |
| XIII  | -H               | -CH <sub>3</sub> | -H               | $\text{C}=\text{O}$     | -1278.6756            |
| XIIIa | -H               | -CH <sub>3</sub> | -H               | $\text{C}(\text{OH})_2$ | -1354.7162            |
| XIV   | -H               | -H               | -CH <sub>3</sub> | $\text{C}=\text{O}$     | -1278.6696            |
| XIVa  | -H               | -H               | -CH <sub>3</sub> | $\text{C}(\text{OH})_2$ | -1354.7062            |

Although the energy computed for PQQH<sub>2</sub> is lower than that of PQQ, the electronic energy of formaldehyde is significantly higher than that of methanol. This brings the overall electronic energy difference (calculated as the sum of the individual species) to 0.0107 Hartree/mol (6.74 kcal/mol) in favor of the reactants. In the aqueous phase, however, formaldehyde is completely hydrated. As a first-order approximation of the energy involved, gas-phase energies of water and the hydrated form of formaldehyde were computed. The total energy difference for the reaction PQQ + CH<sub>3</sub>OH + H<sub>2</sub>O → PQQ<sub>2</sub> + CH<sub>2</sub>(OH)<sub>2</sub> amounts to 4.1 kcal/mol in favor of the products (Table IV). This number is still substantially smaller than the number  $-nF\Delta E_0 = -2*96.5*(0.09-(-0.272))/4.18 = -13.2$  kcal mol<sup>-1</sup> calculated for the Gibbs free energy of the oxidative half reaction (pH 7, standard conditions). Most likely, preferential solvation of the product formaldehyde is an important factor.

*Conclusions from the calibration.*

The geometries of the available X-ray structures can be satisfactorily reproduced by the computations. The pyrrole- and pyridine rings are found to be consistently planar. Their relative position is determined both by the hybridization state of the C(4)- and C(5)-carbon atoms (and the aromatic character of the middle ring) and the presence of a hydrogen bond between the N(1)-hydrogen and the C(9) carboxylic acid moiety. The least structural changes are observed when the C(5) carbon changes its hybridization from a sp<sup>2</sup> to a sp<sup>3</sup> upon addition of water to the carbonyl group. These changes appear to be readily accommodated by the PQQ structure. In the case of addition to C(4), the rotation of the C(7) carboxylic acid moiety changes appreciably. Also the pyrrole nitrogen is seen to dip below the plane of the pyridine ring. Of the three carboxylic

**Table IV.** Calculated energies for methanol, formaldehyde and hydrated formaldehyde and corresponding energy differences for the oxidative half reaction. All energies were calculated at the 6-31G(d,p) level of theory.

| Compound  | Hartree/mole | kcal/mole    |
|---|--------------|--------------|
| Methanol  | -115.0467    | -72187.2232  |
| Formaldehyde  | -113.8697    | -71448.7214  |
| Formaldehyde(aq)  | -189.9106    | -119161.3325 |
| $\Delta E(\text{PQQ}+\text{methanol}) - (\text{PQQH}_2+\text{formaldehyde})$                | -0.0107      | -6.7422      |
| $\Delta E(\text{PQQ}+\text{methanol}+\text{H}_2\text{O}) - (\text{PQQH}_2+\text{form(aq)})$ | 0.0065       | 4.0818       |

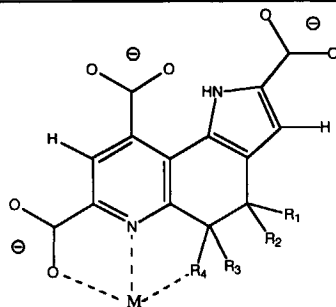
groups, the C(7)-carboxylic acid group is observed to respond most prominently to structural changes. The C(2)-carboxylic acid retains coplanarity with the pyrrole ring, throughout. Most probably, this carboxylic acid group is least affected by steric interactions [48]. The C(9)-carboxylic acid group is primarily positioned by way of hydrogen bonding to the N(1)H, an interaction that remains intact in all studied PQQ structures except for the N(1)-methyl derivative of PQQ. Substitution of the C(3) position by a methyl group does not induce any major changes in the structure. Hydration of the C(5) carbonyl forces the C(7) carboxylic acid group to become more planar, but this could be a side effect of the different hybridization of the C(5) carbon. Substituents introduced at the C(8)- and N(1)-position have considerably more effect on the overall structure. Both C(7)- and C(9)-carboxylic acid groups are forced out of the plane of the molecule. In the case of hydration of the C(5) carbonyl the C(7)-carboxylic acid group retains its original position when placing a substituent at the N(1) position.

Protonation of the respective carboxylic acid groups changes the bond lengths, as the bonds become more localized in nature. A further effect is the rotation of the C(7)-carboxylic acid group, a near planar configuration with respect to the pyridine ring is adopted. This carboxylic acid group is, however, not expected to be protonated as it is one of the  $\text{Ca}^{2+}$  binding ligands.

The results of the calculations performed on the ground-state PQQ structures thus provide a suitable basis for the study of the proposed reaction mechanism.

### 3.2 Postulated reaction intermediates.

With a suitable frame of reference established, energies of intermediates that might be involved in a hydride transfer reaction have been computed. For direct hydride transfer from methanol to PQQ, both the carbons (C(5) or C(4)) and the carbonyl oxygens are candidates. Zheng and Bruice studied the possible role of the C(4) carbonyl oxygen as a primary hydride acceptor [18]. The *ab initio* energies of the PQQ-hydroxy-dienones species formed after transfer of the hydride are summarized in Table V. As expected, (IX [18]) is the most stable of the iso-electronic structures. Somewhat surprisingly, (VII) is the next stable species. Considering the intuitive notion that an electron-rich oxygen can hardly be considered an attractive hydride acceptor, we decided to investigate the energetic demands of direct hydride transfer to the C(5)-carbon in more detail. Formation of  $\text{PQQH}_2$  will then require tautomerization in a consecutive step.

**Table V.** Structures and energies of hydrated PQQ, protonated and deprotonated PQQ-hydroxy-dienones. All energies are calculated at the 6-31G(d,p) level of theory

| Entry | R <sub>1</sub> | R <sub>2</sub> | R <sub>3</sub> | R <sub>4</sub> | M                | Energy (Hartree/mole) |
|-------|----------------|----------------|----------------|----------------|------------------|-----------------------|
| III   |                |                |                |                | -                | -1315.6759            |
| IV    |                |                |                |                | -                | -1315.6557            |
| V     |                |                |                |                | -                | -1240.8108            |
| VI    |                |                |                |                | -                | -1240.7848            |
| VII   |                |                |                |                | -                | -1239.8946            |
| VIII  |                |                |                |                | -                | -1239.8913            |
| IX    |                | -              |                | -              | -                | -1239.9161            |
| X     |                | -              |                | -              | Ca <sup>2+</sup> | -1917.1783            |
| XI    |                |                |                |                | Ca <sup>2+</sup> | -1917.1601            |

The electronic energy of the postulated intermediate, PQQ-C(5)H-O<sup>-</sup> (VII), can not be directly compared to either of these systems (PQQ or PQQH<sub>2</sub>), as the number of atoms is not equal. Nevertheless, a comparison can be made with the hydrated intermediate, PQQ-C(5)H-OH (V)/formaldehyde couple. The calculated energy for this couple compares favorably with the PQQH<sub>2</sub>/formaldehyde state by 0.0077 Hartree/mol (4.84 kcal/mol). The corresponding PQQ-C(4)H-OH (VI) is higher in energy (0.0182 Hartree/mol, 11.44 kcal/mol). This intermediate lies 0.0290 Hartree/mol (18.18 kcal/mol) above the energy level of the PQQ/methanol state. It therefore seems reasonable to assume that if the reaction proceeds via hydride transfer it will most likely form a C(5)-H intermediate. The same trend is observed in the non-protonated form of the postulated



intermediates. PQQ-C(4)H-O<sup>-</sup> (VIII) is less stable than PQQ-C(5)H-O<sup>-</sup> (VII) by 2.11 kcal (0.0034 Hartree/mol). However, the energy difference between the unprotonated forms is much smaller (16.35 kcal/mol for the protonated forms versus 2.11 kcal for the unprotonated ones). The C(5)-deprotonated form of PQQH<sub>2</sub>, PQQ-C(4)OH-C(5)-O<sup>-</sup>, which already has a double bond formed and lengthened carbonyl bonds, is more stable than both PQQ-C(4)H-O<sup>-</sup> and PQQ-C(5)H-O<sup>-</sup> (15.56 kcal (0.0248 Hartree) and 13.45 kcal (0.0214 Hartree), respectively).

*Geometries of protonated and deprotonated PQQ-hydroxy-dienones (V-VIII).* The optimized structures much resemble the PQQ-C(4)- and C(5)-hydrates. Again reversal of the C(3A)-C(4)-C(5)-C(6A) dihedral angle sign takes place, placing the carbon that exhibits sp<sup>3</sup> character above the plane of the PQQ. As a consequence the N(1)-C(1A)-C(9A)-C(9) dihedral also reverses sign, driving the pyrrole ring below the plane of the pyridine ring when the C(4) changes from sp<sup>2</sup> (carbonyl) to sp<sup>3</sup>. This induces no change in the C(9) carboxylic acid position while the C(7) carboxylic acid experiences some changes. The O(7B) oxygen occupies a position beneath the plane of the pyridine ring. The PQQ-C(5)H structure remains the same. The bond distances for the carbonyl carbon and the hydrogen are 1.09 in both cases. Addition of a hydride to the PQQ-C(5)-carbon is favored over the C(4)-position by 0.0034 Hartree/mol (entry VII vs. VIII, Table V). Energies of these intermediates can be compared to that of iso-electronic deprotonated PQQH<sub>2</sub>. Consecutive rearrangement to C(5)-deprotonated PQQH<sub>2</sub> is favored by 0.02 Hartree/mol (entry IX, Table V). Upon protonation the difference in energy between the corresponding C(4)- and C(5)-addition complexes increases to 0.026 Hartree/mol (entries V and VI, Table V).

### 3.3 Role of Calcium

The resemblance of structural features of PQQ and well-known chelating agents, e.g.  $\alpha$ -picolinic acid [57] and 8-hydroxyquinoline [58] has been noticed in an early stage. Two positions for chelation seem available to divalent cations; (1) between the two carbonyl groups or (2) between the C(5) carbonyl and C(7)-carboxylic acid group. The first has been observed for the Na<sup>+</sup> and K<sup>+</sup> salts of PQQ [48,49], but not for divalent cations. In the crystal structure of the acetone-adduct, the position between C(5) and C(7)-COOH is taken up by a water molecule. Also K<sup>+</sup> [49] and Cu<sup>2+</sup> [59-61] have been shown to occupy this particular position. In the available high-resolution X-ray structures of MDH [50,52]

and s-GDH [21], PQQ binds  $\text{Ca}^{2+}$  through the C(5) carbonyl oxygen, C(7) carboxylate and, surprisingly, the pyridyl nitrogen, N(6). The remaining ligand positions are taken by oxygen bearing residues in the protein environment or water molecules. No severe restrictions are placed on the character of the amino acid functioning as a ligand. In s-GDH from *A. calcoaceticus* [21], main chain oxygen atoms from Gly247 and Pro248 and two water molecules serve as ligand (coordination number  $n=7$ ), while in MDH from *M. extorquens* both oxygens from the carboxylate of Glu177 and the amide oxygen of Asn261 fill the coordination sphere ( $n=6$ ) [52]. In this case, two waters are located close by and might be subject to rapid ligand exchange as is well known for calcium (i.e.  $n=6-8$ ).

Calcium was included in the computations of the possible reaction intermediates to estimate the effect of its presence on the relative energies. Fragments mimicking the protein environment were not included in the calculations (i.e. taking (neutral) formic acid to model the catalytic Asp)[62]. The complexation of  $\text{Ca}^{2+}$  by C(5)-deprotonated PQQH<sub>2</sub> (Table V, entry IX and X) induces some minor changes in its structure (Table VI.A). The distances between the  $\text{Ca}^{2+}$ -ion and the O(7A), N(6) and O(5) position are 2.24, 2.29 and 2.21 Å, respectively (Table VI.B). As a result the bond length of the carbonyl and carboxylic acid group slightly changes. The C(5)-O(5) bond length increases from 1.29 to 1.36 Å, while the partially double bond character of the oxygens in the C(7) carboxylic acid group is increased. The bond C(7A)-O(7B) shortens by 0.04 Å, while the bond length of the oxygen liganded to the  $\text{Ca}^{2+}$ -ion increases by 0.05 Å. The tilting angle between the heterocycles decreases and the dihedral angle of the C(9) carboxylic acid group with the pyrrole ring diminishes as a result of the complexation. The C(7) carboxylic acid group is forced in the plane, that is ligated to the calcium. The dihedral angle O(7B)-C(7A)-C(7)-C(8) decreases to -3.3 degrees (-34.8 in the calcium-free compound).

Addition of  $\text{Ca}^{2+}$  to the deprotonated C(5)-hydroxy-dienone (Table V, entry VII and XI) results in a flat structure for this postulated reaction intermediate. The C(7) carboxylic acid is again rotated into the plane of the pyridine ring by complexation to the calcium ion (O(7B)-C(7A)-C(7)-C(8) angle decreases from -42.0 to -9.3). The same holds for the C(9)-COO group (O(9B)-C(9B)-C(9)-C(9A) dihedral changing from -47.5 to 36.0 degrees). The calcium ion is ligated to O(7A), N(6) and O(5) with distances of 2.24, 2.32 and 2.17 Å, respectively (Table VI.B). The bond length between C(5) and the hydrogen is shortened, 1.15 vs. 1.11 Å, while the C(5)-O(5) bond length increases from 1.30 to 1.36

Å. The difference in energy between the two calcium complexed PQQ intermediates amounts to 11.41 kcal, while between the corresponding calcium-free compounds the energy difference equals 13.45 kcal. A net stabilization of the deprotonated C(5)-hydroxy-dienone form of PQQ of 2.04 kcal upon complexation with calcium occurs (Table V).

The distances between the divalent calcium ion and the chelating atoms of PQQ are in general too short with respect to the reported distances for the various X-ray structures (Table VI.B).

**Table VI.A.** Selected geometrical features for C(5)-deprotonated PQQ derivatives and their corresponding Calcium complexes. Roman numbers in parentheses correspond to entries in Table 5

| Bond length (Å)          |     | PQQ-C(5)H-C(5)O <sup>-</sup><br>(VII) | PQQ-C(5)H-C(5)O <sup>-</sup> ---Ca <sup>2+</sup><br>(XI) | PQQ-C(4)OH-C(5) <sup>-</sup><br>(IX) | PQQ-C(4)OH-C(5) <sup>-</sup> ---Ca <sup>2+</sup><br>(X) |        |         |
|--------------------------|-----|---------------------------------------|--|--------------------------------------|---|--------|---------|
| C5                       | HC5 | 1.11                                  | 1.15   | -                                    | -   |        |         |
| C5                       | O5  | 1.36                                  | 1.30   | 1.29                                 | 1.36  |        |         |
| C7A                      | O7A | 1.29                                  | 1.23   | 1.24                                 | 1.29  |        |         |
| C7A                      | O7B | 1.20                                  | 1.25   | 1.25                                 | 1.21  |        |         |
| Dihedral angle (degrees) |     |                                       |  |                                      |   |        |         |
| N1                       | C1A | C9A                                   | C9   | 10.61                                | 12.97   | 2.40   | -179.30 |
| C3A                      | C4  | C5                                    | C6A  | 32.55                                | 38.24   | 1.78   | 1.21    |
| O7B                      | C7A | C7                                    | C8   | -42.03                               | -9.33   | -34.76 | -3.27   |
| O9B                      | C9B | C9                                    | C9A  | -47.48                               | -36.01  | -46.76 | -38.98  |

**Table VI.B.** Coordination distances between PQQ and Calcium as found in the *ab initio* structures and experimental X-ray structures. All distances are in ångstroms. The resolution of the X-ray structures is given in italics.

| Bond                   | Calculated |      | Experimental               |   |      |   |      |                          |                                 |                                  |
|------------------------|------------|------|----------------------------|---|------|---|------|--------------------------|---------------------------------|----------------------------------|
|                        | X          | XI   | s-GDH<br>1.5Å <sup>a</sup> | MDH<br>(M. W3A1)<br>2.4Å <sup>b</sup> 1.9Å <sup>c</sup> |      | MDH<br>(M. extorquens)<br>2.4Å <sup>d</sup> 1.9Å <sup>e</sup> |      | EDH<br>2.6Å <sup>f</sup> | PQQ-K <sup>+</sup> <sup>g</sup> | PQQ-Na <sup>+</sup> <sup>h</sup> |
| N6 - Ca <sup>2+</sup>  | 2.29       | 2.32 | 2.49                       | 2.35  | 2.63 | 2.56  | 2.45 | 2.94                     | 2.72                            | 2.48(2.53)                       |
| O5 - Ca <sup>2+</sup>  | 2.21       | 2.17 | 2.48                       | 2.51  | 2.46 | 2.95  | 2.77 | 2.81                     | 2.77                            | 2.61(2.64)                       |
| O7A - Ca <sup>2+</sup> | 2.24       | 2.24 | 2.41                       | 2.38  | 2.68 | 2.96  | 2.52 | 2.90                     | 2.48                            | 2.40(2.40)                       |

(a) ref. 21 (b) ref. 35 (c) ref. 48 (d) ref. 49 (e) ref. 50 (f) ref. 52 (g) ref. 73 (h) ref. 74. Values in parentheses are coordination distances for the other PQQ molecule present in the unit cell.

This may be attributed to an overestimation of the electronic forces in the *ab initio* calculations. Increased distances were found for the complex of neutral PQQ with  $\text{Ca}^{2+}$  (N(6)- $\text{Ca}^{2+}$  2.47 Å, O(5)- $\text{Ca}^{2+}$  2.30 Å and O(7A)- $\text{Ca}^{2+}$  2.36 Å) by Zheng and Bruice [18]. However, it should also be taken into account that the charges are geometrically not as well balanced in these calculations as they obviously are in an enzyme structure or crystallographic unit cell. It should be noted that distances between PQQ and calcium appear to be highly variable within the different types of quinoproteins as is evident from the data presented in Table VI.B. The distances obtained from the *ab initio* structures are nevertheless too short and fall outside the observed range. Identical values are found in hybrid QM/MM calculations employing model systems comprising acetate or propanoate complexed calcium [63]. These complexes are bidentate and the interactions are very strong due to the attractive interaction of the charged species. Typical distances are in the range of 2.2 to 2.3 Å. Amide (unidentate) complexes with  $\text{Ca}^{2+}$  (complexation to the carbonyl function) give even shorter distances for the purely quantum chemical calculations (~ 2.15 Å), whereas distances between ethylimidazole and calcium are slightly longer (~ 2.35 Å). Quantum chemical calculations of the condensed phase using the self-consistent reaction field (SCRF) method for the bidentate complex of acetate with  $\text{Ca}^{2+}$  show slightly longer distances (~ 2.4 Å) [64]. The large dipole moment of acetate (~ 5 D) is held responsible for these interactions.

### 3.4. Transition state structures.

*Model compound.* Location of the transition state structure of the hydride transfer between a carbonyl moiety and methanolate complexed with a calcium ion was done for a model complex. The formal charge of the calcium was balanced by addition of an extra methanolate and water molecule. This resulted in a final coordination number of 4 (Fig. 3). Coordination numbers for  $\text{Ca}^{2+}$  are required to range from 6 to 9 [65]. However, gas-phase *ab initio* calculations with only one or two ligands have been found to give satisfactory results regarding structural and energetic properties [63,64,66]. The use of filled coordination spheres, as applied in the calculation of hydration of divalent cations [65], was judged unnecessary in the current context.

While the distances between the hydride and the respective carbons of the methanolate and formaldehyde were restrained, all other structural variables were optimized. The analytical Hessian matrices obtained for structures close to the TS were used to locate the first-order saddlepoint using a mode-following protocol (i.e. the energy

is maximized along one of the eigenvectors of the Hessian, while the other modes are minimized). To ensure that a first order saddlepoint was indeed located the eigenvalues of the Hessian were reanalyzed. A single imaginary frequency corresponding to the motion of the hydride ( $\nu = 1123.81 \text{ cm}^{-1}$ ) was found. The frequencies belonging to the translational and rotational modes have wavenumbers between  $0.7$  and  $8.3 \text{ cm}^{-1}$ . Intrinsic Reaction Coordinate (IRC) runs were performed in both directions to establish the symmetry of the potential energy surface. Starting from the TS, both reactant and product state were reached. This confirms that the located TS indeed connects both states and is located on a reaction pathway.

The eigenvalues of the Hessian matrix belonging to the final states of the IRC run, which are identical in this case, were calculated. These showed the final states to be true minima. The energy difference between the TS and the reactant/product state at this level of theory (MC) amounts to  $24.13 \text{ kcal/mol}$  ( $0.0389 \text{ Hartree/mol}$ ).

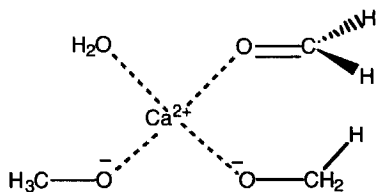


**Figure 3.** Structure of the model calcium complex used to locate the TS of the hydride transfer reaction.

*PQQ complex.* The values obtained for the distances between the hydride and the carbon atoms were copied to a model including PQQ, methanolate and calcium. This complex was minimized at the STO-3G(d) level while restraining the distances between PQQ-C(5) carbon and the hydride and the carbon of the methanolate and the hydride (Fig. 5A). The Hessian belonging to this minimized structure was analyzed and used to locate the TS using a mode following procedure. This resulted in a structure with a single imaginary frequency corresponding to a true TS ( $\nu = 1387.07 \text{ cm}^{-1}$ ) (Fig 4). Rotational and translational frequencies between  $0.42$  and  $4.09 \text{ cm}^{-1}$  were obtained.

In the transition state the distance between PQQ-C(5) position and the hydride is  $1.307 \text{ \AA}$ , between hydride and methanolate carbon  $1.389 \text{ \AA}$ . This compares favorably with the distances usually found for reactions involving hydride transfer [67]. The total distance between the PQQ-C(5) carbon and the methanolate carbon is  $2.59 \text{ \AA}$ . This

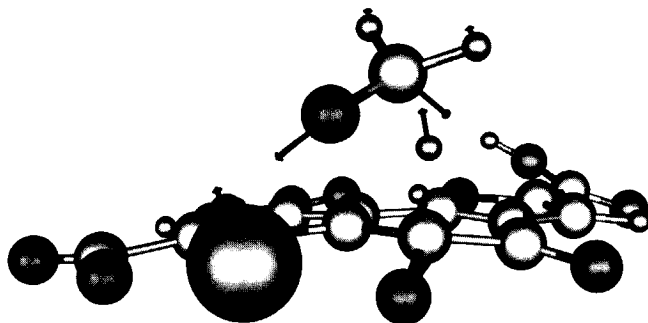


**Figure 4.** Structure of the located TS for the transfer of a hydride between methanol and the C(5) carbon of PQQ. Contributions to the single imaginary frequency found ( $\nu = 1387.07 \text{ cm}^{-1}$ ) are depicted as vectors (scaled to appropriate size). Carbon atoms in light grey, nitrogen in black, oxygen in dark grey, hydrogens in grey (small spheres) and calcium ion as large grey sphere. These calculations were performed at the STO-3G(d) level of theory. Picture was created using MacMolPlt<sup>47</sup>.

implies an angle of 147.6 degrees. The methanolate is complexed to the calcium ion through its oxygen (distance 2.17 Å). The direction of the carbon-oxygen bond in the methanolate slightly deviates from the plane including the calcium, PQQ-C(5) and the central atom of the substrate (11.0 degrees).

A grid search was performed by varying the distances between the hydride and the carbon atom of the methanolate and the PQQ C(5) carbon atom in steps of 0.1 Å to yield information on the potential energy surface of the reaction (Fig. 5A,B). As can be inferred from the contour lines, the transition state barrier is slightly more than 8 kcal mol<sup>-1</sup>, when measured from the lowest energy complex present on this grid.

Both forward and backward IRC runs, starting at the located TS, were performed to ensure that the TS is a point on the reaction pathway (Fig. 6). Starting at the TS, the energy for the forward reaction (going to the “product” state, PQQ-C(5)-H and formaldehyde complexed by Ca<sup>2+</sup>) drops relatively slowly compared to the backward reaction. The energy difference between the TS and the “product” state is only 8.16 kcal mol<sup>-1</sup>. The length of the PQQ-C(5)-H bond deviates 0.1 Å from the value found in the corresponding equilibrium structure (Structure VII), which indicates that the final

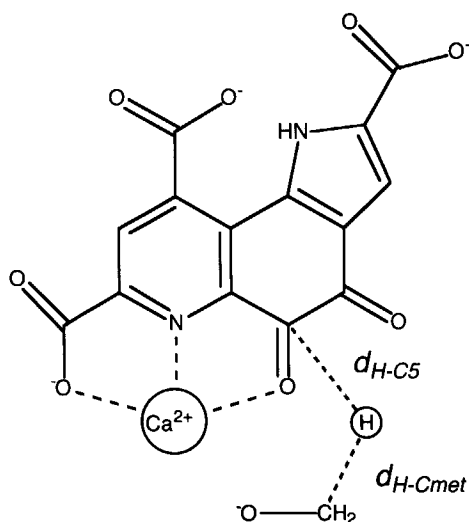


**Figure 5A.** Schematic drawing of the complex used in the grid search performed to locate the TS for the direct hydride transfer reaction between methanol and PQQ. Labeled distances were varied systematically, while all remaining variables were free to move.

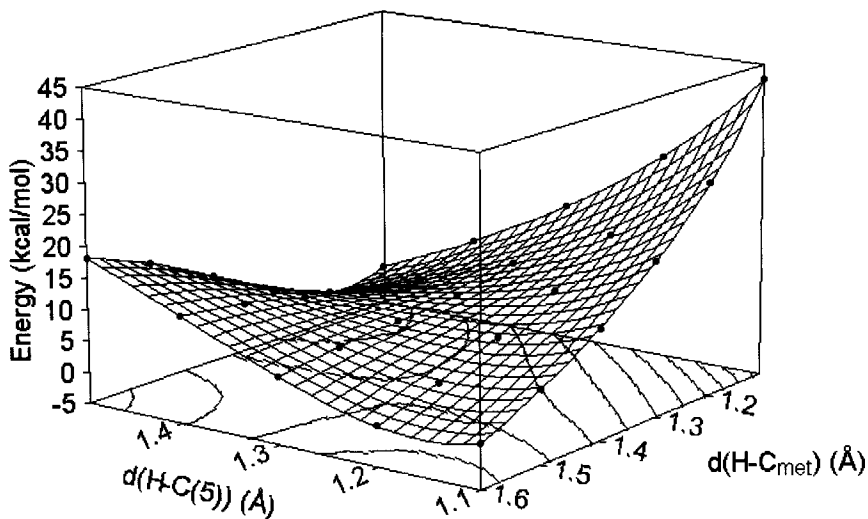


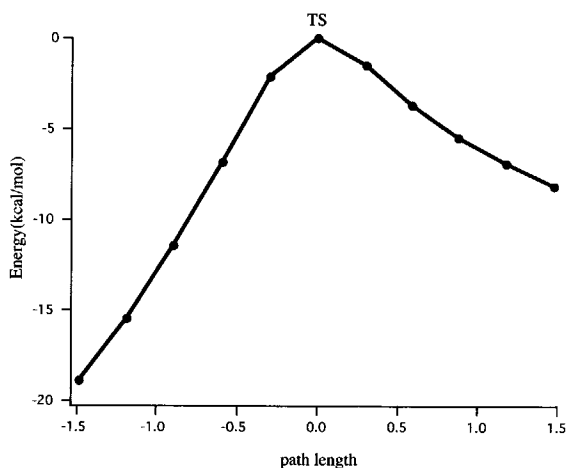
**Figure 5B.** Potential energy surface calculated for the direct hydride transfer reaction between PQQ and methanol. X- and Y-axes correspond to the distances labeled in Fig. 5A. Calculated structures are denoted with black dots. All energies are in kcal/mol and given relative to the lowest energy structure (1.5, 1.2). All calculations were performed at the STO-3G(d) level of theory.

"product" state has not yet been reached during the IRC run. The energy drop for the backward reaction is significantly larger measured over the same path length. The bond length between the hydride and the carbon of the substrate is 1.103 Å at this point, comparable to the other H-C distances (1.099 Å and 1.098 Å). The energy difference of 18.9 kcal/mol might thus be taken to represent the energy barrier for the described hydride transfer. This value is in the same range as that found by Zheng & Bruice for hydride transfer to the PQQ-O(4) (18.5 kcal/mol at the B3LYP/3-21G(d) level of theory) [18].

### 3.5 Mechanistic implications

The reaction mechanism of quinoprotein dehydrogenases has long been subject to debate. The chemistry of free PQQ in solution with regard to the ready addition of various nucleophiles, has focussed on the formation of a hemiketal intermediate as the initial step. Formation of covalent adducts with water, alcohols and amines has been well-documented [23,24]. Addition of acetone and aldehyde at the C(5)-position of PQQ has been shown to lead to strongly fluorescent compounds [23]. Observation of a fluorescent compound thus suggests the addition of a substance at the C(5)-position of PQQ. The recent observation of a fluorescent transient in the reaction of s-GDH with glucose seems to lend credit to such a mechanism [19,68]. However, the actual redox step would either require hydride transfer from the substrate to the C(4)=O group or the C(5) oxygen. Whereas the latter is relative electron rich, the C(4) carbonyl oxygen is not particular well-known for its high affinity for hydrides. Several mechanism have been

**Figure 6.** Minimum energy path connecting the TS found for the oxidation of methanol by PQQ to the reactant and product state. The path length is given in mass weighted Cartesian coordinates, while the energy for the TS has been taken as zero kcal/mol.





suggested in the literature to solve these problems. Formation of a *p*-quinone structure via loss of the N(1)-hydrogen has been suggested by several groups [10,53]. This proposal had to be rejected when N(1)-methylated PQQ derivatives showed activity in reconstitution assays with apo-QHADH from *C. testosteroni* [54]. The involvement of calcium in the catalytic mechanism has been established by mutagenesis studies performed in the group of Anthony [34]. Mutations in the *moxA*, *moxK* and *moxL* genes involved in methanol oxidation by *M. extorquens* lead to the synthesis of an inactive calcium-free MDH. Reconstitution with calcium restores the original activity and spectral features of the fully reduced normal MDH. MDH in which the  $\text{Ca}^{2+}$  ion is replaced by  $\text{Ba}^{2+}$  showed decreased affinity for both substrate and activator ( $K_m(\text{Ca}^{2+})$  for methanol is 3  $\mu\text{M}$ ,  $K_m(\text{Ba}^{2+})$  3.5 mM,  $K_A(\text{Ca}^{2+})$  for ammonia is 2 mM,  $K_A(\text{Ba}^{2+})$  is 52 mM) [69]. Zheng & Bruce have shown the calcium to play a role in the activation of the substrate [18]. They also suggested the hemiketal to be a 'dead-end' complex. However, hydride transfer from the substrate to the C(4)-carbonyl oxygen, as proposed by these authors, is questionable on the basis of steric and electronic arguments.

Based purely on bond lengths and electronic considerations direct hydride transfer to the C(5) carbon of PQQ offers a plausible alternative. With the methanolate liganded to the  $\text{Ca}^{2+}$  ion, the hydrogens come very close to the C(5) carbon, which is also in an electron deficient state.

Taking the protein environment into account further strengthens the notion of direct hydride transfer to the C(5) position of PQQ. Looking into the active site funnel of MDH, the C(5)=O moiety of PQQ is exposed, whereas the C(4)=O group is shielded from sight by the protein. Recent X-ray crystallographic studies on both MDH and s-GDH have indicated the presence of substrate molecules in the respective active site funnels [50,70]. These high resolution data do not resolve the location of the hydrogens, but suggest the carbon atom from which the hydride is to be abstracted to point in the direction of the C(5) position of PQQ. Oubrie *et al.* located the substrate binding site of s-GDH by soaking s-GDH-PQQ crystals in a solution containing excess glucose and in the absence of electron acceptors [70]. This led to reduction of PQQ to PQQH<sub>2</sub> in the final ternary s-GDH-PQQH<sub>2</sub>-glucose complex crystals. Based on the minimal differences observed in the geometries of the different redox states of the cofactor, a s-GDH-PQQH<sub>2</sub>-glucose complex was assumed to mimic a reactive s-GDH-PQQ-glucose complex. Binding of glucose to s-GDH shows the glucose C1 atom to be located directly above the PQQH<sub>2</sub> C(5) atom. The catalytic base, His144, is situated close to the O1-oxygen of the

substrate. Inspection of the binding site shows major rearrangements to be necessary in order to facilitate an addition-elimination reaction. Favorable interactions between positively charged amino acids and the developing negative charge at the deprotonated O1 atom have to be disrupted. Formation of a covalent bond between the glucose O1 atom and the PQQ-C(5) atom would lead to energetically expensive rearrangements. The authors conclude that an addition-elimination reaction would be highly unlikely in the case of *s*-GDH. It was noted that the position of the glucose molecule was ideally suited for direct hydride transfer from the C1 atom of glucose to the PQQ-C(5) atom. The distance between the two carbon atoms involved is only 3.2 Å. The geometric parameters ensure a fast reaction to be possible. Observation of a fluorescent intermediate in kinetic experiments performed on the oxidation of *s*-GDH by glucose, could be explained by the formation of a C(5) reduced PQQ species [19,68]. The subsequent rate-determining step would then be the tautomerization of the intermediate to PQQH<sub>2</sub>. Similar observations have been made regarding the oxidation of methanol by MDH [17,25,71]. A deuterium effect of 6, as found for MDH, can be perfectly well explained by the direct hydride transfer mechanism. An even higher deuterium kinetic isotope effect of 7.8 has recently been reported for the oxidation of β-D-glucose by *s*-GDH in which the calcium has been replaced with Ba<sup>2+</sup> [19]. Replacement of PQQ with its nitrated PQQ derivative, which seems unable to form the hemiketal intermediate, leads to the disappearance of the fluorescing intermediate upon reaction with hydrazine. The initial fast formation of the fluorescent C(5)-reduced PQQ intermediate would be followed by a much slower, rate-limiting, tautomerization step to PQQH<sub>2</sub>.

The calculations described in this article have culminated in the notion that the direct hydride transfer from the substrate molecule to the C(5) carbon of PQQ is energetically feasible. The height of the computed energy barrier is comparable to that found by Zheng and Bruice for the postulated direct hydride transfer from the methanol carbon to the PQQ-O(4) position. The formation of a C(5) reduced PQQ species is in good agreement with the observation of a fluorescent transient in the oxidation of glucose by *s*-GDH [19,68] and methanol by MDH [17,25,71]. The investigated mechanism offers a consistent explanation of the observed experimental data.

When this work was completed a recent article of Zheng and coworkers [72] published a re-evaluation of the x-ray crystallographic data of MDH from *M. methylotrophus* W3A1 in a second crystal form [50]. Convincing evidence for the actual

presence of the C(5)-reduced intermediate of PQQ (Structure as in Table 5, entries V, VII, viz. XI) strongly supports the findings presented here.

#### 4. Conclusion

High level *ab initio* gas-phase calculations have been performed to study the feasibility of direct hydride transfer in the oxidation of methanol by PQQ. The applied computational methods were calibrated against available experimental data. *Ab initio* energies for different possible reaction intermediates were computed. A transition state for the oxidation of methanol by PQQ in the presence of calcium was located and characterized. The computed energy barrier was in the same range as that calculated for a mechanism involving direct hydride transfer from the methanol carbon to the PQQ-O(4) position. Comparison of these values and the observed experimental phenomena support a reaction mechanism involving direct hydride transfer from the Ca-position of the substrate molecule to the C(5) position of PQQ. A similar mechanism has recently been proposed on experimental grounds for the oxidation of glucose by soluble quinoprotein glucose dehydrogenase from *Acinetobacter calcoaceticus* [21]. Future calculations should incorporate the effects of the protein environment and solvent in order to obtain more accurate data. Mechanistic studies, including the measuring of kinetic isotope effects, are currently explored.

#### 5. Acknowledgements

The authors would like to thank Jana Vasiljev (HPaC) and Ronald van Pelt (Silicon Graphics, De Meern, The Netherlands) for their help in installing and maintaining the GAMESS distribution on the CRAY T3E at the High Performance Applied Computing (HPaC) Centre of the Delft University of Technology, The Netherlands. The authors would also like to acknowledge the HPaC for generously providing the computer facilities and time to perform the calculations.

This research has been financed by the Netherlands Organization for Advancement of Pure Research (NWO).

## References

- (1) Duine, J. A.; *Eur. J. Biochem.*, **200** (1991), 271-284.
- (2) McIntire, W. S.; *FASEB Journal*, **8** (1994), 513-521.
- (3) Anthony, C. and Ghosh, M.; *Current Science*, **72** (1997), 716-726.
- (4) Geerlof, A.; Rakels, J. J. L.; Straathof, A. J. J.; Heijnen, J. J.; Jongejan, J. A. and Duine, J. A.; *Eur. J. Biochem.*, **226** (1994), 537-546.
- (5) Matsushita, K.; Yakushi, T.; Toyama, H.; Adachi, O.; Miyoshi, H.; Tagami, E. and Sakamoto, K.; *Biochim. Biophys. Acta*, **1409** (1999), 154-164.
- (6) Anthony, C.; *Int. J. Biochem.*, **24** (1992), 29-39.
- (7) Dales, S. L. and Anthony, C.; *Biochem. J.*, **312** (1995), 261-265.
- (8) Schrover, J. M. J.; Frank, J.; van Wielink, J. E. and Duine, J. A.; *Biochem. J.*, **290** (1993), 123-127.
- (9) Matshushita, K.; Yamashita, Y.; Aoki, N.; Toyama, H. and Adachi, O.; *Biochemistry*, **38** (1999), 6111-6118.
- (10) Duine, J. A.; Frank, J. J. and Jongejan, J. A.; *Adv. Enzymol.*, **59** (1987), 169-212.
- (11) Anthony, C.; *Biochem. J.*, **320** (1996), 697-711.
- (12) Anthony, C.; *Biochem. Soc. Trans.*, **26** (1998), 413-417.
- (13) de Jong, G. A. H.; Geerlof, A.; Stoorvogel, J.; Jongejan, J. A.; de Vries, S. and Duine, J. A.; *Eur. J. Biochem.*, **230** (1995), 899-905.
- (14) Yasuda, M.; Cherepanov, A. and Duine, J. A.; *FEMS Microbiol. Lett.*, **138** (1996), 23-28.
- (15) Stigter, E. C. A.; Lugt, J. P. v. d. and Somers, W. A. C.; *J. Mol. Catal. B: Enzymatic*, **2** (1997), 291-297.
- (16) Matsushita, K.; Toyama, H. and Adachi, O.; *Adv. Microb. Physiol.*, **36** (1994), 247-301.
- (17) Frank, J. J.; van Krimpen, S. H.; Verwiël, P. E. J.; Jongejan, J. A.; Mulder, A. C. and Duine, J. A.; *Eur. J. Biochem.*, **184** (1989), 187-195.
- (18) Zheng, Y.-J. and Bruice, T. C.; *Proc. Natl. Acad. Sci. USA*, **94** (1997), 11881-11886.
- (19) Dewanti, A. R. and Duine, J. A.; *Biochemistry*, **39** (2000), 9384-9392.
- (20) Oubrie, A.; Rozeboom, H. J.; Kalk, K. H.; Duine, J. A. and Dijkstra, B. W.; *J. Mol. Biol.*, **289** (1999), 319-333.
- (21) Oubrie, A.; Rozenboom, H. J. and Dijkstra, B. W.; *Proc. Natl. Acad. Sci.*, **96** (1999), 11787-11791.
- (22) Jongejan, A.; Machado, S. S. and Jongejan, J. A.; *J. Mol. Catalysis B*, **8** (2000), 121-163.
- (23) Dekker, R. H.; Duine, J. A.; Frank, J. J.; Verwiël, J. P. E. and Westerling, J.; *Eur. J. Chem.*, **125** (1982), 69-73.
- (24) Ohshiro, Y. and Itoh, S.; In: "*Principles and applications of quinoproteins*", V. L. Davidson, Ed., Marcel Dekker, Inc: New York, 1993; pp 309-329.
- (25) Frank, J. J.; Dijkstra, M.; Duine, J. A. and Balny, C.; *Eur. J. Biochem.*, **174** (1988), 331-338.
- (26) Frank, J.; Dijkstra, M.; Balny, C.; Verwiël, P. E. J. and Duine, J. A.; In: "*PQQ and Quinoproteins*", J. A. Jongejan and J. A. Duine, Ed., Kluwer Academic Publishers: Dordrecht, 1989; pp 13-22.
- (27) Anthony, C.; *Adv. Microbial. Physiol.*, **27** (1986), 113-210.
- (28) Anthony, C. and Zatman, L. J.; *Biochem. J.*, **92** (1964), 614-627.
- (29) Bamforth, C. W. and Quayle, J. R.; *Biochem. J.*, **169** (1978), 677-686.
- (30) Duine, J. A.; Frank, J. and Westerling, J. A.; *Biochim. Biophys. Acta*, **524** (1978), 277-287.
- (31) Ghosh, R. and Quayle, J. R.; *Biochem. J.*, **199** (1981), 245-250.

- (32) Andres, J.; Moliner, V. and Krechl, J.; *Bioorganic Chemistry*, **22** (1994), 58-71.
- (33) Andres, J.; Moliner, V.; Domingo, L. R.; Picher, M. T. and Krechl, J.; *J. Am. Chem. Soc.*, **117** (1995), 8807-8815.
- (34) Richardson, I. W. and Anthony, C.; *Biochem. J.*, **287** ( Pt 3) (1992), 709-15.
- (35) Anthony, C.; Ghosh, M. and Blake, C. C. F.; *Biochem. J.*, **304** (1994), 665-674.
- (36) de Graauw, C. F.; Peters, J. A.; van Bekkum, H. and Huskens, J.; *Synthesis*, (1994), 1007-1017.
- (37) Sheldon, J. C.; Bowie, J. H.; Dua, S.; Smith, J. D. and O'Hair, R. A. J.; *J. Org. Chem.*, **62** (1997), 3931-3937.
- (38) McLean, A. D. and Chandler, G. S.; *J. Chem. Phys.*, **72** (1980), 5639-5648.
- (39) Eyring, H.; *J. Chem. Phys.*, **3** (1935), 107-115.
- (40) Truhlar, D. G.; Hase, W. L. and Hynes, J. T.; *J. Phys. Chem.*, **87** (1983), 2664-2682.
- (41) Truhlar, D. G.; Garrett, B. C. and Klippenstein, S. J.; *J. Phys. Chem.*, **100** (1996), 12771-12800.
- (42) Schmidt, M. W.; Baldrige, K. K.; Boatz, J. A.; Elbert, S. T.; Gordon, M. S.; Jensen, J. H.; Koseki, S.; Matsunaga, N.; Nguyen, K. A.; Su, S. J.; Windus, T. L.; Dupuis, M. and Montgomery Jr., J. A.; *J. Comput. Chem.*, **14** (1993), 1347-1363.
- (43) Fogarasi, G.; Zhou, X.; Taylor, P. W. and Pulay, P.; *J. Am. Chem. Soc.*, **114** (1992), 8191-8201.
- (44) Pulay, P.; Fogarasi, G.; Pang, F. and Boggs, J. E.; *J. Am. Chem. Soc.*, **101** (1979), 2550-2560.
- (45) Baker, J.; Kessi, A. and Delley, B.; *J. Chem. Phys.*, **105** (1996), 192-212.
- (46) Schaftenaar, G. and Noordil, J. H.; *J. Comput.-Aided Mol. Design*, **14** (2000), 123-134.
- (47) Bode, B. M. and Gordon, M. S.; *J. Mol. Graphics. Mod.*, **16** (1999), 133-138.
- (48) Ishida, T.; Doi, M.; Tomita, K.; Hayashi, H.; Inoue, M. and Urakami, T.; *J. Am. Chem. Soc.*, **111** (1989), 6822-6828.
- (49) van Koningsveld, H.; Jongejan, J. A. and Duine, J. A.; In; "*PQQ and Quinoproteins*", J. A. Jongejan and J. A. Duine, Ed., Kluwer Academic Publishers: Dordrecht, 1989; pp 243-251.
- (50) Xia, Z.-X.; He, Y.-N.; Dai, W.-W.; White, S. A.; Boyd, G. D. and Mathews, F. S.; *Biochemistry*, **38** (1999), 1214-1220.
- (51) Kano, K.; Mori, K.; Uno, B.; Kubota, T.; Ikeda, T. and Senda, M.; *Bioelectrochemistry and Bioenergetics*, **24** (1990), 193-201.
- (52) Ghosh, M.; Anthony, C.; Harlos, K.; Goodwin, M. G. and Blake, C.; *Structure*, **3** (1995), 177-187.
- (53) Itoh, S.; Ogino, M.; Fukui, Y.; Murao, H.; Komatsu, M.; Ohshiro, Y.; Inoue, T.; Kai, Y. and Kasai, N.; *J. Am. Chem. Soc.*, **115** (1993), 9960-9967.
- (54) Jongejan, J. A.; Groen, B. W. and Duine, J. A.; In; "*PQQ and Quinoproteins*", J. A. Jongejan and J. A. Duine, Ed., Kluwer Academic Publishers: Dordrecht, 1989; pp 205-216.
- (55) Duine, J. A.; Frank, J. J. and Verwiel, P. E. J.; *Eur. J. Biochem.*, **118** (1981), 395-399.
- (56) Ribbons, D. W.; Harrison, J. E. and Wadzinski, A. M.; *Ann. Rev. Microbiol.*, **24** (1970), 135-158.
- (57) Suzuki, K.; Yasuda, M. and Yamasaki, K.; *J. Phys. Chem.*, **61** (1957), 229.
- (58) Dwyer, F. P. and Mellor, D. P.; *Chelating agents and metal chelates*; Academic Press: New York, 1964.
- (59) Suzuki, S.; Sakurai, T.; Itoh, S. and Oshiro, Y.; *Inorg. Chem.*, **27** (1988), 591-592.
- (60) Suzuki, S.; Sakurai, T.; Itoh, S. and Oshiro, Y.; *Nippon Kagaku Kaishi*, (1988), 421-424.
- (61) Suzuki, S.; Sakurai, T.; Itoh, S. and Oshiro, Y.; *Chem. Lett.*, (1988), 777-780.
- (62) Siegbahn, P. E. M.; *J. Am. Chem. Soc.*, **120** (1998), 8417-8429.
- (63) Lyne, P. D.; Hodoscek, M. and Karplus, M.; *J. Phys. Chem. A*, **103** (1999), 3462-3471.

- (64) Nara, M.; Torii, H. and Tasumi, M.; *J. Phys. Chem.*, **100** (1996), 19812-19817.
- (65) Pavlov, M.; Siegbahn, P. E. M. and Sandström, M.; *J. Phys. Chem. A*, **102** (1997), 219-228.
- (66) Remko, M.; Liedl, K. R. and Rode, B. M.; *J. Phys. Chem. A*, **102** (1998), 771-777.
- (67) Williams, I. H.; Miller, A. B. and Maggiora, G. M.; *J. Am. Chem. Soc.*, **112** (1990), 530-537.
- (68) Olsthoorn, A. J. J. and Duine, J. A.; *Biochemistry*, **37** (1998), 13854-13861.
- (69) Goodwin, M. G. and Anthony, C.; *Biochem. J.*, **318** (1996), 673-679.
- (70) Oubrie, A.; Rozenboom, H. J.; Kalk, K. H.; Olsthoorn, A. J. J.; Duine, J. A. and Dijkstra, B. W.; *EMBO J.*, **18** (1999), 5187-5194.
- (71) Duine, J. A. and Frank, J. J.; *Biochem. J.*, **187** (1980), 213-219.
- (72) Zheng, Y.-J.; Xia, Z.-X.; Chen, Z.-W.; Mathews, F. S. and Bruice, T. C.; *Proc. Natl. Acad. Sci. USA*, **98** (2001), 432-434.
- (73) Xia, Z.-X.; Dai, W.-W.; Zhang, Y.-F.; White, S. A.; Boyd, G. D.; Mathews, F. S.; *J. Mol. Biol.*, **259** (1996), 480-501.
- (74) Keitel, T.; Diehl, A.; Knaute, T.; Stezowski, J. J.; Höhne, W.; Görisch, H. *J. Mol. Biol.*, **297** (2000), 961-974.

# Deuterium Isotope Effect on Enantioselectivity in the *Comamonas testosteroni* QH-ADH-catalyzed Kinetic Resolution of *rac*-Solketal

Aldo Jongejan, Jaap A. Jongejan and Wilfred R. Hagen

---

## Abstract

Isotopic substitution provides an effective tool to probe the mechanism of enzyme-catalyzed reactions. To our knowledge, kinetic isotope effects on the enantioselectivity of enzymes have not been reported. We investigated the effect of deuterium-substitution on the enantiomeric ratio,  $E$ , of PQQ-containing quinoxinoprotein alcohol dehydrogenase, QH-ADH, from *Comamonas testosteroni* in the ferricyanide-coupled kinetic resolution of *rac*-2,2-dimethyl-4-hydroxymethyl-1,3-dioxolane, solketal. Under otherwise identical conditions, we measured  $E = 30$  for solketal and  $E = 6$  for *rac*-2,2-dimethyl-4-[1,1- $^2\text{H}$ ]hydroxymethyl-1,3-[5,5,4- $^2\text{H}$ ]dioxolane,  $d_5$ -solketal. It is proposed that isotopic substitution affects the relative kinetic weights of the initial hydron/deuteron transfer from substrate to cofactor and the subsequent proton/deuteron shift in the cofactor-product complex. The latter step is becoming more important in the deuterated complex to the extent that the enantiomer discrimination in the first step is partially overruled.

**Key words**

kinetic resolution / enantioselectivity / pyrroloquinoline quinone / solketal /  
quinoxaline alcohol dehydrogenase / deuterium kinetic isotope effects /  
*Comamonas testosteroni*



## Introduction

Enzyme-catalyzed kinetic resolution has proven to be a powerful method for enantioselective synthesis [1-3]. Both practical and fundamental aspects of the enantioselective performance of enzymes have been explored. Extensive documentation of the effects of (co)solvents [4-8], temperature [9-12], (surface)pressure [13-16], substrate modification [9, 17, 18], added salts [19-22], pH [23, 24], and catalyst formulation [25] can be found in the literature. Whereas kinetic isotope effects provide an effective tool to probe the mechanism of enzyme-catalyzed reactions [26-29], explicit investigations of the effects of isotopic substitution of the substrate on the enantioselectivity of enzymes have not yet been reported.

For catalytic, non-enzymatic, kinetic resolution reactions obeying Arrhenius-type equations:  $k = A \exp(-\Delta\varepsilon_{\text{TS-RS}}/RT)$ , with  $\Delta\varepsilon_{\text{TS-RS}}$  the energy difference including zero point energies of the transition state, TS, and reactant state, RS, respectively, primary deuterium kinetic isotope effects (KIEs) are not expected to affect the enantioselectivity. With enantiomeric reactants, *R* and *S*, in isotropic media, assuming pre-exponential factors to be equal and  $\Delta_{\text{D-H}}\text{ZPE}_{\text{RS}}^{\text{R}} = \Delta_{\text{D-H}}\text{ZPE}_{\text{RS}}^{\text{S}}$ ,  $(k^{\text{R}}/k^{\text{S}})_{\text{D}} = (k^{\text{R}}/k^{\text{S}})_{\text{H}}$  follows from  $\Delta_{\text{D-H}}\text{ZPE}_{\text{TS}}^{\text{R}} \approx \Delta_{\text{D-H}}\text{ZPE}_{\text{TS}}^{\text{S}}$  (Figure 1). Indeed, only minor effects on enantioselectivity,  $(k^{\text{R}}/k^{\text{S}})_{\text{H}} = 4.2$ ;  $(k^{\text{R}}/k^{\text{S}})_{\text{D}} = 4.5$ , have been reported for enantiomer-dependent kinetic isotope effects in the (+)-(-8*R*,9*S*)-dihydro-quinidine-catalyzed (non-enzymatic) 1,3-hydride transfer reaction of 1-methylindenes, with primary deuterium KIEs ranging from 5.71 (*S*) to 6.46 (*R*) [30].

For enzyme-catalyzed kinetic resolutions, an intrinsically more complex situation applies. Several kinetic barriers involved in the formation of intermediate (Michaelis) complexes and products contribute to the enantioselectivity. Previously, we showed that the enantiomeric ratio, *E*-value [31], equals the ratio of the sums of the exponentiated barrier contributions relative to the ground state [11, 32] (Figure 2). Despite the 'shared control', differentiation into 'enantioselectivity determining' and 'rate determining' barriers along the reaction coordinate may be opportune [32, 33]. Notably, when isotopic substitution of the substrate enantiomers changes the relative contribution of the individual barriers, effects on the *E*-value can be expected.

Alcohol dehydrogenases containing pyrroloquinoline quinone, 2,7,9-tricarboxy-1*H*-pyrrolo[2,3-*f*]quinolin-4,5-dione, PQQ, and  $\text{Ca}^{2+}$  have been isolated from several sources

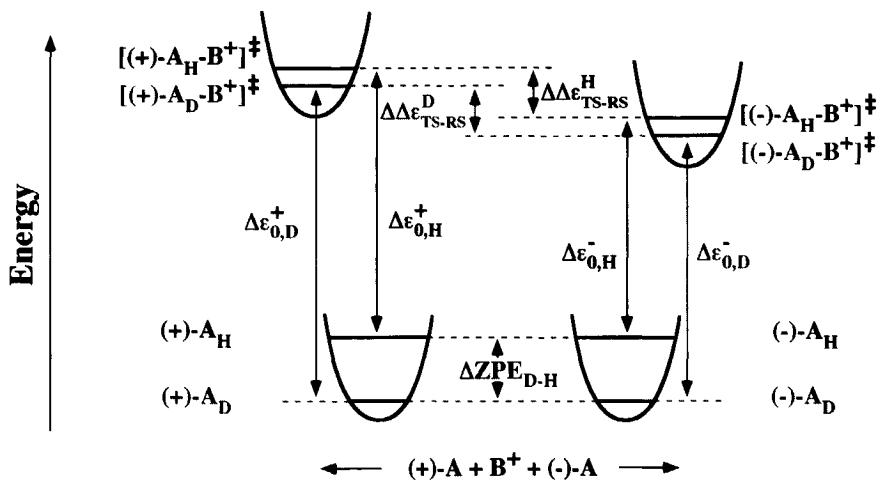


**Figure 1.** Energy diagram summarizing the contribution of kinetic isotope effects in a non-enzymatic enantioselective reaction. (+)- $A_{H/D}$ , (-)- $A_{H/D}$ , reactant enantiomers;  $B^+$ , chiral catalyst;  $\Delta ZPE_{D-H}$ , zero-point energy difference of substrate-H and substrate-D ground states;  $\Delta\Delta\epsilon_{TS-RS}(H)$  and  $\Delta\Delta\epsilon_{TS-RS}(D)$ , activation energy differences of (+)- and (-)-reactants. Adapted from Ref. [30].

[34]. Quinohemoprotein alcohol dehydrogenases, QH-ADHs, contain an additional heme *c* [35, 36]. A high-resolution crystal structure of QH-ADH from *Comamonas testosteroni* has recently been described [37]. The enzyme catalyzes the ferricyanide-coupled oxidation of various alcohols and aldehydes to the corresponding aldehyde and carboxylic acid, respectively, following ping-pong kinetics [38]. *C. testosteroni* QH-ADH has been shown to be a highly enantioselective catalyst for the kinetic resolution of chiral alcohols [32, 39]. Considering the proposed mechanism of action, featuring the intermediate formation of a hydroxy-ketone form of PQQ and subsequent rearrangement to PQQH<sub>2</sub> [32, 37, 40, 41] (Scheme 1), QH-ADH is an attractive target to investigate the effect of isotopic substitution on enzyme enantioselectivity.

## Materials and Methods

QH-ADH (apo-form) from *C. testosteroni* was isolated and purified as described [38]. Upon reconstitution with PQQ in the presence of  $Ca^{2+}$  fully active holoenzyme was obtained ( $k_{cat}$  (ethanol) = 17.5 s<sup>-1</sup>,  $K_M$ (ethanol) = 2.2 mM,  $\epsilon_{416}(\text{red}) = 160,000 \text{ M}^{-1}\text{cm}^{-1}$  [42]).

$$E_{R,S}^H = \frac{\exp(\epsilon_1^S) + \exp(\epsilon_2^S) + \exp(\epsilon_3^S)}{\exp(\epsilon_1^R) + \exp(\epsilon_2^R) + \exp(\epsilon_3^R)} \quad E_{R,S}^D = \frac{\exp(\epsilon_1^S) + \exp(\epsilon_2^S) + \exp(\epsilon_3^S)}{\exp(\epsilon_1^R) + \exp(\epsilon_2^R) + \exp(\epsilon_3^R)}$$

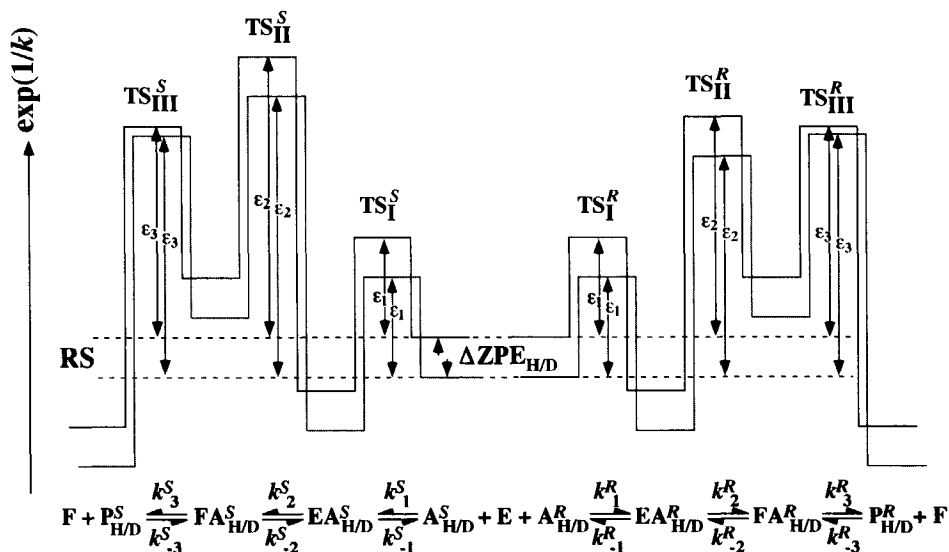
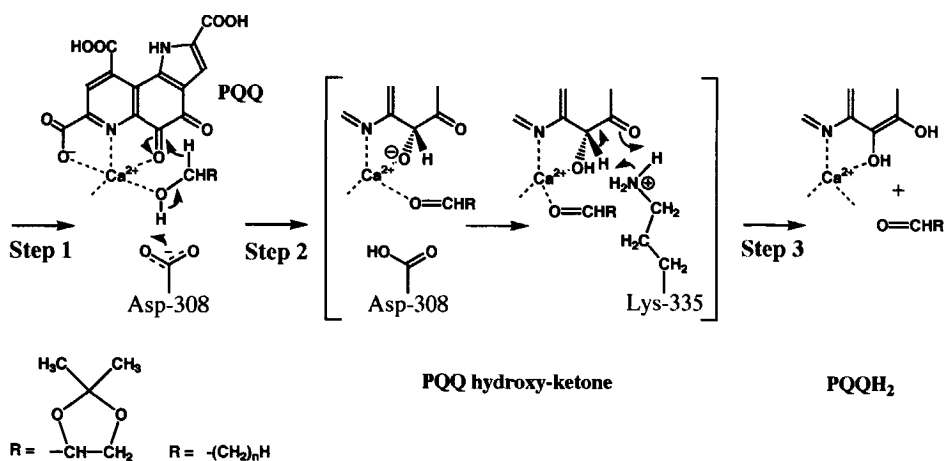


**Figure 2.** Kinetic profile of the initial steps of a bi-bi ping-pong scheme for an enzyme-catalyzed kinetic resolution of a chiral substrate. To emphasize the general features of the profile, kinetic barriers are plotted as 'exp(1/k)' along the reaction coordinate. When the relations that can be derived from Eyring TST (thermodynamic format) hold, there is a one-to-one correspondence between exp(1/k) and  $\Delta G_{TS-RS}^\ddagger$  (the activation free energy difference). Less stringent conditions hold for the *E*-value relations, where pre-exponential factors tend to cancel.  $\Delta ZPE_{H/D}$  represent the zero-point energy difference of H/D-substrate enantiomers in the reactant state, RS. For the choice of transition state ZPEs, and the introduction of an isomerisation step, see text.

(*R*)-(-)-, (*S*)-(+)- and (*R,S*)-Solketal were purchased from Janssen Chimica. *rac*-2,2-Dimethyl-4-[1,1-<sup>2</sup>H]hydroxymethyl-1,3-[5,5,4-<sup>2</sup>H]dioxolane was synthesized from *d*<sub>6</sub>-glycerol (Sigma) and acetone following literature procedures [43]. Inspection of the <sup>1</sup>H-NMR and mass spectra showed the product to be deuterated as expected except for the alcohol function which contained <sup>1</sup>H as a result of exchange during work-up. Chemical purity of the reaction product was confirmed using chiral GC (Chiraldex G-TA, Astec, Whippany, N.J.) [44].



**Scheme 1.** Mechanism of the reductive half-reaction of the QH-ADH-catalyzed oxidation of alcohols. Formation of the Michaelis complex (Step 1) is followed by base-catalyzed hydride transfer from the substrate to PQQ-C5 (Step 2). Rearrangement (possibly: lysine-catalyzed tautomerization, Step 3) of the intermediate hydroxy-ketone produces PQQH<sub>2</sub> and the first product (aldehyde). PQQH<sub>2</sub> is reoxidized by electron acceptor in the oxidative half-reaction

(S)-*d*<sub>5</sub>-Solketal was prepared by QH-ADH-catalyzed kinetic resolution of *rac-d*<sub>5</sub>-solketal in a pH-stat system (Methrom) equipped with a stirred reaction vessel, thermostatted at 25° C. Wet cells of ethanol-induced *C. testosteroni* (3.3 g) were suspended in 15 mL 10 mM Tris/HCl, pH 7.5, containing 2.5 g of ferricyanide. PQQ (9 mM, 120 μL) was added and the cells were left to equilibrate at room temperature (1 hr) before addition of 1.37 g (10 mmol) of *rac-d*<sub>5</sub>-solketal. The reaction was monitored by the addition of 1 M NaOH. After 85% conversion the mixture was extracted with diethyl ether and dried over anhydrous MgSO<sub>4</sub>. The solution was filtered and the solvent removed by evaporation under reduced pressure to yield 111 mg (S)-*d*<sub>5</sub>-solketal (8%). The reaction product was analyzed using <sup>1</sup>H-NMR and MS. The chemical and chiral purity (> 98%) was checked by chiral GC.

Initial reaction rates were determined spectrophotometrically by monitoring the reduction of ferricyanide ( $\Delta\epsilon_{420} = 1020 \text{ M}^{-1}\text{cm}^{-1}$ ) at 25° C in a 1-cm cuvette containing 10 mM MOPS/KOH, pH 7.5, 5 mM CaCl<sub>2</sub>, 1 mM ferricyanide, and a fixed amount of holo-enzyme. The reactions were started by the addition of (enantiomer mixtures of) substrate alcohols.

## Results and discussion

The kinetic resolution of solketal by QH-ADH from *C. testosteroni* has been described [38]. Using the method of initial rates on a range of enantiomer mixtures at otherwise fixed conditions [45], we found  $E_H = 30 \pm 2$ , in good agreement with published results (Figure 3). Applying the same method to determine the  $E$ -value for the oxidation of 2,2-dimethyl-4-[1,1- $^2\text{H}$ ]hydroxymethyl-1,3-[5,5,4- $^2\text{H}$ ]dioxolane,  $d_5$ -solketal, required the synthesis of the enantiomerically-enriched compound. This was accomplished by the condensation of  $d_8$ -glycerol and acetone to give racemic  $d_5$ -solketal, part of which was resolved by selective oxidation of the (*R*)-enantiomer using *C. testosteroni* (whole cells). Measuring initial rates under otherwise identical conditions showed a substantial decrease of the enantioselectivity,  $E_D = 6 \pm 1$ , for the deuterated solketal (Figure 3).

The contribution of microscopic kinetic constants to the  $E$ -value is described by the defining equation,  $E = (k_{cat}/K_M)_R / (k_{cat}/K_M)_S$  [31], or by the equivalent 'translation' into an exponential format [11] (Eqns in Figure 2). Using either representation, it is straightforward to show that kinetic isotope effects are *not* expected to affect the enantioselectivity if: full (classical) primary isotope effects are operative in each and every step to which these kinetic constants apply. In this respect, the current finding represents a remarkable result, indicating that one or more of these restrictions is not met. Probable causes could be: (a) the occurrence of different mechanisms for the oxidation of the enantiomeric substrates or, (b) different (primary) isotope effects for the corresponding steps leading to a redistribution of the relative importance of the individual steps for the  $E$ -value. The occurrence of different mechanistic schemes has been proposed for the hydrolysis of (*R*)- and (*S*)-styrene oxide by the epoxide hydrolase from *Agrobacterium radiobacter* AD1 [46]. In view of our earlier observation that the active site topology of QH-ADH, as deduced from a homology model, would support the accommodation both (*R*)- and (*S*)-*sec*-alcohols depending on whether the alcohol ligates to the calcium site or forms a hemiketal with the PQQ-C5 carbonyl function [47], this would be a possibility.

However, since it is observed (Figure 3) that the decrease in  $E$  results mainly from a lower oxidation rate of the faster-reacting (*R*)-enantiomer, whereas that of the slower reacting (*S*)-enantiomer is hardly affected, we investigated a scenario where isotopic substitution leads to a different distribution of the relative importance of kinetic barriers along the reaction coordinate.

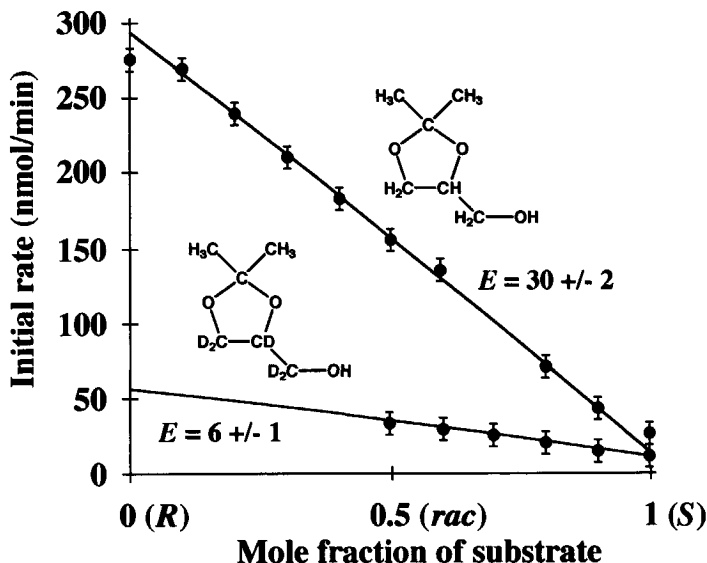


**Figure 3.** Initial rates of QH-ADH-catalyzed oxidations of solketal (upper trace), and  $d_5$ -solketal (lower trace) as a function of the chiral composition of the substrate mixture under otherwise identical conditions. Solid lines represent simulated values according to  $E = \frac{r_R(r_S - r_x) - x}{r_S(r_x - r_x)1 - x}$  with  $r_R$ ,  $r_S$ ,  $r_x$ , the initial enzyme-catalyzed reaction rates for mixtures of solketal and mixtures of  $d_5$ -solketal of mole fraction  $x = 0$ ,  $x = 1$ , and  $x = x$ , respectively

The mechanism of alcohol oxidation by PQQ-containing enzymes has been extensively studied for methanol dehydrogenases, MDHs (for review see [32]), and (soluble) glucose dehydrogenase, sGDH [48]. Despite considerable differences in substrate specificity and turn-over rates, (probably) diffusion-limited formation of a Michaelis complex (Scheme 1, Step 1), base-catalyzed proton abstraction in concert with direct hydride transfer from the substrate to the C5 position of PQQ (Step 2), and subsequent tautomerization of the hydroxy-keto-PQQ intermediate to PQQH<sub>2</sub> (Step 3), seems to be the consensus mechanism of the reductive branch of the reaction. In particular, the similarity of the alcohol oxidation mechanisms for MDH and QH-ADH is supported by the conservation of the catalytic machinery [37].

The identification of three kinetic barriers (Steps 1 - 3) in the reductive branch of the catalytic reaction, in combination with the Eyring TST equation (thermodynamic format),  $k = k_B T / h \cdot \exp\{-\Delta G^\ddagger / RT\}$ , allows a unique assignment of the individual barrier heights

if additional assumptions for the diffusional barrier and the contributions of kinetic isotope effects are incorporated. As a numerical exercise we calculated the barrier heights (Figure 2) assuming  $k_t^{R,S} = 10^8 \text{ s}^{-1}$  (diffusional  $k_{on}$  [49]), and  $\Delta_{D-H}\Delta G_{TS-III}^\ddagger = 5.15 \text{ kJ.mol}^{-1}$  (deuterium KIE of factor 8 at 298 K). Highly satisfactory agreement with the experimental findings is obtained for the following combination:

$$E_H = \frac{\exp(11.04) + \exp(22.95) + \exp(19.16)}{\exp(11.04) + \exp(18.47) + \exp(19.16)} = 30.1$$

$$E_D = \frac{\exp(11.04) + \exp(22.95) + \exp(21.24)}{\exp(11.04) + \exp(18.47) + \exp(21.24)} = 6.1$$

where we have assumed a full deuterium KIE ( $\Delta ZPE/RT = 2.08$  at  $T = 298 \text{ K}$ ) to occur in Step 3 only. For the magnitude of the leading terms, advantage was taken of the fact that at least one of the exponentials should be close to (but not exceeding) the  $\Delta G^\ddagger/RT$  value calculated from  $k_{sp}^R = 19.27 * 10^3 \text{ s}^{-1} \text{ M}^{-1} \Rightarrow \Delta G^\ddagger/RT = 19.59$  (for the denominator), and  $k_{sp}^S = 0.64 * 10^3 \text{ s}^{-1} \text{ M}^{-1} \Rightarrow \Delta G^\ddagger/RT = 23.0$  (for the numerator), the values of the specificity constants for the conversion of solketal at  $T = 298 \text{ K}$  [38].

In order to explore the feasibility of these assumptions, we calculated  $ZPE_{TS} - ZPE_{RS}$  at the STO-3G(d) level of theory for the deuteride-transfer step (Fig 2,  $TS_{II}$ ) using the transition state configuration deduced for the oxidation of methanol by MDH [50]. Partition functions were computed using Gamess-US. We found  $\Delta ZPE/RT = 0.83$ , suggesting that this barrier contributes a factor of slightly over 2 to the deuterium KIE. This result is supported by experimental data for the QH-ADH-catalyzed oxidation of deuterated ethanol,  $C_2D_5OH$ , where we found a KIE of 2 (data not shown). Even more convincing, early work on the oxidation of methanol by MDH from *Hyphomicrobium* X [51] showed that a deuterium KIE of approx. 8 for the oxidation of  $CD_3OH$  in the absence of ammonia, is reduced to only 1.5 in its presence.

These results seem to indicate that the tautomerisation reaction (Step 3), which in the case of QH-ADH does not require the addition of ammonia probably because of the presence of a residue, Lys335, that is suitably oriented for catalysis [37, 47], carries most of the deuterium KIE. In order for this step to be incorporated into the equations that relate the  $E$ -value and the kinetic barriers, we have to assume that product release takes

place after, or at least concomitantly with, the tautomerisation. A possible mechanism for this step is included in Figure 3.

### Conclusions

Analysis of the contributions of the catalytic steps of the *C. testosteroni* QH-ADH-catalyzed kinetic resolution of (deuterated) solketal to the *E*-value suggests that the relative importance of the kinetic barriers shifts from the hydride-transfer step (for solketal) to the tautomerisation step (for  $d_5$ -solketal). An important prerequisite for this interpretation to hold is that the release of the first product (aldehyde) forms part of the reductive branch of the kinetic scheme.

We can not discard the possibility that the lower *E*-value results (in part) from secondary isotope effects, however, in view of the marginally higher steric demands of the deuterium-labeled solketal, the fact that the chiral center is not directly involved in the oxidation reaction, and the matching decrease of overall rate and enantioselective performance, this appears unlikely.

It should be emphasized that even though the present finding falls onto a long line of negative effects on enantioselectivity, beneficial effects of isotopic substitution may well be observed for enzymatic reactions that perform near the diffusion limit. For such systems, increasing the enantioselectivity-determining barrier relative to the diffusion-related barrier could, in principle, raise the enantioselectivity at the expense of the overall rate, exemplifying the intuitive notion that 'slower processes allow better selectivity'. Although, the introduction of deuterium in the substrate (*i.e.* deuteration of the  $\alpha$ -position only) could afford the non-isotopically substituted product of interest, it is doubtful whether such a strategy would have any merits.



## References

- (1) Benkovic, S.J. and Ballesteros, A. (1997) *TIBTECH* **15**, 385-386.
- (2) Sheldon, R.A. (1996) *J. Chem. Tech. Biotechnol.*, **67**, 1-14.
- (3) Johnson, C.R. (1998) *Acc. Chem. Res.* **31**, 333-341.
- (4) Wescott, C.R. and Klibanov, A.M. (1994) *Biochim. Biophys. Acta*, **1206**, 1-9.
- (5) Jongejan, J.A.; van Tol, J.B.A. and Duine, J.A. (1994) *ChimicaOggi*, 15-24.
- (6) Carrea, G.; Ottolina, G. and Riva, S. (1995) *TIBTECH* **13**, 63-70.
- (7) van Tol, J.B.A.; Stevens, R.M.M.; Veldhuizen, W.J.; Jongejan, J.A. and Duine, J.A. (1995) *Biotechnol. Bioeng.* **47**, 71-81.
- (8) Wolff, A.; Zhu, L.; Wong, Y.W.; Straathof, A.J.J.; Jongejan, J.A. and Heijnen, J.J. (1998) *Biotechnol. Bioeng.* **62**, 125-134.
- (9) Pham, V.T. and Phillips, R.S. (1990) *J. Am. Chem. Soc.* **112**, 3629-3632.
- (10) Phillips, R.S. (1996) *TIBTECH* **14**, 13-16.
- (11) Anthonen, T. and Jongejan, J.A. (1997) *Methods Enzymol.* **286**, 473-495.
- (12) Overbeeke, P.L.A.; Ottosson, J.; Hult, K.; Jongejan, J.A. and Duine, J.A. (1999) *Biocatal. Biotransform.* **17**, 61-79.
- (13) Rogalska, E.; Ransac, S. and Verger, R. (1993) *J. Biol. Chem.* **268**, 792-794.
- (14) Kamat, S.V.; Beckman, E.J. and Russell, A.J. (1993) *J. Am. Chem. Soc.* **115**, 8845-8846.
- (15) Fantin, G.; Fogagnolo, M.; Guerzoni, M.E.; Lanciotti, R.; Medici, A.; Pedrini, P. and Rossi, D. (1996) *Tetrahedron: Asymmetry* **7**, 2879-2887.
- (16) De Crescenzo, G.; Ducret, A.; Trani, M. and Lortie, R. (2000) *J. Mol. Catal. B: Enzymatic* **9**, 49-56.
- (17) Öhrner, N.; Martinelle, M.; Mattson, A.; Norin, T. and Hult, K. (1994) *Biocatalysis* **9**, 105-114.
- (18) Hoff, B.H.; Anthonen, H.W. and Anthonen, T. (1996) *Tetrahedron: Asymmetry* **7**, 3187-3192.
- (19) Ke, T.; Rariy, R.V.; Schmidtke, J.L. and Klibanov, A.M. (1999) *Biocatal. Biotransform.* **17**, 81-93.
- (20) Ke, T. and Klibanov, A.M. (1999) *J. Am. Chem. Soc.* **121**, 3334-3340.
- (21) Shin, J.-S.; Luque, S. and Klibanov, A.M. (2000) *Biotechnol. Bioeng.* **69**, 577-583.
- (22) Hsu, W.-T. and Clark, D.S. (2001) *Biotechnol. Bioeng.* **73**, 231-237.
- (23) Keinan, E.; Hafeli, E.K.; Seth, K.K. and Lamed, R. (1986) *J. Am. Chem. Soc.* **108**, 162-169.
- (24) Secundo, F. and Phillips, R.S. (1996) *Enzyme Microb. Technol.* **19**, 487-492.
- (25) Secundo, F.; Carrea, G.; Soregaroli, C.; Varinelli, D. and Morrone, R. (2001) *Biotechnol. Bioeng.* **73**, 157-163.
- (26) Cleland, W.W. (1976) *Isotope effects on enzyme-catalyzed reactions*, University Park Press, Baltimore.
- (27) Cook, P.F. (1990) *Enzyme mechanisms from isotope effects*, CRC Press, Boca Raton, FL.
- (28) Adams, K.A.H.; H., C.S. and Klibanov, A.M. (1990) *J. Am. Chem. Soc.* **112**, 9418-9419.
- (29) Rucker, J. and Klinman, J.P. (1999) *J. Am. Chem. Soc.* **121**, 1997-2006.
- (30) Aune, M.; Bergson, G. and Matsson, O. (1995) *J. Phys. Org. Chem.* **8**, 400-406.
- (31) Chen, C.S.; Fujimoto, Y.; Girdaukas, G. and Sih, S.J. (1982) *J. Am. Chem. Soc.* **104**, 7294-7299.
- (32) Jongejan, A.; Machado, S.S. and Jongejan, J.A. (2000) *J. Mol. Catal. B: Enzymatic* **8**, 121-163.
- (33) Jongejan, A.; Machado, S.S. and Jongejan, J.A. (2001) *J. Mol. Catal. B: Enzymatic* **13**, 57.
- (34) Anthony, C. (1998) *Biochem. Soc. Trans.* **26**, 413-417.
- (35) Groen, B.W.; Frank, J.J. and Duine, J.A. (1986) *Biochem. J.* **223**, 921-924.

- (36) Matsushita, K.; Toyama, H. and Adachi, O. (1994) *Adv. Microb. Physiol.* **36**, 247-301.
- (37) Oubrie, A.; Rozeboom, H.J.; Kalk, K.H.; Huizinga, E.G. and Dijkstra, B.W. (2002) *J. Biol. Chem.* **277**, 3727-3732.
- (38) Geerlof, A.; Rakels, J.J.L.; Straathof, A.J.J.; Heijnen, J.J.; Jongejan, J.A. and Duine, J.A. (1994) *Eur. J. Biochem.* **226**, 537-546.
- (39) Geerlof, A.; van Tol, J.B.A.; Jongejan, J.A. and Duine, J.A. (1994) *Biosci. Biotech. Biochem.* **58**, 1028-1036.
- (40) Anthony, C.; Ghosh, M. and Blake, C.C.F. (1994) *Biochem. J.* **304**, 665-674.
- (41) Zheng, Y.-J.; Xia, Z.-X.; Chen, Z.-W.; Mathews, F.C. and Bruice, T.C. (2001) *Proc. Natl. Acad. Sci. USA* **98**, 432-434.
- (42) de Jong, G.A.H.; Geerlof, A.; Stoorvogel, J.; Jongejan, J.A.; de Vries, S. and Duine, J.A. (1995) *Eur. J. Biochem.* **230**, 899-905.
- (43) Lorette, N.B. and Howard, W.L. (1973) in *Organic Synthesis* (Baumgarten, H.E., ed.), Vol. Coll. Vol. 5, pp. 5-7, Wiley & Sons, New York.
- (44) Geerlof, A.; van Tol, J.B.A.; Jongejan, J.A. and Duine, J.A. (1993) *J. Chromatogr.* **648**, 119-129.
- (45) Jongejan, J.A.; van Tol, J.B.A.; Geerlof, A. and Duine, J.A. (1990) in *5th European Congress on Biotechnology* (Christiansen, C., Munck, L. and Villadsen, J., eds.), Vol. III, pp. 268, Munksgaard Intl. Publisher, Copenhagen.
- (46) Rink, R. and Janssen, D.B. (1998) *Biochemistry* **37**, 18119-18127.
- (47) Jongejan, A.; Jongejan, J.A. and Duine, J.A. (1998) *Protein Engineering* **11**, 185-198.
- (48) Dewanti, A.R. and Duine, J.A. (2000) *Biochemistry* **39**, 9384-9392.
- (49) Job, D.; Jones, P. and Dunford, H.B. (1993) *J. Phys. Chem.* **97**, 9259-9262.
- (50) Jongejan, A.; Jongejan, J.A. and Hagen, W.R. (2001) *J. Comput. Chem.* **22**, 1732-1749.
- (51) Frank, J.; Dijkstra, M.; Balny, C.; Verwiël, P.E.J. and Duine, J.A. (1989) in *PQQ and Quinoproteins* (Jongejan, J.A. and Duine, J.A., eds.), pp. 13-22, Kluwer Academic Publishers, Dordrecht.

# Summary

---

The present-day combination of quantum theory and computing power has opened the possibility to investigate (bio)chemically interesting systems *in silico*. A selection of successes and failures has been collected in Chapter 1. It is concluded that the accuracy of the prediction of various properties of small molecules using computational techniques is still increasing steadily, up to the point where chemically accepted values are within reach. Application to enzyme catalysis is, however, still hampered by the size of the systems. Examples involving the calculation of binding affinities, electron transfer, and reaction rates are provided. The quinohemoprotein alcohol dehydrogenase (QH-ADH) from *Comamonas testosteroni* is introduced as a suitable target for further investigations using computational methods.

Alcohol dehydrogenases containing pyrroloquinoline quinone (2,7,9-tricarboxy-1*H*-pyrrolo[2,3,*f*]quinoline-4,5-dione, PQQ) as an organic cofactor are of fundamental and practical interest. The quinoprotein methanol dehydrogenases, MDHs, from methylotrophic organisms have been particularly well studied. However, much less is known of the quinohemoprotein alcohol dehydrogenases (containing PQQ, Ca<sup>2+</sup> and heme *c*), of which the QH-ADH from *C. testosteroni* is an example. In Chapter 2 the current status of this field is reviewed. Attention is given to the structural and mechanistic features involved in the catalytic action of these enzymes. Proposed mechanistic schemes are discussed. Considering available experimental evidence, two mechanisms are highlighted: 1) formation of a covalent, hemiketal adduct at the PQQ-C(5) position and 2) direct hydride transfer of the substrate  $\alpha$ -hydrogen to the PQQ-C(5) position promoted by the nearby Ca<sup>2+</sup>-ion.

Applying various molecular modeling approaches and a combination of energetic and geometric criteria, the intermediate calcium-alcohol complex involved in the direct hydride transfer reaction is concluded to offer a better explanation for the observed enantioselectivity than does the PQQ-C(5) adduct.

The construction of a homology-based model of the QH-ADH from *C. testosteroni* is described in Chapter 3. Although the sequence identity is low, related methanol dehydrogenases have been used as templates for the catalytically active PQQ-domain. A crude model of the covalently bound cytochrome *c* domain could be build using the minimal sequence homology with cytochromes *c* for which structural information was available at the time. Emphasis is on locating the position of this domain relative to the PQQ-domain with regard to electron transfer properties.

Results of the investigations regarding the reaction mechanism of quinohemoprotein alcohol dehydrogenases are described in Chapter 4. The mechanism involving direct hydride transfer is studied by calculation of the reaction of PQQ and various PQQ-derivatives with methanol using moderate to high level *ab initio* theory. All possible intermediate states are calculated and the Transition State for the reaction between PQQ and methanol in the presence of calcium is located. Although the absolute value for the energetic barrier calculated in this way is too high, direct hydride transfer from the substrate  $\alpha$ -hydrogen to the PQQ-C(5) position appears to be a likely reaction mechanism.

Chapter 5 describes the use of isotopes to probe the enzyme-catalyzed reaction. For the first time kinetic isotope effects (KIEs) on the enantioselectivity of an enzyme are reported. To investigate the actual reaction mechanism of QH-ADH from *C. testosteroni* the effects on the enantiomeric ratio, *E*, in the ferricyanide-coupled kinetic resolution *rac*-2,2-dimethyl-4-hydroxymethyl-1,3-dioxolane (solketal) is measured. The observed difference in *E*-values for the non-deuterated and deuterated form of solketal, *E* = 30 vs. *E* = 6, respectively, is rationalized by assuming different relative kinetic weights of the initial hydron/deuteron transfer from substrate to cofactor and the subsequent proton/deuteron shift in the cofactor-product complex. In case of the deuterated complex, this latter step seems to partially overrule the enantiomeric discrimination in the first step.

At the start of this research, knowledge of the three-dimensional structure of QH-ADHs was not available. In view of the large body of experimental observations, and especially the elucidation of the primary sequence of the QH-ADH from *C. testosteroni*, a computational strategy was adopted to construct a 3D model using homology modeling

protocols. Recently, a high resolution X-ray structure of the QH-ADH from *C. testosteroni* became available. A comparison of the homology model of QH-ADH with the elucidated X-ray structure is included in Chapter 1. It is rewarding to see that the major structural features were predicted correctly. More importantly, it appears that with this new information the computational techniques that have been explored and developed in this thesis can now provide more reliable guidelines to interpret the available experimental data. This may well lead to a better understanding of the electronic and kinetic properties of this intriguing and fascinating enzyme and of biocatalysts of similar complexity.

*Summary*

---

# Samenvatting

---

De combinatie van quantum theorie en rekenkracht van de huidige computer maakt het mogelijk interessante (bio)chemische systemen *in silico* te bestuderen. Een selectie van successen en mislukkingen is verzameld in Hoofdstuk 1. Geconcludeerd kan worden dat de nauwkeurigheid van de rekenmethoden wat betreft het voorspellen van de eigenschappen van kleine moleculen gestaag toeneemt en de grens nadert waarop voorspellingen met chemische nauwkeurigheid kunnen worden verricht. Bij het toepassen van deze technieken op enzymgekatalyseerde processen vormt de grootte van deze systemen een probleem. Voorbeelden van de berekening van bindingswaarden, elektronen transport, en reactie snelheden worden besproken. Aan het eind van Hoofdstuk 1 wordt het quinohemoproteïne alcoholdehydrogenase uit *Comamonas testosteroni* geïntroduceerd als een geschikt enzym om met rekenmethoden te onderzoeken.

Alcoholdehydrogenasen die pyrroloquinolinequinon (2,7,9-tricarboxy-1*H*-pyrrolo-[2,3,*f*]quinoline-4,5-dion, PQQ) bevatten als organische cofactor zijn interessant, zowel vanuit fundamenteel als vanuit praktisch oogpunt. De quinoproteïne methanoldehydrogenases, MDHs, uit methylootrofe organismen zijn zeer goed bestudeerd. Veel minder is bekend over quinohemoproteïne alcohol dehydrogenases, die naast PQQ ook een  $\text{Ca}^{2+}$ -ion en een heem c bevatten. Hiervan is het QH-ADH uit *C. testosteroni* een voorbeeld.

In Hoofdstuk 2 wordt een overzicht gegeven van de huidige inzichten op het gebied van quinoproteïne enzymen. De aandacht gaat vooral uit naar de structurele en mechanistische aspecten die van belang zijn bij de katalytische eigenschappen van deze enzymen. Voorgestelde mechanismen worden besproken. Gelet op de beschikbare experimentele data blijven twee mechanismen over als zijnde meest waarschijnlijk: 1) vorming van een covalent-gebonden, hemiketaal adduct op de PQQ-C(5) positie; 2) directe hydride overdracht van het waterstof atoom op de a positie van het substraat naar de PQQ-C(5) positie, gestimuleerd door het dichtbij gelegen  $\text{Ca}^{2+}$ -ion.

Op basis van moleculaire modelleer technieken en een combinatie van energetische en geometrische criteria, lijkt de vorming van een intermediair calcium-alcohol complex, gevormd tijdens de directe hydride overdracht, een betere verklaring te geven voor de waargenomen enantioselectiviteit dan vorming van het PQQ-C(5) adduct.

De constructie van een ruimtelijk model voor het QH-ADH op basis van sequentie homologie met MDHs wordt beschreven in Hoofdstuk 3. Ondanks de matige overeenkomst konden verwante MDHs gebruikt worden als referentie structuren voor het katalytisch actieve PQQ-domein. Een grof model van het covalent gebonden heem domein kon worden gebouwd door de beschikbare structurele informatie van enkele cytochromen te gebruiken, alhoewel die slechts minimale overeenkomst in primaire sequentie vertoonden. De nadruk is daarom gelegd op bepaling van de locatie van dit domein relatief ten opzichte van het PQQ-domein, in de wetenschap dat er elektronen transport plaats moet kunnen vinden tussen PQQ en heem.

In Hoofdstuk 4 worden de resultaten van het onderzoek aan de mogelijke reactie mechanismen van de QH-ADHs beschreven. Het mechanisme, uitgaand van een directe overdracht van het hydride, is bestudeerd door berekeningen te verrichten aan de reactie van PQQ en PQQ-derivaten met methanol op verschillende theoretische niveaus. Mogelijk relevante intermediairen zijn in de berekening betrokken zodat de overgangstoestand van de reactie tussen PQQ en methanol in de aanwezigheid van calcium kon worden gelokaliseerd. Ondanks het feit dat de absolute waarde van de berekende energetische barrière te hoog uitvalt, wordt aannemelijk gemaakt dat de directe overdracht van een hydride tussen de C<sub>α</sub> positie van het substraat en de C(5)-positie van het PQQ zeer waarschijnlijk is.

Het gebruik van isotopen om het mechanisme van enzymgekatalyseerde reacties te achterhalen is het onderwerp van Hoofdstuk 5. Voor het eerst wordt hier de invloed van het kinetisch isotoop effect op de enantioselectiviteit van een enzym gerapporteerd. Om het mechanisme van QH-ADH uit *C. testosteroni* te onderzoeken werd het effect op de enantiomere ratio, *E*, in de ferricyanide-gekoppelde kinetische resolutie van *rac*-2,2-dimethyl-4-hydroxymethyl-1,3-dioxolaan (solketal) gemeten. Het berekende verschil in *E*-waarde voor de niet-gedeutereerde en gedeutereerde vorm van solketal, *E* = 30 vs. *E* = 6, kan worden verklaard door aan te nemen, dat er verschillen in kinetische bijdrage zijn



voor de initiële overdracht van een hydron/deuteron van het substraat naar de cofactor en de daaropvolgende omlegging van het proton/deuteron in het cofactor-product complex. In het geval van het gedeutereerde complex, lijkt dit de enantiomeer discriminatie in stap 1 gedeeltelijke teniet te doen.

Bij aanvang van dit onderzoek was er weinig bekend van de driedimensionale structuur van QH-ADHs. Gelet op de beschikbare hoeveelheid experimentele data zoals de primaire structuur van QH-ADH uit *C. testosteroni*, leek het construeren van een 3D-model door middel van homologie bouw wenselijk.

Recent werd de structuur van een kristal van QH-ADH uit *C. testosteroni* opgehelderd. In Hoofdstuk 1 is het homologie model (Hoofdstuk 3) vergeleken met deze structuur. Het geeft voldoening te zien, dat de belangrijkste elementen van de structuur correct voorspeld zijn. Belangrijker is, dat met deze nieuwe informatie de gebruikte reken technieken, die werden ontwikkeld tijdens dit onderzoek, met meer vertrouwen ingezet kunnen worden om de beschikbare experimentele informatie te interpreteren. Dit zal hopelijk leiden tot een beter begrip van de elektronische en kinetische eigenschappen van dit intrigerende en fascinerende enzym en biokatalysatoren van vergelijkbare complexiteit.



# List of publications

---

A. Jongejan, J. A. Jongejan and J. A. Duine.

*Homology model of the quinohemoprotein alcohol dehydrogenase from Comamonas testosteroni*

Protein Engineering, **11** (1998), 185-198.

A. Jongejan, S. S. Machado and J. A. Jongejan.

*The enantioselectivity of quinohemoprotein alcohol dehydrogenases: Mechanistic and structural aspects.*

Journal of Molecular Catalysis B: Enzymatic, **8** (2000), 121-163.

Corrigendum in Journal of Molecular Catalysis B: Enzymatic, **13** (2001), 57.

A. Jongejan and J. A. Jongejan.

*Enantioselectivity of PQQ-containing alcohol dehydrogenases: Kinetic, thermodynamic, and molecular modelling.*

In: M. Martinez-Carrion, A. J. Iriarte, H. M. Kagan, (eds.): Biochemistry and Molecular Biology of Vitamin B6 and PQQ-dependent Proteins. Birkhauser Verlag, Basel, 2000, p. 209-212.

A. Jongejan, J. A. Jongejan and W. R. Hagen.

*Direct hydride transfer in the reaction mechanism of quinoprotein alcohol dehydrogenases: A quantum mechanical investigation.*

Journal of Computational Chemistry, **22** (2001), 1732-1749.

A. Jongejan, J. A. Jongejan and W. R. Hagen.

*Deuterium isotope effect on enantioselectivity in the Comamonas testosteroni QH-ADH-catalyzed kinetic resolution of rac-solketal.*

Biochimica et Biophysica Acta, **1647** (2003), 297-302.

S. S. Machado, A Jongejan, A. Geerlof, J A Jongejan and J A Duine.

*Entropic and enthalpic contributions to the enantioselectivity of quinohaemoprotein alcohol dehydrogenase of Acetobacter pasteurianus and Comamonas testosteroni in the oxidation of primary and secondary alcohols.*

*Biocatalysis and Biotransformation*, **17** (1999), 179-207.

A. Hacisalihoglu, A. Jongejan, J. A. Jongejan and J. A. Duine.

*Enantioselective oxidation of amphetamine by copper-containing quinoprotein amineoxidases from Escherichia coli and Klebsiella oxytoca.*

*Journal of Molecular Catalysis B: Enzymatic*, **11**(2000), 81-88.

P. Casarosa, W. M. Menge, R. Minisini, C. Otto, J. van Heteren, A. Jongejan, H. Timmerman, B. Moepps, F. Kirchoff, Th. Mertens, M.J. Smit and R. Leurs.

*Identification of the first non-peptidergic inverse agonist for a constitutive active viral-encoded G-protein coupled receptor.*

*Journal of Biological Chemistry*, **278** (2003), 5172-5178.

# Curriculum Vitae

---

Aldo Jongejan werd geboren op 2 april 1970 in Delft. Hij behaalde zijn VWO diploma aan het Montessori Lyceum in Den Haag. Daarna ging hij scheikunde studeren aan de Rijksuniversiteit Leiden (RUL). Tijdens zijn studie studeerde hij 1 jaar aan de Universiteit in Århus (Denemarken) in het kader van het ERASMUS uitwisselingsprogramma. De afstudeerstage omvatte de synthese van PQQ-derivaten (sectie Enzymologie, TU Delft, prof. dr. ir. J. A. Duine en dr. ir. J. A. Jongejan) en de daaropvolgende koppeling aan polypyrrole derivaten (TNO Voeding, Zeist, dr. W. A. C. Somers) ter ontwikkeling van biosensoren. De afsluitende literatuurstudie had betrekking op de moleculaire identiteit van het Cu<sub>A</sub>-centrum van cytochroom c oxidase (prof. dr. G. W. Canters, RUL).

Na voltooiing van zijn studie (1994) was hij een half jaar werkzaam als junior onderzoeker aan het Gesellschaft für Biotechnologische Forschung (GBF) in Braunschweig, Duitsland. Hier werden onder begeleiding van dr. F. A. Bückmann FAD- en NAD-derivaten gesynthetiseerd met het doel FAD- en NAD-afhankelijke enzymen te gebruiken in biosensoren.

In 1995 aanvaardde hij een aanstelling bij de sectie Enzymologie aan de TU Delft als onderzoeker in opleiding. Tot medio 2000 werkte hij hier onder begeleiding van prof. dr. ir. J. A. Duine (later opgevolgd door prof. dr. W. R. Hagen) en dr. ir. J. A. Jongejan aan het in dit proefschrift beschreven onderzoek.

Vanaf januari 2001 is hij werkzaam als postdoc onderzoeker op het gebied van moleculair modellering van G-eiwit gekoppelde receptoren in de groep van prof. dr. R. Leurs bij de afdeling Farmacochemie van de Vrije Universiteit Amsterdam.



# Dankwoord

---

In 1978 werd de structuur van pyrroloquinoline quinone (PQQ) opgehelderd door Salisbury en medewerkers. Mijn vader is vanaf het begin erg betrokken geweest bij het onderzoek in Delft aan deze nieuwe cofactor en de quinoproteïnen. De verhalen thuis over het PQQ-onderzoek heb zekër invloed gehad op mijn studiekeuzes. Ik was toch erg nieuwsgierig geworden naar de scheikunde.

Nu, 25 jaar later, ben ik waarschijnlijk de laatste onderzoeker in opleiding in Delft, die op een aan quinoproteïnen gerelateerd onderzoek hoop te promoveren. Net nu de kristal structuur van een van de meest intrigerende en fascinerende (quino)proteïnen opgehelderd is, is het onderzoek aan deze klasse van enzymen in Nederland bijna geheel verdwenen. En dat is, denk ik, heel erg jammer. PQQ, bedankt!

Ik wil graag degene bedanken, die mij de kans heeft gegeven onderzoek te doen in dit veld. Hans, ook al ben je niet lang betrokken geweest bij mijn promotieonderzoek vanwege je pensionering, bedankt voor mijn aanstelling. Fred, bedankt voor het overnemen van Hans z'n taken en het feit dat je begreep, dat ik ondertussen in Amsterdam ook druk aan het modelleren was. Jaap (als begeleider), bedankt voor je begeleiding, de discussies en je kennis van quinoproteïnen, organische chemie, biochemie, enzymologie en thermodynamica. Het is vast niet makkelijk geweest de rollen van begeleider en opvoeder te scheiden. Samen zijn we er, denk ik, wel in geslaagd 'computational enzymology' op de kaart te zetten in Delft. Wel is duidelijk geworden dat het volgen van tutorials (die werken altijd!) en handleidingen niet altijd voldoende is om de vraagstellingen in de praktijk te beantwoorden.

Simon, bedankt voor je pogingen mij het kloneren bij te brengen. Helaas lieten QH-ADH en *C. testosteroni* zich niet zo makkelijk manipuleren.

Natuurlijk zijn er ook dagen, weken, maanden, in het leven van een OIO dat het allemaal wat minder gaat. Gelukkig kon ik dan met Evelien altijd heel vroeg koffie

drinken en gezellig praten. Evelien, bedankt. Daarnaast is er natuurlijk een hoop gekletst, gemopperd (ook wel) en lol gemaakt tijdens de koffiepauzes met de mensen van 'beneden' en de stagiaires (Barend, Ton, Mark (2x), Esengul, Arjen, Aster, Alexei, Richard, Thomas, Erwin, Marco, Laura, Natascha en alle anderen)

'Boven' kon ik altijd luisteren naar het 'hakken en zagen' van Bart, de succesverhalen van Toine (maar wat wil je ook als je je enzym met kilo's tegelijk kunt kopen) en de ideeën van Peter. Dat het maken van plaatjes (zoals jullie mijn computer-werk omschreven) toch iets meer tijd moest vergen dan 'even' hebben jullie volgens mij nooit begrepen.

Christian, tusend takk for din hjælp med computeren. Jeg er meget glad for at du var in Delft og synes det har jo vaeret meget morsomt. Og, som du sees, jeg kan nok ikke skrive på svensk...(eller italiensk).

Graag wil ik de broertjes Lispet, naast alle andere mensen in Delft, nog speciaal bedanken voor al hun ondersteunend werk. Volleyballen zullen jullie echter wel nooit meer leren....

Peter, bedankt voor je hulp bij het kweken van *Comamonas* in de grote 100 liter pijp. Door de gevoeligheid van *Comamonas* voor infecties, leverde dit echter voornamelijk mooie foto's op. Marijke en Jack, bedankt voor het kweken van *Comamonas* in een continue-cultuur. Dachten we eindelijk het lek boven te hebben, moesten jullie op congres en werd de stekker eruit getrokken! Maar jullie weten het, mochten jullie ooit uitgekeken raken op die rare gist, dan is er altijd nog *Comamonas testosteroni*.

Ondanks het feit dat ik nog niet gepromoveerd was (en het ook nog wel even op zich liet wachten uiteindelijk) hebben Rob en Ton mij de gelegenheid gegeven als postdoc aan de slag te gaan op het gebied van G-eiwit gekoppelde receptoren aan de Vrije Universiteit in Amsterdam. En daar ben ik ze nog steeds dankbaar voor. Verder wil ik iedereen in de groepen Farmacochemie en Moleculaire Toxicologie bedanken voor hun steun (en het geduld). Jennifer, Marola en Peter, jullie natuurlijk extra bedankt!

De laatste woorden zijn gewoontegetrouw voor de familie en daar ga ik geen uitzondering op maken. Laurian, zusje, ben je toch mooi eerder gepromoveerd. Bedankt voor je steun in de discussies met Jaap over het AIO-schap. En natuurlijk (samen met



Evert) voor het oppassen en spelen met Nynke. Sjoukje en Jaap (daar heb je 'm weer, nu als vader), jullie kan ik nooit genoeg bedanken. Ik hoop nog eens een keer zoveel te weten als jullie.

Tenslotte, Ant, nu weet ik ook wat een bevalling is. Die van Nynke en Nils gingen heel wat vlotter.

Jeg elsker dig (en dat zegt alles).

Aldo



*In the end there still is curiosity*



